ABSTRACTS BOOK

AMCTURKEY 2022

ADDITIVE MANUFACTURING CONFERENCE

OCTOBER 6 - 8, KUŞADASI PINE BAY HOLIDAY RESORT



SPONSORS

Platin Sponsors

KROMAŞ Better surfaces for life... | AM solutions 3D post processing technology | ERMAKSAN ADDITIVE THINK 3D

Gold Sponsors

ADD-ME Additive Manufacturing Excellence | RENA | SLM SOLUTIONS represented by digiMEDE

Silver Sponsors

eos | infoTRON | NORM ADDITIVE | promakim | TEI | voestalpine ONE STEP AHEAD.

Bronze Sponsors

aselsan | ESTAS | Hardline | INTECRO | NETFORM | SENTES BİR | ZEISS | etim | YORSEC

3D PRINTED CORES DEDICATED TO SINGLE CRYSTAL CASTING 1
3D PRINTING FOR SURGICAL PLANNING: CASE REPORT 3
3D PRINTING OF ALKALI-ACTIVATED MORTAR USING ROBOT 5
A CASE STUDY ON THE INJECTION MOLDING WITH A 3D PRINTED INJECTION MOLD 7
A CASE STUDY ON THE TOPOLOGY OPTIMIZATION OF PEDESTAL OF A STABILIZED ANTENNA FOR ADDITIVE MANUFACTURING 9
A NUMERICAL AND EXPERIMENTAL INVESTIGATION ON BUCKLING BEHAVIOR OF ADDITIVELY MANUFACTURED RIBBED CASINGS 11
A STUDY OF DIFFERENT TOOL PATH STRATEGIES FOR LASER METAL DEPOSITION PROCESS 13
ADDITIVE MANUFACTURING OF CLINICAL PRACTICE TRAINING MODELS USED IN MEDICINE AND DENTISTRY 15
ADDITIVE MANUFACTURING TECHNOLOGY CONFORMITY ASSESSMENT MODEL (TCA.M.) FOR AUTOMOTIVE APPLICATIONS 18
AN ALGORITHM FOR POWDER CLEANING OF ADDITIVELY MANUFACTURED PARTS WITH INTERIOR CHANNELS 20
AN INVESTIGATION ON THE EFFECTS OF PROCESS PARAMETERS ON THE GEOMETRICAL CHARACTERISTICS OF LASER DEPOSITED SINGLE TRACKS USING PH 13-8 MO STAINLESS STEEL POWDER 22
ANALYSIS OF THE FORCES AND VIBRATIONS ACTING ON THE CUTTING TOOL IN THE MICRO-DRILLING PROCESS OF TI6AL4V MATERIAL PRODUCED THROUGH EBM METHOD 24
ANGLE DEPENDENT PRODUCTIVITY RESEARCH OF CONFORMAL CHANNEL GEOMETRY SECTION IN LPBF 26
ASSESSMENT OF THE MECHANICAL AND CORROSION PROPERTIES OF AlSi10Mg PARTS PRODUCED THROUGH SELECTIVE LASER MELTING (SLM) AFTER VARIOUS POST PROCESSING CONDITIONS 28
BINDER JETTING OF PURE COPPER PARTS AND THEIR CHARACTERIZATION 30
CASE STUDY ON PRODUCTION OF MEDIUM TO LARGE SCALE PARTS BY WIRE + ARC ADDITIVE MANUFACTURING 32
CHARACTERIZATION OF METAL POWDER REUSED MULTIPLE TIMES FOR LASER POWDER BED FUSION 34
COLD SPRAY EFFECT ON OXIDE DISPERSION STRENGTHENING OF INCONEL 718 35
COMBINATION OF PERIDYNAMICS AND GENETIC ALGORITHM BASED TOPOLOGY OPTIMIZATION METHODS FOR AM-FRIENDLY DESIGNS 37
COMPARISON OF DYNAMIC MECHANICAL PROPERTIES OF AlSi10Mg LATTICE STRUCTURES PRODUCED BY SELECTIVE LASER MELTING 39
COMPARISON OF SINGLE AND TWIN SCREW EXTRUDERS FOR THE PRODUCTION OF GLASS AND CARBON REINFORCED HIGH DENSTIY POLYETHYLENE (HDPE) FILAMENTS 41
CONTACT-FREE SUPPORT STRUCTURES EFFECT ON DIMENSIONAL DEVIATION OF LPBF PRINTED COMPONENTS WITH OVERHANG FEATURES 43
COORDINATION OF SPATIAL & TEMPORAL LASER BEAM PROFILE TOWARDS ULTRA-FINE FEATURE FABRICATION IN LPBF 45
CREEP BEHAVIOR OF 3D PRINTED CB/PEI COMPOSITES 47
DEFECT DETECTION WITH IMAGE PROCESSING AND DEEP LEARNING IN POLYMER POWDER BED ADDITIVE MANUFACTURING SYSTEMS 48

DESIGN AND ADDITIVE MANUFACTURING OF PEEK IMPLANTS FOR PATIENT-SPECIFIC CRANIOPLASTY SURGERY 49

DESING OF A COMPLIANT CLAMPING MECHANISM FOR FDM BED IN ADDITIVE MANUFACTURING .. 51

DEVELOPMENT AND STATIC LOAD TESTİNG OF ADDITIVELY MANUFACTURED STAINLESS STEEL NOSE LANDING GEAR AIRCRAFT PART FOR CIVIL AVIATION APPLICATIONS 52

DEVELOPMENT OF A DIGITAL IMAGE PROCESSING ALGORITHM FOR ANOMALY DETECTION IN LARGE SCALE ADDITIVE MANUFACTURING 54

DEVELOPMENT OF ALUMINUM ALLOY POWDERS FOR ADDITIVE MANUFACTURING 55

Materials.DEVELOPMENT OF MULTIFUNCTIONAL 3D PRINTED SCAFFOLD FOR BIOMEDICAL APPLICATIONS 56

DIMENSIONAL ACCURACY INVESTIGATION OF TiO_2 REINFORCED POLYMER NANOCOMPOSITE PARTS PRINTED BY DLP 59

DIMENSIONAL VARIATIONS IN EBM PRODUCED STRUT-BASED AND TPMS LATTICES 60

DIRECTED ENERGY DEPOSITION OF REFRACTORY CR10MO25TA25TI15V25 HIGH ENTROPY ALLOY 62

Effect of heat treatments on the microstructure and mechanical properties of Inconel 718 alloy fabricated by Laser Powder Bed Fusion method 63

EFFECTS OF DESIGN PARAMETERS ON SURFACE ROUGHNESS OF ADDITIVELY MANUFACTURED THIN WALL STRUCTURES 65

EFFECTS OF DIFFERENT PRODUCTION PARAMETERS ON MECHANICAL PROPERTIES IN FDM-PRINTED PRODUCTS 67

EFFECTS OF LATTICE STRUCTURES ON ADDITIVELY MANUFACTURED METAL PARTS 69

ELECTROMAGNETIC CHARACTERIZATION OF 3D PRINTED METAMATERIAL ABSORBER WITH CONDUCTIVE PAINT 70

ENERGY DENSITY DETERMINATION FOR L-PBFP OF TI-6AL-4V ALLOY FOR VARIOUS BEAM DIAMETERS AND HATCH DISTANCES 71

ESTABLISHING THE EFFECT OF PROCESS PARAMETERS ON THE MECHANICAL PROPERTIES OF 3DPRINTED PETG 73

Experimental analysis of R-phase NiTi tube actuators using conductive/convective heating stage 75

EXTRUDER DESIGN OF PRINTABLE COMPOSITES 76

FOAMING PLA PARTS PRODUCED BY FUSED FILAMENT FABRICATION 78

HEAT PIPE EMBEDED COLD PLATE DESIGN WITH ADDITIVE MANUFACTURING TECHNOLOGIES 80

HIGH CYCLE FATIGUE PERFORMANCE OF AGE HARDENED AND HIPPED AM-ALSI10MG: INVESTIGATION ON POST PROCESS EFFECTS 82

HYBRID THERMOPLASTIC COMPOSITE MANUFACTURING BY ADDITIVE MANUFACTURING 83

INFLUENCE OF CERAMIC-BASED ADDITIVES ON THE DRY SLIDING WEAR BEHAVIOUR OF PA 12 PRODUCED BY SLS 85

INJECTION MOLDING OF MICROFLUIDIC DEVICES WITH 3D PRINTED INSERT TOOLS 87

INVESTIGATION FOR EFFECTS OF HEAT SUPPORT DESIGN FACTORS ON OVERHANGS IN DMLS PROCESS 89

INVESTIGATION OF ELECTROCHEMICAL POLISHING ON THE SURFACE OF THE γ-TiAl PARTS PRODUCED BY ADDITIVE MANUFACTURING 91

INVESTIGATION OF FLUID FLOW CHANNEL GEOMETRIES FOR FUEL MANIFOLD BASED ON ADDITIVE

MANUFACTURING PROCESS LIMITS 93

INVESTIGATION OF LASER POWDER BED FUSION DEFECT INSPECTION BY IN-SITU MONITORING AND COMPUTED TOMOGRAPHY 95

INVESTIGATION OF SKINCORE STRATEGY TO INCREASE PRODUCTIVITY FOR LARGE PARTS IN LASER POWDER BED FUSION SYSTEM 97

INVESTIGATION OF THE EFFECT OF LATTICE PARAMETERS ON MECHANICAL PROPERTIES AND RELATIVE DENSITY IN OPTIMIZATION OF LATTICE STRUCTURES IN ADDITIVE MANUFACTURING 99

LASER WELDABILITY OF LASER POWDER BED FUSED ALSI7MG0.6 101

MECHANICAL PROPERTIES OF CONTINUOUS CARBON FIBER-REINFORCED THERMOPLASTIC PARTS PRODUCED BY FUSED FILAMENT FABRICATION 103

MICROSTRUCTURE AND BONDING MECHANISM EVALUATION FOR BI-METALLIC SS 316-INCONEL718 PRODUCED BY DIRECTED ENERGY DEPOSTION PROCESS 105

MICROSTRUCTURE AND STRENGTH OF 3D PRINTED PART USING MICROPLASMA WIRE ARC ADDITIVE MANUFACTURING 107

MICROSTRUCTURES AND MECHANICAL PROPERTIES OF OXIDE DISPERSION STRENGHTENED INCONEL 718 ALLOYS PRODUCED BY SELECTIVE LASER MELTING 109

MULTI-TRACK, MULTI-LAYER FINITE ELEMENT ANALYSIS OF THE TEMPERATURE FIELD DURING SELECTIVE LAYER MELTING OF 316L STAINLESS STEEL 111

NEW APPROACH FOR USAGE OF VIRGIN AND REUSED POWDERS TOGETHER IN LASER POWDER BED FUSION 112

NOVAL DESIGN OF ANTI-BACKLASH MOTOR BRACKET MECHANISM AND BENCHMARK TEST 114

ON THE MECHANICAL BEHAVIOR AND MICROSTRUCTURAL CHARACTERIZATION OF WIRE + ARC ADDITIVE MANUFACTURING OF Mn-Si BASED STEEL ALLOY (ER70S-6) 116

OPTIMIZATION OF STRAIN ENERGY IN CRACK INDUCED STRUCTURE VIA MICRODEFECTS USING PERIDYNAMIC INFORMED TOPOLOGY OPTIMIZATION 118

PERIDYNAMIC INVESTIGATION OF SURFACE CRACKS IN OPTIMALITY CRITERION-BASED TOPOLOGY OPTIMIZATION FOR ADDITIVE MANUFACTURING 120

POLYACRYLIC ACID-BASED SHAPE-MEMORY, SELF-HEALING HYDROGELS FABRICATED BY STEREOLITHOGRAPHY 122

POLYMER-METAL HONEYCOMB COMPOSITES PRODUCED BY ADDITIVE MANUFACTURING AND ELECTROPLATING 123

POST-PROCESSING OF SURFACE TOPOGRAPHY DATA FOR AS-BUILT METAL ADDITIVE SURFACE TEXTURE CHARACTERIZATION 125

PRELIMINARY INVESTIGATION OF TRIBOLOGICAL CHARACTERIZATION OF 3D PRINTED AN AMORPHOUS THERMOPLASTIC WITH DIFFERENT INFILL DENSITIES 127

QUALIFICATION METHOD FOR THE PROCESS DEPENDENT FACTORS AND AFFECTING THE FATIGUE BEHAVIOR OF LASER POWDER BED FUSION METHODS FOR Ti6AL4V 128

SURFACE CHARACTERIZATION OF ELECTRON BEAM MELTING PROCESSED γ-TIAL 129

SURFACE ROUGHNESS ASSESSMENT OF POST-PROCESS EFFECTS ON LPBF ALLOY 718 131

SURFACE TREATMENT EFFECTS ON CHEMICAL MILLING PERFORMANCE OF L-PBF PRODUCED TI6AL4V ELI 133

TEETH SUPPORT STRUCTURES EFFECT ON DIMENSIONAL DEVIATION OF LPBF PRINTED COMPONENTS WITH OVERHANG FEATURES 135

THERMAL SIMULATION AND EXPERIMENTAL VERIFICATION STUDY FOR TI-6AL-4V ALLOY PROCESSED BY METAL LASER MELTING 137

THERMO-MICRO-MECHANICAL SIMULATION OF A TI-6AL-4V SINGLE WALL STRUCTURE MANUFACTURED BY DIRECTED ENERGY DEPOSITION 139

TOPOLOGY OPTIMIZATION OF THE CONSOLIDATED STRUCTURAL BRACKET AND VALIDATION BASED ON MIL-STD 141

USING COBOTS FOR ADDITIVE MANUFACTURING OF BUILDING ELEMENTS 143

VERIFICATION TESTS of Ti6Al4V ALLOY by TIG BASED WAAM METHOD 145

WIRE + ARC ADDITIVE MANUFACTURE OF 17-4 PH STAINLESS STEEL: EFFECT OF PROCESSING CONDITIONS ON THE GEOMETRICAL AND MECHANICAL PROPERTIES 147

WIRE ARC ADDITIVE MANUFACTURING OF THIN-WALLED LOW ALLOY STEEL COMPONENTS USING SOLID AND METAL CORED WIRES 149

3D PRINTED CORES DEDICATED TO SINGLE CRYSTAL CASTING

Roux Arnaud[1], Coulon Philippe[2], Chaput Christophe[1]
[1]*3DCERAM SINTO – 4 rue du Parc Maison Rouge, 87270 Bonnac-La-Côte, France*
[2]*AVIGNON CERAMIC - Route de Noirlac, 18200 Bruère-Allichamps, France*

ABSTRACT

Due to the need for more efficient engines and gas turbine in the aerospace industry, foundry cores must be more and more complex and are becoming difficult to produce by the conventional ceramic injection molding process (especially new generation cores). The additive manufacturing process allows to produce complex cores with high resolution to meet the need for investment casting. 3DCeram Sinto, a turnkey provider for 3D printing ceramics (machine, materials and process) and Avignon Ceramic, manufacturer of cores for investment casting since 1990, by injection molding and recently 3D printing, have joined forces within U3DC to provide the precision foundry world with proven solutions in the production of 3D printed ceramic cores and to offer a complete printing solution.

Thanks to this partnership with the use of specific ceramic powders dedicated to single crystal casting and to the tailored suspension development, we could obtain optimal properties, thermal expansion, porosity, flexural strength and microstructure analysis of the sintered material. This presentation will highlight the technical results for both technologies, 3D printing compared with injection molding.

Keywords: Foundry cores, stereolithography, ceramic 3D printing, single crystal casting

1. INTRODUCTION

Foundry cores are an essential part of the production of blades for combustion engines. Efficiently cooled blades allow to insure higher temperature of working media, which leads to increase engine power and efficiency. To meet this challenge, the blades are hollowed with integrated cooling channel. As the alloys that make up the turbines' blades are not easily machinable or forgeable, investment casting is used for their production. In this complex process that involves many steps, the ceramic core is the sacrificial material that will be used as a negative once the alloy is melted over the core [1]. Today, the need for complex core design has increased dramatically with customers' demands for smaller, more efficient and cost-effective engines [2, 3]. These new complex cores are difficult to produce using usual industrial processes like ceramic injection molding [4, 5] because it requires to make the core in several pieces that are then assembling manually, which is very complex and can induce an extremely high waste rate. Moreover, the lead time to develop new forms of cores with the traditional methods can be very long due to the complex natures of the molds, so little modifications can be made to the cores during production.

2. MATERIALS AND METHODS

In this context, 3DCERAM has developed a process of producing ceramic foundry cores based on the laser stereolithography (SLA) 3D printing technology. This process consists in a layer-by-layer fabrication procedure in which the selective curing of a photopolymerizable ceramic suspension by a computer-controlled UV laser beam enables the fabrication of a three-dimensional part [6, 7, 8, 9]

3. RESULTS AND DISCUSSION

High accuracy foundry cores with complex geometry and tailored properties were produced through a breaking stereolithography 3d printing process. For this, a specific parts' supporting technology was developed to build parts with low section and fine details with a dimensional accuracy of +/-0.2 mm. This technique is time and cost-effective compared to conventional support creation methods and can be used for industrial production of cores since it allows the manufacture of several dozen parts in a few days.

The properties of the sintered cores were optimized thanks to the use of a specific ceramic powder and to a custom suspension development. Indeed, mechanical properties of the material (flexural strength about 16.7MPa) are in accordance with the specifications. Moreover, a porosity of 37.5 % combined with a cristobalite content of 2% ensure a high dimensional stability during heat treatment (confirmed by dilatometry analysis) as well as a good leachability of the ceramic core.

4. CONCLUSIONS

This innovative technology brings a new dimension to the traditional industrial process used for cores production. Indeed, in addition to saving time and increasing productivity, additive manufacturing delivers the following benefits: flexibility of design, possibility of increased complexity of cores, quick creation of new designs (no mold used, parts are produced directly from CAD files), better responsiveness and increased profitability (lower investment and change costs, no tool maintenance and storage costs).

REFERENCES

1 Ram Prasad, Progress in Investment Castings, Science and Technology of Casting Processes, 2012.
2 Je-Chin Han and al., Enhanced internal cooling of turbine blades and Vanes, The Gas Turbine Handbook, 2006, US Dept. of Energy, 321-346.
3 T. Ravi Teja and al., Case study on Turbine Blade Internal Cooling, International Journal of Engineering Research & Technology, Vol. 2 Issue 3, 2013.
4 EP0497682A1, Procédé de réalisation de noyaux complexes en céramique pour fonderie, Snecma, 1992.
5 Ceramic cores for turbine blades via injection moulding, Magdalena Gromada and al., Journal of Materials Processing Technology, vol 220, 2015, 107-112.
6 C. Hinczewski and al., Ceramic suspensions suitable for stereolithography, J. Eur. Ceram. Soc., vol. 18, no 6, 583-590, 1998.
7 T. Chartier and al., Additive Manufacturing to Produce Complex 3D Ceramic Parts, J. Ceram. Sci. Technol., vol. 6, no 2, 95-104, 2014.
8 Griffith, Freeform Fabrication of Ceramics via Stereolithography, Journal of the American Ceramic Society, 1996.
9 A. Brady and al., Curing behavior of ceramic resin for stereolithography in solid free form fabrication proceedings, 403-410, 1996.

3D PRINTING FOR SURGICAL PLANNING: CASE REPORT

Mihrigül Altan[1,2], Halil İbrahim Canter[3]
[1]*Department of Mechanical Engineering, Yildiz Technical University, Besiktas, İstanbul, Turkey,34349, meksi@yildiz.edu.tr*
[2]*Department of Biomedical Engineering, Yildiz Technical University, Esenler, İstanbul, Turkey, 34220 , meksi@yildiz.edu.tr*
[3]*Department. of Plastic Reconstrucitve Surgery, Liv Hospital Vadistanbul, Sariyer, İstanbul, Turkey, 34346, hicanter@gmail.com*

ABSTRACT

Surgeons use to perform their surgery depending on their experiences as well as visual aids from medical imaging techniques such as magnetic resonance imaging (MRI) or computed tomography (CT). However, due to the anatomical complexity of the surgery, two dimensional or virtual images are not sufficient to achieve successful structural details. 3D printing technologies have brought a new era in medicine by providing surgical planning. In this study, case reports about 3D printing application for surgical planning for maxillofacial surgery are presented. By the usage of 3D printing techniques and related software, planning of surgical cutting and designing of drilling guides in skeletal surgery could be done. In this regard, data on computer from radiological imaging were converted to three-dimensional visualization of the anatomic structures and then virtual surgical planning of the operations were done by the surgeons. Finally, 3D models were manufactured by additive manufacturing in order to verify the design and usability of the implants before the surgery. As a result, it has been shown that additive manufacturing methods have great importance in production of custom-made implants and fixation plates for the treatment of skeletal deformities with complex anatomy.

Keywords: surgical planning, 3D printing, implant, additive manufacturing

1. INTRODUCTION

Surgeons have been carrying out surgeries on complex anatomical structures of human body depending on their experiences as well as the collected data from medical imaging techniques. By the help of medical imaging tools such as computed tomography (CT) and magnetic resonance imaging (MRI), surgeons can determine diagnosis. However, these imaging tools provide two-dimensional images and they are limited depict complex 3dimensional (3D) structures. Therefore, todays virtual 3D reconstruction methods have been started to be used for better understanding of structural complexity of any kind of defect such as bone losses, tumor, congenital heart defects and aneurysms. (Ou et al., 2007). However, there are still differences between real anatomical structures and the interpretation of virtual 3D images . (Shiraishi et al., 2010).

With the development of digital technology, it has been seen that virtual surgery, computer aided design and 3D printing techniques have become a part of the medical treatment. 3D printing is now being used to create physical models of patient anatomies for surgical simulation and planning. Surgical simulations provide surgeons to prepare themselves for specific and risky operations without the use of patients, cadavers, or animal models. With recent advancements in the field of 3D printing, MRI or CT images can now be used to fabricate 3D anatomical models (Ganguli et al., 2018, Silvina 2021, Stephany et al., 2021). In this study, surgical planning for maxillofacial surgery by 3D printing are given and it has been reported that complex anatomical surgeries can be carried in short time and with less blood loss with high precision.

2. MATERIALS AND METHODS

A neurofibromatosis case with facial skeletal deformity due to the expanding tumor at the right side of the patient is reported. Medical image processing software Materialise Mimics (Belgium) and 3D modelling software Materialise 3-matic (Belgium) were used for modelling the implant. Before titanium based implant manufacturing, verification of the design was done on multi jet fusion process (HP Jet Fusion 3D). Finally, Ti6Al4V ELI implant was manufactured on M2 cusing (L-PBF) with the set process parameters for titanium material.

3. RESULTS AND DISCUSSION

The extend of the deformity is confirmed my mirror imaging of the facial skeleton of the patient on the midfacial axes. The amount of the bony structures that would be removed on the right facial skeleton and the titanium implant that would be used to fill that defect were planned as given in Figure 1.

Surgical cutting guides for removal of the deformed bones and titanium implant for reconstruction were manufactured with SLM. The surgery of each patient was done as planned without any intraoperative unexpected problem related with the implants. The recovery period was uneventful and surgical wounds were healed as expected. Both patients were satisfied with the facial contour achieved by the introduced implants.

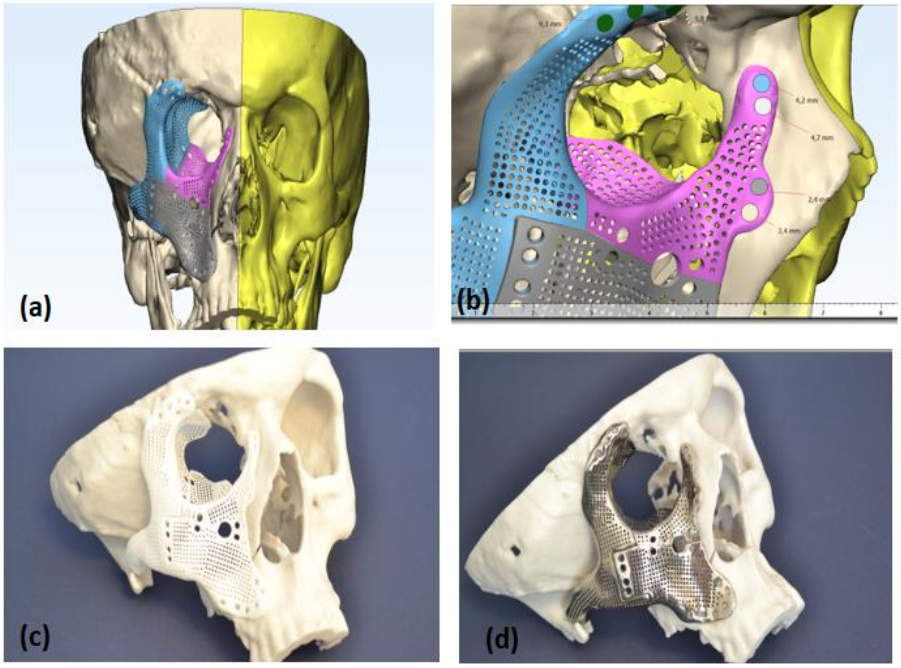

Figure 1. Surgical planning by 3d printing techniques for maxillofacial surgery: (a) , (b) Design and modeling by Materialise Mimics and 3-matic (c) Poliamid12 modeling by multijet fusion (d) Ti6Al4V ELI implant by selective laser melting

4. CONCLUSIONS

It has been seen that for successful and short time surgeries, surgical planning has critical importance. From designing step to the final step of manufacturing of the titanium based implant, additive manufacturing related software and processes are promising for biomedical applications.

REFERENCES

Ou, D.S., Celermajer, G. , Calcagni, F., Brunelle, D., Bonnet, D., Sidi, (2007) Three-dimensional CT scanning: a new diagnostic modality in congenital heart disease. *Hear,t* 93(8), 913.

Shiraishi, I. , Yamagishi, M., Hamaoka, K., Fukuzawa M., , T. Yagihara, T.(2010), Simulative operation on congenital heart disease using rubber-like urethane stereolithographic biomodels based on 3D datasets of multislice computed tomography. *European Journal of Cardio-Thoracic Surgery*, 37(2), 306.

Ganguli, A., Pagan-Diaz, G. J., Lauren, C., Caroline, B., Mathew, V., John, K., Thenkurussi, B., Rashid (2018), 3D printing for preoperative planning and surgical training: a review. *Biomedical Microdevices*, 20(65), 24.

Silvina Z.T. (2021), Biomodeling and 3D printing: A novel radiology subspecialty. *Annals of 3D Printed Medicine*, 4, 24

Stephany, L.S., Jon Z.J., Maria Elena, R.G., Juan Jose, G.Z., Luis M M. (2021).Three-dimensional printed models used for personalized precision thoracic surgery. *Annals of 3D Printed Medicine*, 2,3.

3D PRINTING OF ALKALI-ACTIVATED MORTAR USING ROBOT

Erman Tunçer[1], Sepehr Seyedian Choubi[2] Çağla Meral Akgül[3]
[1] *Department of Civil Engineering Middle East Technical University, Ankara, Turkey, erman.tuncer@metu.edu.tr*
[2] *Department of Civil Engineering Middle East Technical University, Ankara, Turkey, sepehr.seyedian@gmail.com*
[3] *Department of Civil Engineering Middle East Technical University, Ankara, Turkey, cmeral@metu.edu.tr*

ABSTRACT

Ram extruder combined with Universal Robot 10e was used to print a 35-layer structure with thicknesses of 0.7cm for each layer and a 10cm diameter. For printing material, an alkali-activated mortar (cementitious composite) was developed using ground granulated blast slag (slag) and red mud -bauxite residue- as binders, NaOH as an activator and continuous graded sand. Flexure and compressive strength tests were conducted to measure hardened properties.

Keywords: 3D Printing, Universal Robot, Alkali-activated Mortar

1. INTRODUCTION

Additive manufacturing (AM) is attracting increasing interest in construction industry, especially in concrete technology[1]. Using robots as a new way of construction reduces material consumption and total waste, eliminates the need for formwork (considerable time and cost-saving) and increases the geometrical flexibility [2, 3]. 3D printing of cementitious materials requires a variety of material qualities, some of which are listed in ***Hata! Başvuru kaynağı bulunamadı.*** (a) [2]. Both pumpability a nd buildability are linked to the rheology of fresh cementitious materials. Aggregates take up a significant portion of the total volume of cementitious materials; hence, aggregate gradation highly affects its rheological property. Continuous aggregate gradation contributes to high density and good rheological properties of materials ***Hata! Başvuru kaynağı bulunamadı.*** (b)[4].

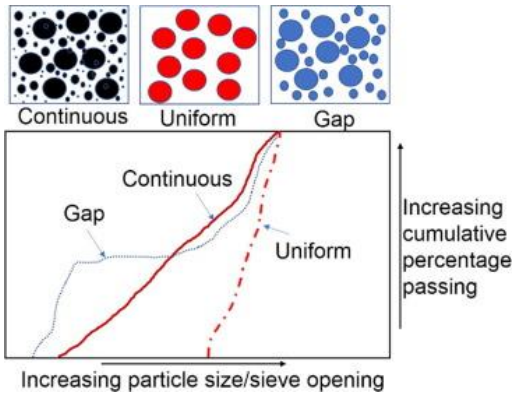

(a) (b)

Figure 1 (a) Selected requirements of printable concrete in fresh and hardened state, (b) Three types of sand gradation

The authors of this paper develop an alkali-activated mortar (type of cementitious composite) suitable for 3D printing technology. The extrusion technology was applied to determine the printability of the mortar mix.

2. MATERIALS AND METHODS

In this study, slag and red mud were collected from İsdemir (İskenderun Demir ve Çelik A.Ş.) and Eti Aluminyum A.Ş. High purity NaOH (>98%) collected from Koruma Group Companies was used as an activator. Silica sand and quartz powder were used to prepare mortar. The mix design for mortar is given in *Hata! Başvuru kaynağı bulunamadı.*.

Table 1 Mix design for $1m^3$

	Binder		Sand			Activator	
Materials (Kg)	Slag	Red mud	0.2-0.5 mm	0.1-0.3mm	Quartz powder	NaOH	Water
Mortar mix	390	260	520	455	325	65	292.5

Ram extruder ***Hata! Başvuru kaynağı bulunamadı.*** a was used to inject fresh mortar into the 3D p

rinting pipe by applying 2 bar pressure. Universal Robots 10e was used to print 35 layers of mortar with thicknesses of 0.7cm for each layer and 10cm diameter by moving speed of nozzle at 4cm/s. 4*4*16cm prisms were cast to measure compressive and flexure strength for hardened mortar at 1, 3 and 7 days.

3. RESULTS AND DISCUSSION

Aggregates of different sizes and quartz powder were mixed in specific portions to achieve continuous gradation as possible, an essential factor in achieving printable mortar mix **Hata! Başvuru kaynağı b ulunamadı.**c. As a result, the freshly mixed mortar was successfully printed with air driven ram type extruder **Hata! Başvuru kaynağı bulunamadı.**b. During the printing process, the printed part did m aintain its shape throughout 35 layers **Figure 2** b. Mechanical test results are as follows: Flexture test results showed 1.3,1.5 and 2 MPa strength at 1,3 and 7 days, respectively, and compressive test results showed 4.7,15.45 and 20.75 MPa strength at 1,3 and 7 days, respectively.

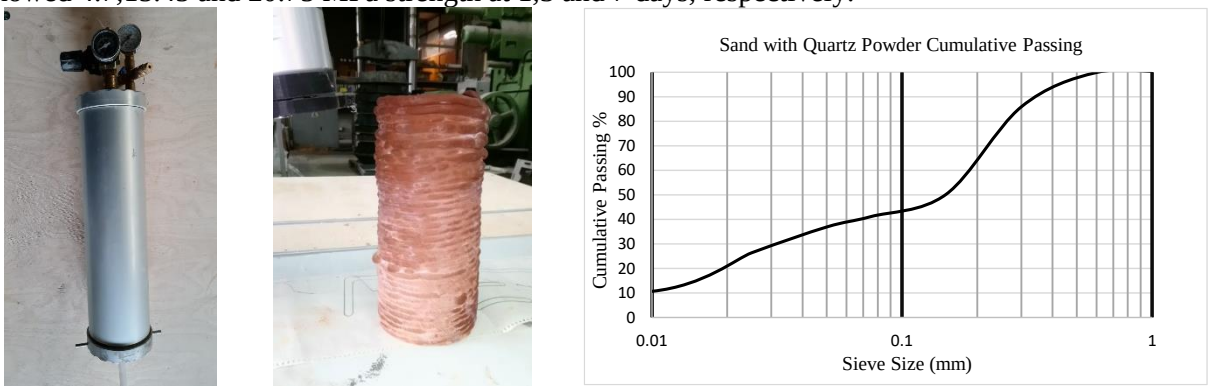

(a) (b) (c)

Figure 2 (a) Ram extruder,(b) Final product, (c) Gradation of sand

4. CONCLUSIONS

Developed mortar resulted in flexure and compressive strength suitable for construction. Freshly printed 35-layer cylinder remained stable through printing. These preliminary tests gave acceptable results for continuing the study for improving the mix and trying to print structures with more complex geometries and bigger dimensions.

REFERENCES

1. Asprone D, Auricchio F, Menna C, Mercuri V (2018) 3D printing of reinforced concrete elements: Technology and design approach. Constr Build Mater 165:218–231. https://doi.org/10.1016/J.CONBUILDMAT.2018.01.018
2. Nerella VN, Mechtcherine V (2019) Studying the Printability of Fresh Concrete for Formwork-Free Concrete Onsite 3D Printing Technology (CONPrint3D). 3D Concr Print Technol 333–347. https://doi.org/10.1016/B978-0-12-815481-6.00016-6
3. Skibicki S, Pułtorak M, Kaszyńska M, et al (2022) The effect of using recycled PET aggregates on mechanical and durability properties of 3D printed mortar. Constr Build Mater 335:127443. https://doi.org/10.1016/J.CONBUILDMAT.2022.127443
4. Weng Y, Li M, Tan MJ, Qian S (2018) Design 3D printing cementitious materials via Fuller Thompson theory and Marson-Percy model. Constr Build Mater 163:600–610. https://doi.org/10.1016/J.CONBUILDMAT.2017.12.112

A CASE STUDY ON THE INJECTION MOLDING WITH A 3D PRINTED INJECTION MOLD

Alper Atak[1], Kerem Güngör[2]
[1]*Aselsan, Yenimahalle-ANKARA, alperatak@aselsan.com.tr*
[1]*Aselsan, Yenimahalle-ANKARA, kgungor@aselsan.com.tr*

ABSTRACT

Injection molding is the most common method for mass production of plastic parts. It's perfect for producing large numbers of identical parts with precise tolerances in a short amount of time. Previously, 3D printing was mainly utilized in the design and production process to build and test prototypes that would be injection molded later. 3D printers can now directly build molds thanks to advancements in printer accuracy, surface polish, and materials.

Keywords: Injection Molding, 3D Printed Molds,

1. INTRODUCTION

Injection molding is the method of making components by injecting molten material into a die under pressure. Because of the significant initial setup costs associated with injection molding, this technology is only cost-effective when used in large quantities. These costs are mostly related to the extremely high standards for designing, producing, and manufacturing injection molding dies. As a result, injection molding is often reserved for producing large quantities of similar parts at a low cost.

Low-run injection molding, which refers to production runs of 10 to 100 components is not financially feasible due to the enormous expenses of tooling (the injection molding dies). Thanks to the recent improvements in additive manufacturing technology, now it is possible to generate items with great accuracy and outstanding surface polish. When this is combined with modern temperature-resistant 3D printing materials and the design freedom that 3D printing provides, 3D printed molds have become a feasible option for producing low-volume injection molding dies. Mold designs can also be quickly verified with 3D printed molds, reducing the financial risk of investing in an expensive metal mold.

This case study a discusses the benefits of using 3D printing for manufacturing low-run injection molds on traditional injection molding process and gives advice on the possible mold configurations, the available 3D printing mold materials and the best design practices for creating 3D printed injection molds

2. MATERIALS AND METHODS

Case study is started with the mold design of the part that will be injected. Traditional injection mold design concepts, rules, and procedures apply to 3D printed injection molds as well, however some adjustments are required to compensate for the mechanical, thermal, and dimensional characteristics of the plastic mold. The mold design for this case study is shown in Figure 1a.

For printing the designed mold Stratysy J750 3D printer and Digital ABS material combination is used. With Stratysy J750 3D printer it is possible to built in 30 micron layers with accuracy as high as 0.1mm. These production features provide high dimensional accuracy and smooth surface finish so post processing is not needed in most cases. The Digital ABS material combines strength and toughness together with high temperature resistance, therefore it is selected as mold material. The printed molds are shown in Figure 1b.

For injection molding process 3D printed Molds are mounted in MUD base (Figure 1c). Injection molding with 3d printed molds requires adjustment to the traditional molding process.

To avoid causing damage to the tool, it's best to start with conservative values. The process settings are changed using the test shoots until the desired parts are produced.(Figure 1d).

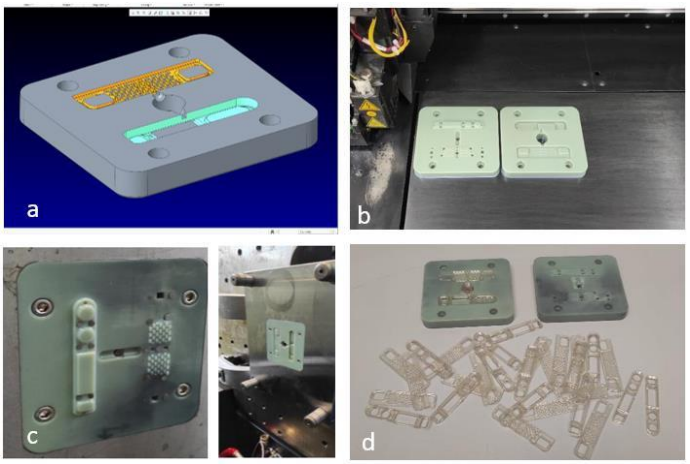

Figure 1. Experimental Procedure, a)Designing the Mold, b)3D Printing the Mold, c)Injection Molding Process, d)Printed Parts

3. RESULTS AND DISCUSSION

The cost and lead times for traditional injection molding process and injection molding with 3D Printed molds for this case study are shown in Table 1. As shown in table total costs with 3D Printed Molds are almost 25 times lower compared to traditional IM. Also building a 3D printed mold is relatively quick, a mold can be built within a few hours as compared to days or weeks to create traditional molds. In cases where design changes are required, a new iteration of the mold can be created in-house allows designers and engineers greater design freedom.

Table 1. Cost of manufacturing the ABS fitting

	Traditional Injection Molding	Injection Molding with 3D Printed Molds
Cost of Mold	$70.85	$1660.72
Cost per Part	$0.05	$1.89
Total Cost for 25 Part	$72.10	$1711.48
Lead Time	2 days	8-10 days

4. CONCLUSIONS

With 3D printed molds it is possible to produce prototypes using the same injection molding process and materials, allowing them to take functional testing to a new level. Companies can obtain superior performance statistics and establish certification confidence with this technology.

REFERENCES

[1]Stratasys Technical Application Guide, Polyjet for Injection Molding
[2]Stratasys Case Study “Durable Prototying”
[3]Stratasys Precision Prototyping,”The Role of 3D Printed Molds in the Injection Molding Industry”

A CASE STUDY ON THE TOPOLOGY OPTIMIZATION OF PEDESTAL OF A STABILIZED ANTENNA FOR ADDITIVE MANUFACTURING

Akın Arslan[1], Emre Esen[2]
[1]*Aselsan, Yenimahalle-ANKARA, akinarslan@aselsan.com.tr*
[2]*Aselsan, Yenimahalle-ANKARA, eesen@aselsan.com.tr*

ABSTRACT

Antenna pedestal is an electromechanical structure that provides the movement and control of an antenna system with two or three axes of motion in a stabilized manner. In this study, mechanical foundation of the pedestal which previously consisted of 4 different aluminum parts connected with screws and washers is re-designed for additive manufacturing as one single body that topology optimization was applied. Topology optimization goal is performed in order to reduce the total weight while keeping or strengthening the pedestal stiffness and modal behavior which is very important for antenna stabilization.

Keywords: Topology optimization, antenna system, design for additive manufacturing, lightweighting, metal additive manufacturing

1. INTRODUCTION

Antenna pedestal is a structure that supports electronic and electromechanical parts that will provide bi- or tri- axial movement of the antenna and is controlled in stabilized or unstabilized forms. In order to provide this movement and control, there are targeted stiffness, modal behavior and mass requirements. At the same time, the antenna system must withstand environmental conditions such as vibration or shock that it will be exposed to on the platform (air, land or sea) on which it will operate.

Topology optimization methods try to find the optimal geometry of the design by solving the material distribution problem. Lightweight parts with complex design geometry can be achieved by topology optimization, with the help of the additive manufacturing methods, parts with complex shapes can be produced by adding materials layer by layer. (Esen, 2021)

In this case study, it is aimed to redesign the antenna base, which was previously designed by combining four different mechanical parts with screws and washers, and produced by conventional manufacturing methods. By performing topology optimization methods, it is aimed to design a one-piece structure that will be lighter, more rigid and whose mechanical behavior will be more efficient in the aspect of control and stabilization framework.

2. MATERIALS AND METHODS

The pedestal structure, which was previously produced from Aluminum 6061-T6 material by conventional methods was re-evaluated during the topology optimization and alternatives of Ti6Al4V and AlSi10Mg material were studied. Before the topology optimization, maximum design area was defined to the algorithm. The topology optimization was carried out using this maximum design space. (Figure 1)

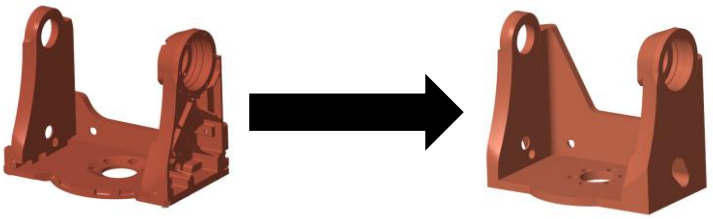

Figure 1. a) Conventionally manufactured antenna pedestal b) Maximum design space input geometry

Density-based method was used in topology optimization. During the optimization, considering that the antenna structure will be used on the aerial platform, it was considered that the weight should be low and therefore weight reduction was determined as an output target. Likewise, since the modal behavior and mechanical environmental resistance of the antenna must be high for proper stabilization and control of the antenna it was determined that the first natural frequency value should be at least as much as obtained in conventional methods as a secondary output target.

3. RESULTS AND DISCUSSION

As a result of optimization studies, different outputs were obtained for aluminum and titanium powder materials. When these outputs were evaluated, it was seen that the aluminum material alternative was more advantageous than titanium. (Table 1) The reason for this is that when titanium is used, since it is desired to completely keep the motor and roller bearing housings in the desired geometry, it has been observed that these housings have a very large effect on the total weight. For this reason, it was concluded that the goal of weight reduction would not be possible with titanium material.

Table 1. Comparison of original geometry and topology optimization output geometries

	Original Design	Topology Optimization Output (Aluminum)	Topology Optimization Output (Titanium)
Mass (kg)	1.40	1.08	1.38
First Natural Frequency (Hz)	36.7	73.3	63.0

The geometry obtained with aluminum material is 23% lighter in weight than the original design and first natural frequency of this geometry is 100% higher. Accompanied with these results, the targets set before the optimization were achieved. Final geometry was manufactured by SLM method and mounted on an antenna system. (Figure 2)



Figure 2. Original Design (far left) Final Geometry (left and right), Antenna Assembly (far right).

4. CONCLUSIONS

In this study, it was concluded that the structure obtained as a result of topology optimization in terms of mechanical behavior, control-stabilization and weight criteria and manufactured by metal additive manufacturing methods, can be used in antenna pedestal systems. It can be interpreted that there is a shortening of assembly times by making the structure one-piece. At the same time, this structure does not have a cost disadvantage compared to the original structure, since the AlSi10Mg powder material is inexpensive and cost-effective. (Guo & Leu, 2013)

REFERENCES

Esen, E. (2021). Topology Optimization of Stabilized Antenna Platform for Additive Manufacturing. (Master's thesis) Istanbul Technical University.

Guo, N. & Leu, M. (2013). Additive manufacturing: Techology, applications and research needs. Frontiers of Mechanical Engineering. 8. https://doi.org/10.1007/s11465-013-0248-8

A NUMERICAL AND EXPERIMENTAL INVESTIGATION ON BUCKLING BEHAVIOR OF ADDITIVELY MANUFACTURED RIBBED CASINGS

Burak Sivri[1*], Emre Özeren[2], Barış Pehlivanoğulları[2], Ahmet Okudan[1], Ceren Çelebi Şen[2], Akın Orhangül[2], Kübra Nur Ulukaya[1], Utku Cemal Ünlü[1]
[1]*Numesys İleri Mühendislik A.Ş., burak.sivri@numesys.com.tr*
2TUSAS Engine Industries, Inc.

ABSTRACT

Laser Beam Powder Bed Fusion (LB-PBF) is an additive manufacturing technology that enables manufacturing of complex structures with the advantages such as design freedom and reduced machining needs. However, LB-PBF process is a thermomechanical process and the plastic deformations, and residual stresses that occur in the component may affect its geometrical stability. Buckling is, on the other hand, a type of failure mode for materials, also known as instability that leads thin materials to buckle under compressive loads. To have a more stable buckling behavior in gas turbine engine casings, ribbing structures are being used due to their high compression strength-to-weight ratio. With the advantages of LB-PBF process such as the ability to create complex ribs and reducing machining needs, it can be preferred to manufacture ribbed engine casings via LB-PBF method.

In this study, different ribbed engine casings with identical volumes are designed and plastic shape deformations, residual strains, and stresses caused by LB-PBF are inspected. Along with these studies, buckling and post-buckling simulations are performed on the designed and process simulation-derived casings including the residual strains and stresses, and compressive tests are physically carried out on manufactured parts in order to compare with simulation results.

Keywords: Laser beam powder bed fusion, process simulation, ribbing, buckling, post-buckling.

1. INTRODUCTION

The casings are thin-walled components of aero-engines, which require adequate stiffness and reduced weight. The casing is ought to have sufficient buckling behavior against the compression loads arising during operating conditions [1]. Ribbing structures are used on casing surfaces to improve buckling behavior and stiffness due to their high compression strength-to-weight ratio. Also, ribbing provides the ability to overcome vibration problems [2], enabling cooling and noise reduction, and it can be used as a mounting interface.

These structures are relatively complex structures that require long machining times if produced by conventional fabrication methods. Laser Beam Powder Bed Fusion (LB-PBF) is an additive manufacturing process with the ability to create complex three-dimensional (3D) structures via melting materials layer by layer on a build plate. With the ability to manufacture complex structures, it plays an important role in creating such parts. Ribbed casings can be efficiently manufactured via LB-PBF process without any machining needs. However, LB-PBF process is a thermomechanical process and it includes plastic shape deformation, residual strains, and stresses during and after the process. Therefore, in these conditions, thin-walled structures are relatively hard to be built in terms of achieving intended geometrical accuracy. In this regard, it is quite important to understand the process behavior before manufacturing to ensure good quality parts.

In this study, casings with the same volume that have different ribbing structures are designed and manufactured with LB-PBF process. LB-PBF process simulations are performed before production to understand the thermomechanical effects of the process on designed parts. Also, buckling and post-buckling of the casings are simulated to understand the effect of ribbing on thin parts. Simulation results are compared with buckling test results performed on the parts.

2. MATERIALS AND METHODS

In this study, different ribbed casings are designed as seen Figure 1. with Siemens NX software.

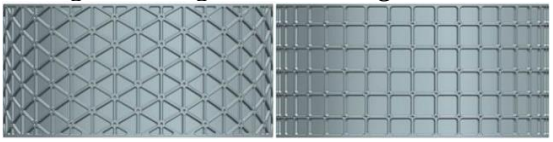

Figure 1. Casings with Isogrid and orthogrid ribbigs

LB-PBF process simulations are carried out using Ansys Additive Suite. Together with nominal CAD geometries, deformed ribbed casing geometry which is derived from process simulation is also used for buckling and post-buckling behavior. Ansys Mechanical is used for buckling and post-buckling analysis. Concept Laser M2 cusing S5 system is used as LB-PBF process and non-virgin Ti6Al4V ELI material is used as powder feedstock. Ribbed casings are heat-treated as annealing with a build plate according to AMS2801. Then, the casings are partially cut from the build plate surface by Charmilles Cut 300Sp W-EDM machine. The casings are geometrically inspected with CMM Laser scanning measurements using LK (Nikon) Altera 15.10.8 CMM 59” x 39” x 31” with LC15Dx. For compression tests, a compressive testing machine with a 1000 kN load capacity is used.

3. RESULTS AND DISCUSSION

By simulating the additive manufacturing and post-heat treatment processes of ribbed casings, 3D models with plastic deformation were obtained. Deformed casing models were analyzed dimensionally, shrinkage of up to 1 mm in diameter and plastic deformations varying along height were investigated. Critical load factors and post-buckling behavior of nominal and deformed frame models under 1000 kN compressive load were numerically compared. Preliminary FEA studies have shown that plastic deformations and internal stresses that occur in the manufacturing process need to be carefully reviewed as they can cause the part to fail sooner than expected, especially if the part is thin-walled and large-diameter. The produced orthogrid and isogrid ribbed casing geometries were forced to bend under pressure load and the maximum axial forces reached during the test were compared with the simulation outputs. As a result of the comparison of the first test results with the simulations made using the developed simulation methodology, it was seen that the critical buckling loads can be calculated with more than 90% accuracy. By comparing the outputs of the buckling simulations performed with nominal and deformed frame models with the test data, it is evaluated that the effect of plastic deformations and residual stresses due to AM on thin-walled structures such as frames can be understood more clearly and will shed light on future studies.

4. CONCLUSIONS

The study shows that thin-walled casings are manufactured efficiently via LB-PBF method. Besides, process simulation and understanding its effects on casings with ribbings is quite important to correctly define the buckling and post-buckling behavior of ribbed engine casings. The study also demonstrates that compressive test results are compatible with simulation results obtained from Ansys Additive and Ansys Mechanical.

REFERENCES

[1] Ananth, S. (2015). *Stability analysis of additively manufactured isogrid* (Master’s thesis). Retrieved from https://etd.ohiolink.edu/.

[2] Senthil kumar, K. K., Sharath, R., Manjunatha Babu, N. S., Mohan Kumar, K. and Nazar, P. (2019). *Structural design analysis of bypass casing for an aero engine.* International Research Journal of Engineering and Technology

A STUDY OF DIFFERENT TOOL PATH STRATEGIES FOR LASER METAL DEPOSITION PROCESS

Omer Faruk Yazici[1], Talha Muslim[2], Taner Karagoz[3], Oguzhan Yilmaz[4], Recep Ozkok[5], Metin Calli[6], Alperen Bayram[7], Orkun Tekelioglu[8]

[1] *Coşkunöz Holding R&D Center, ofyazici@coskunoz.com.tr*
[2] *Coşkunöz Holding R&D Center, tmuslim@coskunoz.com.tr*
[3] *Coşkunöz Holding R&D Center, TKARAGOZ@coskunoz.com.tr*
[4] *Advanced Manufacturing Technologies Research Group (AMTRG), Gazi University, oguzhanyilmaz@gazi.edu.tr*
[5] *Coşkunöz Holding R&D Center, rozkok@coskunoz.com.tr*
[6] *Coşkunöz Holding R&D Center, MCALLI@coskunoz.com.tr*
[7] *Coşkunöz Holding R&D Center, abayram@coskunoz.com.tr*
[8] *Coşkunöz Holding R&D Center, otekelioglu@coskunoz.com.tr*

ABSTRACT

Laser Metal Deposition (LMD) is an additive manufacturing process that is used to manufacture three-dimensional parts. To produce zero-defect parts, it is essential to minimize defects and maximize density. LMD involves the stacking of layers and has complex thermal history affecting the geometrical, metallurgical and mechanical properties. Tool path strategy directly impacts the thermal history affecting the density, microstructure, and stresses originating in the part during deposition. In literature, very few studies correlate the tool path strategies with density, hardness and final microstructure of the part. This study aims to understand in detail the effect of tool path strategies on the geometrical, metallurgical and mechanical properties. Five different 316L-Si stainless steel U shape geometries were deposited with varying tool paths using Erlaser hard + clad LMD system.

The deposits are still being analyzed for hardness, density, microstructure and presence of defects. The influence of different tool path geometries will be reported in detail in the full paper submission.

Keywords: Laser Metal Deposition, Tool path strategies, 316L-Si stainless steel, Microstructure, Density.

1. INTRODUCTION

Laser Metal Deposition (LMD) is an additive manufacturing process in which a laser beam creates a melt pool in which metal powder is fed and melted. A track forms as the heat source moves away. Depositing tracks side by side forms a layer which can be stacked to form a three dimensional part. The LMD systems can be programmed to deposit parts in a particular way also known as tool paths. The tool path strategies in LMD are the paths that the robot head follows to deposit a part. When adjacent tracks are deposited, there must be sufficient overlap to prevent empty voids to maximize the density of the part. Ribeiro et al. reported that tool paths significantly influence the microstructure and density in the LMD process. Defects such as porosity are very common in the LMD process. The pores may originate due to feedstock material, trapped shielding gas or unmelted powder particles, especially at the interface of two adjacent tracks or layers. Tool paths directly influence the thermal history of the part, which directly influences the microstructure and the final mechanical properties. A suitable tool path can help to minimize porosity, increase density, and reduce distortion and residual stresses. Ribeiro et al. mentioned that the best tool paths are those which minimize temperature gradient during deposition. To maintain a stable process, the thick and thin sections of the same part must be considered separately, especially for a part with complex geometry. More work is required to find optimal tool path strategies that can be used for different sections of the same part to maintain a stable process. In the present study, five different tool path strategies to build three dimensional U shape parts are studied and the effect on porosity, hardness and microstructure are investigated.

2. MATERIALS AND METHODS

ERLASER HARD + CLAD LMD system was used to deposit U shape coupons of dimension (52.5 mm x 51 mm x 10 mm). Gas atomized AISI 316L-Si stainless steel powder with the particle size distribution of 45 -106 microns was used. The laser spot diameter was fixed at 3.5mm. The same process parameters were used to deposit all coupons as shown in Table 1.

Table 1. Process Parameters used to deposit U shape coupons

Laser Power (W)	Scan Velocity (mm/s)	Powder flow rate (Revolution/minute)	Shield Gas (Argon) flow rate (L/min)	Carrier Gas (Argon) flow rate (L/min)
1500	8	4	8	8

Figure 1 shows the different tool path strategies used and some of the deposited U shape coupons.

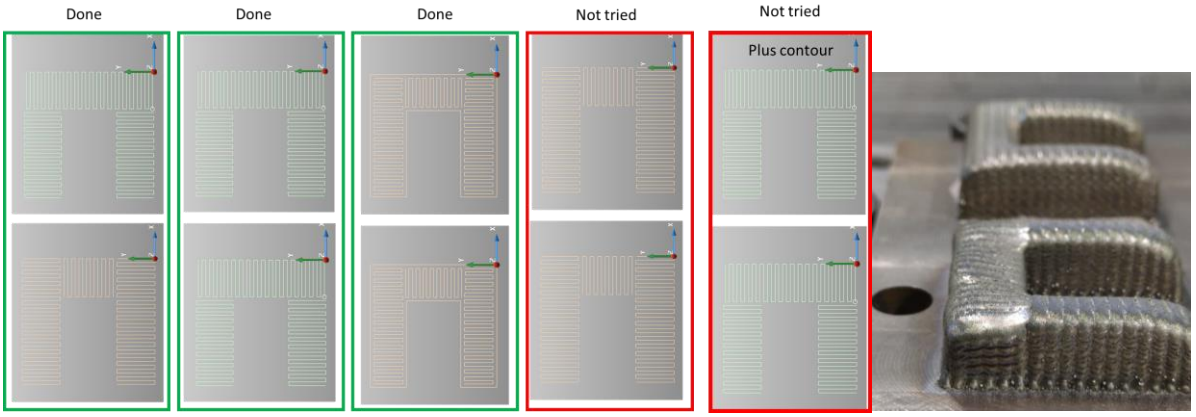

Figure 1. Five different tool path strategies (alternating layers) used and U shape coupons

For the individual track in all coupons, an X increment of 1.5 mm and Z increment of 1 mm were used. All samples will be machined and the Archimedes test will be performed to find the density for each coupon. The density will give an idea of volumetric porosity in each coupon. Vickers hardness (HV) will be measured on 5 equidistant points at the centre of each side of the U shaped coupons. The hardness will be averaged out and compared. It must be noted that higher hardness is expected near the substrate due to the heat sink effect. For each individual U shape, small sections from different regions will be cut and prepared for metallographic analysis.

3. RESULTS AND DISCUSSION

The authors want to bring to the attention of the reviewers that we have deposited the U shape coupons however analysis of the coupons will be done. The samples will be cut and microstructure, hardness, density and presence of defects will be compared for different scan strategies and will be reported in the full paper.

4. CONCLUSIONS

The deposits are still being analyzed for hardness, density, microstructure and presence of defects. The influence of different tool path geometries will be reported in detail in the full paper submission.

REFERENCES

Ribeiro, K. S., Mariani, F. E., & Coelho, R. T. (2020). A Study of Different Deposition Strategies in Direct Energy Deposition (DED) Processes. Procedia Manufacturing, 48, 663–670. https://doi.org/10.1016/j.promfg.2020.05.158

ADDITIVE MANUFACTURING OF CLINICAL PRACTICE TRAINING MODELS USED IN MEDICINE AND DENTISTRY

Osman Tunç[1], Halit Yosunçığır[2]
[1]*Trabtech, osman.tunc@trabtech.co*
[2]*Trabtech, halit.yosuncigir@btech.com.tr*

ABSTRACT

The study mentioned in this article aims to investigate the role of three-dimensional anatomical models in clinical education. Considering the study plan, the training models that the users need for learning and experience applications in the education processes of medicine and dentistry were determined as the first task. After that, DICOM data digital anatomical data files, namely STL files, were obtained from appropriate CT/CBCT/MRI radiological images. Educational models were produced by using an SLA 3D printer. Radiological images were segmented from special images related to image processing methods and 3D printed with specific materials for application in clinical training within the scope of these findings. On the training model developed within the scope of this work, a patient-specific clinical training phantom model has been made. Repetition of clinical training on 3D-printed physical models specific to the scenario has removed the physical constraints for surgical training. As a result of this work, dependence on high-cost foreign phantom models has decreased. The advantages of the study are that it can reduce operator-dependent variables, shorten the operation time, reduce radiation exposure, and increase the success of the procedure, thanks to the patient-specific planning and application of the surgical procedure with three-dimensional models.

Keywords: Training Model, Medical Education, 3D Anatomical Modelling, 3D Printing, SLA

1. INTRODUCTION

The 3D training models have started to be used in digital applications as well as classical education in medicine and dentistry education, where the pandemic period has had a great impact. These applications have been actively used not only by students but also in the continuous training of doctors and dentists. In dentistry education, practising artificial teeth made of appropriate materials played an active role in the prevention of cross-infection, instead of working on teeth extracted from patients which are standard in preclinical training. It is aimed to standardize education by using the same model developed for different clinical scenarios in certain education groups and determined for each student. Since cadavers cannot be easily obtained in the field of neurosurgery in medical education, a neurovascular surgery model is required for craniotomy and clipping applications from certain anatomical points. Although endovascular embolization is a popular treatment option for MCA aneurysms, a surgical procedure with microsurgical clipping in this area is less risky. [1-2]. In this case-specific training model, the preoperative planning of the surgery and the rehearsal of the surgery were made.

2. MATERIALS AND METHODS

Imaging data including Computed Tomography(CT), Cone Beam Computed Tomography(CBCT), Magnetic Resonans Imaging(MRI) scans were used to reconstruct the patient-specific digital 3D model.

Mimics Innovation Suite 23.0 software (Materialise, Leuven, Belgium) was used for 3D anatomical

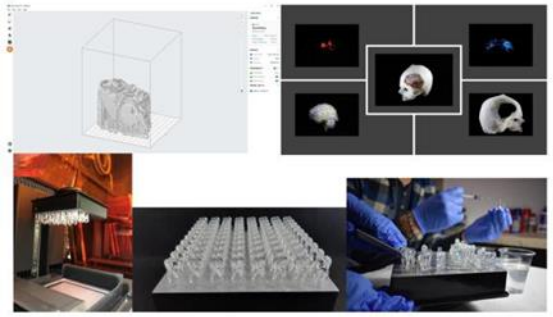

modelling and surgical planning. DICOM files were imported into Mimics. 2D radiological images were opened in axial, coronal and sagittal image projections. Masking was performed on 2D radiological images using Hounsfield Unit (HU) and Gray Value values. Segmentation of the structures was performed according to the anatomical boundaries. Design module 3-Matic 15.0 software (Materialise, Leuven, Belgium) was used for detailed anatomical modelling and surgical planning. All surgical scenario steps from pterional craniotomy to aneurysm clipping are modelled on the neurovasculargery training model. In the case of the endodontic education model, the canal and pulp models are plotted specifically for the case. For 3D printing production, texture models were exported in STL file format, and a production plan was made. Models were produced on the Formlabs Form 3 (Formlabs Inc., Massachusetts, USA) printer working with SLA (Stereolithography) technology, which is an additive manufacturing method in the production of the relevant models. For the production of the model of neurovascular surgery training, "durable" resin for bone tissue and "elastic" resin for brain hemisphere tissue and vascular structure were used. The endodontic education model is produced with a transparent"clear" resin so that the canal inside the tooth can be observed during the practice phase.

Figure 1. Production Phases

3. RESULTS AND DISCUSSION

Tissue-specific sequences of radiological data were determined. MRI T1 and T2 were used for brain hemisphere tissue, and contrast angiography CT and TOF sequence MRI data were used for the vascular structure. CT scanning was used to model the tooth and cranium structure. Shore value, which generally defines the hardness value of rubber, elastomer and polymers, was determined as <50 A for vascular structure and soft tissue, and 80 A for tooth and cranium hard tissue in this study. Students and clinicians who practice on 3D educational models have evaluated that these models are suitable, useful and practical for the anatomical structure. In addition, the domestic production of models reduces production costs and makes them more accessible.

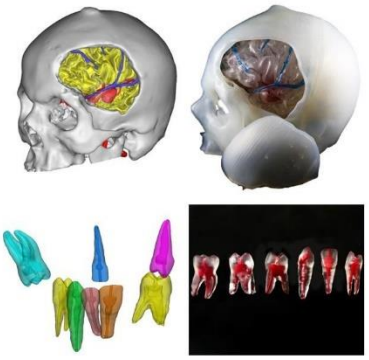

Figure 2. The Design and Additive Manufacturing of Samples for Each Training Model

4. CONCLUSIONS

Thanks to innovations in design and production technology, realistic educational resources have been created. Through this study, in medicine and dentistry education, pre-surgical planning and phantoms which surgical and treatment steps can be applied to the model contributed to the education of students and clinicians, and the need for cadaver and patient tissue was reduced.

REFERENCES

[1]Bakker, N. A., Metzemaekers, J. D. M., Groen, R. J. M., Mooij, J. J. A., & van Dijk, J. M. C. (2010). International subarachnoid aneurysm trial 2009: endovascular coiling of ruptured intracranial aneurysms has no significant advantage over neurosurgical clipping. Neurosurgery, 66(5), 961–962. https://doi.org/10.1227/01.NEU.0000368152.67151.73

[2]Molyneux, A. J., Kerr, R. S., Yu, L. M., Clarke, M., Sneade, M., Yarnold, J. A., & Sandercock, P. (2005). International subarachnoid aneurysm trial (ISAT) of neurosurgical clipping versus endovascular coiling in 2143 patients with ruptured intracranial aneurysms: a randomised comparison of effects on survival, dependency, seizures, rebleeding, subgroups, and aneurysm occlusion. Lancet (London, England), 366(9488), 809–817. https://doi.org/10.1016/S0140-6736(05)67214-5

ADDITIVE MANUFACTURING TECHNOLOGY CONFORMITY ASSESSMENT MODEL (TCA.M.) FOR AUTOMOTIVE APPLICATIONS

Zafer Çağatay Öter[1], Cenk Kılıçaslan[2*], Korhan Ondoğan[3], İlhan Yiğit Başar[4]
1Norm Additive, cagatay.oter@normadditive.com
*2Norm Additive, cenk.kilicaslan@normadditive.com, *Corresponding author*
3Norm Additive, korhan.ondogan@normadditive.com
4Norm Additive, yigit.basar@normadditive.com

ABSTRACT

Over the last decade, Additive Manufacturing (A.M.) has encountered vast adoption from aviation, defense, white goods and automotive industries as an innovative and sustainable low-volume mass production technology. There are a number of commercial A.M. technologies and systems developed for the fabrication of various metal, polymer and composite materials, and choosing the right technology is the foremost stage of the sector-oriented investment plan of any company. Several technology selection tools, guideline books etc. were already published. However, an accessible industry-specific method or tool that evaluates the systems released by equipment manufacturers in terms of technical specifications has not been developed yet. Organizations have to base their equipment selection on benchmarks provided by manufacturers, and choosing the wrong equipment in terms of technical specifications is where an organization could potentially suffer the most. Mathematical tools are most useful for solving complex multiple-criteria problems, involving a lot of human perceptions and judgments, whose decisions have a long-term impact. In this paper, a problem was created using the technical specifications provided by a number of A.M. equipment manufacturers, and a Technology Conformity Assessment Model (TCA.M.) was developed and applied to select the most suitable equipment for automotive industry applications, reducing the human factor and improving investment processes.

Keywords: Automotive Industry, Decision Making, Technology Analysis

1. INTRODUCTION

Unequalled freedom of design and the ability of mass customization resulted in the global prevalence of additive manufacturing technology over a wide range of applications in recent years (Khorasani, 2020). Currently, there are many commercial systems in the market that produce with various types and forms of raw materials, technologies and technical capacities (Bahnini, 2018). Determining the most suitable system for the needs of a particular industry is a complex process consisting a number of parameters as well as human judgement. This study offers an unbiased method that can be applied to all decision-making processes.

2. MATERIALS AND METHODS

A Technology Conformity Assessment Model (TCA.M.) was developed and applied to select the most suitable equipment for automotive industry applications, reducing the human factor and improving investment processes. Interviews were held with industry professionals in automotive companies and academics/researchers operating in the field of additive manufacturing, thus collecting information on raw materials, part properties, part dimensions, etc. demanded for actual industrial applications. In the light of this information, six different additive manufacturing machinery manufacturers were contacted, virtual tours and interviews were held with each manufacturer and technologies suitable for the sector's needs were determined. Brief information about these manufacturers is provided in Table 1. To select the most suitable machine, a TCA matrix was produced, evaluating a total of 68 technical and operational parameters grouped under 13 titles (raw materials, technical specs, print properties, occupational safety, sustainability, service, additional system needs and training opportunities etc.).

Table 1. Suppliers contacted within the scope of the evaluation study.

Supplier Name	Information	Country of Origin
Supplier 1	SLM system manufacturer	Germany
Supplier 2	SLM system manufacturer	Germany
Supplier 3	Metal Binder Jet system manufacturer	USA

Supplier 4	Metal Binder Jet system manufacturer	USA
Supplier 5	Metal Binder Jet system manufacturer	Sweden
Supplier 6	Metal FDM system manufacturer	USA

3. RESULTS AND DISCUSSION

5 technology conformity indicators (TCIs) were defined to ensure optimized decision making by taking into account all 68 parameters. These TCIs were Technical Specifications (TS), Market Range (MR), Business Model (BM), Technical Training (TT) and Partnership Potential (PP). Each individual TCI was associated with a score, calculated based on technical interviews and evaluations. In order to incorporate the practical information obtained from the interviews with sector professionals and researchers in the decision process, TCIs were also aggregated with their weighting factors. These weighting factors were calculated through the pairwise-comparison by the technical team depending on pre-defined priorities.

Table 2. Summary of technology conformity indicators, weighting factors and supplier scores.

	TCI							Overall Score					
TCI	**Priority**	**TS**	**MR**	**BM**	**TT**	**PP**	**WF**	**Supp. 1**	**Supp. 2**	**Supp. 3**	**Supp. 4**	**Supp. 5**	**Supp. 6**
TS	High		3	6	6	6	0.31	1.55	1.55	0.62	1.24	0.93	0.93
MR	High	3		6	6	6	0.31	1.55	1.55	0.93	1.24	0.93	0.93
BM	Mid	1	1		3	6	0.16	0.64	0.64	0.32	0.32	0.32	0.48
TT	Mid	1	1	3		6	0.16	0.80	0.80	0.16	0.64	0.64	0.64
PP	Low	1	1	1	1		0.06	0.30	0.18	0.06	0.24	0.24	0.24
Total Score								4.84	4.72	2.09	3.68	3.06	3.22

4. CONCLUSIONS

This study introduces a decision making problem, and suggests an unbiased method to determine the most suitable additive manufacturing system for actual automotive industry applications. 5 technology conformity indicators (TCIs) were defined to run an assessment by taking into account 68 different parameters. Supplier 1, an SLM system manufacturer based in Germany, was determined to be the most suitable choice with a score of 4.87/5.00.

REFERENCES

Bahnini, I., Rivette, M., Rechia, A., Siadat, A. & Elmesbahi, A. (2018). Additive manufacturing technology: the status, applications and prospects. The International Journal of Advanced Manufacturing Technology, 97, 147–161. doi:10.1007/s00170-018-1932-y

Khorasani, A.M., Gibson, I., Veetil, J., K. & Ghasemi, A. H. (2020). A review of technological improvements in laser-based powder bed fusion of metal printers. The International Journal of Advanced Manufacturing Technology, 108, 191–209. doi:10.1007/s00170-020-05361-3

AN ALGORITHM FOR POWDER CLEANING OF ADDITIVELY MANUFACTURED PARTS WITH INTERIOR CHANNELS

Alptuğ Öztaşkın[1], Ulaş Yaman[2]
[1]*AddPark İleri Mühendislik A.Ş., alptug.oztaskin@btech.com.tr*
[2]*Department of Mechanical Engineering, Middle East Technical University, uyaman@metu.edu.tr*

ABSTRACT

With the increasing adoption of Additive Manufacturing (AM) technologies, direct manufacturing of parts with complex interior geometries has become possible. However, for most of the Powder Bed (PB) approaches, powder removal is the bottleneck for manufacturability, it constitutes a design limit. Even on technologies like Selective Laser Melting (SLM), where the powder is not strictly adhered to the surface and gravity would be enough to clean the inner powder, complex channel structures made the cleaning by manual rotation virtually impossible. In this study, an algorithm is proposed to detect inner channels and exit points of a mesh file (of STL or OBJ format) and to form a graph of the inner channel structure. Furthermore, for each node on the graph, the shortest path to exit points is found, which allows the formation of a tree-type data structure. The algorithm is realized using Python programming language and the related libraries. Series of rotational motions (lists of angles and durations) that would allow total powder removal are obtained. Even though the skeleton generation and exit point detection take time, the algorithm is promising with some performance enhancements.

Keywords: Powder Based Additive Manufacturing, Powder Cleaning, Powder Cleaning Algorithm, Automated, Post Process

1. INTRODUCTION

One of the advantages of AM methods is the ability to produce complex inner structures. Of those structures, especially heat exchanger applications require intricate channels. However, regarding PB technologies, powder removal is an important post-processing operation. Even though the company Solukon offers such a machine that can depowder SLM parts[3], no detailed information is provided regarding their algorithmic approach. Moreover, no previous study is found in the literature related to powder removal algorithms. Therefore, using mostly open-source tools, a powder removal algorithm is developed in this study. The algorithm detects the inner channels of a part and generates a rotation series (an ordered list of angles and time separate motions) for each exit on a part. With the application of the given rotations, powder evacuation would be possible with the help of gravity.

2. MATERIALS AND METHODS

To achieve the targeted results, firstly convex hull of the input mesh is determined. Then, by Boolean subtraction of the input mesh, one or more meshes that corresponds to channel structures are isolated. The skeleton of the channel structure is obtained via Local Separators Method described by Bærentzen & Rotenberg [1]. Intersection points of the channel and the convex hull (of the original part) are obtained in order to define the channel exits. For each node on the skeleton, a line segment is formed for each exit point. By performing ray tracing on each line segment, and counting intersection number for each point, exit nodes on the skeleton are found. For each exit node, Dijkstra method [2] with weights is used to find the shortest path from any node to the exit node. Then, a spanning tree is formed from the graph using the shortest paths. The rotation series starts with the deepest leave (by weight rather than just node precedence) on the tree and descends towards the shallowest leaves that are closer to the root representing the exit node.

3. RESULTS AND DISCUSSION

In Figure 1, the spanning tree of a part is presented. By comparing it with Figure 2 one can notice that the spanning tree accurately gives the shortest distance to the exit node (at the bottom of the part in Figure 2).

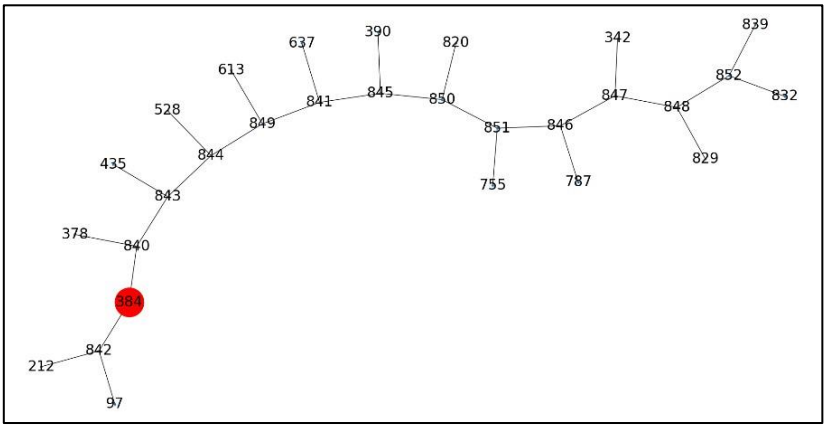

Figure 1. The Spanning Tree Acquired from a Golf Ball Injection Mold Part (Red point representing the exit node)

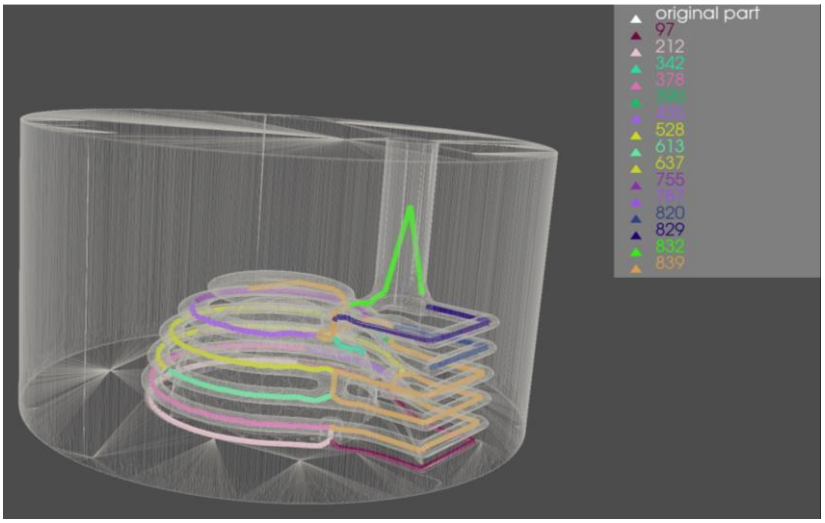

Figure 2. Representation of the Spanning Tree on the Channel Structure (Each color representing one leaf)

4. CONCLUSIONS

Through visual inspection, the spanning tree and the related solutions are validated, and the algorithm is available to be used on a physical device. However, throughout this study, it was assumed that the channels have a constant cross-section. In future works, cross-sections between consecutive nodes will be considered in a detailed manner and the algorithm will be updated accordingly. Such an improvement can be employed by performing a ray tracing perpendicular to each node edge. Moreover, modified multiple travelling salesman algorithms may be developed to evacuate powder from multiple exits on the same application.

REFERENCES

[1] Bærentzen, A., & Rotenberg, E. (2020). Skeletonization via Local Separators. ACM Transactions on Graphics, 40(5). https://doi.org/10.48550/arxiv.2007.03483
[2] Dijkstra, E. W. (1959). A note on two problems in connexion with graphs. Numerische Mathematik 1959 1:1, 1(1), 269–271. https://doi.org/10.1007/BF01386390
[3] Solukon Maschinenbau GmbH, (2022) Solukon Digital Factory Tool: Solukon launches a Sensor and Interface Kit for the Digital Thread and Quality Validation [Press release]

AN INVESTIGATION ON THE EFFECTS OF PROCESS PARAMETERS ON THE GEOMETRICAL CHARACTERISTICS OF LASER DEPOSITED SINGLE TRACKS USING PH 13-8 MO STAINLESS STEEL POWDER

Talha Muslim[1], Taner Karagoz[2], Omer Faruk Yazici[3], Oguzhan Yilmaz[4], Recep Ozkok[5], Metin Calli[6], Alperen Bayram[7], Orkun Tekelioglu[8]

[1] *Coşkunöz Holding R&D Center, tmuslim@coskunoz.com.tr*
[2] *Coşkunöz Holding R&D Center, TKARAGOZ@coskunoz.com.tr*
[3] *Coşkunöz Holding R&D Center, ofyazici@coskunoz.com.tr*
[4] *Advanced Manufacturing Technologies Research Group (AMTRG), Gazi University, oguzhanyilmaz@gazi.edu.tr*
[5] *Coşkunöz Holding R&D Center, rozkok@coskunoz.com.tr*
[6] *Coşkunöz Holding R&D Center, MCALLI@coskunoz.com.tr*
[7] *Coşkunöz Holding R&D Center, abayram@coskunoz.com.tr*
[8] *Coşkunöz Holding R&D Center, otekelioglu@coskunoz.com.tr*

ABSTRACT

Laser Metal Deposition (LMD) is a well-known Additive Manufacturing method used to manufacture parts, coating applications to enhance surface properties of high value parts, add features on already existing parts, repair applications and to manufacture functionally graded parts. The single bead geometry and melt pool penetration depth below the substrate that is the portion of the substrate that melts and gets mixed with the deposited material significantly influence the final mechanical properties of the part. It is therefore necessary to select and control LMD process parameters in order to obtain single bead tracks with the optimum geometry. This study investigates the effect of process parameters on the geometry of single bead tracks using PH 13-8 MO stainless steel powder. This study shows that the process parameters can be effectively controlled to achieve the required outcome.

Keywords: Laser metal deposition, PH 13–8Mo stainless steel, Process parameter, Single bead track geometry

1. INTRODUCTION

Additive Manufacturing (AM) refers to a group of technologies that can be used to manufacture complex 3D parts directly from the Computer-aided design (CAD) data. Laser metal deposition (LMD) is a metal AM process. A focused laser beam melts the substrate and creates a melt pool. The powder is fed into the melt pool and melts. As the heat source moves away, the melt solidifies to form a track. Tracks can be deposited side by side to form a layer which can be stacked to manufacture a 3D part. Sun et al. mentioned that different combinations of process parameters have different effects on the track geometries, and metallurgical/mechanical properties (hardness, surface roughness, and microstructure). PH 13-8 Mo stainless steel is a precipitate hardening material that is difficult to process conventionally and is very suitable to be processed via LMD. Very few studies investigate how precipitate hardening stainless steels (PHSS) can be effectively processed via LMD. Therefore the current study was performed to understand the influence of critical LMD process parameters on the single bead track geometries deposited using PH 13-8 Mo stainless steel. Tracks are the building blocks of a laser deposited part, therefore it is necessary to understand how track geometry is affected as process parameters are varied.

2. MATERIALS AND METHODS

ERLASER HARD + CLAD laser cladding system was used in this experiment. The system consists of an industrial robot used as a manipulator. A fibre coupled laser is used as a heat source. Gas atomized PH 13-8 Mo stainless steel powder was used as feedstock material with the particle size distribution of 45-106 microns. Argon was used as shielding gas. AISI 1050 stainless steel substrate was used with the dimensions of 300mm x150mm x 20mm. Unidirectional 60 mm long single bead tracks were deposited. Laser power (W), scan velocity (mm/s), and powder feed rate (rev/min) were varied and all other process parameters remained unchanged. Table 1 shows the range of process parameters used.

Table 1. Process Parameter ranges used in experimental trials

Parameter	Range
Laser Power (W)	1200, 1300, 1400, 1500
Scan Velocity (mm/s)	7, 8, 9, 10
Powder flow rate (Rev/min)	3, 3.5, 4, 4.5
Gas flow rate (L/min)	8

Spot diameter (mm)	3.5

3. RESULTS AND DISCUSSION

Track height and width increase with ED. Lee et al. reported that the heat input increases with ED. More powder gets melted therefore the height increases. The heat influences the melt pool shape and size increasing the width as well as shown in Figure 2.

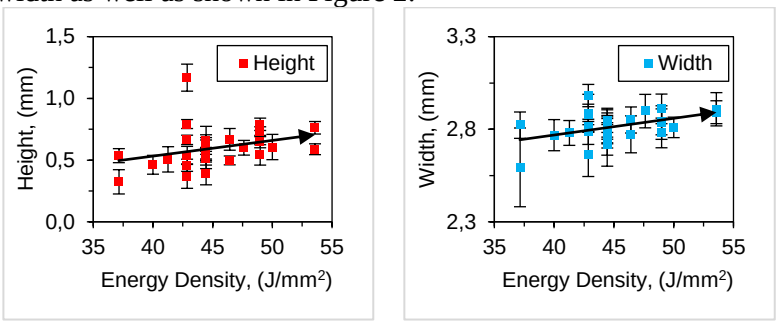

(a) (b)

Figure 2. Effect of energy density on (a) height, (b) width.

Melt pool penetration depth below the substrate increases with ED because more heat gets transmitted into the substrate. The width to height ratio decreases along with ED. This may be explained by the fact the increase in height is relatively more than the increase in width as ED increases. Track height and width also increase with PFD. This is because as more powder gets delivered in the melt pool region, more powder gets melted resulting in increased height and width. The melt pool penetration depth below the substrate reduces ith increasing PFD. This is because as PFD increases, relatively more powder interacts with the laser beam mid-air. This reduces the heat incident on the substrate resulting in the reduction of the melt pool depth.

4. CONCLUSIONS

The track height and width increase along with ED and PFD due to the availability of additional energy and powder particles per unit area. Melt pool penetration depth increases along with ED and decreases along with PFD. In future work, different models (physics-based, machine learning and mathematical) will be generated to predict the single track geometry without doing expensive experimental trials.

REFERENCES

Lee, E. M., Shin, G. Y., Yoon, H. S., & Shim, D. S. (2017). Study of the effects of process parameters on deposited single track of M4 powder based direct energy deposition. Journal of Mechanical Science and Technology, 31(7), 3411–3418. https://doi.org/10.1007/s12206-017-0239-5

Sun, Y., & Hao, M. (2012). Statistical analysis and optimization of process parameters in Ti6Al4V laser cladding using Nd:YAG laser. Optics and Lasers in Engineering, 50(7), 985–995. https://doi.org/10.1016/j.optlaseng.2012.01.018

ANALYSIS OF THE FORCES AND VIBRATIONS ACTING ON THE CUTTING TOOL IN THE MICRO-DRILLING PROCESS OF TI6AL4V MATERIAL PRODUCED THROUGH EBM METHOD

Barkın BAKIR[1], Murat ŞEN[2], Sertaç ACER[3]
[1]*Marmara University, Engineering Faculty, İstanbul / Turkey*
[2]*Marmara University, Engineering Faculty, İstanbul / Turkey*
[3]*Marmara University, Institute of Pure and Applied Sciences, İstanbul / Turkey*

ABSTRACT

Thanks to its multiple usage areas, Ti6Al4V alloy is a highly preferred and researched material. Recently, with the development of additive manufacturing technologies, studies on this alloy have intensified. Additive manufacturing has recently become a very important alternative for designs which cannot be manufactured by traditional methods. Work pieces produced by additive manufacturing cannot be used directly in the areas of use. Because they may not have the desired features directly. Generally, various machining processes are applied after additive manufacturing. The most used of these processes are turning, milling and drilling. There are many reference studies on the processes on the parts produced with traditional methods. However, since the materials produced by additive manufacturing have different properties, they should be examined separately. In machining, cutting parameters, surface quality, tool life, labor costs, energy costs, geometric tolerances, etc. have a direct impact on many details. Micro hole drilling is used in special fields (aerospace, defence, automotive, medical). It is also a process that needs to be worked very carefully. Micro drills can break easily because they have very small diameters. In this study, cutting forces and vibration affecting tool life and quality were investigated. Ti6Al4V alloy produced with EBM was used in the study. Three different diameters (0.3mm, 0.4mm, 0.5mm) of micro drills were tested at different feed rates and different speeds in dry cutting conditions. A 3-axis high-precision CNC workstation was used in the studies.

Keywords: Ti6Al4V, EBM, Micro Drilling, Vibration, Additive Manufacturing, Cutting Forces

1. INTRODUCTION

Additive manufacturing (AM) is becoming more common day by day due to the advantages it provides [1], [2], [3]. Some of these advantages include freedom of design, no need for fixtures, avoidance of waste and an excellent alternative for prototyping. Selective laser melting method (SLM) and electron beam melting method (EBM) are among the most preferred additive manufacturing methods in metal additive manufacturing. Titanium alloys are highly preferred in areas such as aerospace, defense industry and automotive, thanks to their high strength in tough conditions. It is also widely used in the medical field, thanks to its compatibility with the human body. Therefore Titanium alloys are the most studied materials in additive manufacturing field [4]. Titanium alloys are both light and durable materials and Ti6Al4V alloy is generally used in cockpit, accelerator, wings and engine in aviation. Titanium alloys are highly preferred in the medical field, especially since they do not react with the body [5]. Thanks to the micro holes, assembly operations can be done. It is difficult to produce complex designs with conventional methods, and machining hard materials such as Titanium alloys makes the process even more difficult. Although additive manufacturing has many advantages, it is difficult to use the parts produced by additive manufacturing directly. The parts produced by additive manufacturing undergo processes such as turning, milling, drilling, polishing and grinding to provide the desired properties. Microholes are used in pressurized fluid passages and especially in implants. Drilling is one of the post-processing processes after additive manufacturing, like other machining processes. Two major factors affecting the life of the drill and the quality of the hole are cutting force and vibration. In this study, micro holes were drilled under dry cutting conditions to find suitable micro hole drilling parameters with a carbide drill. There are many post processing studies after additive manufacturing in the literature, but studies on micro hole drilling are limited [6]. Drilling holes of the appropriate quality in materials produced by additive manufacturing is one of the biggest challenges facing industries [7]. Drilling studies larger than micro size are more common in the literature. In a study, the surface quality and geometric dimensions of the hole in the titanium alloy produced by additive manufacturing were investigated [8]. In another study, the surface quality of the hole was analyzed and noted that feed rate is significant [9]. Yusuf Kaynak and his team mate have studied drilling process in additively manufactured Inconel 718. They worked on hole quality, micro structure and surface roughness. They explored that increasing feed rate provides quality surface and micro hardness [7]. In another study, micro-drilling study of Titanium alloy produced by DMLS method was carried out [10]. As a result of

the research, it was determined that the amount of burr at the exit is higher than the amount of burr at the entrance [10]. In his study, Dang investigated the cutting forces of Ti-6Al-4V alloy produced by DMLS method under dry drilling conditions. He found that as the feed rate decreases, the cutting forces decrease [11]. The highest machining temperature was observed at 0.12 mm/rev feed rate and 1500 rev/mm cutting speed and hence it was concluded that the higher production can be achieved at a higher cutting speed and feed rate [11]. In another study, chip morphology of Ti6Al4V alloy produced by additive manufacturing was investigated under dry drilling conditions [6]. The chip emerging in the drilling process directly affects the surface quality and tool life. As a result of the research, it was seen that the chip morphology changed as the cutting speed changed [6]. In the studies, generally subjects such as materials, drill diameters, surface quality, geometric position tolerances, cutting conditions, drill coatings, cutting speed, feed rate and depth of cut were studied. Ti6Al4V alloy is used in very critical areas and is becoming widespread. In the field of metal additive manufacturing, it is one of the most used materials together with Inconel. Machining works on parts produced with traditional methods have been done since the past and are very common. There are structural differences between materials produced by traditional methods and materials produced by additive manufacturing. Therefore, it should be examined how the materials produced by additive manufacturing will behave in machining. Appropriate parameters must be found. Such analysis studies that have been done or will be made will contribute greatly to research and development studies. Micro hole drilling is also normally a difficult process. In a hard material such as Ti6Al4V, the conditions become a little more difficult. Micro-sized drills are more fragile than normal. There are many factors that affect the quality of the hole and the cutting tool. These factors are coolant, cutting speed, drill coating, feed rate, speed, etc. are factors. Vibration and shear forces were analysed in this study. It has been determined which factors should be used in which diameters.

REFERENCES

Karunakaran, K., et al., Low cost integration of additive and subtractive processes for hybrid layered manufacturing. Robotics and Computer-Integrated Manufacturing, 2010. 26(5): p. 490-499.

Shamsaei, N., et al., An overview of Direct Laser Deposition for additive manufacturing; Part II: Mechanical behavior, process parameter optimization and control. Additive Manufacturing, 2015. 8: p. 12-35.

Bartolo, P., et al., Biomedical production of implants by additive electro-chemical and physical processes. CIRP annals, 2012. 61(2): p. 635-655.

Trosch, T., et al., Microstructure and mechanical properties of selective laser melted Inconel 718 compared to forging and casting. Materials letters, 2016. 164: p. 428-431.

Rong, T. and D. Gu, Formation of novel graded interface and its function on mechanical properties of WC1− x reinforced Inconel 718 composites processed by selective laser melting. Journal of Alloys and Compounds, 2016. 680: p. 333-342.

Ming, W., et al., Chip formation and hole quality in dry drilling additive manufactured Ti6Al4V. Materials and Manufacturing Processes, 2020. 35(1): p. 43-51.

Karabulut, Y. and Y. Kaynak, Drilling process and resulting surface properties of Inconel 718 alloy fabricated by Selective Laser Melting Additive Manufacturing. Procedia CIRP, 2020. 87: p. 355-359.

Ilčík, J., D. Koutný, and D. Paloušek, Geometrical accuracy of the metal parts produced by selective laser melting: Initial tests, in Modern Methods of Construction Design. 2014, Springer. p. 573-582.

Vandenbroucke, B. and J.P. Kruth, Selective laser melting of biocompatible metals for rapid manufacturing of medical parts. Rapid Prototyping Journal, 2007.

Rysava, Z., et al., Micro-drilling and threading of the Ti6Al4 v titanium alloy produced through additive manufacturing. Procedia CIRP, 2016. 46: p. 583-586.

Dang, J., et al., Experimental investigation on machinability of DMLS Ti6Al4V under dry drilling process. Materials and Manufacturing Processes, 2019. 34(7): p. 749-758.

ANGLE DEPENDENT PRODUCTIVITY RESEARCH OF CONFORMAL CHANNEL GEOMETRY SECTION IN LPBF

Mustafa Safa Yılmaz[1], Cemal İrfan Çalışkan[2], Gökhan Özer[3]
[1] *Fatih Sultan Mehmet Vakif University, Aluminium Test, Training, and Research Center (ALUTEAM), TR 34445, Halic Campus, Beyoglu, Istanbul, Turkey, msyilmaz@fsm.edu.tr,*
[2] *FSMVU, ALUTEAM, cicaliskan@fsm.edu.tr,*
[3] *FSMVU, ALUTEAM, gozer@fsm.edu.tr.*

ABSTRACT

It is known that channel orientation at different angles is a necessity in CCC design strategies developed by focusing on regions exposed to intense heat in molds. In the design studies carried out in this area, it is seen that the channel geometries produced without support in LPBF (laser powder bed fusion) production systems complete the geometry by being oriented at 90°, 180°, 45° and intermediate angles throughout the entire channel geometry. Within the scope of this study, which will not affect the efficiency of the duct geometry in terms of overall flow in CCC applications, and ideal positioning where the sagging problem in the duct cross-section is minimal, and suggestions on duct design, duct section productions in cylindrical and pentagonal forms at different scales and angles, then laboratory work and SEM examination constitute the general content of the study.

Keywords: Conformal cooling channels (CCC), Laser powder bed fusion (LPBF), Design for additive manufacturing (DFAM), Maraging Steel (MS1).

1. INTRODUCTION

The subject of cooling channels, which cannot be produced with traditional production methods and designed in accordance with the mold form, is a research topic that is being discussed more and more every day as an important advantage of AM technologies. In studies with mostly metal materials, manufacturability (Çalışkan, Özer, Coşkun, & Koç, 2021), design capability (Tan et al., 2020), material properties (Sanaei & Fatemi, 2020), shortening the thermal cycle time (Çalışkan, Özer, Koç, et al., 2021) some CCC studies can be mentioned. Within the scope of this research, the evaluation of the orientation of conformal channels in the geometries following the mold form at different angles and their position on the production platform within the scope of manufacturability is discussed. In this context, the pentagonal channel geometry (Çalışkan, Coşkun, Özer, et al., 2021), which stands out in terms of flow efficiency in previous studies, and the cylindrical geometry preferred in general CCC applications, the sections produced at different scales and angles are compared with different position effects on the production platform. are considered. In this context, the geometry of the channel section, which continues along the mold length, was examined within the scope of three angles and X-Y positioning, and some suggestions were presented.

2. MATERIALS AND METHODS

In the study, MS1 (maraging steel) material with integrated conformal cooling channels and DMSL (direct metal laser sintering) from LPBF systems were used in the production of test samples. The cylindrical and pentagonal forms of the test specimens shared in Figure 1b were studied with three different angles of the channel geometry in four different sizes. In the research; The sagging state of the upper section of the channel formed by the downskin parameter in the channels was examined.

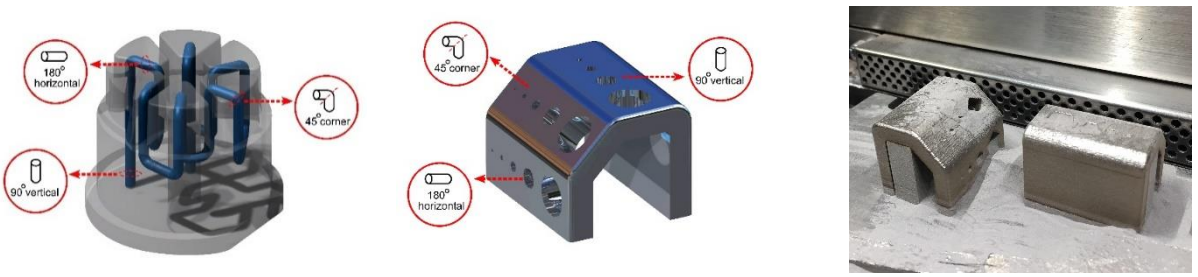

a *b* *c*

Figure 1. *a.* CCC integrated mold insert (Çalışkan, Özer, Koç, et al., 2021) and channel positioning graphic used in the automotive industry, b. Test sample and hole positioning graphic produced within the scope of the study, c. Test samples production positioning.

3. CONCLUSIONS

- According to to the results of the laboratory work done on the test samples produced;
- Channel geometry can be produced with different sensitivity values in different angles and planes in molds with CCC integrated.
- The manufacturability of the duct sections and the sagging rates in the downskin area vary in different planes and angles.
- In 180° and angled channel geometries where the sagging ratio is higher, it is recommended to divide the CAD data and apply a different process parameter to that region in order to increase the cross-section quality.
- In the evaluation of the cooling channel position and angle, the direction with the channel density throughout the mold or the channel direction in the region where the cooling sensitivity is intense can be positioned on the LPBF production system table 90° in terms of cross-section quality, so that more precise production can be achieved.

REFERENCES

Çalışkan, C. İ., Coşkun, M., Özer, G., Koç, E., Vurkır, T. A., & Yöndem, G. (2021). Investigation of manufacturability and efficiency of micro channels with different geometries produced by direct metal laser sintering. *The International Journal of Advanced Manufacturing Technology*, 1–13.

Çalışkan, C. İ., Özer, G., Coşkun, M., & Koç, E. (2021). Investigation of direct metal laser sintering downskin parameters' sagging effect on microchannels. *The International Journal of Advanced Manufacturing Technology*, *114*(9), 2567–2575.

Çalışkan, C. İ., Özer, G., Koç, E., Sarıtaş, U. S., Yıldız, C. F., & Çiçek, Ö. Y. (2021). Efficiency Research of Conformal Channel Geometries Produced by Additive Manufacturing in Plastic Injection Mold Cores (Inserts) Used in Automotive Industry. *3D Printing and Additive Manufacturing*.

Sanaei, N., & Fatemi, A. (2020). Analysis of the effect of surface roughness on fatigue performance of powder bed fusion additive manufactured metals. *Theoretical and Applied Fracture Mechanics*, *108*, 102638.

Tan, C., Wang, D., Ma, W., Chen, Y., Chen, S., Yang, Y., & Zhou, K. (2020). Design and additive manufacturing of novel conformal cooling molds. *Materials and Design*, *196*(September), 109147. https://doi.org/10.1016/j.matdes.2020.109147

ASSESSMENT OF THE MECHANICAL AND CORROSION PROPERTIES OF ALSI10MG PARTS PRODUCED THROUGH SELECTIVE LASER MELTING (SLM) AFTER VARIOUS POST PROCESSING CONDITIONS

Güler Deniz SERTTAŞ[1], Mehmet Emre ŞENSES[2], İpek KANDEMİR[3], Ömer Faruk KOCAOĞLU[4]
[1]*Alp Aviation, gdserttas@alp.com.tr*
[2]*Alp Aviation, mesenses@alp.com.tr*
[3]*Tübitak Sage, ipek.bayraktar@tubitak.gov.tr*
[4]*digiMODE, omer@digi-mode.com.tr*

ABSTRACT

In this paper, investigation of mechanical and corrosion properties of was carried out on AlSi10Mg components produced with SLM technique, results different microstructures and mechanical properties, that are undergoing various post-processing conditions such as hot isostatic pressing (HIP), T6 heat treatment, shot peening, anodizing and alodining. For comparison, the same examination was also performed on samples of non machined AlSi10Mg alloy without any post-processing. HIP treatment consists of the application of heating to 520 °C and applying 1000 bar of pressure in inert gas atmosphere while maintaining the temperature and pressure for 120 minutes. A two-stage T6 heat treatment included solid solution at 535 ºC and artificial aging at 158 ºC for 10 h. Shot peen proceed according to AMS 2430, anodizing is done in accordance with MIL-A-8625, Type I and type II, and alodining is carried on AMS-C-5541 Class 1A. The process tensile specimens, designed according to ASTM standard, were printed and tensile tests were carried out. The results obtained showed that differences can be outlined among the samples at different post processing conditions. Corrosion test is performed on ASTM B117 on all specimens which is produced with SLM. The results of this study is to provide informations into the control of corrosion protection and mechanical evaulation of AlSi10Mg alloy by adressing suitable post processes.

Keywords: Additive manufacturing, Selective laser melting, AlSi10Mg, Mechanical properties, Corrosion resistance

1. INTRODUCTION

Additive manufacturing technologies are gaining incredibly interest over the last years thanks to the several advantages. Particularly, selective laser melting (SLM) is a metal additive manufacturing technique that engaging interest for various industrial applications including aerospace and defence industries. Despite the clear advantages related to this technique, there are some issues focus on the components qualification, that still inhibit a extensive industrial application of SLM. Qualification and certification of the parts manufactured through SLM for aero structural applications requires an complete understanding of the relation within this technique in terms of microstructural, thermal, tensile, fatigue and corrosion performance. This requires the application of customized post processings to improve the quality of SLM fabricated AlSi10Mg components. The present contribution, being aimed at SLM applications for the aerospace sector, deals with the AlSi10Mg alloy, the most convenient and studied Al-alloy, produced with an industrial grade SLM system operated by a worldwide known established AM service provider in the sector. The overall objective is the determination of the link between the as-fabricated and various post processing conditions by examining microstructures, corrosion resistance and mechanical properties.

2. MATERIALS AND METHODS

The raw material for powder to be used in selective laser melting process is AlSi10Mg powder shall be as specified, chemical composition has been shown in Table 1, supplied by SLM Solutions. The featured particles were spherical shape with particle diameters in the range of 20~63 µm.

Table 1. Chemical composition [Mass fraction in %]

Alloy Designation	Si	Fe	Cu	Mn	Mg	Zn	Ti	Ni	Pb	Sn	Other Total
AlSi10Mg	9 - 11	0.55	0.05	0.45	0.20-0.45	0.10	0.15	0.05	0.05	0.05	0.15

The mechanical test samples were printed according to ASTM standard [1] for general tensile test with the process parameters suggested by the manufacturer. Tensile test specimens were printed in two building directions. These angles were chosen considering the affect of the building directions on

mechanical properties. Principally, the building directions chosen respect to the position of the building plate and the specimens manufactured horizantally and vertically. For the 2 specimen from different building direction specimens undergo HIP treatment consists of the application of heating to 520 °C and applying 1000 bar of pressure in inert gas atmosphere while maintaining the temperature and pressure for 120 minutes. Subsequently, a two-stage T6 heat treatment included solid solution at 535 ºC and artificial aging at 158 ºC for 10 h. Also, to determine the affect of shot peening on mechanical properties, shot peen proceed according to AMS 2430. Further, several selective laser melting specimens exposed in a standardized corrosive environment subjected to a salt spray test according to ASTM B117 used to produce relative corrosion resistance information. Furthermore, to investigate the affect of various post processing on the microstructure of the specimens, the microstructural examination is employed via optically (OM), samples mechanically polished and etched using Keller's solution which contains following contents and together with their amounts (Distilled water H_2O 190 ml, Nitric acid HNO_3 5 ml, Hydrochloric acid HCl 3 ml, Hydrofluoric acid HF 2 ml).

3. RESULTS AND DISCUSSION

The stress vs strain curves obtained and the yield strength (YS), the ultimate tensile strength (UTS), elongation and reduction of area (R. of A.) to fracture are determined in tensile tests for the horizontally manufactured and vertically manufactured orientation samples in the T6 and HIPped conditions. It is clearly appear that the high thermal gradients that are inherently exists in the SLM process cause a lot of residual stresses in the fabricated specimens. If these stresses are not relieved, it could get distorted and become dimensionally inaccurate. So, aforementioned post processes are very crucial for the qualification and reliability of the such fabricated parts. Also, it is known that corrosion weakens the structural integrity and reliability of the parts in an aircraft can lead to significant safety hazards. So, protective coatings are a very efficient way to minimize the corrosion, by limiting the exposure of the metal to a corrosive environment. For this purpose, for selective laser melting fabricated components it should be well known how these parts exposed to a corrosion and their resistance. Additionally selective laser melting fabricated parts may demonstrate distinctive microstructures after numerous post processes. A microstructure it can be seen in Figure 1, which at fabricated condition.

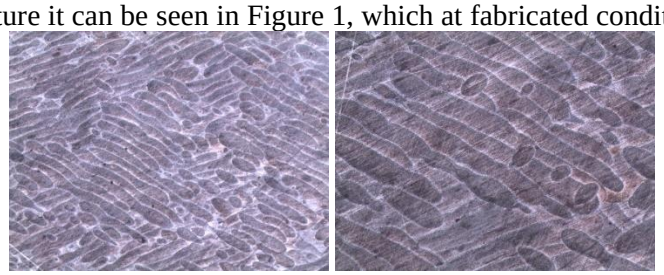

Figure 1. Microstructure of selective laser melting AlSi10Mg specimen at as fabricated condition, examined with optical microscope at 25x and 50x magnifications.

4. CONCLUSIONS

In this work, the influence of the building direction and the affect of the post processing treatments on the mechanical properties are obtained with the results shown. Specimens in the as-built (AB), HIPped (HP), HIPped and heat-treated (HP + HT), and shot peened (SP) conditions were considered. The mechanical properties are enhanced by the post processes. Also, it is seen that coated specimens shows better corrosion resistance compared to as fabricated conditions. This is primarily due to the comparatively large amounts of cavities and other surface defects that were formed at the external surface of the selective laser melting part as a result of the production process.

REFERENCES

[1] ASTM E8/E8M-16a standard test methods for tension testing of metallic materials. ASMI

BINDER JETTING OF PURE COPPER PARTS AND THEIR CHARACTERIZATION

Diego Comi[1,2], Ali Gokhan Demir[1], Baris Kirim[2], Emrecan Soylemez[2*]
[1] *Department of Mechanical Engineering, Istanbul Technical University, Istanbul, TÜRKİYE*
[2] *Department of Mechanical Engineering, Politecnico di Milano, Milano, ITALY*
* *esoylemez@itu.edu.tr*

ABSTRACT

Complex designs enabled by metal additive manufacturing can strongly improve the pure copper parts performance. Only a few studies, however, assess the additively manufactured pure copper parts. Here, we focus on binder jetting additive manufacturing process to characterize the part densities, mechanical strength, thermal conductivity, and electrical conductivity. Two differently sized powder printed at two different layer thicknesses and sintered in different regimes to optimize the process. Results provide the pure copper material property that gives an insight into designing complex copper parts with binder jetting.

Keywords: copper additive manufacturing, binder jetting, copper sintering

1. INTRODUCTION

Pure copper is one of the highest thermally and electrically conductive material with high corrosion resistance. It is commonly used in heat management applications. Complex designs need to be enabled where the material performance reaches its limit. Therefore, metal additive manufacturing (AM) researchers has been working on to optimize the copper printing process to benefit from the full capacity of the copper conductivity properties (Jiang et al., 2021). Arguably, the most common metal AM process is laser powder bed fusion (LPBF) because it gives the high resolution, fine surface roughness, and above 99% density of the metal parts. However, copper is a challenging material for LPBF. The wavelength of the fiber laser commonly used in the conventional LPBF machines is reflected up to 98% from the copper surface. Moreover, the high thermal conductivity of copper leads to an unstable melt pool. Hence, LPBF of Cu is a highly demanding task resulting in a relatively more cumbersome process (Colopi, Demir, Caprio, & Previtali, 2019). Concerning another powder bed fusion process, the electron beam melting, the high optical reflectivity is no more an issue. Instead, the high thermal dissipation and high electrical conductivity of the material make the process control difficult and result in density variations in the parts and low surface roughness (Tran et al., 2019). An alternative metal additive manufacturing to fusion processes is binder jetting additive manufacturing (BJAM). In binder jetting additive manufacturing, inkjet head squirts binder to the programmed surface area and green parts are printed in layer-by-layer. Then, green parts are sintered to reach the final shape and strength. This eliminates all the problems related to fusion of the copper in additive manufacturing. One of the first studies of copper binder jetting provided 80% sintered density results (Bai & Williams, 2015). They used 75 µm and 15 µm mean powder sizes and printed parts at 60, 80 and 100 µm layer thicknesses with ~55% green part densities. Later, they improved the sintered density results up to 92%, and after hot isostatic pressing up to 99.7% (Kumar, Bai, Eklund, & Williams, 2017). Thermal conductivity (335-370 W/m-K) and electrical conductivity ($3 - 5.2 \times 10^7$S/m) reported in another study (Yegyan Kumar, Wang, Bai, Huxtable, & Williams, 2019). Sintering density improved by using bimodal powders, a mixture of 5 µm and 30 µm. More recent study showed an alternative to the bimodal powders which is a 5 µm mean powder size to print the parts (Miyanaji, Rahman, Da, & Williams, 2020). Although green part density dropped to 45%, 91% sintered density was achieved. They used a state-of-the-art binder jetting printer to be able to spread the fine powders. However, depowdering of the green parts are still not fully automated, and fine powders require extra care for health safety of the personnel. This study focuses BJAM of copper powders that do not include smaller than 5 µm powder size. Two different powder size distributions are studied with different sintering strategies. Sintered density, mechanical strength, thermal conductivity and electrical conductivity results are presented.

2. MATERIALS AND METHODS

Binder jetting samples were printed using a Sinterjet binder jetting printer with their SR7 solvent based polymer binder. The powder bed volume is $65 \times 65 \times 160\ mm^3$, and 500 W power infrared lamp is used to dry the binder jetted layers. Custom powder bed heating set up was built to be able to keep the copper powder bed at ~55 °C. Layer thicknesses were selected as 65 µm and 85 µm. Two different pure copper

powders were studied with the median diameter of 19.8 µm (10 – 38 µm) and 25.1 µm (15 – 45 µm) provided by Sentes-BIR. Four different geometries were printed. To study the effects of layer thickness and sintering strategies, 10 mm × 10 mm × 10 mm prismatic parts were printed. Sintered densities were calculated by dividing measured mass with a precision scale to measured volume with a caliper. Same parts were also utilized for electrical conductivity experiments measured by FYTRONIX four probe resistance system. The other two different geometries were needed to conduct thermal capacity, cylinder diameter = 3 mm and length = 30 mm, and thermal diffusivity, cylinder diameter = 12.7 mm and length = 30 mm, experiments. Thermal conductivity is derived from these measured values. Final geometry is a tensile bar according to ISO-6892-1 with a 5 mm diameter and 50 mm gauge length. All samples were oversized to account the shrinkage effects and machined to satisfy standard geometry sizes except prismatic samples. Prismatic samples were used to optimize the sintering process. Copper samples sintering recipes are developed based on the variables in Table 1 under inert-hydrogen mixture atmosphere conditions.

Table 1. Sintering process parameters

Debinding Temperature (°C)	440	**Sintering Temperature (°C)**	1060 – 1075
Soaking Temperature (°C)	none, 700 and 900	**Heating Ramp (°C/min)**	3 and 5

Densification and material properties were compared to LPBF produced samples. The same geometries were produced with fixed processing conditions able to produce high density parts.

3. RESULTS AND DISCUSSION

All results will be ready during the revision period. Figure 1 presents the green part and sintered part pictures of the initial trial of a heat exhanger.

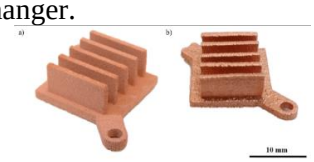

Figure 1. Heat exchanger **(a)** green part, **(b)** sintered part

4. CONCLUSIONS

Conclusions will be presented when the abstract is going to be revised.

REFERENCES

Bai, Y., & Williams, C. B. (2015). An exploration of binder jetting of copper. *Rapid Prototyping Journal*, *21*(2), 177–185. https://doi.org/10.1108/RPJ-12-2014-0180

Colopi, M., Demir, A. G., Caprio, L., & Previtali, B. (2019). Limits and solutions in processing pure Cu via selective laser melting using a high-power single-mode fiber laser. *International Journal of Advanced Manufacturing Technology*, *104*(5–8). https://doi.org/10.1007/s00170-019-04015-3

Jiang, Q., Zhang, P., Yu, Z., Shi, H., Wu, D., Yan, H., … Tian, Y. (2021). A review on additive manufacturing of pure copper. *Coatings*, *11*(6). https://doi.org/10.3390/coatings11060740

Kumar, A., Bai, Y., Eklund, A., & Williams, C. B. (2017). Effects of Hot Isostatic Pressing on Copper Parts Fabricated via Binder Jetting. *Procedia Manufacturing*, *10*, 935–944. https://doi.org/10.1016/j.promfg.2017.07.084

Miyanaji, H., Rahman, K. M., Da, M., & Williams, C. B. (2020). Effect of fine powder particles on quality of binder jetting parts. *Additive Manufacturing*, *36*(September). https://doi.org/10.1016/j.addma.2020.101587

Tran, T. Q., Chinnappan, A., Lee, J. K. Y., Loc, N. H., Tran, L. T., Wang, G., … Ramakrishna, S. (2019). 3D printing of highly pure copper. *Metals*, *9*(7), 12–20. https://doi.org/10.3390/met9070756

Yegyan Kumar, A., Wang, J., Bai, Y., Huxtable, S. T., & Williams, C. B. (2019). Impacts of process-induced porosity on material properties of copper made by binder jetting additive manufacturing. *Materials and Design*, *182*, 108001. https://doi.org/10.1016/j.matdes.2019.10800

CASE STUDY ON PRODUCTION OF MEDIUM TO LARGE SCALE PARTS BY WIRE + ARC ADDITIVE MANUFACTURING

Nevzat Bol[1], Masoud Abbaszadeh[1], Ozge Ece Kara[1], A. Ali Sen[1], Oguzhan Yılmaz[2]
[1]*INTECRO Robotics company, Ankara, Turkey, nevzat.bol@intecro.com.tr*
[2]*Advanced Manufacturing Technology Research Group (AMTRG), Gazi University, Ankara, Turkey, oguzhanyilmaz@gazi.edu.tr*

ABSTRACT

Wire + Arc Additive Manufacturing (WAAM) is a metal additive manufacturing (AM) technique that enables the production of medium to large-scale near-net-shape structural parts with a high deposition rate. During this process, the filler wire is melted using current arc and deposited on a substrate or already solidified part to build up the structures in a layer-by-layer manner. This manufacturing method has recently attracted the attention of different industrial sectors such as aerospace, aviation, and shipbuilding due to its outstanding advantages such as lower buy-to-fly ratio and consequently lower cost, ability to repair operations as well as being environmentally friendly. In the current case study, the production of an ellipsoid-like structure with height of one meter using ER70S-6 steel wire is examined by the WAAM method. Determining the ideal parameters to produce this structure and corresponding tool path strategy, production of the part with the created tool path strategy and the verification of the part geometry with 3D scanning after the part production are discussed.

Acknowledgments: This work has been supported by The Scientific and Technological Research Council of TURKEY (TUBITAK) under the Project Grant No: 3200280.

Keywords: WAAM, Tool Path Strategies, ER70S-6, 3D scanning

1. INTRODUCTION

Wire + Arc Additive Manufacturing (WAAM) is a wire-based direct energy deposition technique that employs electrical arc as heating source and filler wire as a feedstock material to build relatively large and complex engineering parts. Unlike traditional machining from solid and rather than subtracting the material in this technique, WAAM produces the components by adding the material in a layer by layer and free-form manner. This feature enables WAAM process to create complex shaped three-dimensional parts which can be difficult or impossible to obtain by conventional manufacturing processes (Tiago A. Rodrigues, 2019). WAAM is a promising technology to reduce the material waste, lead times, design constraints and ultimately in the total cost of the finished product compared to traditional machining methods (John Coykendall, 2014). Although other additive manufacturing (AM) technologies such as powder-based AM methods are able to produce highly precise components, they are affected by high material costs, low deposition rates and consequently long production time (Filomeno Martina, 2015).

In this case study, the production process including parameters determination, toolpath strategy, part production and geometry verification with 3D scanning of a one-meter-high ellipsoid-like structure using ER70S-6 steel wire is explained by WAAM process. A preliminary study was carried out to obtain the optimized parameters, i.e., wire feed speed (WFS), torch travel speed (TTS) for production of this structure. The selected parameters lead to minimum level of porosity in the produced part as well as higher surface quality.

2. MATERIALS AND METHODS

One meter ellipsoid-like structure with a base diameter of 150 mm, and midpoint diameter of 300 mm is produced by wire + arc additive manufacturing based on cold metal transfer (CMT) system. Fronius TPS500i CMT welding machine and Kuka KR6 R 1820 ARC HW 6-axis industrial robotic arm were used for the production of the part. ER70S-6 low carbon steel wire with diameter of 1.2 mm was used as feedstock material. Wire feed speed (WFS) and torch travel speed (TTS) are considered to be 4.8 m/min and 0.45 m/min, respectively. In order to avoid overheating during production, the inter-layer waiting time of 1 minute was applied before deposition of new layer. %93 Ar, %2 O_2, %5 CO_2 gas mixture, at a speed of 18L/min was used as shielding gas. Tool path of the part was generated starting from 4 different points with 90-degree angles. The direction of movement of the robot changes so as to be clockwise and counterclockwise at each layer pass.

3. RESULTS AND DISCUSSION

In this article, ER70S-6 welding wire was implemented in wire + arc additive manufacturing process to build one meter ellipsoid-like structure. In order to manufacture this structure, 45 kg of ER70S-6 welding wire was consumed and deposited layer by layer in 18 hours. The total production time was 38 hours including 18 hours working time and 20 hours waiting time which were distributed after deposition of each layer. The wire + arc additive manufacturing setup as well as the final produced ellipsoid-like structure is shown in Figure 1a. The 3D scanning of the manufactured part was performed and compared with the CAD data, see Figure 1b. this figure shows that the part was produced within ±2 mm tolerances in the majority of the areas. These geometrical deviations are dimensional deviations that are caused by material flow and tool path slip (Z displacement) during stacking due to the nature of the WAAM process.

From internal experience, if the production of this part had been carried out with traditional manufacturing methods, it could have been produced in approximately 50 hours using approximately 840 kg of raw material. The result of this study shows that WAAM has significant advantages in terms of raw material efficiency and production cost and time.

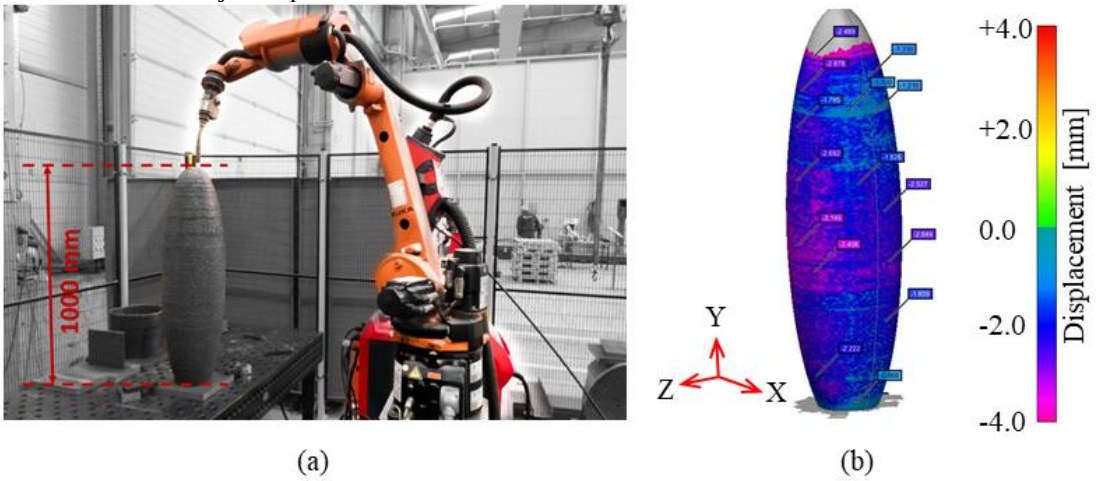

Figure 1. (a) Wire + arc additive manufacturing set-up and final ellipsoid-like structure, (b) 3D scanning of the built structure and corresponding tolerance compared to initial 3D CAD model.

4. CONCLUSIONS

In this case study, the advantages of WAAM in producing medium to large scale structural parts are examined. The results show that WAAM has an advantage over traditional manufacturing methods in terms of production costs and times. 3D scanning of the deposited ellipsoid-like structure using WAAM process showed that the deviation from chosen target 3D CAD model remains in the range of ±2 mm that can be removed during post machining process.

REFERENCES

Filomeno Martina, S. W. (2015). Wire + Arc Additive Manufacturing vs. Traditional Machining from Solid: A Cost Comparison. Cranfield University.

John Coykendall, M. C. (2014). 3D Opportunity in Aerospace and Defense: Additive Manufacturing Takes Flight. A Deloitte series on additive manufacturing.

Tiago A. Rodrigues, V. D. (2019). Current Status and Perspectives on Wire and Arc Additive Manufacturing (WAAM). Materials, 12(7), 1121. doi:https://doi.org/10.3390/ma12071121

CHARACTERIZATION OF METAL POWDER REUSED MULTIPLE TIMES FOR LASER POWDER BED FUSION

E. Özeren[1*], G. M. Bilgin[1], B. Ertekin[1], A. Taş[1], Z. Cavcar[1], M. B. Gökcan[1], A. Orhangül[1] and G.Kara[1]
[1] *TUSAS Engine Industries, Inc., Eskişehir, Turkey*
* *Corresponding author, email: emre.ozeren@tei.com.tr*

ABSTRACT

Laser Powder Bed Fusion (L-PBF) enables the manufacturing of highly complex parts with less material consumption for being used in various industrial applications. Metal powders are commonly used as feedstock material and the powder can be reused several times. Especially in aerospace applications, the reused powder characteristics are quite important in terms of traceability over the part quality since the aerospace industry requires high-quality and reliable end-use parts. In this study, Alloy 718 metal powder, which is generally utilized in high-temperature applications in gas turbine engines due to their good creep and corrosion resistance, were characterized over a 20 series of L-PBF build cycles. The powder characterization was performed in order to investigate the flow behavior of powder reused multiple times by using several methods such as powder rheology, particle size distribution (PSD), and quantitative morphology analysis along with apparent and tap density measurements. The results showed that no major and meaningful difference was seen among 20 times reused powder in terms of PSD and their morphology whereas there is a prominent difference seen by density measurements and with shear cell measurements by powder rheology. These methods revealed that reusing powder causes worse flowability trend.

Keywords: Laser powder bed fusion, powder reuse, powder characterization, powder rheology, particle size distribution and morphology.

CONCLUSIONS

In the present paper, we explored the effect of powder reuse for Alloy 718 produced with the L-PBF method by characterizing powder reuse cycles via PSD and morphology analysis, powder density measurements and powder rheology. The following conclusions can be drawn from the present study:

- Powder reuse causes shifting PSD curves both left and right side by decreasing the median size of the curve. This shows that not only agglomerated particles increase but also a small size of particles caused by spattering or soot increases. The trend of width or span of the PSD curve is also increasing due to the abovementioned phenomenon.
- Quantitative morphology analysis by DIA requires detailing investigation in order to define the powder characteristics. Furthermore, the particle count plays an important role to compare the reuse cycles.
- Tap and apparent powder density measurements revealed that the trend of hausner ratio increases with reusing powder. This result shows that the flowability of powders becomes worse with reusing number of the powder increases.
- Powder shear cell measurements by rheometer show that the powder flowability trend via defining flow functions decreases with increasing reusing of powder.
- In the powder cohesion strength measurement by rheometer, there was not seen a meaningful and clear correlation between the reuse cycles. Additional tests with different amounts of materials are required to evaluate the reused powder characteristics.

The future work will continue with performing additional build cycles with the same powder batch. Furthermore, different powder characterization methods will be used such as a scanning electron microscope for the evaluation on morphological analysis for a better understanding of reused powder characteristics. Moreover, the influence of reused powder on chemical composition, microstructure, and mechanical properties including fatigue behavior, is an ongoing study.

COLD SPRAY EFFECT ON OXIDE DISPERSION STRENGTHENING OF INCONEL 718

B Berk TANRISEVDİ[1], Eda AYDOĞAN[2]
Department of Metallurgical and Materials Engineering, Middle East Technical University (METU), Ankara, 06800, Turkey
[1]berk.tanrisevdi@metu.edu.tr [2]aydogane@metu.edu.tr

ABSTRACT

Oxide dispersion strengthened Inconel 718, ODS In718, produced by Low Pressure Cold Spray method. The Cold Spray was conducted with He / N pressure of 8 bar, max temperature of 130-330 °C, %20 powder density, %25 air flow, 2 mm/s tracking speed, and 2mm hatch distance with 14 mm stand-off distance. Mechanical alloying was applied to the powders using a Fritsch Pulverisette P6 classic line planetary mono mill machine with hardened stainless steel veil in Argon atmosphere at a rate of 300 rpm. With and without the balls 1 hour tries are conducted up to 5 hours. Stainless steel 10 mm grinding balls are used with 1 to 1 ball to powder ratio. The smples heat treated for 1,2 and 3 hours at 1050 °C. The results obtained from EDX analysis satisfied the estimated composition. TEM analysis of cold spray samples showed a homogeneous distribution of nano sized Y-Ti (Hf, Zr, Al) oxides through the microstructure of obtained material. Heat treatment of the cold sprayed samples effectively decreased the porosity of the coating. The observations showed comparable results with that of selective laser melting technique.

Keywords: Nano-oxide, ODS, Superalloy, Cold-Spray, Coating

1. INTRODUCTION

It is well accepted that oxide dispersion strengthened alloys show high strength, creep resistance, thermal stability, oxidation and radiation resistance at high temperatures. The presence of Y-Ti (Hf, Zr, Al)-O nano-oxides in the microstructure of Inconel 718 stabilizes and improves the mechanical properties by pinning dislocations and grain boundaries at elevated temperatures (Yalcin *et al.*, 2022). Fusion-based and solid state kinetic-based additive manufacturing methods are considered as of those promising techniques which take advantages of auto-mixing along with the effect of surface tension differences (Tan *et al.*, 2020). During the cold spraying pressurized and heated gasses are loaded with the micron size powders. The speed of the sprayed mixture can be increased up to speed of sound. Such kind of highspeed results in kinetic sintering between both powder-substrate and powder-powder. The concurrence of severe plastic deformation along with adiabatic shear instability phenomenon results in mechanical locking of powder and substrate (Singh *et al.*, 2021) . The mechanical alloying (MA) is necessary to incorporate the fine oxide particle of Y2O3/ FeO and Hf precursor to Inconel 718 powder body. As the bow shock effect is increasing with decreasing the particle size, so mechanical alloying is applied to produce bigger particles to minimize the aforementioned effect. The objective of this study is to modify the composition of the Inconel 718 alloys by mechanical alloying and low-pressure cold spray methods to produce equiaxed grain structures with high volume fraction of nano-oxide dispersions.

2. MATERIALS AND METHODS

Oxide dispersion strengthened Inconel 718, ODS In718, produced by Low Pressure Cold Spray method. Cold Spray conducted using He or N gasses with 8 bar pressure at temperatures 130 and 330 °C, respectively. The parameters for the feeder were applied by %20 powder density and %25 air flow. The scan speed of the nozzle was 2 mm/s and the distance between consecutive lines was 2 mm (hatch distance), and the distance between the deposition surface and the nozzle was 14 mm. Four to one ratio of converging diverging nozzle is used with 14 mm diameter nozzle opening. Mechanical alloyed Inconel 718 powders are sprayed upon 2xxx series Al, pure Zr, 1050 steel, Inconel 718 with 800 grinded surfaces. Mechanical alloying was applied to the powders using a Fritsch Pulverisette P6 classic line planetary mono mill machine with hardened stainless steel veil in Argon atmosphere at a rate of 300 rpm. Mechanical alloying was done with and without balls for different durations from one to 5 hours. Stainless steel grinding balls were used with the diameter of 10 mm with equal proportions (1 to 1 ball to powder ratio). Heat treatment of samples were done at 1050 °C for 1, 2 and 3 hours. Optical microscopy, scanning electron microscopy (SEM) and transmission electron microscopy (TEM), and Energy dispersive X-ray spectroscopy were used to characterize the obtained microstructures.

The percentage and the size of the used powders were 0.84 wt.% Hf (5-25 µm), 0.67 wt.% Y2O3 (20-40 nm) and 0.33 wt.% FeO (<100 nm) precursor and oxides balanced with Inconel 718 (0-25 µm).

3. RESULTS AND DISCUSSION

Cold spraying of Inconel 718 particles with incorporated oxides and precursors using N gass reduced the top velocity of powders. Therefore, He was applied instead of N gass and process optimized by changing hatch distance, speed, feeding ratios and stand-off distance. The modification resulted in successful thin coating. The figure 1. Depicts the formation of a continuous interface between Inconel 718 coating and Zr substrate. EDX analysis showed that the mechanical alloying introduced a very homogeneous composition in the microstructure of the coating (0.34- 0.92 wt.% Y and 1.03% to 2.87% Hf). The variation of the Hf percentage is more likely related to the mechanical alloying and deflect ratio to bow shock phenomenon. The porosity of cold sprayed samples tended to decrease by the heat treatment process. Furthermore, TEM investigations showed that nano sized Y-Ti (Hf, Zr, Al) were distributed homogeneously through the microstructure of the coated layer.

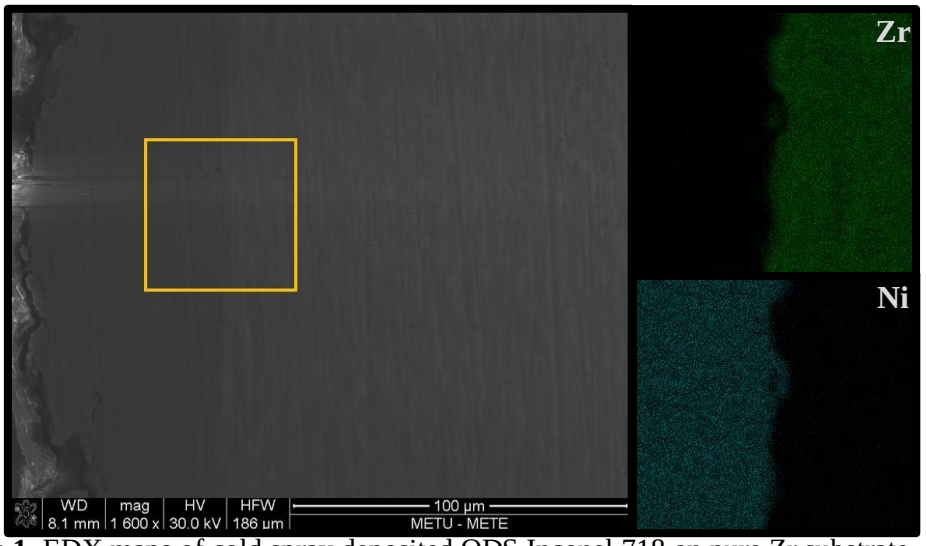

Figure 1. EDX maps of cold spray deposited ODS Inconel 718 on pure Zr substrate.

4. CONCLUSIONS

Inconel 718 is strengthened with Y-Ti- (Al)-O nano particles. Heat treated and as produced samples had the desired composition. TEM characterization showed the formation of homogeneous and nano-sized oxide particles inside the coating.

REFERENCES

[1] Yalcin, M. Y., Derin, C. B., & Aydogan, E. (2022). Development and additive manufacturing of oxide dispersion strengthened Inconel 718: Thermochemical and experimental studies. *SSRN Electronic Journal*. doi:10.2139/ssrn.4034430

[2] Tan, L., Wang, G., Guo, Y., Fang, Q., Liu, Z., Xiao, X., . . . Huang, L. (2020). Additively manufactured oxide dispersion strengthened nickel-based superalloy with superior high temperature properties. *Virtual and Physical Prototyping, 15*(Sup1), 555-569. doi:10.1080/17452759.2020.1848283

[3] Singh, S., Raman, R. K., Berndt, C. C., & Singh, H. (2021). Influence of cold spray parameters on bonding mechanisms: A Review. *Metals, 11*(12), 2016. doi:10.3390/met11122016

COMBINATION OF PERIDYNAMICS AND GENETIC ALGORITHM BASED TOPOLOGY OPTIMIZATION METHODS FOR AM-FRIENDLY DESIGNS

Abdullah Kendibilir[1,2,3*], Mehmet Furkan Polat[1,2,3*], Omer Safa Cavus[1,2,3], Sina Khalilvandi Behrouzyar[1,2,3], Peyman Lahe Motlagh[3,4], Bahattin Koc[1,2,3**], Adnan Kefal[1,2,3**]

[1] *Faculty of Engineering and Natural Sciences, Sabanci University, Tuzla, Istanbul 34956, Turkey*

[2] *Composite Technologies Center of Excellence, Sabanci University-Kordsa, Istanbul Technology Development Zone, Sanayi Mah. Teknopark Blvd. No: 1/1B, Pendik, 34906 Istanbul, Turkey*

[3] *Integrated Manufacturing Technologies Research and Application Center, Sabanci University, Tuzla, 34956, Istanbul, Turkey*

[4] *Department of Mechanical Engineering, Gebze Technical University,Gebze, 41400, Kocaeli, Turkey*

[*] *The authors contributed equally to this work*

[**] *Corresponding authors: bahattin.koc@sabanciuniv.edu (B. Koc), adnankefal@sabanciuniv.edu (A. Kefal)*

ABSTRACT

Topology optimization (TO) is a practical tool to generate light-weighted engineering structures for various manufacturing industries. However, manufacturing constraints and surface smoothing are still considerable challenges for TO algorithms. Existing TO frameworks utilize mechanical analysis approaches that discretize the whole domain with elements or particles. Therefore, obtained geometries from TO have been criticized for their complex shapes. In this study, we propose a coupled framework to generate AM-friendly designs which result in less support structure and higher surface quality. For this purpose, the generative topology optimization method (GTO), which uses genetic algorithm to search for the best alternative set of geometry within all the possible topology results, is coupled with the peridynamics topology optimization (PD-TO) method to evolve the PD-TO results into AM-friendly shapes. The PD- TO method discretizes the problem domain using equally spaced particles during the TO process. Hence, PD-TO generates a point cloud file with relevant artificial material density values in the final state. Then, GTO method utilizes the point cloud and material densities as an input file to achieve better final geometry. Consequently, AM-friendly designs achieved from GTO are compared with the initial results obtained from PD-TO to demonstrate the efficiency and capability of the proposed method.

Keywords: AM-friendly design, generative topology optimization, peridynamic, additive manufacturing, topology optimization

1. INTRODUCTION

In recent years, the utilization of topology optimization studies according to additive manufacturing constraints has become more attractive for researchers. Since the overhang constraint have great impact on the manufacturability, TO for overhang constraints is necessary for support-free manufacturing or support minimization studies (Bi et al., 2020). Moreover, geometry redesigning after TO applications can become complicated processes due to fragmented surface. Several methods and studies have been conducted for overcoming those issues in the literature (Brackett et al., 2011).

2. MATERIALS AND METHODS

In this study, a novel GA-based approach is developed to create a TO process that includes AM constraints and obtain a parametric surface outcome that is ready to print. This approach will utilize PD-TO results as input to generate smooth and ready-to-print AM-friendly designs by the GTO method for the first time. The general PD equation of motion for a material point initially located at x can be written as (Kefal et al.,2019):

$$\rho(\boldsymbol{x})\boldsymbol{u}(\boldsymbol{x},t) = \int \left(\boldsymbol{t}(\boldsymbol{u}'-\boldsymbol{u},\boldsymbol{x}'-\boldsymbol{x}) - \boldsymbol{t}'(\boldsymbol{u}-\boldsymbol{u}',\boldsymbol{x}-\boldsymbol{x}')\right) dH_x + \boldsymbol{b}(\boldsymbol{x},t) \quad (1)$$

The non-local nature of the PD approach can be illustrated for the 3D domain as shown in Figure 1.

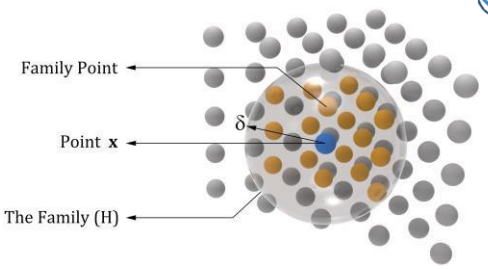

Figure 1. The family of the material point x

3. RESULTS AND DISCUSSION

After we optimize a given domain with the PD-TO method, the GTO method turns this solution into a smooth ready-to-print geometry by generating parametric surfaces. One example of the GTO result and ANSYS result is shown in Figure 2. to emphasize the surface quality difference between GTO and ANSYS results.

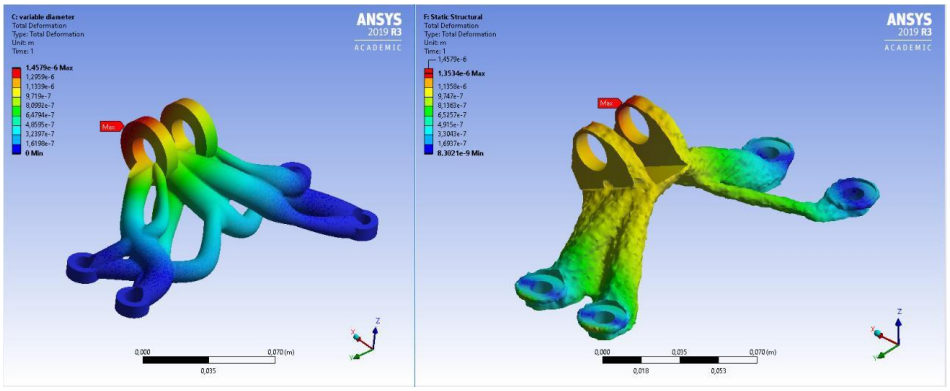

Figure 2. Total deformation comparison between GA and ANSYS Result

4. CONCLUSIONS

We performed the PD-TO and GTO methods sequentially to obtain topologically optimized and smooth designs while minimizing the support structures for additive manufacturing processes. The results showed that the proposed method can decrease the support volume drastically compared to the results obtained from commercial software while having less maximum displacement value. In addition to those enhancements, the resultant geometries have smoother surfaces, so the local stress concentration of the resultant part can also be reduced.

REFERENCES

Bi, M., Tran, P., & Xie, Y. M. (2020). Topology optimization of 3D continuum structures under geometric self- supporting constraint. *Additive Manufacturing*, *36*, 101422.

Brackett, D., Ashcroft, I., & Hague, R. (2011, August). Topology optimization for additive manufacturing. In *2011 International Solid Freeform Fabrication Symposium*. University of Texas at Austin.

Kefal, A., Sohouli, A., Oterkus, E., Yildiz, M., & Suleman, A. (2019). Topology optimization of cracked structures using peridynamics. *Continuum Mechanics and Thermodynamics*, *31*(6), 1645-1672.

COMPARISON OF DYNAMIC MECHANICAL PROPERTIES OF ALSI10MG LATTICE STRUCTURES PRODUCED BY SELECTIVE LASER MELTING

Mustafa Caliskan[1], Hakan Hafizoglu[2], Ahmet Sever[3] and Nazim Babacan[4]
[1]*Sivas University of Science and Technology, Department of Mechanical Engineering, Sivas 58140, Turkey, mustafaclskn96@gmail.com*
[2] *TUBITAK Defense Industries Research and Development Institute, Ankara 06261, Turkey, hakan.hafizoglu@tubitak.gov.tr*
[3]*ERMAKSAN, Bursa 16065, Turkey, ahmet.sever@ermaksan.com.tr*
[4] *Sivas University of Science and Technology, Department of Mechanical Engineering, Sivas 58140, Turkey, nazimbabacan@sivas.edu.tr*

ABSTRACT

Three different AlSi10Mg lattice structures, face-centered cubic (FCC), diamond and auxetic, were produced by selective laser melting (SLM). Dynamic compression tests were applied to as-build samples at two different strain rates (750 s^{-1} and 1100 s^{-1}) by Split-Hopkinson Pressure Bar (SPHB). While the maximum compressive strength was found as 43 MPa in FCC structure, diamond structure had the lowest compressive strength with 24 MPa. Initial results of additive manufactured AlSi10Mg lattice structures showed that the maximum load carrying capacity of the FCC structure is higher than that of diamond and auxetic lattices.

Keywords: Selective laser melting, AlSi10Mg, Lattice structures, Split-Hopkinson Pressure Bar, Mechanical properties

1. INTRODUCTION

Selective laser melting (SLM), as one of the additive manufacturing methods, are more useful than traditional methods in the production of complex structures such as lattice structures. Lattice structures consisting of struts with a diameter of several hundred microns have attracted significant attention in recent years due to their high specific strength, high specific modulus, and energy absorption capabilities (Schaedler et al. 2015)

AlSi10Mg alloy is a traditional cast alloy that is often used for die-casting. Because of its high strength and good mechanical properties, this alloy has been widely used in the automotive and aerospace industry. Moreover, it has good weldability due to its near eutectic composition of Al and Si (Liu et al. 2019). These properties make this alloy as ideal candidate for the additive manufacturing.

Dynamic responses of the lattice structures are generally investigated by different test set-ups, such as drop test or Split-Hopkinson pressure bar (SHPB). High deformation rates obtained with SHPB simulate the dynamic behavior of the materials successfully, which is highly beneficial to forecast the energy absorption capacity of the structures during exposing a dynamic load. Studies in the literature show how important it is to choose the appropriate lattice structure type and geometry to meet the loading conditions. (Hazeli et al. 2019 and Sienkiewicz et al. 2020)

The purpose of the present work is to investigate the dynamical mechanical performances of three different AlSi10Mg lattice structures fabricated with SLM at high strain rates and find the optimal structure for dynamic responses.

2. MATERIALS AND METHODS

In this study, there layer of lattice structures with unit cell dimensions of 4 x 4 x 4 mm^3 were fabricated on a SLM device (Ermaksan Enavision 250) using AlSi10Mg powder. Relative density of the all structures were arranged to approximately 25% by modifying the strut diameter. 0.79, 0.97 and 1.09 mm strut diameters were used for auxetic, diamond and FCC structures, respectively. Layer thickness was kept constant at 30 µm.

SHPB test setup in TUBITAK SAGE was used for dynamic compression tests. As-built specimens were attached directly to the pressure bar and dynamic compression tests were performed for each lattice structures at strain rates of 750 s^{-1} and 1100 s^{-1}. The compression test was applied parallel to the building direction.

3. RESULTS AND DISCUSSION

True stress-strain graph of the additively manufactured AlSi10Mg lattice structures obtained from the

SHPB test is given in Figure 1. While the yield strength of FCC and auxetic structures increased with the increase in strain rates, ultimate compressive strength did not change prominently. On the other hand, ultimate compressive strength of the diamond structure increased with the increase in strain rate, while yield strength was not affected clearly. The ductility of the all samples increased by increase in strain rate.

The maximum compressive strengths obtained for FCC, auxetic and diamond structures are 43, 29 and 27 MPa, respectively. The maximum strain values of the samples tested at the same strain rate were found similar. The load-bearing capacity and energy absorption capacity of the FCC lattice structure are superior to its counterparts

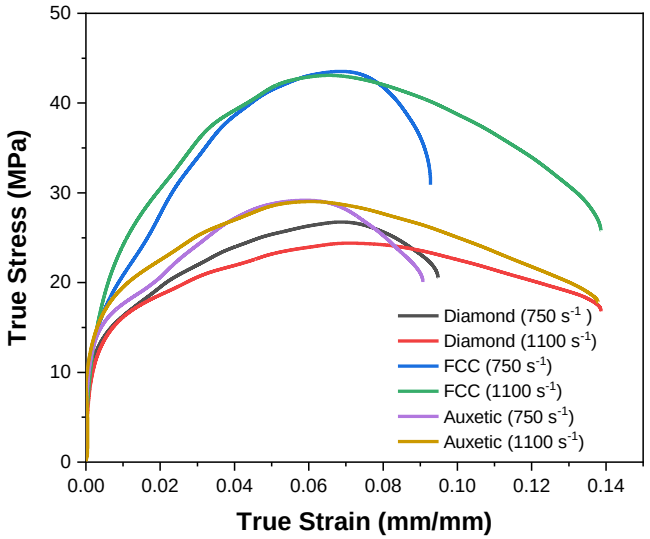

Figure 1. True stress-strain curves of diamond, FCC and auxetic lattice structures at 750 s^{-1} and 1100 s^{-1} strain rates

4. CONCLUSIONS

According to the obtained results, the FCC lattice structure is found to be more efficient compared to diamond and auxetic structures in terms of dynamic mechanical performance. The ballistic penetration response of the same lattice structures will be analyzed comprehensively as a future study.

REFERENCES

Schaedler, T.A., Jacobasen, A.J., Torrents, A., Sorensen, A.E., Lian, J., Greer, J.R., Valdevit, L., & Carter, W.B. (2011). Ultralight metallic microlattices. Science, 18;334(6058), 962

Hazeli, K., Babamiri, B. B., Indeck, J., Minor, A., & Askari, H. (2019). Microstructure-topology relationship effects on the quasi-static and dynamic behavior of additively manufactured lattice structures. Materials and Design, 176, 107826.

Liu, X., Zhao, C., Zhou, X., Shen, Z., & Liu, W. (2019). Microstructure of selective laser melted AlSi10Mg alloy. Materials and Design, 168, 107677.

Sienkiewicz, J., Płatek, P., Jiang, F., Sun, X., & Rusinek, A. (2020). Investigations on the mechanical response of gradient lattice structures manufactured SLM. Metals, 10(2), 213

COMPARISON OF SINGLE AND TWIN SCREW EXTRUDERS FOR THE PRODUCTION OF GLASS AND CARBON REINFORCED HIGH DENSTIY POLYETHYLENE (HDPE) FILAMENTS

Ayberk Sözen[1], Gökdeniz Neşer[1]
[1]*Institute of Marine Sciences and Technology, Dokuz Eylul University, Izmir, Turkey,*
gokdeniz.neser@deu.edu.tr, ayberk.sozen@deu.edu.tr

ABSTRACT

HDPE is a newly used thermoplastic for additive manufacturing but there is some problem to overcome. They need to be strengthened with various micro size additives. The distribution of the fibers in the matrix is of vital importance. The production process is affected by many parameters such as temperature, extrusion speed, cooling rate, matrix, and fiber particle size. In this study, a comparison was made by using single and twin-screw extruders to produce 10% glass and carbon and reinforced HDPE filaments. Mechanical properties were evaluated based on tensile tests. Reinforcing fiber to the HDPE matrix increases the tensile strength. If the matrix and fiber particle size are reduced to 250µ before the extrusion, it is possible to achieve high tensile results close to twin screw extrusion with single screw extrusion, but homogeneous distribution of fibers in the matrix is not satisfactory.

Keywords: Single screw extruder, twin screw extruder, filament production, additive manufacturing

1. INTRODUCTION

In marine industry, for almost ten years, HDPE with its good resistance to environmental degradation effects such as UV, marine organism, and corrosion (Rajeshwari & Dey, 2014) has been care into prominence. Using HDPE in production of small marine craft by additive manufacturing techniques needs to overcome the difficulties of thermal defects. To improve mechanical performance of HDPE, it needs to be reinforced with various additives such as micro-sized glass and carbon fiber (Guo, Finkenstadt, & Nimmagadda, 2019). During this reinforcement process, the distribution of the fibers in the matrix is of vital importance. The production process is affected by many parameters such as temperature, extrusion speed, cooling rate, matrix, and fiber size (Grande & Torres, 2005). While the single screw extrusion process is easier, simpler, and less costly, it is more vulnerable to manufacturing errors.

2. MATERIALS AND METHODS

In this study, a comparison was made by using single and twin-screw extruders to produce 10% glass and carbon and reinforced HDPE filaments. Mechanical were evaluated based on tensile tests. PETILEN YY I668 product of PETKİM company was used as the matrix. For single screw extrusion, pellet sizes were reduced to 250 µ by grinding and the surface area was increased. The mixture is tried to be homogenized with an ultrasonic mixer in single screw extrusion. Recycled glass and carbon fibers with a diameter of 100-400 µ were used as filament with fiber sizes vary. 1,75 mm diameter filament was extruded. D638 ASTM type V size tensile specimens were printed, and mechanical properties were investigated. In addition, the homogeneous distribution of the fibers in the matrix was observed in SEM images.

3. RESULTS AND DISCUSSION

As can be seen in the table, adding fiber to the HDPE matrix increases the tensile strength. Carbon fiber resulted a significant increase as expected. If the matrix and fiber particle size are reduced, it is possible to achieve results close to twin screw extrusion with single screw extrusion, but homogeneous distribution of fibers in the matrix cannot be guaranteed. Considering the higher production and operating costs of the twin screw extruder, this method may be a good alternative for low-cost production.

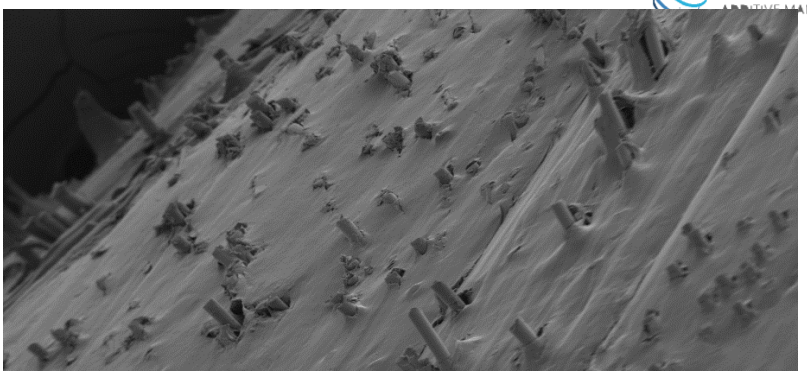

Figure 1. SEM images of twin screw extruded filament *(single screw will be added soon.)*

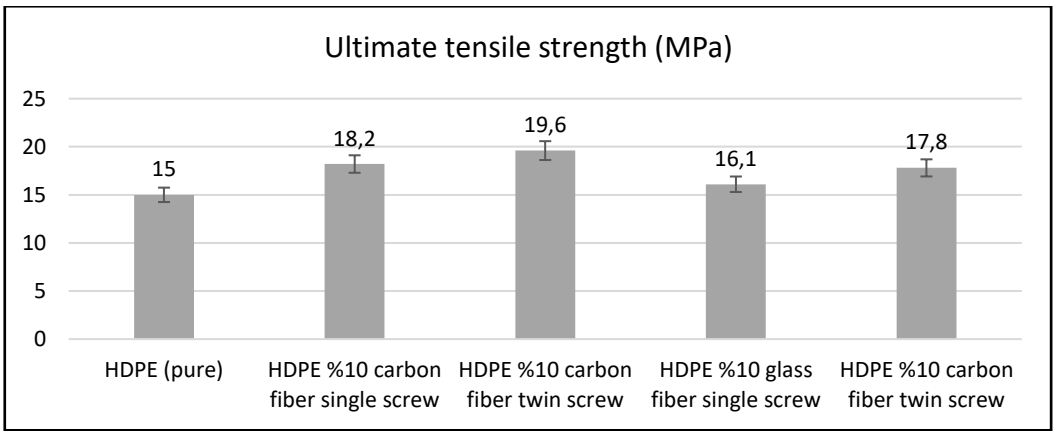

Figure 2. Tensile test results

4. CONCLUSIONS

Although fiber-reinforced HDPE composite filament production with single screw extrusion is low-budget, it is not suitable for industrial uses due to poor homogeneous distribution. HPDE composite filaments shows commercialization activities as new. HDPE is generally difficult to 3D printing due to its low surface adhesion and flexibility, but the addition of carbon and glass fiber increases tensile strength, brittleness to some extent but facilitates surface adhesion to the heated printing plate and allows printing on inexpensive entry level 3d printers.

REFERENCES

Grande, C., & Torres, F. G. (2005). Investigation of fiber organization and damage during single screw extrusion of natural fiber reinforced thermoplastics. Advances in Polymer Technology, 24(2), 145–156. doi:10.1002/adv.20037

Guo, G., Finkenstadt, V. L., & Nimmagadda, Y. (2019). Mechanical properties and water absorption behavior of injection-molded wood fiber/carbon fiber high-density polyethylene hybrid composites. Advanced Composites and Hybrid Materials, 2, 690–700. doi:10.1007/s42114-019-00116-5/Published

Rajeshwari, P., & Dey, T. K. (2014). Structural and thermal properties of HDPE/n-AlN polymer nanocomposites. Journal of Thermal Analysis and Calorimetry, 118(3), 1513–1530. doi:10.1007/s10973-014-4063-1

CONTACT-FREE SUPPORT STRUCTURES EFFECT ON DIMENSIONAL DEVIATION OF LPBF PRINTED COMPONENTS WITH OVERHANG FEATURES

Orhan Gülcan[1], Kadir Günaydın[2], Alican Çelik[3] and Evren Yasa[4]
[1]*General Electric Aviation, Gebze, Kocaeli, Turkey, orhan.gulcan@ge.com*
[2]*General Electric Aviation, Gebze, Kocaeli, Turkey, kadir.gunaydin@ge.com*
[3]*General Electric Aviation, Gebze, Kocaeli, Turkey, alican.celik@ge.com*
[4]*Eskişehir Osman Gazi University, Mechanical Engineering Department, Eskişehir, Turkey, eyasa@ogu.edu.tr*

ABSTRACT

Laser powder bed fusion (LPBF) process has gained great attention in recent years since it enables the production of very complex parts with acceptable dimensional accuracy, cost and mechanical properties. Since LPBF process is a thermal process and very high thermal stresses occur during production, dimensional deviations occur especially in very thin and overhang regions. The aim of this study is to show the feasibility of using contactless supports at thin and overhang regions for reducing dimensional deviation of the final part. For this purpose, 1.5 mm thick overhang parts with 30^0 inclination angles with respect to build plate were manufactured with LPBF process from In718 material. Contactless supports with different amount of gaps between the overhang surface and the support (0.23, 0.31 and 0.38 mm) were used during production. The produced parts were 3D scanned with a blue light device. Results show that contactless supports are good alternative to solid supports in the production of overhang parts with LPBF method and contactless support gaps directly affect the dimensional deviation of the final part.

Keywords: dimensional deviation, contactless support, LPBF

1. INTRODUCTION

Laser powder bed fusion (LPBF) method is a sub-branch of powder bed fusion additive manufacturing processes where laser energy is used as the energy source to melt the metal powder laid on a build platform with a recoater blade. With the movement of build plate, the part is produced layer by layer according to the machine specific tool path based on 3D computer aided design (CAD) file sliced in a virtual environment (Cheng and Chou, 2015). During production, high amount of thermal stresses occur resulting in dimensional variations in especially thin and overhang areas. To solve this problem, supports can be added to these areas which serve as an anchorage to the build platform. However, these support structures need to be removed after production since they are not a part of the final component. Contactless supports where there is no direct contact between the support and the overhang surface seems to be a good alternative to solid supports to eliminate the need for machining of the support structures after production. In contactless supports, the gap between the support and the overhang surface is a key factor that affects the producibility of the final component. Smaller gaps reduce the part distortion, but they increase the risk of melting/sintering of metal powders in the gap especially when the melt pool is deeper than the gap (Leary, 2020). This study focuses on the effect of contactless support gap on dimensional variation of LPBF produced In718 parts.

2. MATERIALS AND METHODS

Overhang specimens with 30^0 inclination angles with respect to build plate were modelled with Siemens NX software (Figure 1). Contactless supports with three different gaps (0.23, 0.31 and 0.38 mm) were used during production. Concept Laser M2 LPBF machine was used for the production of the specimens. In718 powder material and standard vendor process parameters were used. After production, supports and the final parts were removed from the build platform with GF Agiecharmilles wire electrical discharge machine. Specimens were scanned with ATOS ScanBox 4105 blue light device and GOM Inspect software was used to evaluate the dimensional deviations of the produced specimens from the original CAD geometry.

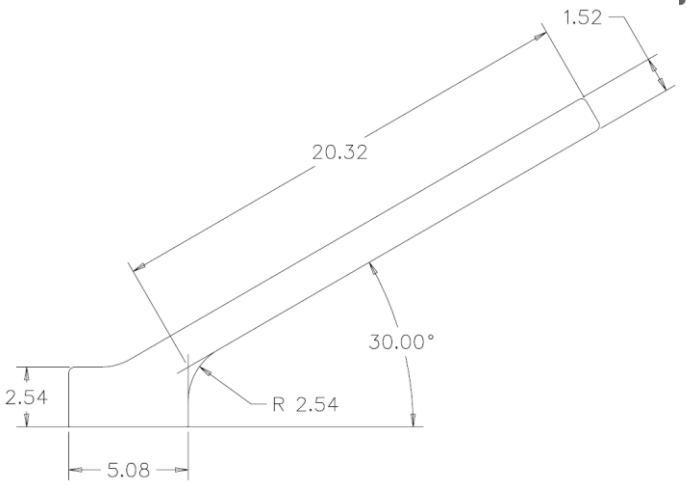

Figure 1. Overhang specimen

3. RESULTS AND DISCUSSION

For each gap value, three specimens and total 9 specimens were produced without any specific production problem (Figure 2).

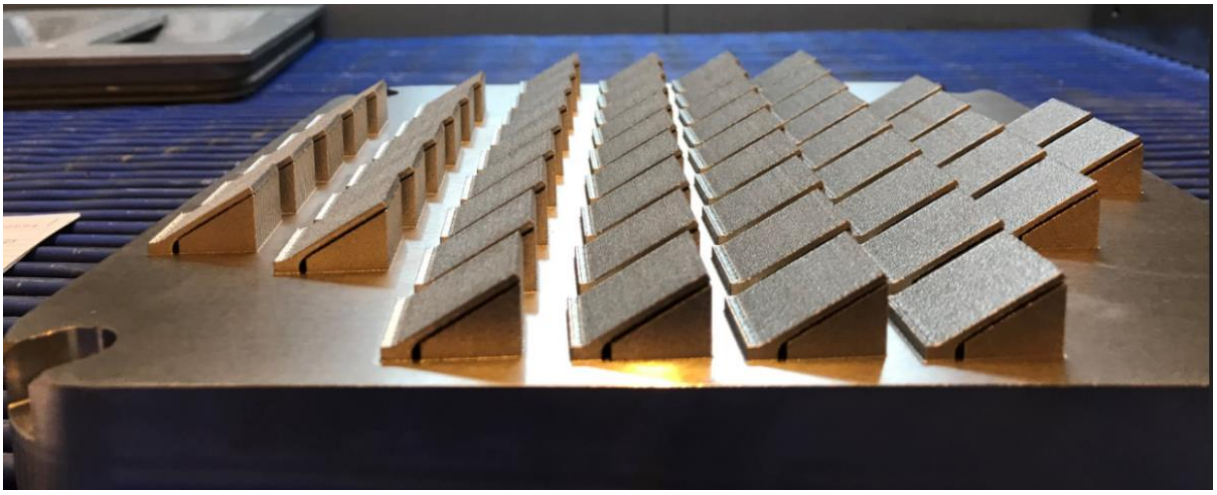

Figure 2. Produced specimens.

4. CONCLUSIONS

The comparison between bluelight scanned 3D data of the produced specimens and the original CAD data reveals that gap value between the support and the part directly affects the dimensional variation of the overhang surface. As a future work, the effect of contactless support gap on surface roughness, microhardness through thickness and microstructural changes will be investigated.

REFERENCES

Cheng, B., Chou, K. 2015. “Geometric consideration of support structures in part overhang fabrications by electron beam additive manufacturing”, Computer-Aided Design, 69: 102-111.
Leary, M. 2020. “Powder bed fusion”, Editor(s): Martin Leary, In Additive Manufacturing Materials and Technologies, Design for Additive Manufacturing, Elsevier, 295-319.

COORDINATION OF SPATIAL & TEMPORAL LASER BEAM PROFILE TOWARDS ULTRA-FINE FEATURE FABRICATION IN LPBF

Ali Aktas[1,*], Leonardo Caprio[1], Francesco Galbusera[1], Barbara Previtali[1], Ali Gökhan Demir[1]
[1] *Department of Mechanical Engineering, Politecnico di Milano*
**Corresponding author: ali.aktas@polimi.it*

ABSTRACT

Laser powder bed fusion (LPBF) is a layer-wise metal additive technology that provides high shape and dimensional flexibility compared to conventional technologies. Thanks to the distinctive manufacturing characteristics, the process can be theoretically described as free-form fabrication technique. Therefore, it is generally used in applications that are required high performance and structural complexity. Lattice structures, twin skinned high-performance parts, complex heat exchangers, custom biomedical parts can be given as generic examples for the application range. Nonetheless, despite the provided shape and dimension flexibility, the fabrication of parts with ultra-fine geometrical features such as wall thickness or strut size under 200 µm still pose a problem for the technology. Particularly, the geometrical fidelity of ultra-fine features is decreasing when their dimensions become comparable to the laser beam diameter (typically 50-100 µm) and the powder grain size (typically 50-100 µm). Therefore, the mismatch between the digital model and final geometry is counted as one of the main obstacles.

The studies presented in the literature have generally addressed ultra-fine features in terms of process parameters and different scanning strategies, and most of them remarked the importance of using optimum process parameters with correct scanning strategy for reducing the dimensional mismatch between the actual and final part (Abele et al., 2015). However, the technological limitations of the LPBF machines in terms of temporal-spatial synchronization and control of the laser beam, which can be described briefly as scanning performance, were mostly neglected. Although there were specific studies which investigated the problem in parameter, geometry and technology domains together, scanning performance of different LPBF machines were not regarded during the research (Wang et al., 2017), (Kranz et al., 2015). Nevertheless, even though the process parameters and/or design rules are well-defined for specific structures in the ultra-fine segment, repeatability and validation of these works are still a controversial issue because of variability in the technological capacity of the LPBF machines (Lopez Taborda et al., 2021), (Thompson et al., 2016). Often industrial grade LPBF systems do not operate at their full potential for producing fine features, since they are initially developed for producing larger dimensions. The scanner systems and the fiber laser sources used in these machines are capable of a greater control of laser spatial and temporal emission profile essential for the ultra-fine dimensions. However, these features have been hardly explored due to the rigid machine architectures not allowing the end-user to access parameters related the scanner dynamics and laser temporal emission profile independently. Principally, for developing the process towards ultra-fine features and preventing any misdirection, process parameter and scanning induced errors should be detected and separated at the initial stage. The correct detection of processing capability and system precision are required to be identified at a 2D scan layer level prior to moving towards complex 3D geometries.

In this study, temporal-spatial coordination of the laser beam during the different scanning conditions were studied towards the future manufacturing of ultra-fine struts by LPBF. An industrial grade LPBF system with open architecture was used for the purpose (3DNT LLA 150, Solbiate Olona, Italy). The laser emission could be controlled at a vector level allowing to operate the laser in continuous wave (CW), pulsed wave (PW) or single point exposure (SPE) flexibly with dedicated control software (Direct Machining Control, Vilnius, Lithuania). The machine operated with a single mode fiber laser (AFX1000, nLIGHT, Vancouver, WA, USA) coupled to a scanner head (MS-III, Raylase, Wessling, Germany).

The shape and dimensional errors emerged due to incorrect trajectory and temporal control of the laser beam were investigated with the aid of laser marking tests. Laser power, scan speed and hatch distance were studied in range close to what is employed in LPBF with a conventional hatch strategy. Al 5457 substrate, and simple 2D circular geometry with different nominal radii (R_{nom}) were used to realize the study. The scanned geometries on the substrate were characterized with optical microscopy. Shape and dimensional fidelity were evaluated in terms of actual radius and circularity of the area. In Figure 3, tabulated data of characterized samples are representatively shown, and the errors are physically described via characterized samples. According to the different scanning speeds, the scanning performance of the LPBF system was evaluated in terms of fine ($200 \leq D \leq 1000\ \mu m$) and ultra-fine

fabrication segments ($\leq 200\ \mu m$), and the scan-related errors were shown for different dimension scales (Figure 3-B). Technological feasibility map of the employed LPBF system was deducted. The laser marking tests aided the definition of process parameter ranges for the different feature sizes involved. Especially the link between the scan speed and the minimum vector length for a stable laser emission profile was established. The results show that complete scan trajectories based on hatching can be carried out with sufficient geometrical accuracy if the correct scan parameters are selected.

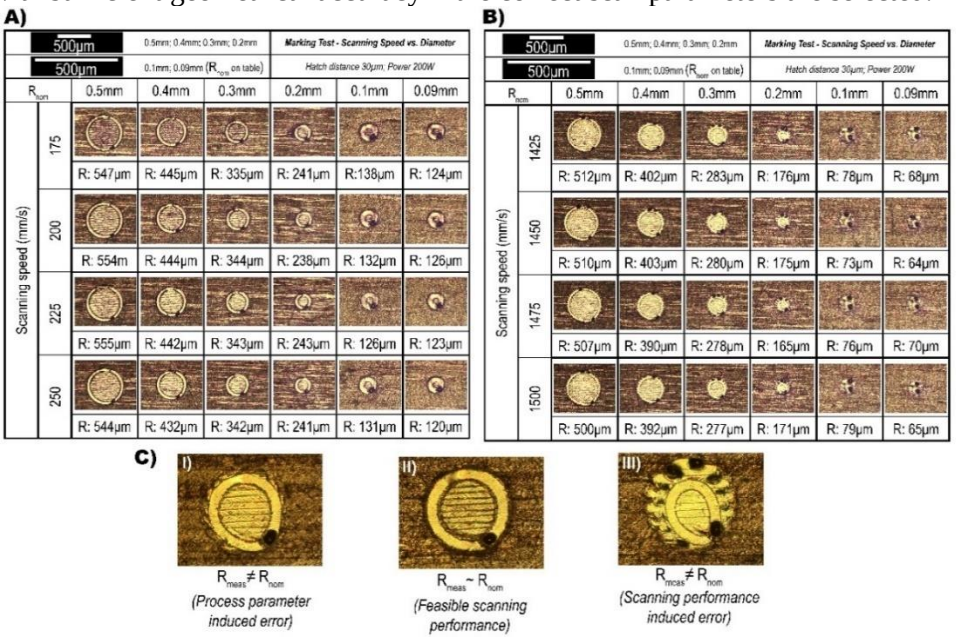

Figure 3. Representative sample characterization tables: A) Low scanning speeds and expected scanning performance (only dimensional error that is caused by the nonoptimal laser power). B) Relatively high scanning speeds and poor scanning performance for ultra-fine segment (shape and dimension error). C) Process and scan induced error description.

REFERENCES

Abele, E., Stoffregen, H. A., Klimkeit, K., Hoche, H., & Oechsner, M. (2015). Optimisation of process parameters for lattice structures. *Rapid Prototyping Journal*, *21*(1), 117–127. https://doi.org/10.1108/RPJ-10-2012-0096

Kranz, J., Herzog, D., & Emmelmann, C. (2015). Design guidelines for laser additive manufacturing of lightweight structures in TiAl6V4. *Journal of Laser Applications*, *27*(S1), S14001. https://doi.org/10.2351/1.4885235

Lopez Taborda, L. L., Maury, H., & Pacheco, J. (2021). Design for additive manufacturing: a comprehensive review of the tendencies and limitations of methodologies. *Rapid Prototyping Journal*, *April 2020*. https://doi.org/10.1108/RPJ-11-2019-0296

Thompson, M. K., Moroni, G., Vaneker, T., Fadel, G., Campbell, R. I., Gibson, I., Bernard, A., Schulz, J., Graf, P., Ahuja, B., & Martina, F. (2016). Design for Additive Manufacturing: Trends, opportunities, considerations, and constraints. *CIRP Annals - Manufacturing Technology*, *65*(2), 737–760. https://doi.org/10.1016/j.cirp.2016.05.004

Wang, D., Wu, S., Bai, Y., Lin, H., Yang, Y., & Song, C. (2017). Characteristics of typical geometrical features shaped by selective laser melting. *Journal of Laser Applications*, *29*(2), 022007. https://doi.org/10.2351/1.4980164

CREEP BEHAVIOR OF 3D PRINTED CB/PEI COMPOSITES

Fulden Kaygınok[1,6], Merve Karabal[2,6], Alptekin Yıldız[3,6], Uğur Emanetoğlu[4,6], Hülya Cebeci[5,6]
[1]*Advanced Materials Technologies Research Division, ASELSAN Inc., Istanbul 34906, Turkey*
f.kayginok@gmail.com
[2]*Department of Aeronautical Engineering, Istanbul Technical University, Istanbul 34469, Turkey*,
karabal17@itu.edu.tr
[3]*Aviation Institute, Istanbul Technical University, Istanbul 34469, Turkey, alyildiz@itu.edu.tr*
[4]*Polymer Science and Technology, Istanbul Technical University, Istanbul 34469, Turkey*,
ugur.emanetoglu@gmail.com
[5] *Department of Aeronautical Engineering, Istanbul Technical University, Istanbul 34469, Turkey*,
geyikh@itu.edu.tr
[6]*Aerospace Research Center, Istanbul Technical University, Istanbul 34469, Turkey*

ABSTRACT

Reinforcing polymeric materials used in many 3D printed parts may bring several advantages such as multifunctionality by Fused Filament Fabrication (FFF). In this study, carbon black (CB) reinforced polyetherimide (PEI) filaments at 5, 10, and 20 wt.% CB contents were fabricated in a twin-screw extruder with a ratio of L/ D = 22 at 360℃ and 210 rpm. CB/PEI composites were printed using a custom-made 3D printer with 390℃ of nozzle temperature, -45°/+45° raster angle, and 100% infill. Thermogravimetric analysis showed that the thermal stability of neat PEI did not significantly change with the presence of CB. However, dynamic rheology analysis introduced CB-PEI interaction by a 5E5% increase for 20 wt.% CB/PEI in the storage modulus and a decrease in the frequency dependency of neat PEI. Besides, thermomechanical and mechanical properties improved with CB content and the highest flexural modulus was obtained from 20 wt.% CB/PEI as 1.8 GPa at 170℃. On the other hand, a short-term creep test was conducted to evaluate the in-service performance of the composites, and the results showed that the increase in CB concentration decreased the creep compliance by 40% for 5 wt.% CB/PEI compared to neat PEI at 30℃. With such a low-cost filler as CB, the addition can bring the tunability of PEI for several advanced applications.

Keywords: CB/PEI composites, high performance, creep behavior, TTSP

DEFECT DETECTION WITH IMAGE PROCESSING AND DEEP LEARNING IN POLYMER POWDER BED ADDITIVE MANUFACTURING SYSTEMS

E. Arslan[1,2], D. Ünal[1], O. Akgün[2], T. Çonka Yıldız[2]
[1]*R&D Prototyping Departman, Arçelik A.Ş., Istanbul, Turkey E-mail*
[2]*Departmant of Mechatronics Engineering, Turkish-German University, Istanbul, Turkey*
**Corresponding Author: deha.unal@arcelik.com*

ABSTRACT

Selective Laser Sintering (SLS) is a type of additive manufacturing process which uses a laser to fuse polymer particles on the powder bed. The process critically relies on controlling the heat and uncontrolled thermal gradients can cause the parts to curl during the process, which may fail the ongoing build with a cost. This layer-wise manufacturing process needs to monitor the continuing build to ensure the process is free from problems. In this paper, deep learning-based defect detection system has been developed to detect any defect (curling, part shifting, short feed). The developed detection system aims to detect the existence of the anomaly during powder bed fusion process and send instant error notifications to the operator. Detection of the anomaly is a binary classification problem and it is solved with the scratch model. The novelty of the developed defect detection algorithm is, it can work independently from the size of the build area, the shape of the part and the location of the part. This study shows the detection system's effectiveness developed by the deep learning method without continuous human supervision in polymer powder bed additive manufacturing processes.

DESIGN AND ADDITIVE MANUFACTURING OF PEEK IMPLANTS FOR PATIENT-SPECIFIC CRANIOPLASTY SURGERY

M. Onur Demirak[1], Harun Demirci[2]
[1]*Trabtech, onur.demirak@trabtech.co*
[2]*Ankara Yıldırım Beyazıt Üniversitesi, Tıp Fakültesi, Cerrahi Tıp Bilimleri, Beyin ve Sinir Cerrahisi, hdemirci@ybu.edu.tr*

ABSTRACT

Additively manufactured patient-specific implants are developed for the cases where the standard implant solutions are inadequate. Steps to obtain an accurate patient-specific implant require knowledge of medical and engineering sciences, hence, physician-engineer cooperation. This study aimed to generate a tailor-made implant design for bilateral cranial defect and fabrication of the implant by using a fused filament fabrication(FFF) additive manufacturing technique. Computed tomography belonging to the patient was converted to 3D models via medical image processing. 3D anatomical models of the patient were printed by using SLA technology to plan the surgery. Implant design has been made through medically certified software by adopting design for additive manufacturing rules. Additive manufacturing technology-material combination has been determined depending on the mechanical behavior of the material after implementation, biological requirements of the region, and producibility of the material by selected AM technology. According to those, the implant has been produced in polyetheretherketone(PEEK) material using FFF technology. As a recently emerging technique in the biomedical field, printing ready-to-use, medical-grade PEEK material requires optimization of process parameters. The studies are made and a comparison analysis between digital and physical implant models has been done. After implementation, clinical experience has been reported and radiological results were evaluated.

Keywords: Medical Additive Manufacturing, Patient-Specific, PEEK, Implant, Cranioplasty

1. INTRODUCTION

Additive manufacturing technologies make alternative approaches possible for the medical field. They revolutionize modern personalized medicine. While the need for patient-specific implants rises, advancements in additive manufacturing technologies are increased, and 3D printers which are specialized in the medical field are commercialized. Craniomaxillofacial implant development is one of the most plentiful research fields for additive manufacturing and its materials. Titanium and its alloys with the combination of powder bed fusion have been utilized for years. However, their mechanical properties such as high elastic modulus cause stress shielding effect in the long term[3]. Also, the bioactive structure of one of the most used Ti alloys, Ti-6Al-4V has been mentioned in the follow-ups with an excessive immune response, [2] . Polyetheretherketone (PEEK) has been used as a consistent alternative to metals and alloplastics, especially in reconstruction surgery. PEEK exhibits good biocompatibility with its bioinert structure, high chemical resistance and low density (1.32 g/cm2) [1]. The fused filament fabrication method made it feasible to create irregular anatomically shaped PEEK geometries which is fully adaptable to the defect site. The need has been increased and there is a current trend to develop FFF machines and PEEK material specializing in the medical field. In this study, we present a workflow to generate patient-specific PEEK implants using FFF technology. The clinical applicability of the design and fabrication parameters has been assessed through the bilateral cranioplasty case.

2. MATERIALS AND METHODS

After computed tomography (CT) of the patient was gathered, the Digital Imaging and Communications in Medicine (DICOM) data was imported to the medical imaging software (Mimics 24.1, Materialise, Leuven, Belgium). Hard tissue segmentation has been realized using Hounsfield units and a 3D model of the cranium was created. Medically certified computer-aided design software (3-matic Medical 16.0, Materialise, Leuven, Belgium) has been utilized to generate accurate cranial prostheses. The wall thickness analysis has been made and the part was exported in standard tessellation language (.STL) format. The STL file was then imported to the 3D slicer (Simplify3D 4.1.2, Simplify3D, Cincinnati, ABD) and pre-fabrication planning has been done. FFF PEEK 3D printer (M220, Apium Additive Technologies GmbH, Karlsruhe, Germany) which maintains a sterile environment following biocompatibility standards (ISO 10993) while fabrication has been preferred for additive manufacturing. The filament has been chosen as a medical-grade 1.75 mm PEEK filament ((Evonik VESTAKEEP ® i4 G resin, Evonik Industries AG, Essen, Germany). After 3 months from the implementation post-

operational CT is gathered. DICOM data is imported to medical imaging software and part comparison analysis has been made.

3. RESULTS AND DISCUSSION

The results after fabrication by using optimized process parameters (Table 2) showed that the roughness of the implant was low according to the clinical perspective except for the areas of the support structures were located. Due to the controllable printing conditions thanks to the closed chamber build platform, majorly a light tan color has been observed which is a sign of good thermal distribution and a high level of crystallization.

Table 2. Optimized process parameters.

Parameter	Unit	Value
Layer Thickness	µm	0.1
Infill Rate	%	100
Nozzle Temperature	˚C	480
Airflow Temperature	˚C	140
Infill Pattern	-	Rectilinear

The post-operational radiological results showed that the implants were successfully fitted on to defect site. The part comparison analysis showed a clinically acceptable dimensional difference between digital and physical implant models. The deviations varied from 1.9 mm to -1.16 mm. This range is majorly caused by the challenging imaging and processing phase of PEEK due to its radiolucent surface. According to the clinician's statement, the clinical experience was positive due to the implant's proper design and fabrication.

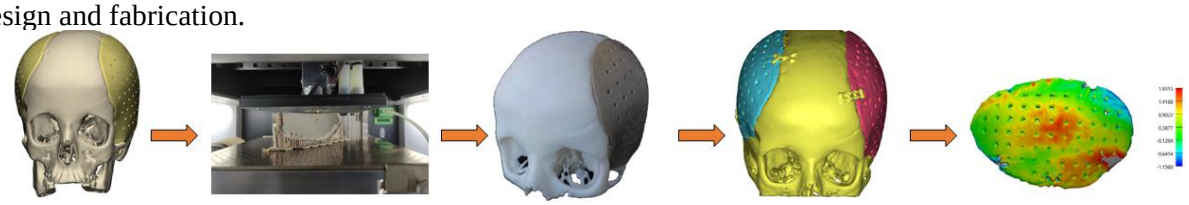

Figure 4. Schematic demonstration of the study evolution from left to right (1) implant design, (2) FFF additive manufacturing, (3) assessment of the implant with anatomical model (4) assessment of the implant radiography after implementation (5) dimensional comparison

4. CONCLUSIONS

In this study, the design and fabrication workflow for patient-specific PEEK cranial implants has been developed. The FFF process parameters for large cranial implants have been developed and assessed with clinical approaches. The promising results proved that personalized medicine will be much more accessible with the help of additive manufacturing.

REFERENCES

[1] Panayotov, I. V., Orti, V., Cuisinier, F., & Yachouh, J. (2016). Polyetheretherketone (PEEK) for medical applications. Journal of Materials Science: Materials in Medicine 2016 27:7, 27(7), 1–11. https://doi.org/10.1007/S10856-016-5731-4

[2] Souza, J. C. M., Apaza-Bedoya, K., Benfatti, C. A. M., Silva, F. S., & Henriques, B. (2020). A Comprehensive Review on the Corrosion Pathways of Titanium Dental Implants and Their Biological Adverse Effects. Metals 2020, Vol. 10, Page 1272, 10(9), 1272. https://doi.org/10.3390/MET10091272

[3] Torres, Y., Trueba, P., Pavón, J., Montealegre, I., & Rodríguez-Ortiz, J. A. (2014). Designing, processing and characterisation of titanium cylinders with graded porosity: An alternative to stress-shielding solutions. Materials & Design, 63, 316–324. https://doi.org/10.1016/J.MATDES.2014.06.012

DESING OF A COMPLIANT CLAMPING MECHANISM FOR FDM BED IN ADDITIVE MANUFACTURING

Çağıl Merve Tanık[1], Raşit Karakuş[2]
[1]*ASELSAN Inc., Ankara, Turkey, cagilmerve@aselsan.com.tr*
[2]*Department of Mechanical Engineering, Hacettepe University, Ankara, Turkey, rasitkarakus@hacettepe.edu.tr*

ABSTRACT

Nowadays spread of 3D printers is accelerated all over the world because of the recent developments in Additive Manufacturing (AM). Through AM complex geometries can be produced easier than the traditional manufacturing methods. Obviously, cost and time savings are one of the most important factors in manufacturing components with additive processes. However, large-size products have difficulties of transfer of research results in physical items in AM for various industries. Fused deposition modeling (FDM) is the most widely used type of 3D printing for most consumers. To have a successful print, proper 3D print bed platform adhesion is critical. For a supporting base of the design, multiple layers of filament are extruded in a pattern-like mesh that is called Raft. If the materials of the model are prone to wrapping, tip over, and fail later in the print rafts are very useful. Addition to the Raft, bed adhesives are also used to form a stickier layer for prints. Temperature-controlled chambers are also useful for avoiding wrapping. However, while printing larger parts that are spread through the print bed, these anti-wrap methods would not be sufficient due to the inequivalent cooling processes. For these types of 3D prints, a compliant bistable clamping mechanism will be designed and it will be actuated automatically with the aid of the algorithm embedded in the code. Once the printing operation is started, the designed clamps are activated at a certain point for stabilizing the product.

Keywords: Additive manufacturing, 3D printing, clamping mechanism, compliant mechanism

DEVELOPMENT AND STATIC LOAD TESTİNG OF ADDITIVELY MANUFACTURED STAINLESS STEEL NOSE LANDING GEAR AIRCRAFT PART FOR CIVIL AVIATION APPLICATIONS

Talha Muslim[1], Omer Faruk Yazici[2], Taner Karagoz[3], Furkan Ercel[4], Dilara Ergin[5], Oguzhan Yilmaz[6], Recep Ozkok[7], Metin Calli[8], Alperen Bayram[9], Orkun Tekelioglu[10]

[1] *Coşkunöz Holding R&D Center, tmuslim@coskunoz.com.tr*
[2] *Coşkunöz Holding R&D Center, ofyazici@coskunoz.com.tr*
[3] *Coşkunöz Holding R&D Center, TKARAGOZ@coskunoz.com.tr*
[4] *Coşkunöz Holding R&D Center, fercel@coskunoz.com.tr*
[5] *Coşkunöz Holding R&D Center, dergin@coskunoz.com.tr*
[6] *Advanced Manufacturing Technologies Research Group (AMTRG), Gazi University, oguzhanyilmaz@gazi.edu.tr*
[7] *Coşkunöz Holding R&D Center, rozkok@coskunoz.com.tr*
[8] *Coşkunöz Holding R&D Center, MCALLI@coskunoz.com.tr*
[9] *Coşkunöz Holding R&D Center, abayram@coskunoz.com.tr*
[10] *Coşkunöz Holding R&D Center, otekelioglu@coskunoz.com.tr*

ABSTRACT

Coskunoz and Industry partners have been working towards manufacturing process development to reduce costs and lead times for parts used in civil aviation applications in Turkey with the goal to reduce the overall production cost. One technique evaluated is laser metal deposition (LMD). The aim was to design, develop and test a full scale additively manufactured stainless steel part for the nose landing gear of an aircraft. Conventionally the part was made by machining a forged stainless steel billet. To advance the manufacturing process further, Coskunoz investigated the feasibility to manufacture such a large critical component via additive manufacturing (LMD). Multiple materials were tried to find a suitable replacement for the conventional material. LMD process parameters were optimized, and the part was successfully manufactured and tested. This paper describes the design, development, manufacturing and testing of a critical component of a nose landing gear of a civil aviation aircraft and the lessons learnt throughout the design and development process.

Keywords: Metal Additive Manufacturing, Laser Metal Deposition, Process Development, Precipitate Hardening Stainless Steels

1. INTRODUCTION

Additive manufacturing (AM) technologies continue to mature creating new opportunities for applications in civil aviation. Metal AM technologies enable benefits such as significant reduction in lead times, reduction in buy to fly ratio, enhanced part performance due to added functionalities, and cost reduction. Landing gear of aircraft operates in very harsh conditions making their design and manufacturing expensive and time consuming due to many manufacturing techniques involved. AM offers design and manufacturing feature not previously possible with conventional manufacturing processes. Additive Manufacturing is not a process that will replace all traditional manufacturing techniques, however it does provides substantial advantages. Coskunoz is exploring the use of AM for medium to large sized critical landing gear parts used in aircraft through design, development and static load testing.

2. MATERIALS AND METHODS

The aim was to design, develop, manufacture and test a medium to a large-sized critical component of the aircraft landing gear. A precipitate hardening stainless steel (PH SS) part was selected that attaches the nose landing gear assembly to the body of the aircraft. Initially, the boundary conditions were defined and finite element analysis was performed to identify the most critical regions of the part. To maximize the benefit of producing the part with AM, the part geometry was optimized. Many designs were obtained. The part was to be produced with laser metal deposition (LMD) process. As compared to powder bed fusion techniques, LMD offers relatively less design freedom. A design was finalized that was manufacturable with a weight reduction of 10.77%. PH 17-4 stainless steel was chosen as the material of choice to manufacture the part additively. To successfully produce the part, process parameters were developed taking into account the geometrical, metallurgical, and mechanical properties with minimal presence of defects such as pores/cracks. Many experimental trials were conducted and 1D, 2D and 3D optimizations were performed. Destructive testing in different directions was performed. This is because AM is an anisotropic process and generally mechanical properties are

lower, especially in the build direction. Tensile and Charpy coupons were heat-treated with different heat treatment conditions to understand and choose the most appropriate heat treatment condition. Once process parameter ranges were developed, tool paths were generated and part was deposited. The near net-shaped part underwent machining and heat treatment with hot isostatıc pressing (HIP). The part underwent an X-ray CT examination post to identify the presence of internal defects if any. Later the part was tested on the specially designed fixture to simulate the real-life boundary conditions and the part successfully passed the static load test. Figure 1 shows the process workflow.

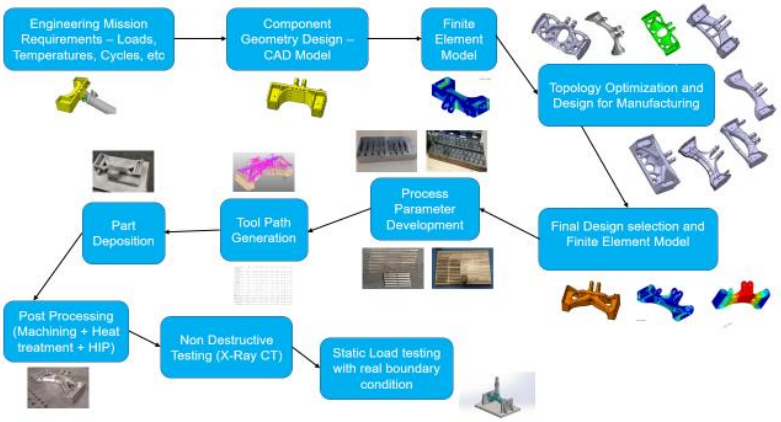

Figure 1. Process Workflow

3. RESULTS AND DISCUSSION

Valuable lessons were learnt during the whole process. It was leant that it is hard to manufacture sharp corners with LMD because they can be affected by the accelerations and decelerations of the robot. Curved surfaces are more suitable, especially around the sharp corners. Heat accumulates as the height of the deposit increases. It is critical to maintaining a thermally stable process to minimize stresses induced in the part due to continuous heating and cooling cycles. Suitable dwell time can be chosen and temperature must be monitored in real-time to prevent defects. Heat treatment was observed to significantly enhance the mechanical properties due to the precipitation of Copper precipitates. Porosity can be minimized by choosing suitable energy densities.

4. CONCLUSIONS

Precipitate hardening stainless steel (PH SS) was successfully designed, developed, additively manufactured and tested. The part successfully passed the static load test proving that LMD can be used to fabricate medium to large-sized critical parts that can perform in harsh conditions.

REFERENCES

Gradl, P. R., Protz, C., Greene, S. E., Ellis, D., Lerch, B., & Locci, I. (2017). Development and Hot-fire Testing of Additively Manufactured Copper Combustion Chambers for Liquid Rocket Engine Applications. 53rd AIAA/SAE/ASEE Joint Propulsion Conference. https://doi.org/10.2514/6.2017-4670

DEVELOPMENT OF A DIGITAL IMAGE PROCESSING ALGORITHM FOR ANOMALY DETECTION IN LARGE SCALE ADDITIVE MANUFACTURING

Sinan Keskin[1], Omer Eyercioglu[2], and Engin Tek[3]
[1]*sinankeskin15@gmail.com*
[2]*eyercioglu@gantep.edu.tr*
3engintek@outlook.com

ABSTRACT

Large Scale Additive Manufacturing (LSAM) defines a system that can be used for printing components on the order of several meters at high extrusion rates (up to 50 kg/hr). The feedstock material is in the form of thermoplastic or fiber-reinforced thermoplastic pellets which are almost 20 times cheaper than the filament-based feedstock. The system has the potential to significantly affect the automobile, aerospace, and energy industries. However, by increasing the scale of additive manufacturing, more numerous and diverse problems arise. Particularly, the variety of errors, long-term production costs, and energy inefficiency in 3D printing processes exceeding one cubic meter constitute a major hindrance to development in this field. The formation of defects such as warping, distortion, porosity, surface roughness, etc. needs to be monitored in real-time under the supervision of the operator for preventing permanent deformations. Recently, the developments in the field of image processing make it more convenient to monitor these problems in situ and to intervene in the process during printing. In this study, the common anomalies in the LSAM of ABS parts that can be recognized by image processing algorithms were reviewed.

Keywords: Large scale additive manufacturing (LSAM), Image processing, Anomaly detection,

DEVELOPMENT OF ALUMINUM ALLOY POWDERS FOR ADDITIVE MANUFACTURING

Beyza Bilgiler[1], Mustafa Safa Yılmaz[2], İrem Şebnem Sorucu[1], Selin Alanyalı[1], Bülent Genç[1]
[1]*Sentes-BIR, R&D Center, beyza.bilgiler@sentes.com.tr*
[2]*Aluminum Test Training and Research Center(ALUTEAM), Fatih Sultan Mehmet Vakif University (FSMVU), m.safayilmaz@gmail.com*

ABSTRACT

This study aims to the production of AlSi10Mg powders with gas atomization and examines the effects of atomization parameters on powder characteristics and usability for the Laser Powder Bed Fusion (PBF-LB) process. 3 different powders were produced and characterized and then parts were produced with 18 different production parameters in the EOS M290 machine. The parts' surface roughness, porosity, hardness, optical microscope, and scanning electron microscope analyses were investigated. The particle size of powder used in the production is 20-63 µm, the oxygen/hydrogen level is appropriate, and its chemical composition is similar to the standard AlSi10Mg alloy. The results demonstrated that surface roughness (Ra) differed around 4-5% compared with parts produced with manufacturer A powder. Ra values on different surfaces were investigated with different parameters. Standard levels were achieved in porosity analyzes (99.86%). It has been observed that the thermal stresses caused by the heat generated by the parameters in the system cause significant differences in the hardness value (122±12 Vickers). In OM and SEM studies, parameter-related errors (energy deficiency, formation of gas pores, fusion errors, etc.) and differences in structures were determined.

(Manufacturer A powder is used in AM systems at the TRL9 level.)

Keywords: AlSi10Mg alloy, metal powder, gas atomization, powder characterization, parameter optimization

1. INTRODUCTION

Laser powder bed fusion (PBF-LB) is an additive manufacturing (AM) method that provides the fabrication of functional complex parts. PBF-LB is a layer-by-layer process, and the laser beam is used as a heat source that fuses the particles. Aluminum alloys are used in the AM sector to produce parts that cannot be produced with traditional methods such as casting or forging. Metallic powders are raw materials for this method and are usually produced by gas atomization. Gas atomization with a close-coupled atomizer (CC) is used for the AM metal powders due to the smaller particle size efficiency. During the process, molten metal is poured through a nozzle or orifice into an atomization chamber where the melt is atomized by flowing inert gas *(Jose Alberto Muñiz-Lerma, 2018)*. The purpose of this paper, compare the results of the powder characteristics of various atomization temperatures with the manufacturer A powder. Chemical composition, microstructure, liquidus.-solidus temperature and phase analyses were observed. Also, the usability of AlSi10Mg powders and effects of process parameters (laser power, laser speed, and hatch distance) on the PBF-LB process with different characterization methods such as surface roughness, porosity, hardness, and microstructure were investigated.

2. MATERIALS AND METHODS

AlSi10Mg powders were produced with CC Gas Atomization with different atomization temperatures in Sentes-BIR. The atomization temperature of P1, P2, and P3 is 860 ºC, 820 ºC, and 780 ºC respectively. The atomization gas is nitrogen, and the charge weight is 20 kg. Chemical composition was measured with ICP-OES and fusion methods. The particle size was measured by Laser Diffraction. The microstructure of powders was analyzed with OM and SEM. XRD analysis was conducted. Parts were produced with the 18 different process parameters (Laser power between 15-370 W, scan speed between 700-1600 mm/s, hatch distance between 0.1-0.19 mm, and layer thickness was set at 0.03 mm) by the PBF-LB machine at ALUTEAM and then parts were characterized.

3. RESULTS AND DISCUSSION

Table 1 illustrates the chemical composition of P1, P2, P3, and PA AlSi10Mg powder. Changing the atomization temperature has resulted in the change of Si and Mg values, but still in ASTM E3061 limits. Moreover, all powders were examined in SEM and they are mostly spherical and satellite free.

Table 1. Chemical composition results of P1, P2, P3, and PA AlSi10Mg powder.

	ASTM E3061 AlSi10Mg	P1 AlSi10Mg	P2 AlSi10Mg	P3 AlSi10Mg	PA AlSi10Mg
Al	Balance	Balance	Balance	Balance	Balance
Si	9.0-11.0	10.01	9.52	9.44	10.42
Mg	0.25-0.45	0.35	0.32	0.31	0.40
Fe	0.40 max.	0.11	0.12	0.10	0.16
Cu	0.03 max.	0.00	0.02	0.03	0.02
Ni	0.05 max.	0.01	0.01	0.01	0.03
Zn	0.10 max.	0.02	0.02	0.02	N/A
Ti	0.15 max.	0.01	0.01	0.02	0.01

Figure 1 shows the characterization results of the additively manufactured samples.

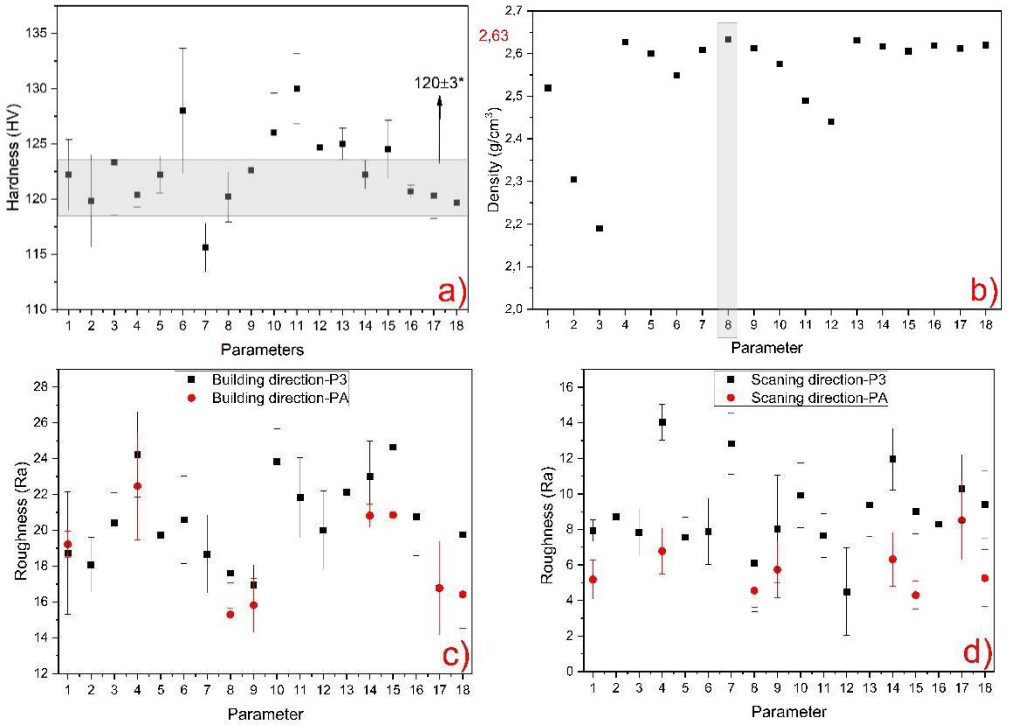

Figure 1. Additively manufactured samples characterization results; a) Hardness, b)Density, c-d) Roughness

4. CONCLUSIONS

- AlSi10Mg powders were produced with CC gas atomization, in ASTM E3061 alloy limits successfully.
- According to powder characterization results, similar results were obtained compared to PA.
- Production did not have to stop in any of the 18 parameters.
- Parameter differences caused production-related errors and decreases in density values occurred. This also affected the hardness values. In addition, the changes in the parameter created differences in the building and scanning direction roughness values of the material. With these characterizations, it has been determined that the most appropriate parameter is Parameter-8 (370 W, 100 mm/s, 0.19 mm).

REFERENCES

Jose Alberto Muñiz-Lerma, A. N.-N. (2018). A Comprehensive Approach to Powder Feedstock characterization for Powder Bed Fusion Additive Manufacturing: A Case Study on AlSi7Mg.

MATERIALS.

DEVELOPMENT OF MULTIFUNCTIONAL 3D PRINTED SCAFFOLD FOR BIOMEDICAL APPLICATIONS

İlknur Kökcü[1], Meltem Eryıldız[1,2], Mirigül Altan[1,3], Sedat Odabaş[4]
[1]*Department of Mechanical Engineering, Yildiz Technical University, Istanbul, Turkey, ikokcu@gmail.com*
[2] *Department of Mechanical Engineering, Beykent University, Istanbul, Turkey, meltemeryildiz@beykent.edu.tr*
[3] *Department of Biomedical Engineering, Yildiz Technical University, Istanbul, Turkey, meksi@yildiz.edu.tr*
[4]*Ankara University, Department of Chemistry, Ankara, Turkey, sodabas@ankara.edu.tr*

ABSTRACT

Additive manufacturing (AM) has become significant in biomedical applications due to necessity of customized fabrication of the patients. Fused deposition modeling (FDM) is one of the low cost additive manufacturing (AM) techniques that can provide fast and accurate solutions in biodegradable hard tissue applications. However, commercial filaments do not provide patient-specific requirements. In this study, it was aimed to develop a multifunctional filament for scaffold fabrication by FDM process that could carry the drug and provide sustainable drug release. Metformin (MET) was selected for drug loading onto halloysite nanotube (HNT). In the matrix of polylactic acid (PLA), HNT was responsible for both carrying the metformin and improving the mechanical properties of the scaffold. Scaffolds with infill design of grid porous structure was fabricated. Tensile test properties and controllable drug release of the printed scaffolds were investigated. According to the results, scaffolds have shown about 125% of increment in tensile strength. Drug release was quite sustainable till five days and 50% of the loaded drug were gradually released over time. It has been seen that the developed drug loaded scaffold has potential to be used in biomedical application of hard tissues.

Keywords: Fused deposition modeling, filament, scaffold, HNT, drug loading

1. INTRODUCTION

Recent breakthroughs in additive manufacturing and biomaterials have proven that drug-eluting scaffolds have a lot of promise. Scaffolds offer the necessary mechanical support at the implantation site and then resorb over time, shifting the load to newly created tissue and eliminating the need for a revision operation to remove the scaffold. The flexibility of FDM method also allows to combine polymeric materials with drugs. This is especially important for implanted scaffolds that have a high infection risk (Shaqour et al., 2020). When the studies on the manufacturing of drug-loaded structures by the FDM method are reviewed, two different types of applications are encountered. The first is the manufacturing of capsules or tablets with the FDM method (Saviano et al., 2019; Matijašić et al., 2019). Hovewer, these studies are not about the manufacturing of a scaffold, but are about tablet drug fabrication. The second technique can be accomplished by immersing the filament in drug solutions (Farto-Vaamonde et al., 2019).

Polylactic acid (PLA) has high mechanical properties, but it also has certain drawbacks, such as brittleness, low heat resistance and low shear and crystallisation rates. Thus, there are different PLA nanocomposites to overcome these drawbacks. Incorporating halloysite nanotubes (HNT) into a PLA polymer matrix provides a novel class of materials with a wide set of properties and applications. HNT has a tubular shape so it is good for drug loading applications and biocompatible with the human body (Kamble et al., 2012). A few studies were focused on 3D printing of PLA with HNT for biomedical applications (Luo et al., 2020; Weisman et al. 2017). However, to the best of the authors knowledge, the drug loaded HNT/PLA nanocomposite scaffolds is not much explored. In this study, MET loaded HNT/PLA scaffolds were fabricated by using FDM method. Mechanical properties and drug release of the nanocomposite scaffolds were investigated.

2. MATERIALS AND METHODS

Halloysite nanotube (Sigma-Aldrich) and metformin drug particles were prepared through physical and electrostatic adsorption method. After drug loading, polylactic acid (PLA 3001D, resinex) and MET_HNT was melt mixed by Rondol twin-screw extruder (L/D=10). All the prepared filaments were processed with a Prusa i3 FDM printer to fabricate the scaffold samples. Tensile tests were applied by INSTRON 5982 in compliance with ASTM D412. Drug release tests were performed on the 3D printed scaffolds. The release kinetics of the MET was assessed by using a UV-vis spectrophotometer at 235 nm based on calibration curve.

3. RESULTS AND DISCUSSION

Table 1 shows tensile strength and elongation of PLA/MET_HNT nanocomposite scaffolds fabricated by FDM.

Table 1. Tensile test results

Material	Max Tensile Strength (MPa)	Max Tensile Elongation (mm)
Neat PLA	9,48	1,11
PLA/MET_HNT%1	15,97	1,38
PLA/MET_HNT%3	21,28	1,42
PLA/MET_HNT%5	14,13	1,17

In comparison to neat PLA, tensile strength and elongation increased with the addition of stiffer HNT, as seen in Table 1. According to the drug release results at pH 7.4, more than half of the drug was released by the end of 5 days by weight, as shown in Figure 2.

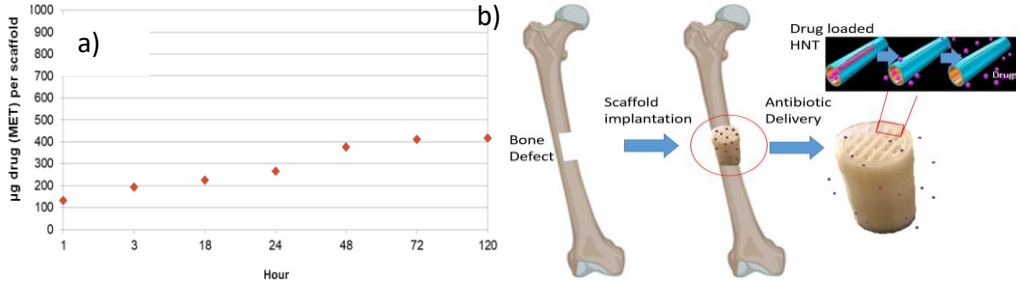

Figure 2. a) Cumulative MET release in scaffolds, b) Drug releasing from 3d printed scaffold

4. CONCLUSIONS

Metformin (MET) loaded halloysite nanotube (MET_HNT)/Polylactic acid (PLA) scaffolds were fabricated by FDM process. Tensile test properties and controllable drug release of the scaffolds were investigated. According to the results, scaffolds have shown about 125% of increment in tensile strength. Drug release was quite sustainable till five days and 50% of the loaded drug were gradually released over time. It has been seen that the developed drug loaded scaffold by 3D printing has potential to be used in biomedical application of hard tissues.

REFERENCES

Shaqour, B., Samaro, A., Verleije, B., Beyers, K., Vervaet, C., & Cos, P. (2020). Production of drug delivery systems using fused filament fabrication: a systematic review. Pharmaceutics, 12(6), 517.

Saviano, M., Aquino, R. P., Del Gaudio, P., Sansone, F., & Russo, P. (2019). Poly (vinyl alcohol) 3D printed tablets: The effect of polymer particle size on drug loading and process efficiency. *International journal of pharmaceutics*, *561*, 1-8.

Matijašić, G., Gretić, M., Vinčić, J., Poropat, A., Cuculić, L., & Rahelić, T. (2019). Design and 3D printing of multi-compartmental PVA capsules for drug delivery. *Journal of Drug Delivery Science and Technology*, *52*, 677-686.

Farto-Vaamonde, X., Auriemma, G., Aquino, R. P., Concheiro, A., & Alvarez-Lorenzo, C. (2019). Post-manufacture loading of filaments and 3D printed PLA scaffolds with prednisolone and dexamethasone for tissue regeneration applications. *European Journal of Pharmaceutics and Biopharmaceutics*, *141*, 100-110.

Kamble, R., Ghag, M., Gaikawad, S., & Panda, B. K. (2012). Halloysite Nanotubes and Applications: A Review. *Journal of advanced scientific research*, *3*(2).

Luo, Y., Humayun, A., & Mills, D. K. (2020). Surface modification of 3D printed PLA/halloysite composite scaffolds with antibacterial and osteogenic capabilities. *Applied Sciences*, *10*(11), 3971.

Weisman, J. A., Jammalamadaka, U., Tappa, K., & Mills, D. K. (2017). Doped halloysite nanotubes for use in the 3D printing of medical devices. *Bioengineering*, *4*(4), 96.ld

DIMENSIONAL ACCURACY INVESTIGATION OF TIO_2 REINFORCED POLYMER NANOCOMPOSITE PARTS PRINTED BY DLP

Metehan Demirkol[1], Bedri Onur Küçükyıldırım[2]
[1]*Yildiz Technical University, Department of Mechanical Engineering, 34349, Istanbul, Turkey, demirkol@yildiz.edu.tr*
[2]*Yildiz Technical University, Department of Mechanical Engineering, 34349, Istanbul, Turkey, kucukyil@yildiz.edu.tr*

ABSTRACT

In this study, it is aimed to obtain 3D-printed polymer nanocomposite parts with the utmost dimensional accuracy and show how the accuracy is affected by varying fractions of reinforcement. Polyurethane acrylate (PUA) is chosen as the matrix material due to its extensive usage and titanium dioxide (TiO2) nanotube is chosen as the reinforcement material due to its photocatalytic properties, which can provide antibacterial properties for future nanocomposite studies. Nanoresins were prepared by ultrasonic mixing of nanotubes in the resin homogeneously. Sample parts were printed using digital light processing (DLP) and dimensional accuracy is discussed using the data of the optical measurements.

Keywords: Titanium dioxide nanotubes, PUA, nanocomposite, DLP, dimensional accuracy

DIMENSIONAL VARIATIONS IN EBM PRODUCED STRUT-BASED AND TPMS LATTICES

Barış Sokollu[1], Orhan Gülcan[2], Erhan İlhan Konukseven[3]
1Turkish Aerospace, Ankara, Turkey, baris.sokollu@tai.com.tr
2General Electric Aviation, Kocaeli, Turkey, orhan.gulcan@ge.com
2Middle East Technical University, Ankara, Turkey, konuk@metu.edu.tr

ABSTRACT

The aim of this experimental study is to investigate the dimensional variations in Ti6Al4V specimens produced by electron beam melting technology from original CAD geometry. Strut-based and triply periodic minimum surface (TPMS) type of lattice structures were produced and investigated by scanning electron microscope (SEM). Face centered cubic (FCC), body centered cubic (BCC), gyroid, primitive and diamond type of lattices with fixed volume fractions were the main focus in this study. The experimental results revealed that the maximum and minimum dimensional variations were observed on gyroid and diamond specimens, respectively. The SEM images exhibited that excessive and more non-fully melted particles were observed on downfacing surfaces of the struts or walls than up facing surfaces.

Keywords: Electron beam melting, dimensional variation, lattice structure

1. INTRODUCTION

Due to their high energy absorption capability, light weights and high specific strengths, lattice structures find its usage in different industries ranging from automotive and aviation to biomedical and power plants. However, producibility of these structures is a big challenge that researchers need to focus on. Today, additive manufacturing (AM) technologies give novel solutions in terms of producibility of lattice structures. Electron beam melting (EBM) is one of the powder bed fusion type AM processes where metal powders on a build plate are melted by electron beams with the help of Argon or Helium gases in vacuum environment (Zhang et al., 2022). Despite the ease of production, EBM manufactured parts undergo some amount of distortion and dimensional variations due to thermal gradients during manufacturing and resulting residual stresses. It is important to have a knowledge about distortion and dimensional deviation of EBM produced lattice parts to make necessary design changes accordingly so that high energy absorption and mechanical strength can be obtained.
To address this issue, face centered cubic (FCC), body centered cubic (BCC), gyroid, primitive and diamond type of lattices with fixed volume fractions were manufactured by EBM and dimensional variations were evaluated in this study.

2. MATERIALS AND METHODS

Rectangular blocks with 40x40x40 mm dimensions for five types of lattices were modelled by nTopology software. 10x10x10 mm unit cell size with 4 cells in each row and column were used for all specimens. Arcam EBM Q20plus EBM machine was used in the production of the specimens. Ti6Al4V Grade 5 powders with 45-106 μm particle size provided from GE Additive were used in the production. QUANTA 400F Field Emission Scanning Electron Microscope (SEM) and Nikon ECLIPSE MA100 Optical Microscope was used to investigate the diameters of the produced struts and the wall thickness of the sheet surfaces as well as the satellite powder particles sticked to the surfaces.

3. RESULTS AND DISCUSSION

All specimens were manufactured without any observed failure. Produced parts are then subjected to the powder removal by using Powder Recovery System (PRS) provided by Arcam as a standard. The related SEM images of parts after powder removal were shown in Figure 1.

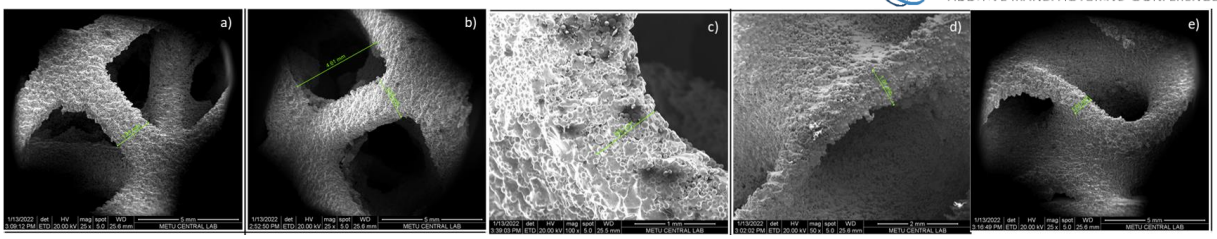

Figure 1. SEM images: a) FCC b) BCC c) Primitive d) Diamond e) Gyroid.

The comparison of the thicknesses obtained from the SEM images with the nominal diameter or wall thicknesses is shown in Table 1.

Table 1. Nominal vs. produced strut diameter / wall thicknesses for different lattices

	FCC	**BCC**	**Primitive**	**Diamond**	**Gyroid**
Nominal (mm)	1.69	1.86	0.73	1.08	1.29
Produced (mm)	1.91	2.06	0.86	1.01	1.01
Error (%)	-13.0	-10.7	-17.8	6.5	21.7

The highest and the lowest errors between nominal and produced strut diameter / wall thickness were observed for gyroid specimens (21.7 %) and diamond specimens (6.5 %), respectively. On the other hand, FCC, BCC and primitive specimens showed 13.0 %, 10.7 % and 17.8 % errors, respectively. Consistent with the literature (Maconachie et al., 2019), it is clear from SEM images that some non-fully melted powder particles were attached to the upper and lower surfaces of the struts/walls and the amount of this adhesion is more on lower surfaces than upper surfaces.

4. CONCLUSIONS

The following conclusions can be drawn from the present experimental study:

- Gyroid specimens showed the highest and diamond specimens showed the lowest amount of dimensional variations
- More non-fully melted powder particles are sticked to the lower surfaces of struts or walls than upper surfaces.

As a future study, compression tests will be performed on these specimens and compressive behavior of different lattice types will be investigated.

REFERENCES

Zhang, L., Wang, J., Liu, Y., Jia, Z. & Liang, S. (2022). Additive manufacturing of titanium alloys. Encyclopedia of Materials: Metals and Allloys, Elsevier Publishing, Amsterdam, Netherlands, pp. 256-274.

Maconachie, T., Leary, M., Lozanovski, B., Zhang, X., Qian, M., Faruque, O., & Brandt, M. (2019). SLM lattice structures: Properties, performance, applications and challenges. Materials and Design, 183, 108137. https://doi.org/10.1016/j.matdes.2019.108137

DIRECTED ENERGY DEPOSITION OF REFRACTORY CR10MO25TA25TI15V25 HIGH ENTROPY ALLOY

O. Umut Tukac1, Eda Aydogan2
[1]*Department of Metallurgical and materials Engineering, Middle East Technical University, umut.tukac@metu.edu.tr*
[2]*Department of Metallurgical and materials Engineering, Middle East Technical University, aydogane@metu.edu.tr*

ABSTRACT

Worldwide growth of energy need requires the increase in the efficiency of energy systems. This results in the increase of operating temperatures and stresses exerted on the used materials especially in nuclear reactors. Therefore, Refractory High Entropy Alloys (RHEAs) due to their high thermal stability and radiation resistance are one of the interest areas of recent studies. In this study CrMoTaTiV RHEA produced by vacuum arc melting and directed energy deposition techniques have been investigated. Process parameter optimization and difference in the resulting products are analyzed and compared with VAM produced samples using XRD, SEM, EBSD and TEM analyses and compression tests.

Keywords: RHEAs, DED, EBSD, TEM

1. INTRODUCTION

Production of refractory high entropy alloys (RHEAs) using conventional methods is challenging due to high melting temperatures and high tendency to oxidize of consisting elements. Therefore, researches on RHEAs are limited with methods like vacuum arc melting(VAM) or powder metallurgy(Müller et al., 2020; Senkov & Woodward, 2011). Moreover, subtractive machining of RHEAs is also difficult due to these alloys have high hardness and their brittle nature. Studies on additive manufacturing of these alloys shown promising results for advanced material production(Dobbelstein, Gurevich, George, Ostendorf, & Laplanche, 2018; Katz-Demyanetz, Gorbachev, Eshed, Popov, & Bamberger, 2020). In this study $Cr_{10}Mo_{25}Ta_{25}Ti_{15}V_{25}$ RHEAs is produced using VAM and directed energy deposition (DED) methods. We present comparative study of the effects these two methods on produced samples. This study shows the possibility of bulk production of RHEAs using in-situ alloying by dynamic powder mixing in DED.

2. MATERIALS AND METHODS

Arc melter samples were manufactured with Compact Arc Melter MAM-1. Granules of Cr, Mo, Ta, Ti and V elements were used in VAM production. DED samples were manufactured with DMG LASERTEC 65 DED hybrid. Powders of Cr, Mo, Ta, Ti and V elements with the size of 50-120 microns were used in DED production.

X-ray diffraction was conducted on the produced samples for phase analysis. Optical microscopy and scanning electron microscopy techniques were used for microstructure analysis. In addition, energy dispersive X-ray spectroscopy (EDX) mapping, electron back scatter diffraction (EBSD), Transmission electron microscopy (TEM) analyses were conducted for both VAM and DED samples.

Mechanical properties of the produced samples were investigated by using microhardness and compression tests. Compression tests were conducted according to ASTM E9-19 standard with a strain rateof10-4s-1.

EFFECT OF HEAT TREATMENTS ON THE MICROSTRUCTURE AND MECHANICAL PROPERTIES OF INCONEL 718 ALLOY FABRICATED BY LASER POWDER BED FUSION METHOD

Özhan Kıtay[1,2], Mert Kaya[2,3], Yusuf Kaynak[2]
[1]*Department of Machine, Bilecik Şeyh Edebali University, Gülümbü Campus, 11230, Bilecik,Turkey*
[2]*Department of Mechanical Engineering, Marmara University, Aydınevler Mah. İdealtepe Yolu no:15 34854 Maltepe/İstanbul,Turkey*
[3]*Department of Mechanical Engineering, Piri Reis University, Postane Mahallesi, Eflatun Sk. No:8, 34940 Tuzla/İstanbul, Turkey*

ABSTRACT

Inconel 718 super alloy fabricated by laser powder bed fusion (LPBF) was subjected to different heat treatments. Microstructures of as-built and heat-treated samples were examined under aging, 980ºC+aging (HT980), and the 1100ºC+aging (HT1100) conditions. The microstructure of the as-built sample in the building direction and scanning direction consists of columnar dendrite and subgrain structures. These structures contain the Laves phase. In aging, most of the melting pools and scanning traces were dispersed and some of the Laves phases were precipitated. After the HT980 and HT1100, all the melting pools and scanning traces disappeared. In both these cases, the majority of the Laves phases collapsed. However, a more homogeneous structure was obtained in H1100. The highest hardness value was HT980 with 39%. However, in HT1100, a more ductile material was obtained despite the 25% increase in hardness.

Keywords: Inconel 718, Additive manufacturing, Heat-treatment, Phase analysis

CONCLUSIONS

Microstructures and precipitation of Inconel 718 samples fabricated by LPBF process and heat treated were examined and their toughness values were determined by Charpy impact test. The main findings can be summarized as follows:

The melting pools of the as-built sample are visible viewed from the building direction, while the scanning traces of the laser beam are visible on the part viewed from the scanning direction. The microstructure of both directions consists of columnar dendrite and subgrain structures.

In aging, melting pools have almost disappeared and grain formation is evident. Some of the Laves phase precipitated in the matrix and the δ phase was concentrated at the grain boundaries.

In HT980, the heterogeneous structure has almost disappeared. However, it was found that 980°C was not a sufficient temperature to completely dissolve the Laves phases. In addition, some of the Nb element precipitated as the δ phase, which decreased the amount of Nb required for the precipitation of the γ" phase.

A homogeneous structure is formed in HT1100. 1100 °C precipitated the δ phase and almost all Laves phases. However, the high pre-heat treatment at 1100 °C caused the recrystallization and dissolution of the particles leaving the subgrain boundaries, causing limitation in grain boundary movement.

The highest hardness increase was 41% in HT980 and 39% in aging. At the same time, in these two cases, the material structure is embrittled. However, although the hardness increase was 25% in HT1100, a more ductile structure was obtained

REFERENCES

1. Li, X., et al., Effect of heat treatment on microstructure evolution of Inconel 718 alloy fabricated by selective laser melting. Journal of Alloys and Compounds, 2018. **764**: p. 639-649.

2. Kaya, M., N. Sunay, and Y. Kaynak, Comparison of finite element and empirical model prediction of surface residual stress in inconel 718 parts fabricated by laser powder bed fusion additive manufacturing. Journal of Additive Manufacturing Technologies, 2021. **1**(3): p. 592-592.
3. Tucho, W.M., et al., Microstructure and hardness studies of Inconel 718 manufactured by selective laser melting before and after solution heat treatment. Materials Science and Engineering: A, 2017. **689**: p. 220-232.
4. Karabulut, Y., E. Tascioglu, and Y. Kaynak, Heat treatment temperature-induced microstructure, microhardness and wear resistance of Inconel 718 produced by selective laser melting additive manufacturing. Optik, 2021. **227**: p. 163907.
5. SUNAY, N., K. Mert, and Y. KAYNAK, CHEMICAL POST-PROCESSING METHODS FOR ENHANCING SURFACE PROPERTIES OF PARTS FABRICATED BY ADDITIVE MANUFACTURING: A REVIEW. Sigma Journal of Engineering and Natural Sciences, 2020. **38**(4): p. 2027-2042.
6. Kim, H., et al., Effect of heat treatment on apatite-forming ability of Ti metal induced by alkali treatment. Journal of Materials Science: Materials in Medicine, 1997. **8**(6): p. 341-347.
7. Huang, X., M. Chaturvedi, and N. Richards, Effect of homogenization heat treatment on the microstructure and heat-affected zone microfissuring in welded cast alloy 718. Metallurgical and materials Transactions A, 1996. **27**(3): p. 785-790.
8. Shan, D. and L. Zhen, Aging behavior and microstructure evolution in the processing of aluminum alloys, in Microstructure Evolution in Metal Forming Processes. 2012, Elsevier. p. 267-297.
9. Thomas, A., et al., High temperature deformation of Inconel 718. Journal of materials processing technology, 2006. **177**(1-3): p. 469-472.
10. Raghavan, S., et al., Effect of different heat treatments on the microstructure and mechanical properties in selective laser melted INCONEL 718 alloy. Materials and Manufacturing Processes, 2017. **32**(14): p. 1588-1595.
11. Huang, W., et al., Heat treatment of Inconel 718 produced by selective laser melting: Microstructure and mechanical properties. Materials Science and Engineering: A, 2019. **750**: p. 98-107.
12. ASTM E23 ‘‘Standard Test Methods for Notched Bar Impact Testing of Metallic Materials”. 2018.
13. Kaynak, Y. and O. Kitay, The effect of post-processing operations on surface characteristics of 316L stainless steel produced by selective laser melting. Additive Manufacturing, 2019. **26**: p. 84-93.
14. Gao, Y., et al., Effect of δ phase on high temperature mechanical performances of Inconel 718 fabricated with SLM process. Materials Science and Engineering: A, 2019. **767**: p. 138327.
15. Komarasamy, M., et al., Microstructure, fatigue, and impact toughness properties of additively manufactured nickel alloy 718. Additive Manufacturing, 2019. **28**: p. 661-675.
16. Wen, D.-X., Y. Lin, and Y. Zhou, A new dynamic recrystallization kinetics model for a Nb containing Ni-Fe-Cr-base superalloy considering influences of initial δ phase. Vacuum, 2017. **141**: p. 316-327.
17. Deng, D., et al., Microstructure and mechanical properties of Inconel 718 produced by selective laser melting: Sample orientation dependence and effects of post heat treatments. Materials Science and Engineering: A, 2018. **713**: p. 294-306.

EFFECTS OF DESIGN PARAMETERS ON SURFACE ROUGHNESS OF ADDITIVELY MANUFACTURED THIN WALL STRUCTURES

Vahap Yogurtcuoglu[1], Ugur Simsek[2], Bahattin Koc[3*]
[1]*Sabanci University, Faculty of Engineering and Natural Sciences, Istanbul, yogurtcuoglu@sabanciuniv.edu*
[2]*General Electric Aviation, Gebze, Kocaeli, ugur.simsek@ge.com*
[3]*Sabanci University, Faculty of Engineering and Natural Sciences, Istanbul, bahattinkoc@sabanciuniv.edu*

ABSTRACT

Additive manufacturing (AM) has enabled the production of complex geometries that are not possible to be manufactured through traditional subtractive methods. Among the AM technologies, direct metal laser melting (DMLM) has gained considerable attention in many engineering industries due to its capability to fabricate components with high resolution. The benefits of DMLM technology have also been utilized in the production of thin-wall structures in the aviation industry. Many internal thin wall surfaces are retained as-build due to inapplicability of surface enhancement methods. Therefore, surface roughness of additively manufactured thin wall structures is thoroughly sensitive to quality of AM process. This may adversely affect the mechanical properties of the end-product. Therefore, in this study, thin-wall specimens made of CoCr are fabricated through DMLM and effects of wall thickness, build angle, laser incidence angle, and spatial distribution of these specimens on the surface roughness are investigated. For that purpose, printed surface topologies are analyzed using an optical profilometer and relationship between the control parameters and standard surface roughness metrics is presented.

Keywords: Surface Roughness, Thin Wall, DMLM, Additive Manufacturing, Design for AM

1. INTRODUCTION

With the numerous advantages provided by the technology, metallic additive manufacturing (AM) has gained great attention from multiple industries, including aviation, automotive, energy and biomedical sectors. Direct metal laser melting (DMLM) is a powder bed fusion technology used in manufacturing of complex shape and thin-walled metallic parts with its ability to fabricate components with high resolution. Besides the advantages, DMLM produces undesired surface roughness due to interaction of several process and design parameters. As-built surface roughness can affect the fatigue and tensile properties adversely. [1,2] Recent growth in the use of AM metals has highlighted the need to understand the effects of process and design parameters on surface finish.

DMLM technique makes it possible to manufacture multiple parts on the same platform simultaneously and provides numerous advantages by using entire working volume of the machine, reducing manufacturing time and raw powder consumption. On the other hand, this method may lead to differences in surface quality of the different parts depending on their location and orientation on the build platform. [3,4] In this study, surface roughness differences of the different thin wall coupons that are manufactured on the same platform are studied. The effects of part thickness, build angle, the angle of incidence of the laser and sample position with respect to the platform on the surface roughness metrics are investigated.

2. MATERIALS AND METHODS

2.1 Design of Experiment

Thin wall flat tensile test coupons are designed in three different thickness values. These coupons are oriented with three different build angles on the build platform. Table 1 summarizes the sample thickness and build orientation values.

Sample Group	Sample Thickness [in]	Build Angle [°]	Number of Sample Printed
1	.035	50	5
2	.055	50	4

3	.075	50	4
4	.035	60	5
5	.055	60	4
6	.075	60	4
7	.035	70	4
8	.055	70	3
9	.075	70	3

Table 1. Design of Experiment

2.2 Material Preparation

Thin wall coupons are manufactured through DMLM (M2, Concept Laser) by using default CoCr build parameters. Coupons are vacuum stress relieved with default VSR parameters for the material (1052°C, 2hrs in vacuum).[5] Coupons, then separated from build platform and support structures are removed with wire EDM.

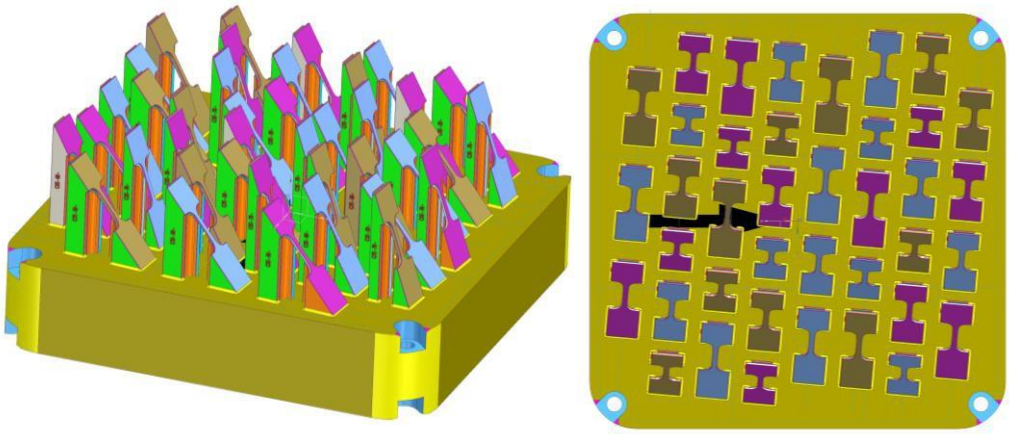

Figure 1. Build Layout

3. RESULTS AND DISCUSSION

Results will be documented.

4. CONCLUSIONS

Relationship between control parameters and surface roughness metrics will be presented.

REFERENCES

[1] J. Gockel, L. Sheridan, B. Koerper and B. Whip, “The influence of edditive manufacturing processing parameters on surface roughness and fatigue life”, International Journal of Fatigue, vol. 124, pp.380-388, 2019. https://doi.org/10.1016/j.ijfatigue.2019.03.025

[2] Everhart, W., Sawyer, E., Neidt, T. et al. “The effect of surface finish on tensile behavior of additively manufactured tensile bars”, Materials Science 51, 3836–3845 2016. https://doi.org/10.1007/s10853-015-9702-9

[3] S. Sendino, M. Gardon, F. Lartategui, S. Martinez, A Lamikiz, “The Effect of the Laser Incidence Angle in the Surface of L-PBF Processed Parts”, Coatings 2020, 10, 1024. https://doi.org/10.3390/coatings10111024

[4] E.E. Covarrubias, M. Eshraghi, “Effect of Build Angle on Surface Properties of Nickel Superalloys Processed by Selective Laser Melting”, JOM 70, 336–342, 2018. https://doi.org/10.1007/s11837-017-2706-y [5]https://www.ge.com/additive/sites/default/files/202007/M2SERIES5_COCRMO_CMDS_REV2.pdf

EFFECTS OF DIFFERENT PRODUCTION PARAMETERS ON MECHANICAL PROPERTIES IN FDM-PRINTED PRODUCTS

Elifnur Kösemen1, Ali Taner Kuzu2, Mustafa Bakkal3
1,3Department of Mechanical Engineering, Istanbul Technical University, Istanbul, Turkey
2Department of Mechanical Engineering, Isik University,İstanbul, Turkey, alitaner.kuzu@isikun.edu.tr

ABSTRACT

FDM, which is a common additive manufacturing technology in producing plastic parts, allows for the comparison of many different production parameters. This article presents the variation of density, hardness, tensile and impact strength depending on the production parameters of the number of contours, infill pattern and orientation angle. 8 different production parameter combinations were created using 2 different contour numbers as 1 and 2, 2 different infill patterns as sparse high density and hexagram, and two different orientation angles as 0o/45o degrees, and sample production was made with FDM technology and ABS material. In the experiments performed on the samples produced with the specified production combinations, no major change in density and hardness was detected, and it was determined that the production parameter combination that gave the best results in both tensile and impact strength was hexagram infill pattern, 45o orientation angle and 2 contour production parameters.

Keywords: FDM, tensile strength, impact strength, ABS.

1. INTRODUCTION

Studies using 3D printers and production technology are increasing day by day and these studies make a great contribution to the production sectors. Its important benefits such as minimizing the production time of large parts with complex design, increasing efficiency, optimizing work flows and ensuring that production is monitored and automated, have enabled the production of many products from spare parts to final products with 3D modeling in the sector. Compared to other production methods, the method that comes to the fore in the 3D printing of plastic materials is fused deposition modelling (FDM). There is no doubt that FDM will contribute greatly to the development with each new study in all industry and the use of the method will continue to increase continuously. Compared to production methods with other 3D printers, FDM is among the most popular methods due to the wide variety of materials available, such as acrylonitrile butadiene styrene (ABS), polycarbonate (PC), PC-ABS, ASA [1].
In this study, it is aimed to examine the changes in the mechanical and internal structure properties of the 3D printer samples produced by using FDM production technology and different production parameters as addition to the studies done with 3D printers in the literature. In the production of the samples, 2 different infill patterns, 2 different contour numbers and 2 different orientation angles were used. For the infill pattern, sparse high density and hexagram, 2 different contour numbers, 1 and 2, and 2 different angles, 0o and 45o, for the orientation angle, a total of 8 different production parameter combinations were obtained. Density measurements of samples with different production parameter combinations were determined by using Archimedes method, and hardness measurements were determined by Shore A measurement. In order to observe the effects of changes in production parameters on tensile and impact strengths, tensile test specimens were first produced in accordance with ISO 527 standard and tensile tests were carried out. Following the tests, the internal structure images of the fracture surfaces were examined with a microscope.

2. MATERIALS AND METHODS

The samples produced for the study were produced using ABS-M30 filament in the Stratasys F370 device. All test specimens were produced with 8 different combinations considering 3 different production parameters: sparse high density and hexagram infill patterns, 0o/45o orientation angle and 1 or 2 contour number. ISO 527 standard was used as a reference in the tensile tests. The production of the samples was accomplished by establishing the appropriate toolpaths. The tests were performed 3 times for each production parameter combination using a Shimadzu 50 kN tensile testing device at a tensile speed of 2 mm/min in accordance with the requirements of the ISO 527 standard. Due to the

anisotropy feature of the parts created using FDM, the impact test specimens were produced by sitting on the XY plane, using two different directions in the production combination, parallel to the production nozzle and perpendicular to the production nozzle. Sample dimensions in accordance with the ISO 180

standard produced and the impact test was performed using the Charpy impact tester. Density measurement of the samples produced using different parameters were carried out by the Archimedes principle measurement method, which states that an object immersed in a liquid loses an amount equal to the weight of the liquid it replaces. The hardness values of the produced samples were made by Shore hardness measurement. The meter is a Shore A meter.

3. RESULTS AND DISCUSSION

The highest density value was obtained in the sample produced using sparse high density infill pattern, 45° orientation angle and 2 contour production parameters, the lowest density value was obtained in the sample with hexagram infill pattern, 45o orientation angle and 2 contours. In addition, the highest Shore A hardness value was obtained in the sample with hexagram infill pattern, 45o orientation angle and 2 contours, while the lowest hardness value was obtained in the sample with sparse high density infill pattern, 0o orientation angle and 1 contour.

Figure 1 shows the internal structure images after the tensile and impact tests of the samples produced with using a combination of 8 different production parameters. Considering the tensile tests, the highest UTS value was obtained in the sample with hexagram infill pattern. On the other hand, the highest value for strain at fracture was measured in the sample with sparse high density infill pattern, 45o orientation angle and 2 contours. Considering the impact tests, while the highest impact energy for Orientation-1 was measured in the sample with hexagram infill pattern, 0o orientation angle and 2 contour production parameters, the highest impact energy was measured in the sample with hexagram infill pattern, 45o orientation angle and 2 contour production parameters for Orientation-2.

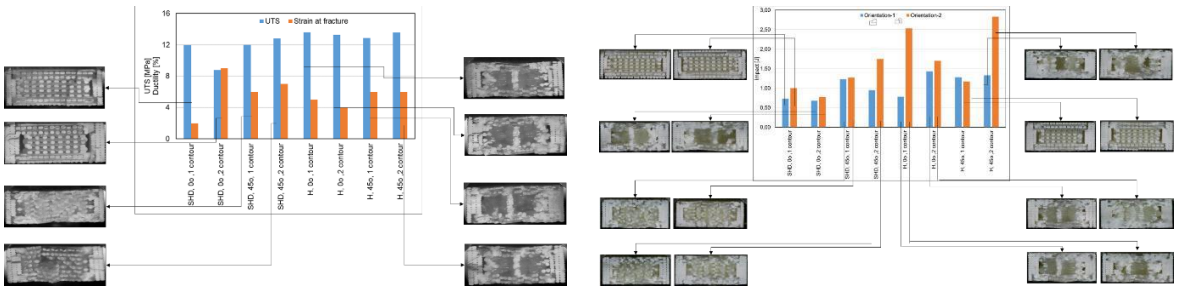

Figure 1: Results of Tensile and Impact Tests.

4. CONCLUSIONS

When the results were examined, no major difference was observed in the density and hardness measurements depending on the production parameter. Maximum UTS was reached with 45o orientation angle and 2 contours in both infill patterns. According to the production combination, the highest impact strength was observed in hexagram infill pattern, 0o orientation angle and 2 contour production parameters in Orientation-1 samples, while the highest impact strength was observed in Hexagram infill pattern, 45o orientation and 2 contour production parameters in Orientation-2 samples.

5. REFERENCES

1. Wong, K. V., & Hernandez, A. (2012). A Review of Additive Manufacturing. ISRN Mechanical Engineering, 2012, 1-10. doi:10.5402/2012/208760

2. A.K. Sood, R.K. Ohdar, S.S. Mahapatra, Experimental investigation and empirical modelling of FDM process for compressive strength improvement, J. Adv. Res. 3 (1) (2012) 81–90. https://doi.org/10.1016/j.jare.2011.05.001.

AMCTURKEY
ADDITIVE MANUFACTURING CONFERENCE

EFFECTS OF LATTICE STRUCTURES ON ADDITIVELY MANUFACTURED METAL PARTS

Yusuf Silik[1,2], Ulaş Yaman[2]
[1]*Roketsan A.Ş., yusufsilik@roketsan.com.tr*
[2]*Middle East Technical University, uyaman@metu.edu.tr*

ABSTRACT

With the recent advancements in the computational tools for additive manufacturing (AM) technologies, topology optimization method is becoming a must before fabricating an end-product with these digital manufacturing approaches. In addition to the structural optimization process, certain dynamic properties are further required for the designed parts especially in some application areas such as automotive and aerospace industries. For this purpose, interior of the parts can be utilized to acquire better dynamic properties. In this study, we will use lattice structures as interior filling patterns to increase the natural frequencies of the parts manufactured with a metal AM method. We will work on cantilever or simply supported beams to prove the advantages of our approach. These beams will be designed using various types of lattice structures and they will further be optimized using the SIMP topology optimization method. After the manufacturing of the samples, we will evaluate them using impact hammer tests. Furthermore, we will perform numerical analysis and compare them with the results of the experiments.

Keywords: Lattice Structures, SIMP Method, Topology Optimization, Metal Additive Manufacturing

ELECTROMAGNETIC CHARACTERIZATION OF 3D PRINTED METAMATERIAL ABSORBER WITH CONDUCTIVE PAINT

Mete BAKIR, Oğuzhan AKGÖL, Abdullah GÖZÜM, Abdullah Gozum[1], Mete Bakir[2], Oguzhan Akgol[3]
[1]*TUSAŞ, abdullah.gozum@tai.com.tr*
[2] *TUSAŞ, mete.bakir@tai.com.tr*
[3]*İSTE, oguzhan.akgol@iste.edu.tr*

ABSTRACT

In this study, electromagnetic characterization of 3D printed metamaterials manufactured by using conductive paint is carried out in terms of their absorption behavior. The samples have been prepared in sizes to fit waveguide setup in the frequency range of 12-18 GHz. 3D printing technique was used to prepare the substrate of the design while conductive paint and copper tape were used for the conductive parts of the structure including the metamaterial resonator and the ground plane. For electromagnetic characterization of the design, different thickness of substrate layers, various raster orientation ($0°, \pm 45°$ and $\pm 90°$), different infill densities have been simulated and experimentally tested in terms of their effects on absorption behavior. In addition, conductivity of the paint was improved by adjusting its formulation and the resulting absorption behaviors have been compared with copper tape using the same metamaterial dimensions. Using 3D printing technology along with conductive paint rather than solid conductors in manufacturing electromagnetic absorbers will provide the possibility of producing flexible and non-planar electromagnetic absorber structures in desired frequency ranges. The design can be easily adopted to different frequencies and this technique can be used to design wideband metamaterial absorbers using 3D layered structures.

Keywords: Additive manufacturing, 3D printing, conductive paint, Metamaterials, Absorber

ENERGY DENSITY DETERMINATION FOR L-PBFP OF TI-6AL-4V ALLOY FOR VARIOUS BEAM DIAMETERS AND HATCH DISTANCES

Mehmet Mollamahmutoglu[1], Oguzhan Yilmaz[1], Cumhur Köseoğlu[2], Hüseyin Tecer[2], Fatih Özaydın[2], Ömer Faruk Kocaoğlu[3], Elif Zeynep Emir[3]

[1] *Advanced Manufacturing Technologies Research Group (AMTRG), Gazi University, Ankara, Turkey, mehmet.mollamahmutoglu@gazi.edu.tr*

[2]*ESTAŞ, Şeyh Şamil OSB Mah. Halis Vermezoğlu Cd. No:57, SİVAS*

[3]*digiMODE, Alınteri Bulvarı, No: 52 Ostim 06374, Yenimahalle, Ankara Türkiye*

ABSTRACT

It is important to determine the appropriate energy densities for an ideal (error-free) production in the laser powder bed fusion process. In this study, energy density levels were determined for the Ti-6Al-4V alloy via volumetric heat source model [1] simulations. Undesirable situations such as fusion problems, balling, excessive evaporation and keyhole regime were accepted as criteria for the evaluation. The developed process window covers analysis for different beam diameters of 50, 80, and 100 micrometers, hatch distances ranging from 30 to 100 micrometers. Laser power and scan speed range from 50 to 200 W and 250 to 1500 mm/s, respectively. It has been found that higher laser powers accompanied with higher laser scan speeds are prone to some production problems such as, keyhole, unstable pools and balling. Consequently, the analysis results are to be used as a guide before further experimental tests.

Keywords: Laser powder bed fusion process, Ti-6Al-4V, additive manufacturing

1. INTRODUCTION

Parameter selection is highly crucial for an ideal production in the laser powder bed process. Various undesired phenomena such as keyhole or balling may occur and result in some defects. These defects are mainly due to fusion problems between layers or between hatches. These fusion problems are caused by insufficient energy and/or large hatch distance. Balling may occur as a further situation, especially for interlayer fusion problems. On the other hand, excessive power input means the waste of material and energy. As an extreme case, the keyhole regime may occur. Overall, high evaporation can cause porosity. In this case, just as with insufficient energy, the quality of the part decreases. Within the scope of this information, a numeric study was carried out for the Ti-6Al-4V alloy.

2. MATERIALS AND METHODS

The parameter selection for an experiment, which will be conducted, was determined via the DOE method. Here, beam diameter (50, 80, 100 µm), laser power (50-200 W), scan speed (250-1500 mm/s), and hatch distance (30-100 µm) were taken as input parameters. Optimization is aimed according to possible defects in the samples to be produced with the selected parameters. Before the designed experiment, the selected parameters were analyzed numerically to predetermine possible defects and problems that might be encountered. Here, different criteria were taken into account to determine whether a parameter is suitable for production. The criteria considered here are as follows: melt pool shape, temperature and fusion between pools.

3. RESULTS AND DISCUSSION

As a result of the simulations carried out, the parameters for the ideal production were determined and presented in Figure 1. Here, suitable parameters are colored green, and unsuitable ones are colored red. Some parameters were not considered appropriate due to possible fusion problems. In a few cases, even balling may occur during production. Apart from these, the parameters in which the keyhole regime is evident due to the intense energy were not considered appropriate. High porosity due to evaporation is likely to be observed in these parameters.

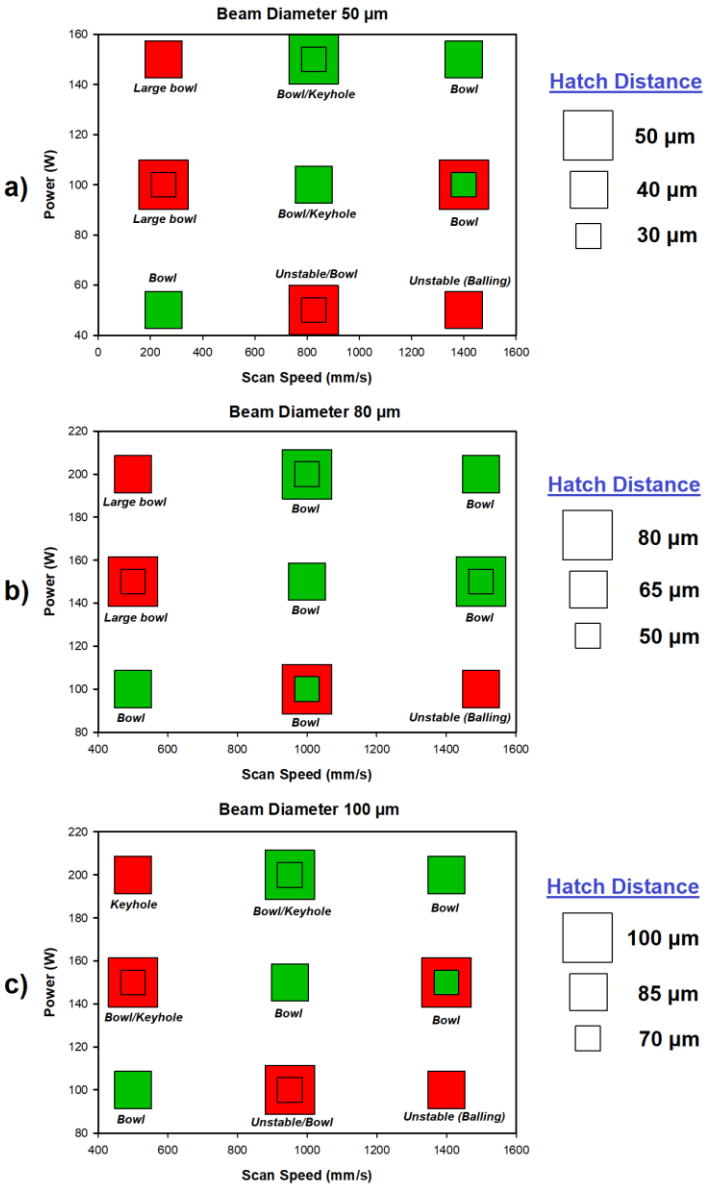

Figure 1. Process window obtained as a result of the simulation via criteria: pool shape and size, temperature, interlayer, and intertrack fusion. a) Beam diameter 50 µm, b) Beam diameter 80 µm, c) Beam diameter 100 µm.

4. CONCLUSIONS

The result of the study can be summarized as follows:

- The beam diameter is the most dominant parameter in the selection of the ideal hatch distance.
- The ideal penetration (melt pool) depth is approximately 1.5 to 2.5 times the layer thickness.
- In addition to the thermo-physical properties of the material used, the powder layer thickness also limits the usable beam diameter and laser power range.

REFERENCES

[1] Mollamahmutoglu, M., & Yılmaz, O. (2021). Volumetric Heat Source Model for Laser-Based Powder Bed Fusion Process in Additive Manufacturing. Therm. Sci. Eng. Progress, 25, 101021. https://doi.org/10.1016/j.tsep.2021.101021

ESTABLISHING THE EFFECT OF PROCESS PARAMETERS ON THE MECHANICAL PROPERTIES OF 3DPRINTED PETG

Buket Parlak[1*], Hülya Cebeci[2]
[1]*TUSAS Engine Industries, Inc.and Istanbul Technical University, *Buket.Taspinar@tei.com.tr*
[2]*Aerospace Research Center (ITU ARC), Istanbul Technical University, *geyikh@itu.edu.tr*

ABSTRACT

FFF is one of the polymer additive manufacturing production methods with an advantage of producing high volume parts in a short time with low cost compared to extrusion. Since the extrusion process results with better mechanical properties than 3D printed parts, a majority od research has been focused to optimize the mechanical properties of additively manufactured parts [1]. Through negative air gap and annealing, it is possible to achieve enhanced mechanical properties. Hence, this research aims to reveal the importance of air gap selection, sample standard types, infill patterns, post process temperature & time on mechanical properties through comparative studies.

Keywords: FFF, PETG, Air gap, Annealing, Specimen Standards

1. INTRODUCTION

3d printing technology which is also known as additive layer manufacturing revealed that its products have good accuracy, faster manufacturing, wide range of materials, and low cost of equipment compared to traditional methods [2]. One of the specified metal extrusion method is the FFF (fused filament fabrication) [1]. The working principle of FFF is through melting the feedstock and extruding into bed with a nozzle.

The selection of the printing parameters plays a vital role to enhance mechanical properties. Most studied printing parameters are specified as raster angle, layer height (layer thickness), raster width, infill pattern, air gap ratio, number of outer shells and heat treatment [2,3]. Another controversial topic on FFF technology is the selection of specimen standards [3]. There is a limited research discussing the effects of sample preparation, testing standards and their validity.

The aim this study is to reveal that the effect of air gap and infill patterns by producing with two different sample standards on mechanical properties. And then, through an optimized parameter set, the annealing effect for time and temperature is studied for further enhancement. set.

2. MATERIALS AND METHODS

The specimens were printed from PETG (glycol modified polyethylene terephthalate) polymer due to its outstanding properties. Specimens fabricated as per ASTM D638 TYPE IV and ASTM 3039 using the CAD software NX. After model creation, G codes were prepared with Ultimaker Cura 4.13.1. RAISED 3D PRO 2 Plus FDM machine was used in order to fabricate samples, as presented in Figure 1.

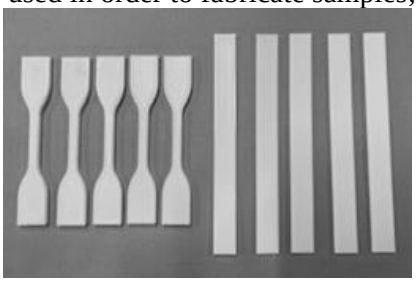

Figure 1. Samples produced from ASTM D638 Type 1(left) and ASTM D3039 (right)

Annealing was performed with two set of temperature and time parameters. The effects of the infill pattern and air gaps on microstructure of the samples was investigated using scanning electron microscopy (SEM) (Jeol Branded). The samples were tested with 2 mm/min deformation rate by using Zwick/Roell Z100 at room temperature.

3. RESULTS AND DISCUSSION

It was observed that the samples produced with concentric infill patterns (and rectilinear) by ASTM D3039 showed the highest elastic modulus (E) and ultimate tensile strength (UTS) properties compared to the rectilinear ones. According to comparison of E and UTS of samples which was produced as per

ASTM D638 Type IV and ASTM D3039, there is no linear relation between two different standards. Effects of the negative air gap on tensile properties were investigated from samples produced concentric and rectilinear infills. Instead of samples produced as concentric infill, rectilinear samples (ASTM D3039) shows that with a 20% negative air gap, E and UTS were achieved as the highest. However, rectilinear samples (ASTM D3039) have lowest E and UTS properties than other samples.

The highest increase on UTS properties was reported with concentric samples manufactured as per ASTM D638. There is a linear relation while increasing negative air gap from 0% to 20% for all samples except concentric ones produced as per ASTM D3039. Due to this reason, it was considered to continue with concentric samples (produced as per ASTM D638) instead of rectilinear samples (produced as per ASTM D3039) for annealing studies (second set). The annealing studies were performed with the samples produced 15% negative air gap per ASTM 638 testing protocol based on the tensile results. The annealing was shown positive improvements on tensile properties.

4. CONCLUSIONS

This study was completed to improve tensile properties of FFF produced samples by application of different parameter configurations. Based on this research following results were investigated:

- Concentric pattern has high tensile properties than rectilinear patterns, % 30-50 for E %33-47 for UTS.
- Air gap is significant parameter that is clearly improve tensile properties of all samples, % 3-11 for E %4-9 for UTS.
- 15% negative air gap has highest results on tensile properties than other air gap configurations.
- The samples produced as per ASTM D638 Type IV was shown highest improvement and tensile properties than ASTM D3039.
- Annealing is also other main factor that is improve tensile properties of samples.

REFERENCES

[1] Gordelier, Tessa Jane, et al. “Optimising the FDM Additive Manufacturing Process to Achieve Maximum Tensile Strength: A State-of-the-Art Review.” *Rapid Prototyping Journal*, vol. 25, no. 6, 2019, pp. 953–971., https://doi.org/10.1108/rpj-07-2018-0183.

[2] Xu, Weiheng, et al. “3D Printing for Polymer/Particle-Based Processing: A Review.” *Composites Part B: Engineering*, vol. 223, 2021, p. 109102., https://doi.org/10.1016/j.compositesb.2021.109102.

[3] Srinidhi, M.S., et al. “Enhancing the FDM Infill Pattern Outcomes of Mechanical Behavior for AS-Built and Annealed PETG and CFPETG Composites Parts.” *Materials Today: Proceedings*, vol. 45, 2021, pp. 7208–7212., https://doi.org/10.1016/j.matpr.2021.02.417.

EXPERIMENTAL ANALYSIS OF R-PHASE NITI TUBE ACTUATORS USING CONDUCTIVE/CONVECTIVE HEATING STAGE

Lehar Asip Khan[1], Hasan Ayub[1], Corné Muilwijk[1],Inam Ul Ahad and Dermot Brabazon
[1] *I-Form Advanced Manufacturing Research Centre, School of Mechanical and Manufacturing Engineering, Dublin City University, Dublin, Ireland*
†Corresponding Author Email: leharasip.khan@dcu.ie

ABSTRACT

In the last few decades, Nitinol (NiTi) actuators have created a massive impact at the commercial level due to their application in various engineering and medical fields. NiTi wires sheets and tube actuators are a useful resource for harvesting any form of heat energy available. In any actuation application, the rate of actuation and actuation force are important parameters that determine the feasibility of the actuator. Current ongoing research aims to critically investigate and develop NiTi R-phased and martensitic phased actuators using commercially available material. Prior heat treatment and shape setting will be performed on the available NiTi material in the research lab facility at Dublin City University. A design test rig will be built capable of providing conductive and convective heating for cyclic heating and cooling of material consequently producing actuation. Input parameters such as heat flux, convective flux, and actuator shape setting will be optimized while the output parameters such as rate of actuation and actuation force will be reported and optimized. In the later stages of the investigations will be diverted towards the additive manufactured materials for a comparison of NiTi build by conventional methods and additive manufacturing. Criticality, of the NiTi actuators, is the rate of solid-solid phase transformation which is linked to the temperature distribution. Therefore, convective heat transfer correlations will be presented for an enormous range of input parameters.

Keywords: **NiTi, Heat Pipes, Actuators, Phase Transformation**

Name	Qualification
Lehar Asip Khan	BS Mechanical Engineering
Corné Muilwijk	Ph.D. in Mechanical Engineering
Hasan Ayub	BS Electronics Engineering
Inam Ul Ahad	Ph.D. in Mechanical Engineering
Dermot Brabazon	Ph.D. in Material Science

EXTRUDER DESIGN OF PRINTABLE COMPOSITES

Amirali Hashemzadeh[1,5], Erman Tunçer[2,7] , Ulaş Yaman[1,3], Hüsnü Dal[1,4], Çağla Meral Akgül[2,6]
[1]*Department of Mechanical Engineering Middle East Technical University, Ankara, Turkey,*
[3]*uyaman@metu.edu.tr,* [4]*dal@metu.edu.tr,* [5]*amir.zadeh@metu.edu.tr*
[2] *Department of Civil Engineering Middle East Technical University, Ankara, Turkey* [6]*cmeral@metu.edu.tr,*
[7]*erman.tuncer@metu.edu.tr*

ABSTRACT

There are many extruder designs in today's standards for the extrusion of known extrudable metals and materials. Yet, when it comes to the design of the materials which were not extruded widely before, there are not many easy solutions for the design. In this paper, we designed a new extruder that works at given conditions for a given range of material properties. We found that the most impactful parameters for the design are: mill rpm, die diameter, outflow diameter, outflow speed, material viscosity, and the distance between the leaf and the inner surface of the extruder.

Keywords: Extruder design, Printable concrete, 3D printing

1. INTRODUCTION

3D printing of concrete has received immense attention from the industry. The number of researches done in the last decade increased exponentially. More than half of the printing applications employ ~6mm to ~50mm pump continuous filament through gantry style or robotic arm to ensure good deposition of the composite. Also, the pumping speed varies between 50 mm to 500 mms per second (Buswell et al., 2018). 3D printable concrete processes are not fully automated and regulated yet. The extruded material should retain its shape during printing process which requires precise mix designs and expertise in controlling the machines that are used for deposition. The flow is generally dominated by arm or gantry speeds, or the speed of ram or screw extrusion Figure 5 .

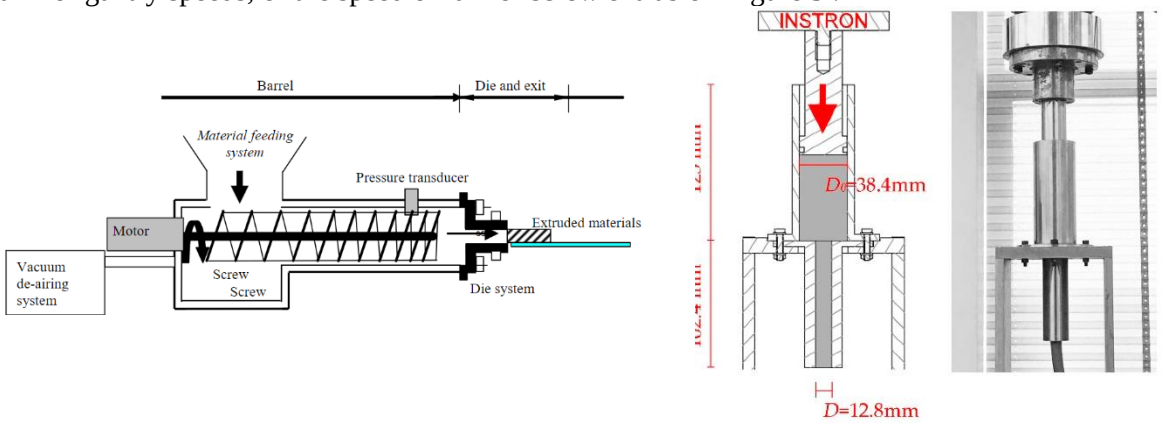

(a) (b)

Figure 5. Extrusion methods for concrete printing a) Screw type extrusion (Perrot, Rangeard, Nerella, & Mechtcherine, 2018) b) Ram extrusion (Chen et al., 2019)

In this study design of the screw type extruder for a printable paste is discussed. Effect of different parameters investigated for optimal extruder design.

2. METHODOLOGY

Formulations driven in (J. F. Carley, Mallouk, & McKelvey, 1953; L. Carley, Strub, & Purday, 1953) adopted for design of the extruder. 3D modelled and manufactured screw and feeding system taken as reference. ΔP(Pressure) vs. d_{out}(diameter of the outlet pipe), P_{total} (power required) vs. c (ratio of D=die diameter to d_{mill}=mill diameter), P_{total} vs. d_{mill}, P_{total} vs. d_{out}, P_{total} vs δ(clearance between leafs and the inner surface of the extruder), P_{total} vs. μ(viscosity), P_{total} vs. N(RPM of the mill), and P_{total} vs. v_{out}(outflow speed) were investigated. If not a variable, the constant values of the parameters were taken as: μ:2000Pa.s, v_{out}= 0.04m/s, d_{out}=0.02m, δ=0.001m, d_{mill}=0.034m, and D=0.098m.

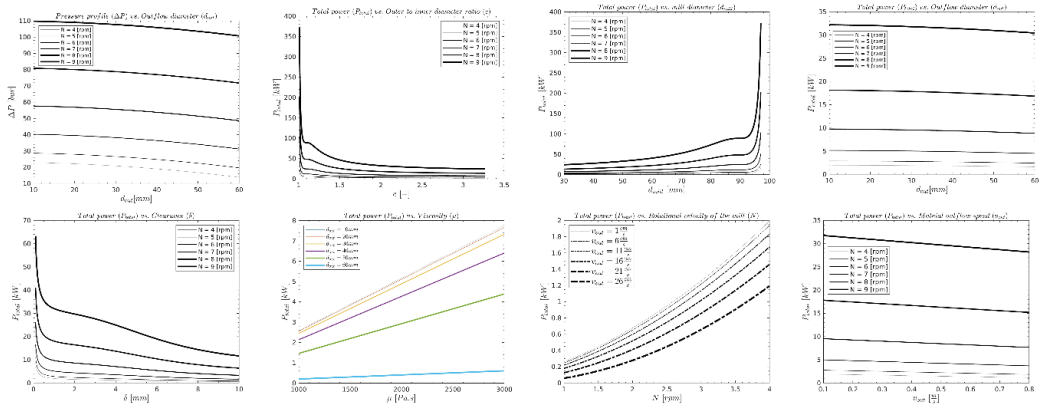

Figure 6. Results of investigated parameters for power requirement and extruder dimensions

3. RESULTS AND DISCUSSION

While RPM of the mill is the most impactful parameter in terms of power needs, P_{total} to d_{mill} analysis shows that selecting a mill and die diameters for the needed flow rate is as vital as rpm selection. Moreover, clearance between screw leaves and the inner surface of the extruder should be appropriately selected for optimal power requirement to the system. These comparisons show some key points that should be analyzed. As the leaf area decreases, the power need increases. According to the P vs N graph, for a constant outflow speed, the power requirement increases as N increases. Also, very low values of clearances are not desired due to the dramatic effect on P. Moreover, higher values of outflow speed and diameter reduce the total required power. As the mill diameter reaches the die diameter, an exponential increase is observed in the P values. To fulfill the low total power requirement, a designer should pick from two possible alternatives; either low values in working rpm, mill diameter, and material viscosity or high values in outflow diameter, extruder diameter, clearance, and outflow speed.

4. CONCLUSIONS

According to the results, an extruder designer should initially measure the viscosity of the material. Also, extrusion speed and output diameter for material deposition should be specified. The 'c' ratio should be determined from the beginning to calculate the surface area of the leaves and the material volume pushed through the extruder. Lastly, the required power and rpm needed for extrusion can be calculated. This way of design leads to a more economical and feasible way of manufacturing extruders for concrete printing.

REFERENCES

Buswell, R. A., Leal de Silva, W. R., Jones, S. Z., & Dirrenberger, J. (2018). 3D printing using concrete extrusion: A roadmap for research. *Cement and Concrete Research*, *112*, 37–49. https://doi.org/10.1016/J.CEMCONRES.2018.05.006

Carley, J. F., Mallouk, R. S., & McKelvey, J. M. (1953). Simplified Flow Theory for Screw Extruders. *Industrial & Engineering Chemistry*, *45*(5), 974–978. https://doi.org/10.1021/IE50521A032

Carley, L., Strub, J. F., & Purday, R. A. (1953). Application of Theory to Design of Screw Extruders. *Industrial & Engineering Chemistry*, *45*(5), 978–982. https://doi.org/10.1021/IE50521A033

Chen, Y., Figueiredo, S. C., Yalçinkaya, Ç., Çopuroğlu, O., Veer, F., & Schlangen, E. (2019). The Effect of Viscosity-Modifying Admixture on the Extrudability of Limestone and Calcined Clay-Based Cementitious Material for Extrusion-Based 3D Concrete Printing. *Materials 2019, Vol. 12, Page 1374*, *12*(9), 1374. https://doi.org/10.3390/MA12091374

Perrot, A., Rangeard, D., Nerella, V. N., & Mechtcherine, V. (2018). Extrusion of cement-based materials - an overview. *RILEM Technical Letters*, *3*, 91–97. https://doi.org/10.21809/RILEMTECHLETT.2018.75

FOAMING PLA PARTS PRODUCED BY FUSED FILAMENT FABRICATION

Abdullah Alduais[1], Sezer Özerinç[2]
[1]*Department of Mechanical Engineering, Middle East Technical University, Ankara, Turkey, abdullah.alduais@metu.edu.tr*
[1]*Department of Mechanical Engineering, Middle East Technical University, Ankara, Turkey, ozerinc@metu.edu.tr*

ABSTRACT

Fused filament fabrication (FFF) is a cost-effective additive manufacturing technique for the printing of polymeric parts. One of the most widely used FFF filament materials is Polylactic acid (PLA), which is a biodegradable and sustainable thermoplastic. In this work, we explored the performance of a novel foaming PLA filament, which enables the manufacturing of polymeric foams. The study focused on the effect of feed rate on the density and tensile strength. The results showed that as feed rate decreases, the porosity level increases, resulting in a decrease in tensile strength. The results demonstrate the great potential of foaming filaments in the additive manufacturing of complex parts with tunable mechanical properties.

Keywords: Additive manufacturing, fused filament fabrication, polylactic acid, polymer foams, mechanical properties.

1. INTRODUCTION

Fused filament fabrication (FFF) is one of the most cost-effective additive manufacturing techniques for the printing of polymeric parts (Bakır, Atik, and Özerinç 2021). One of the most widely used FFF materials is polylactic acid (PLA), which is a biodegradable and sustainable thermoplastic material. In this work, we explored the performance of a novel foaming PLA filament, which enables the manufacturing of polymeric foams.

2. MATERIALS AND METHODS

A systematic set of tensile specimens were manufactured by using An Ultimaker 2+ FFF 3D printer (Netherlands). The foaming filament was a commercial PLA filament manufactured by Colorfabb (Netherlands) under the brand name LW-PLA.
Tensile specimen employed the Type 4 geometry of ASTM D638 Standard Test Method for Tensile Properties of Plastics (ASTM D20 Committee 2014:638). The study focused on the effect of feed rate on the porosity and mechanical performance, as feed rate has been identified as the most effective parameters in adjusting porosity. Table 1 summarizes the printing parameters employed.

Table 1. Printing Parameters Employed in the Study.

Filament Diameter	2.85 mm
Nozzle Temperature	230°C
Bed Temperature	60°C
Infill Ratio	100%
Infill Pattern	±45°
Layer Thickness	0.45 mm
Feed Rate	25%, 50%, 75%, 100%
Printing Speed	50 mm/s
Inwall Layers	3
Top and bottom layers	Same as other layers

3. RESULTS AND DISCUSSION

Figure 1(a) shows the effect of feed rate on the density. As feed rate increases, the density monotonically increases. By adjusting the feed rate, it is possible to tune the density over a wide range of about 300 – 1000 kg/m^3.
When the feed rate is low, the filament goes through the heated nozzle more slowly, providing more time for foaming. Therefore, as the feed rate decreases, the extent of foaming increases, resulting in lower porosity.

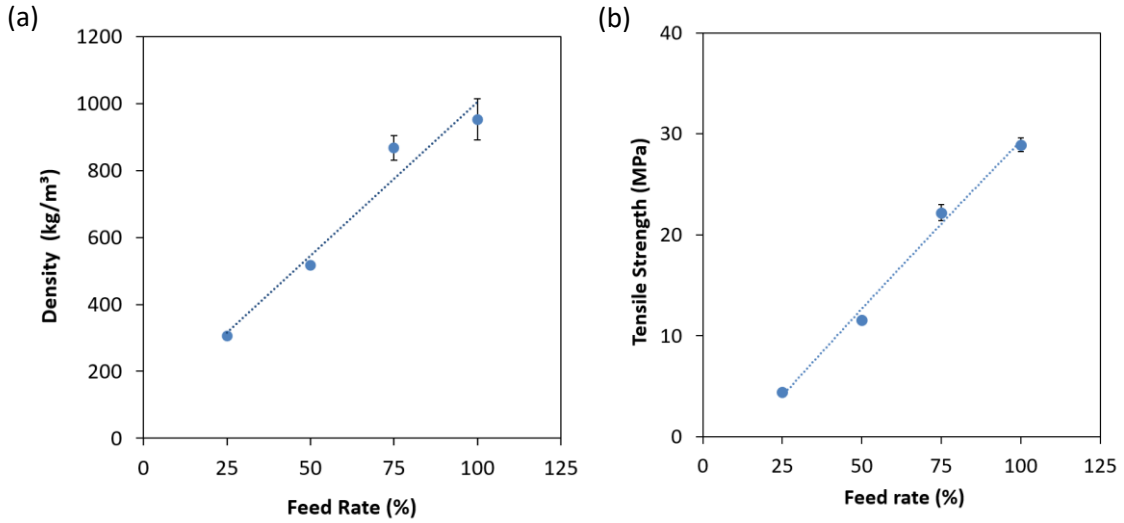

Figure 1. (a) Effect of Feed Rate on Density. (b) Effect of Feed Rate on Tensile Strength.

Figure 1(b) shows the effect of feed rate on tensile strength. As feed rate increases, the tensile strength monotonically increases. By adjusting the feed rate, it is possible to tune the density over a wide range of about 5 – 30 MPa.

The varying mechanical performance is a direct result of the specimen porosity. As porosity increases, the load bearing capacity decreases dramatically. As density of solid PLA is 1250 kg/m^3, the 100% feed rate specimens can be considered to have limited foaming. The resulting mechanical strength, however, is about 25% lower than that reported in the literature for FFF-produced solid PLA parts (Wach, Wolszczak, and Adamus-Wlodarczyk 2018). Therefore, even small amount of porosity can adversely affect the mechanical properties, which we attribute to the stress concentration effects and subsequent cracking and failure.

4. CONCLUSIONS

This study demonstrated the effect of feed rate on the density and mechanical properties of FFF parts produced by a foaming PLA filament. The results show that the feed rate is an effective parameter to tune the mechanical properties of the foaming PLA.

The tunable properties of PLA are promising for applications where lightweight structures are desirable. As opposed to conventional foams, FFF-produced foams also enable the tuning of the porosity and strength spatially over the specimen, providing new opportunities for the design of impact absorbers and soft robotics components.

REFERENCES

ASTM D20 Committee. 2014. *Test Method for Tensile Properties of Plastics*. ASTM.

Bakır, Ali Alperen, Resul Atik, and Sezer Özerinç. 2021. "Mechanical Properties of Thermoplastic Parts Produced by Fused Deposition Modeling:A Review." *Rapid Prototyping Journal* 27(3):537–61. doi: 10.1108/RPJ-03-2020-0061.

Wach, Radoslaw A., Piotr Wolszczak, and Agnieszka Adamus-Wlodarczyk. 2018. "Enhancement of Mechanical Properties of FDM-PLA Parts via Thermal Annealing." *Macromolecular Materials and Engineering* 303(9):1800169. doi: 10.1002/mame.201800169.

HEAT PIPE EMBEDED COLD PLATE DESIGN WITH ADDITIVE MANUFACTURING TECHNOLOGIES

Murat PARLAK[1], Vedat YAĞCI[1]
parlak@aselsan.com.tr, vyagci@aselsan.com.tr

ABSTRACT

Heat pipe embedded/integrated cold plates are mostly preferred to increase the thermal conductivity of the base material to have passive thermal management in reliable products. Thanks to Additive Manufacturing Technology, it became possible to find a high conductive product by simultaneously manufacturing the heat pipe in the cold plate. In this study, the heat pipe embedded cold plate design of an electronic chassis designed for a military product has been investigated in detail. With this study, it is seen that there are many outstanding advantages of using AM technology compared to the conventional heat pipe embedding techniques. Thermal analysis of a 6U size cold plate with a high thermal load is performed for aluminum & copper base material and groove type heat pipe embedded aluminum cold plate (HPECP). After that, the manufacturing constraints of both techniques are compared and important design capabilities with AM technology are discussed in detail. It is seen that by using AM technology, it is possible to have a lighter cold plate with improved thermal conductivity in one piece and even lower cost.

Keywords: Cold Plate, Heat Pipe Embedded Cold Plate, Additive Manufacturing, Groove Type Heat Pipe, Electronic Cooling

1. INTRODUCTION

In electronic cooling applications, depending on the requirement one can find many different packaging techniques. To have a low cost and reliable product, mostly preferred cooling technique is the passive technique which is not required any control, energy or rotating parts. A heat pipe is the most preferred technique to carry heat from the heated zone to the low-temperature locations to have effective cooling passively. Depending on the design approaches, heat pipe type, material, and filling fluid can be selected accordingly and the embedding process can be performed after several stages to provide the requirement. Many experienced companies working in this field can perform heat pipe embedding techniques to the base material. Up to now, one can see that many different shapes have been used in many products both industrial and military applications. With the popularity of additive manufacturing technologies, the point of view on product development has been improving every day. Robinson et al. [1] studied the wicked heat pipe with AM to investigate the thermal performance of a novel cross-hatched porous wick structure and in each layer, the hatch distance is altered to have different wick properties. Characterizing the thermal performance in terms of thermal resistance, an effective two-phase cavity has been performed for different parameters. In recent years, many studies have been published that cover heat pipe production with AM technology for space and earth applications [2-9]. In this study, AM technology is applied to have a highly conductive aluminum plate with a lighter weight for a military product.

2. RESULTS AND DISCUSSION

Analysis results of all solutions are given in the following figures. Using AM technology many advantages have been earned and this makes it possible to find more design versatility to have better thermal results. **Table 1.** is given to compare the pros & cons of using 3 AM technology instead of the conventional embedding approach.

Table 1. Comparation of two different manufacturing techniques in a heat pipe embedded cold plate production.

Conventional Manufacturing Methods	Application of 3D AM Technology
Need to use filler material	No need of using filler or bonding material
Inconsistent different materials	All materials are consistent
Additional thermal contact resistance	No contact resistance
Heavy post-processing	Less post-processing
Difficulties in bending or fitting	Easy production
Difficulties in the manufacturing of heat pipe	Easy production
Loss of performance due to flattening process	No need for flattening, hence no loss in performance

Need to use a thick plate to embed the heat pipe	No need. It can be flat and thin
Using adhesive material can shorten the effective length	No need to use adhesive material so that length of the heat pipe can be more effective

In **Fig. 1a-1b**, thermal modal, cold plate with heat pipes, boundary conditions, the thermal performance and weight comparations of each case are illustrated. Accordingly, depending on the fluid, filling ratio, and gravitational effect, the thermal performance of HPECP changes. It is seen that using constant effective conductivity, the performance of the plate can be comparable with the copper one. Therefore, instead of using copper, an HPECP can serve satisfactory thermal and mechanical results with a much lighter weight.

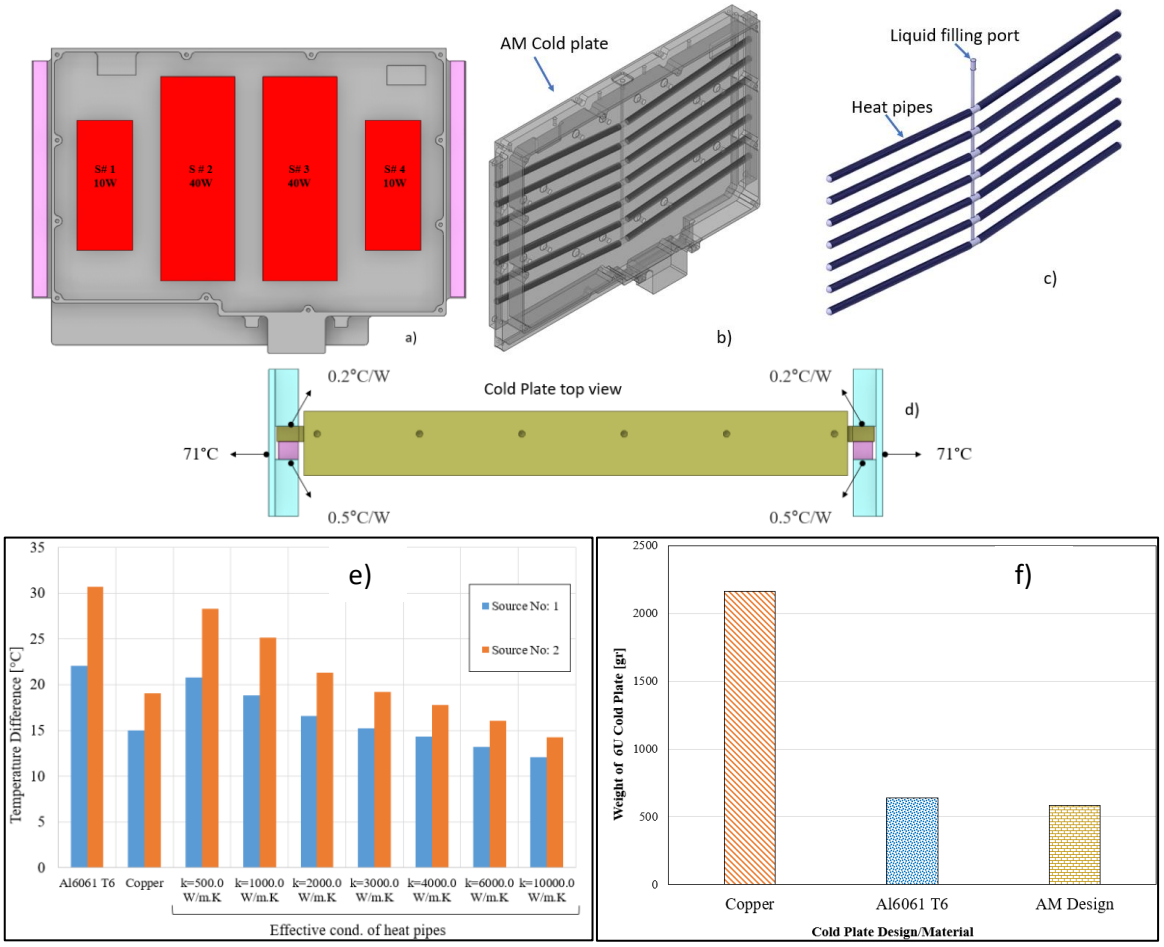

Figure 1. Thermal modal, 3D-AM Modal of Cold plate with heat pipes, boundary conditions, thermal performance and weight comparation of different cold plates

3. CONCLUSIONS

In this study, we have shown that a 6U size cold plate for a PCB can be manufactured with AM technology including groove heat pipes details to increase the conductivity of the aluminum cold plate. Theoretically, it is seen that HPECP can satisfy the thermal requirement as far as the filling is done accordingly. With the proper design, it is possible to change the fluid and its ratio without damaging the base material to perform series tests with a single sample. As a future work; after the filling operation is completed, a thermal test will be conducted for a reliable comparison with different fluids like acetone, water, and CNT added nanofluid to have the desired thermal performance.

Note that: This design is at the Patent Pending stage.

HIGH CYCLE FATIGUE PERFORMANCE OF AGE HARDENED AND HIPPED AM-ALSI10MG: INVESTIGATION ON POST PROCESS EFFECTS

Remzi Ecmel ECE[1], Ömer KELEŞ[2], Bekir Sami YILBAŞ[3,4]
[1]*Turkish Aerospace Industry Inc, reece@tai.com.tr*
[2]*Gazi University, omer@gazi.edu.tr*
[3] *Turkish Japanese Science and Technology University, bsyilbas@tju.edu.tr*
[4] *King Fahd University of Petroleum and Minerals, bsyilbas@kfupm.edu.sa*

ABSTRACT

AM technology has begun to be widely used in the industry. There is an increasing demand on investigation of inevitable inherent defects developing from process parameters and raw material properties. The performing of post-processes to eliminate the production errors plays an important role in increasing the product quality. In this study, high cycle fatigue performance of AM-AlSi10Mg specimens produced by selective laser melting were evaluated. To investigate the effects on mechanical properties of build position, the specimens were prepared with different built directions (0°: horizontal - 45°: diagonal - 90°: vertical). Accordingly, natural ageing and artificial ageing with different temperature and hot isostatic pressure (HIP) were applied to the samples. Fatigue tests were performed under uniaxial load using 20 Hz frequency and a stress ratio of R=-1. Results of post processes were compared with as-built samples according to fracture surface analysis by characterizing porosity and crack propagation evaluation for all build directions. It is found that the ageing reduces the fatigue life. Contrarily, the fatigue life of the HIPped samples showed a great difference compared to the aged and as-built samples. Among the HIPped specimens, the vertical samples have higher fatigue life compared to other directions. It is observed that microstructural transformation of Silicon's size and morphology during the heat treatment is the main cause for fatigue property changes.

Keywords: AlSi10Mg, Post Processes, Ageing, HIP

HYBRID THERMOPLASTIC COMPOSITE MANUFACTURING BY ADDITIVE MANUFACTURING

Alperen DOGRU[1,2], M. Özgür SEYDİBEYOGLU[3,4]
[1]*Ph.D Can. Lecturer, Ege University, alperen.dogru@ege.edu.tr*
[2]*Visiting Researcher, University of Alberta, adogru@ualberta.ca*
[3]*Prof., Izmir Katip Çelebi University ozgur.seydibeyoglu@ikcu.edu.tr*
[4]*Visiting Researcher Prof., University of Maine, ozgur.seydibeyoglu@maine.edu*

ABSTRACT

The most innovative production method of polymer matrix composites is additive manufacturing technologies. It has been a practice for years to optimize the various properties of polymer matrices by reinforcement fibers or particles of different sizes. It is possible to obtain positive results in the mechanical properties of fiber-reinforced polymers in this way. Especially fiber reinforcements made to thermoplastic polymers expand their usage areas and make the use of thermoplastics an important alternative. The recyclability of thermoplastics is critical to a sustainable future. The production of fiber-reinforced thermoplastics by additive manufacturing methods has become the focus of attention in recent years. Thermoplastic polymers reinforced with different fibers have been the subject of many studies. The limitations of existing thermoplastic composite manufacturing methods on geometry and their varying costs depending on the production volume limit the use in certain areas.

In this study, hybrid composite sample production was carried out by combining the positive aspects of two different fibers. Firstly, filament production was carried out with the extrusion process from the compounds in which carbon and glass fibers are used in equal proportions by weight. Polyamide 6 was used for the matrix. Sample production was carried out with the Fused Filament Fabrication method using filaments containing different fibers. Tensile strength and impact resistance values of the produced samples were compared, and thermal characterizations and morphological analyzes were performed.

While the samples produced with carbon fiber showed high tensile strength, glass fiber reinforcement had a lower effect on the tensile strength of the polyamide matrix. In impact resistance, carbon fiber reinforcement made the material brittle, while glass-reinforced samples showed a more ductile feature than carbon fiber reinforced ones.

Keywords: Thermoplastic, hybrid composites, additive manufacturing, carbon fiber, glass fiber, polyamide

1. INTRODUCTION

With the advantages, additive manufacturing methods have gone beyond prototype production in many areas and started to be used in the production of final products. The most innovative production method for polymer matrix composites is additive manufacturing technologies. Existing polymer matrix composite production methods have limitations, especially in part geometry. Thanks to additive manufacturing methods, being able to produce parts with complex geometry in one piece provides significant advantages.

It is possible to improve the mechanical, thermal, or electrical properties of polymer matrix composites with fiber or particle reinforcement of different sizes. It is a known fact in the literature to obtain positive results in the mechanical properties of polymers by reinforcement fiber reinforcement. Variables such as fiber ratio, fiber type, and fiber length affect the properties of composite materials. Especially fiber reinforcements made to thermoplastic polymers expand their usage areas and make the use of thermoplastics an important alternative. It is very important for the future of our world to develop sustainable materials that can replace materials such as thermoset material, which cannot be recycled, and which is one of the most important problems of today. In this context, the recyclability of thermoplastics is critical for a sustainable future. The reinforcement by fibers of thermoplastic matrices, create significant opportunities. The production of fiber-reinforced thermoplastics by additive manufacturing methods has become the focus of attention in recent years. Thermoplastic polymers reinforced with different fibers have been the subject of many studies. The limitations of current thermoplastic composite methods on part geometry and their varying costs depending on the production volume appear as disadvantages. The use of hybrid composites and different fibers together and the production of parts by additive manufacturing methods are important alternatives to eliminate these disadvantages.

2. MATERIALS AND METHODS

In this study, hybrid composite sample production was carried out by combining the positive aspects of two different fibers. Firstly, filament production was carried out with the extrusion process from the compounds in which carbon and glass fibers are used in equal proportions by weight. Materials containing 10% and 20% fiber by weight were produced. At these ratios, pure carbon fiber, pure glass fiber, and hybrid form materials containing both in equal weight ratios were produced. Afterward, using these filaments containing different fibers, sample production was carried out with the Fused Filament Fabrication method. Tensile strength and impact resistance values of the produced samples were compared, and thermal characterizations and morphological analyzes were performed.

3. RESULTS AND DISCUSSION

According to the tensile test results obtained, it was observed that the polyamide 6 matrix samples reinforced with pure carbon fiber showed the highest tensile strength and glass fiber reinforcement had a lower effect on the tensile strength of the polyamide 6 matrix. In impact resistance, it has been observed that carbon fiber reinforcement makes the material more fragile, while glass reinforcement exhibits a more ductile feature compared to carbon fiber reinforced ones.

4. CONCLUSIONS

Carbon fiber offers important opportunities with its mechanical properties. However, it is an expensive fiber due to its production methods and raw materials that require special qualifications. Glass fibers are low-cost fibers. In fact, glass fiber reinforcement reduces the unit price compared to pure polyamide, since it is cheaper than the matrix material. Hybrid structures can offer suitable features and cost-effective opportunities for their areas of use with their mechanical properties.

REFERENCES

Almangour B. Additive manufacturing of emerging materials. Springer; 2018. 1–355 p.
Brenken B, Barocio E, Favaloro A, Kunc V, Pipes RB. Fused filament fabrication of fiber-reinforced polymers: A review. Addit Manuf [Internet]. 2018;21(January):1–16.
Dizon JRC, Espera AH, Chen Q, Advincula RC. Mechanical characterization of 3D-printed polymers. Addit Manuf [Internet]. 2018;20:44–67.
Gibson I, Rosen D, Stucker B. Additive Manufacturing Technologies 3D Printing, Rapid Prototyping, and Direct Digital Manufacturing. 2015.
Huang SH, Liu P, Mokasdar A, Hou L. Additive manufacturing and its societal impact: A literature review. Int J Adv Manuf Technol. 2013;67(5–8):1191–203.
Ivey M, Melenka GW, Carey JP, Ayranci C. Characterizing short-fiber-reinforced composites produced using additive manufacturing. Adv Manuf Polym Compos Sci [Internet]. 2017;3(3):81–91.
Paolini A, Kollmannsberger S, Rank E. Additive manufacturing in construction: A review on processes, applications, and digital planning methods. Addit Manuf [Internet]. 2019;30(October):100894.
Papon EA, Haque A. Fracture toughness of additively manufactured carbon fiber reinforced composites. Addit Manuf [Internet]. 2019;26(December 2018):41–52.
Tofail SAM, Koumoulos EP, Bandyopadhyay A, Bose S, O'Donoghue L, Charitidis C. Additive manufacturing: scientific and technological challenges, market uptake and opportunities. Mater Today [Internet]. 2018;21(1):22–37.
Wohlers T. Wohlers report 2019: 3D printing and additive manufacturing state of the industry annual worldwide progress report [Internet]. Wohlers Associates. Wohlers Associates; 2019.
Zaverl M, Seydibeyoğlu MÖ, Misra M, Mohanty AK. Studies on Recyclability of Polyhydroxybutyrate-co- valerate Bioplastic: Multiple Melt Processing and Performance Evaluations. J Appl Polym Sci. 2011;116(5):2658–67.

INFLUENCE OF CERAMIC-BASED ADDITIVES ON THE DRY SLIDING WEAR BEHAVIOUR OF PA 12 PRODUCED BY SLS

Burçin Özbay Kısasöz[1], İbrahim Tütük[2], Sencer Süreyya Karabeyoğlu[3], Ebubekir Koç[4], Alptekin Kısasöz[5]
[1]*Fatih Sultan Mehmet Vakif University, ALUTEAM , burcinozbay@gmail.com*
[2]*Fatih Sultan Mehmet Vakif University, ALUTEAM, itutuk@fsm.edu.tr*
[3]*Kirklareli University, Department of Mechanical Engineering, sencerkarabeyoglu@klu.edu.tr*
[4]*Fatih Sultan Mehmet Vakif University, ALUTEAM, ekoc@fsm.edu.tr*
[5]*Yildiz Technical University, Department of Metallurgical and Materials Engineering, akisasoz@gmail.com*

ABSTRACT

The Selective Laser Sintering is one of the main methods to fabricate polyamide matrix composites. Various reinforcements are used like metalic, polymeric and ceramic to produce polyamide based composites. Also, ceramic based additives have improved the tribological and thermal behaviour of the polyamide. In this study, Polyamide 12 (PA 12) matrix composites were produced with ceramic microsphere additives by Selective Laser Sintering methods using two different energy density values. Influence of ceramic based additives on the tribological behavior of PA 12 was investigated by wear tests. Dry sliding wear tests were carried out with 5N and 20N test loads, and 100 mm/s sliding velocity. The examinations revealed that the composite sample produced by 0.04 J/mm^3 energy density value provides the highest wear resistance compared to other samples.

Keywords: Polyamide composite, additive manufacturing, dry sliding wear, ceramic-based particulates.

1. INTRODUCTION

Several reinforcement materials have been used to improve mechanical and physical properties of the PA 12 matrix composites including ceramic particulates, metals, carbon fiber and functionalized graphene. Additive manufacturing (AM) is a remarkable fabrication method ensures production of complex-shaped parts layer by layer. AM provides design flexibility, improved mechanical properties and fabrication without the need for any mold compared the conventional methods. Owing to these advantages, AM products are frequently used in fabrication of polymer matrix composites.
Selective Laser Sintering (SLS) has been frequently used for production of polyamide-based composites in order to obtain better physical and mechanical properties. SLS provides better mechanical properties in terms of mechanical strength and modulus. In this study, ceramic particulate reinforced PA 12 composites were fabricated with various energy density values by SLS system. Moreover, dry sliding wear tests were performed and wear behavior of composites depending on energy density values was investigated.

2. MATERIALS AND METHODS

Samples were produced by EOS P 110 (EOS GmbH) SLS production machine. The average grain size of the PA 2200 PA 12 and thermos sphere W75 ceramic powders were determined as 60 µm and 75 µm, respectively. The PA 12 (Sample 1) and PA 12 matrix polymer composites (Sample 2 and Sample 3) were produced by different energy densities. The energy density values were determined as 0.0336 J/mm^3, 0.0400 J/mm^3 and 0.0500 J/mm^3 for Sample 1, Sample 2 and Sample 3, respectively.
Dry sliding wear tests were carried out by using a ball-on-disc type tribometer at room temperature. 6-mm-diameter Al_2O_3 ball was employed as a counterface. Dry sliding wear test parameters were performed with 150 m sliding distance at 0.1 m/s sliding velocity by 5N and 20N test load, respectively.

3. RESULTS AND DISCUSSION

Higher wear rates were recorded when the surface of the samples was subjected to higher test load (Fig. 1). The wear rate values of the composites were higher than the neat PA 12. The lowest wear rate value was obtained in Sample 2. Lower energy density values, applied during the production of PA 12 matrix composite, provided the fabrication of composite with resistant to wear. Also, it has been also noticed that increasing test load causes an increase in the wear track depth of the samples.

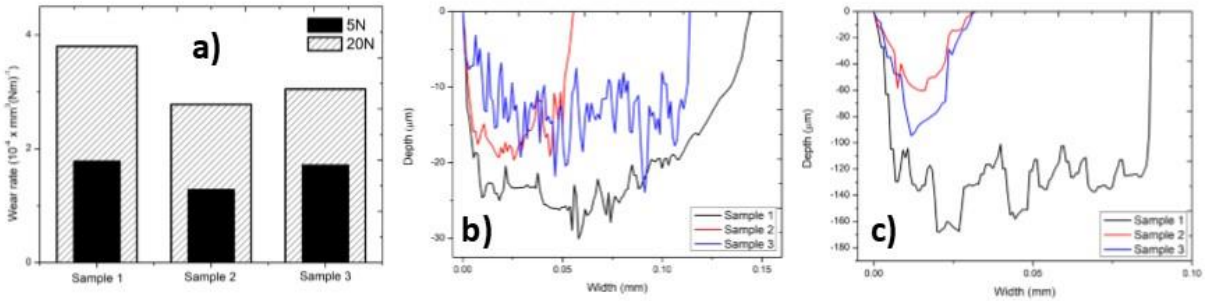

Figure 1. a) Wear rate, b), c) 2-D profiles of the wear tracks

Raising the test load increased the CoF of the all energy density dependent samples, causing more significant material degradation. As a result, the CoF of the Sample 2 sample was determined to be the lowest among all samples. The samples worn at 20N test load reached steady state CoF after a certain sliding distance. However, samples worn at 5N test load showed a heavy fluctuations. High test load provided high pressure on the surface and new contact surfaces were formed between the composite and the counter and steady CoF values were obtained for the 20 N test load.

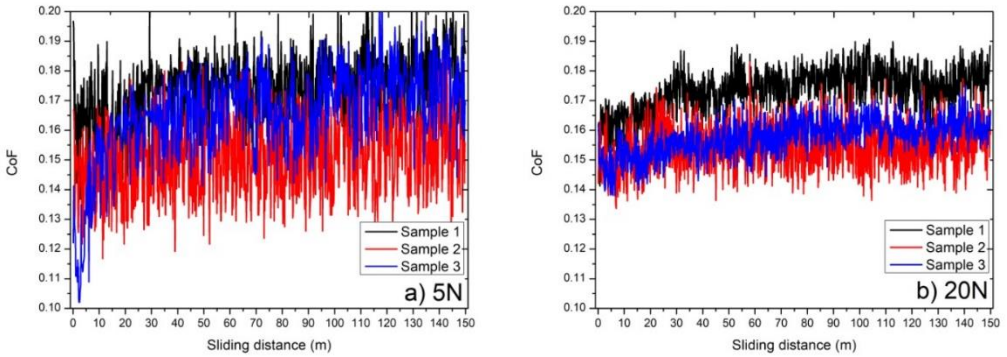

Figure 2. CoF values of the samples a) 5 N test load, b) 20 N test load.

4. CONCLUSIONS

PA 12 matrix composites provided higher wear resistance compared to neat PA 12 sample. Increasing wear test load caused an increase in wear rate and wear loss. Higher test load caused a steady CoF via ensuring new contact surfaces between the worn sample and the counter.

REFERENCES

Farahani, R. D., Dube, M., Therriault, D. (2016). Three-Dimensional Printing of Multifunctional Nanocomposites: Manufacturing Techniques and Applications, *Advanced Materials*, 28(28), 5794-5821. doi: 10.1002/adma.201506215

Hasan, M. M., Zhou, Y., Mahfuz, H., & Jeelani, S. (2006). Effect of SiO_2 nanoparticle on thermal and tensile behavior of nylon-6. *Materials Science and Engineering A*, 429(1-2), 181-188. doi: 10.1016/j.msea.2006.05.124

Martelli, V., Toccafondi, N., & Ventura, G. (2010). Low-temperature thermal conductivity of Nylon-6/Cu nanoparticles, *Physica B: Condensed Matter*, 405(20), 4247-4249. doi: 10.1016/j.physb.2010.06.031

Shiva Kumar, K., & Chennakesava Reddy, A. (2020). Investigation on mechanical properties and wear performance of Nylon-6/Boron Nitride polymer composites by using Taguchi Technique. *Results in Materials*, (5), 100070. doi: 10.1016/j.rinma.2020.100070

INJECTION MOLDING OF MICROFLUIDIC DEVICES WITH 3D PRINTED INSERT TOOLS

Parya Teymoory[1] Ulas Yaman[1], Ender Yildirim[1]
[1]*Mechanical Engineering Department, Middle East Technical University,*
06800 Ankara, Turkey, parya.teymoory@metu.edu.tr, uyaman@metu.edu.tr, yender@metu.edu.tr

ABSTRACT

The use of microfluidic devices has grown in both potential and number of applications in recent years. Micro-injection molding (µIM) is an attractive method of manufacturing these devices due to its excellent process throughput and commodity-priced raw materials. Still, manufacturing microstructured tooling for prototyping remains a slow and costly endeavor. This work investigates the feasibility of utilizing additive manufacturing to produce polymer-based tooling for µIM. Inserts consisting of an array of 100µm-1mm-wide straight protrusions were made by stereolithography (SLA). The high flow rate of melted polymer material was molded in the inserts. The molded samples were characterized using surface profilometry and optical microscopy to investigate process resolution capabilities and replicability. It could be possible to replicate the features down to 100 µm in width at a melt temperature of 260ºC. The experiments revealed that the replication of micro-channels, including feature profiles, were highly sensitive to polymer-based tooling.

Keywords: stereolithography, micro injection molding, microfluidic, replication

1. INTRODUCTION

Microfluidic devices offer the potential for a wide variety of chemical and biological operations that are applicable for diagnostic and therapeutics with higher efficiency, repeatability, and reproducibility (Bendre et al., 2022; Sackmann, Fulton, & Beebe, 2014). With the increasing demand for microfluidic devices made out of thermoplastic materials to reduce compound absorption and increase manufacturability, there is a need for new rapid microfabrication prototyping processes that can be used at the early stages of the device development to accelerate transitioning microfluidic devices from the lab to scalable manufacturing and product deployment (Becker, 2010). In this regard, the use of additive manufacturing and capabilities has opened the door for rapid tooling in conjunction with µIM is becoming increasingly popular, with cost-effectiveness and time benefits to coupling the techniques for the manufacture of such devices, where the microstructure directly impacts the performance of the products (Gheisari, Bártolo, Goddard, & das Neves Domingos, 2017; Walsh, ter Horst, & Markl, 2021). Consequently, this study aims to determine the feasibility of replicating milli/micro-scale features from an SLA mold insert with the µIM. We also investigated the correlations between the surface quality and roughness of the molds and the replication quality of features. Moreover, channel width and height influence on the replication quality of micro features injection molding process are characterized.

2. MATERIALS AND METHODS

The mold was formed by placing a two-part SLA printed polymer insert in a steel holder. Figure 1 shows a top view of the steel holder (a) and 3D printed polymer insert in the steel holder (b). The insert was produced via an LCD-based SLA printer (Photon Mono SE, Anycubic, China) using transparent clear resin (UV Sensitive Resin, Anycubic, China). The layer thickness was set to 10 µm. The printed insert was washed for 9 min. and UV flood post-cured for 3 min. Polypropylene was injected at 260ºC using a benchtop injection molder (MSE Technology, Turkey). The injected sample is shown in Figure 1c.

3. RESULTS AND DISCUSSION

Figure 2 shows the protrusions on the mold and replicated channels on the sample. We observed that all 100 µm, 300 µm, and 1 mm-wide protrusions could be replicated. All protrusions were designed to have a thickness of 200 µm. To investigate the replicability, we measured the profiles of the replicated channels using a handheld surface profilometer (MarSurf PS10, Mahr Inc., Providence, RI, USA). However, the conical profile of the stylus enabled the extraction of only the profile of 1 mm-wide channel (Figure 2e). The profile reveals that 1 mm-wide 200 µm-deep channels can be successfully replicated by using SLA printed insert. The microscope image of the insert (Figure 2a, b) indicates that the 3D printed microstructure is regular and homogeneous across the whole 3D printing area, but there are some surface defects on the protrusions (Figure 2b). Optical images in Figure 2 compare features on

the mold insert and the injection molded part, showing that all the features on the mold insert have been well replicated and the overall quality of the 3D printed channels was good, with near full fidelity of the channel depth. It can be seen from Figure 2c and d that part of the channels without any defects on the mold has a better replication quality than those parts of channels with defects. Sharp edges can be seen free of defects (shown by the black arrow in Figure 2d), indicating that the features are sensitive to defects in the mold.

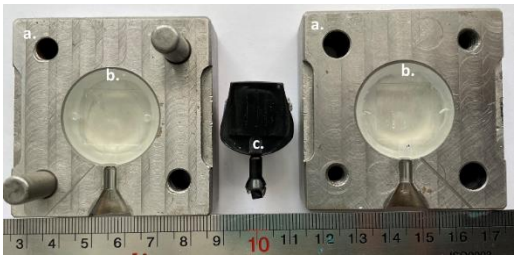

Figure 1. Top view of the mold and the injected part: (a) two-part steel holder, (b) SLA 3D printed two-part insert, and (c) injection molded sample

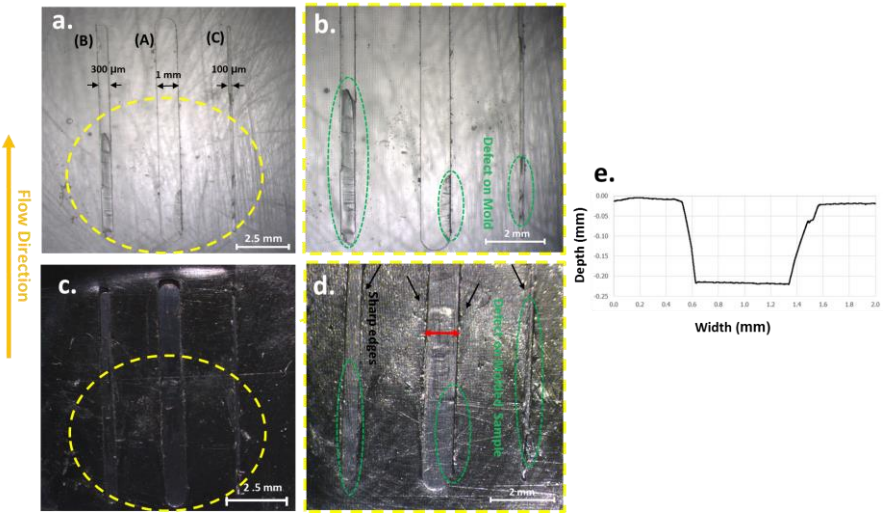

Figure 2. The microscope image of the top of features (a) and (b) on the mold, (c) and (d) on the injected part, and (e) profilometer trace of the channel is indicated by the red arrow in (d).

4. CONCLUSIONS

This work showed that SLA 3D printed inserts could be used to prototype microchannels of widths ranging between 100 µm and 1 mm. The replication of the features was sensitive to mold surface properties, especially the roughness, which has a crucial effect in achieving micro features with high replication quality.

REFERENCES

1) Becker, H. (2010). Mind the gap! *Lab on a Chip*, *10*(3), 271–273.
2) Bendre, A., Bhat, M. P., Lee, K.-H., Altalhi, T., Alruqi, M. A., & Kurkuri, M. (2022).. *Materials Today Advances*, *13*, 100205.
3) Gheisari, R., Bártolo, P., Goddard, N., & das Neves Domingos, M. A. (2017).. *Rapid Prototyping Journal*.
4) Sackmann, E. K., Fulton, A. L., & Beebe, D. J. (2014). *Nature*, *507*(7491), 181–189.
5) Walsh, E., ter Horst, J. H., & Markl, D. (2021). *Chemical Engineering Science*, *235*, 116498.

INVESTIGATION FOR EFFECTS OF HEAT SUPPORT DESIGN FACTORS ON OVERHANGS IN DMLS PROCESS

Furkan Erdogdu[1], Firat Mavi[2], Beyza Bilgiler[1], Prof. Dr. I. Etem Saklakoglu[2]
[1]*Sentes-BIR R&D Center, furkan.erdogdu@sentes.com.tr*
[2]*Ege University Mechanical Engineering Department, firat.mavi@ege.edu.tr*
[1]*Sentes-BIR R&D Center, beyza.hasdemir@sentes.com.tr*
[2]*Ege University Mechanical Engineering Department, i.e.saklakoglu@ege.edu.tr*

ABSTRACT

In this study, the manufacturability of overhangs with heat supports and the effect of design factors characterizing heat supports on part quality were investigated in the DMLS method. For this purpose, the distance between the overhangs and the heat support surface, the width and height of the heat supports, and the scanning order of the overhang and heat support sections are considered as independent factors. Sample productions were carried out using Inconel 625 alloy with different levels of these factors. Images were taken over the powder bed with the optical tomography system during the process. Dimension, roughness, hardness measurements and microstructure examinations were carried out on the produced samples. When the results were evaluated, it was observed that the dimensional deviation and surface roughness decreased with the decrease in the distance between the overhangs and the heat support surfaces. However, it has been observed that the scanning order of the overhang and heat support sections is quite effective on the quality of the part. When the relationship of the heat support width and height factors with the final product properties is evaluated, it is concluded that there is a lower level of relationship compared to the other two factors. When the cube sample produced as a reference in the experiment and the structure of the overhangs are compared, it is thought that the heat support parameters used in the experiment can contribute to subsequent studies.

Keywords: DMLS, Inconel625, heat supports

1. INTRODUCTION

The production of overhangs is one of the challenging problems encountered in metal additive manufacturing processes. Vertical and up facing geometries are built on top of the previous layer, while overhangs are built on loose powders. Since the thermal conductivity of powder particles is lower than the conductivity of bulk material, local overheating and increase in melt pool sizes can be seen during scanning. In addition, due to gravity, the powder bed cannot sufficiently support the liquid metal and the molten pool becomes unstable due to capillarity, turbulent liquid flow and other phenomena. Thus, the tendency to defect formation increases and the production quality is negatively affected (Babu et al. 2022; Chen et al. 2017; Paggi et al. 2019). Distortions can be seen due to the inadequacy of the specified mechanical constraints and the non-uniform stresses acting on the structure. Support structures are added to the designs to reduce these effects. However, it is very difficult to remove these support structures from the main structure with post-processing (Cooper et al. 2018). Nowadays, the effort to provide lightness at the same time with functionality causes part designs to become increasingly complex, and therefore the demands for supportless additive manufacturing processes are increasing. In current studies carried out with different machines and materials, it can be seen that structures with an inclination angle of 30° can be produced without support (Weber et al. 2021).
(Cooper et al. 2018) stated that by changing the thermal properties of the area under the overhangs, the thermal stresses acting on these structures and thus the distortions can be reduced. They stated that heat flow and thermal behavior can be improved by producing overhangs with parts positioned a short distance from the surface without contacting their lower surfaces. Researchers labeled these support parts, which reduce the distortions seen in overhangs, as non-contact heat supports. However, they stated that heat supports are effective in overhang geometries with different curves and shapes and these structures require less finishing compared to traditional support structures. In the same study, the researchers stated that the efficiency of the heat supports depends on the gap distance between the overhang surface and the thickness of the heat support.
In this study, the producibility of overhangs with heat supports in the DMLS method and the effects of factors such as the distance between the overhang surface and the heat support, the height and width of the heat support and the scanning order on the manufacturing quality were investigated.

2. RESULTS AND DISCUSSION

When the distance between the overhangs and the heat support is between 0.24 and 0.48 mm, it has

been observed that the overhangs and the heat support fuse with each other. At 0.52 mm, it was observed that the part did not fuse with the heat support and the block supports could be removed successfully and easily after production. As a result of the dimensional measurements taken from the overhangs, it was observed that the deviation in the Z direction decreased as the distance between the overhang surface and the heat support surface decreased. Also, the deviation detected in the condition of scanning the overhang section before the heat support section was found to be less compared to the opposite condition. However, when the relationship between width and height values and dimensional deviation was examined, no specific trend was observed.

When the roughness measurements were evaluated, it was observed that the Ra value on the overhang surface decreased gradually with the decrease in the distance between the overhang surface and the heat support but did not change in a certain trend on the top surface. It was observed that the roughness on both surfaces increased in the condition that the heat support section was scanned first. However, no high correlation was observed between width and height values and surface roughness.

No cracks and porosity in macro dimensions were observed in the optical microscope examinations of the samples. On the other hand, it was observed that the hardness values measured in the samples were higher than the cube sample produced as a reference, but its relationship with independent factors could not be determined.

3. CONCLUSIONS

In this study, the usability of heat supports in the production of overhangs by using Inconel 625 alloy in the DMLS method. Also, the effect of heat support design parameters on the part quality were investigated. Obtained results are given below.

- As the distance between the overhang and the heat support surface decreases, the dimensional deviation and the Ra value on the downfacing surface decrease.
- The scanning order of the overhang and heat support parts affects the dimensional deviation and surface roughness values.
- The effect of the distance between the overhang and the heat support surface on the production quality is higher than the width and height of the heat support.

REFERENCES

Babu, Joe Joseph, Mehrshad Mehrpouya, Thomas C. Pijper, Gydo Willemsen, and Tom Vaneker. 2022. “An Experimental Study of Downfacing Surfaces in Selective Laser Melting.” *Advanced Engineering Materials* (March):2101562.

Chen, Hongyu, Dongdong Gu, Jiapeng Xiong, and Mujian Xia. 2017. “Improving Additive Manufacturing Processability of Hard-to-Process Overhanging Structure by Selective Laser Melting.” *Journal of Materials Processing Technology* 250(May):99–108.

Cooper, Kenneth, Phillip Steele, Bo Cheng, and Kevin Chou. 2018. “Contact-Free Support Structures for Part Overhangs in Powder-Bed Metal Additive Manufacturing.” *Inventions* 3(1).

Paggi, Umberto, Rajit Ranjan, Lore Thijs, Can Ayas, Matthijs Langelaar, Fred van Keulen, and Brecht van Hooreweder. 2019. “New Support Structures for Reduced Overheating on Downfacing Regions of Direct Metal Printed Parts.” *Solid Freeform Fabrication 2019: Proceedings of the 30th Annual International Solid Freeform Fabrication Symposium - An Additive Manufacturing Conference, SFF 2019* 1626–40.

Weber, Sebastian, Joaquin Montero, Matthias Bleckmann, and Kristin Paetzold. 2021. “Support-Free Metal Additive Manufacturing: A Structured Review on the State of the Art in Academia and Industry.” *Proceedings of the Design Society* 1(August):2811–20.

INVESTIGATION OF ELECTROCHEMICAL POLISHING ON THE SURFACE OF THE γ-TiAl PARTS PRODUCED BY ADDITIVE MANUFACTURING

Safak Nesli[1], Hasan Demirtas[2], Oguzhan Yilmaz[3], Levent Subasi[4], Aydemir Gunaydin[4], Guney Mert Bilgin[4], Akin Orhangul[4], Guray Akbulut[4]

[1]*Advanced Manufacturing Technologies Research Group (AMTRG), Department of Mechanical Engineering, Faculty of Engineering, Ostim Technical University, 06374, Ankara, Turkey, safak.nesli@ostimteknik.edu.tr*
[2]*Samsun University, Engineering Faculty, Department of Mechanical Engineering, Samsun, 55420, Turkey*
[3]*Advanced Manufacturing Technologies Research Group (AMTRG), Department of Mechanical Engineering, Faculty of Engineering, Gazi University, 06570, Ankara, Turkey, oguzhanyilmaz@gazi.edu.tr*
[4]*TUSAS Engine Industries Inc., 26210, Eskisehir, Turkey*

ABSTRACT

Additive manufacturing (AM) technologies play a significant role in the industrial field due to the possibility to build complex, near-net-shape, and porous parts. However, the high surface roughness of AM parts remains a critical drawback, limiting their use as an as-built part. Therefore, the electropolishing (ECP) treatment could be an alternative post-process method for simple, complex, or porous parts to enhance the surface. In this study, the fundamentals of the ECP process, experiments on additive manufactured part surfaces and the roughness reduction has been examined. A cubic γ-TiAl part produced by electron beam melting (EBM) was selected as the sample for the ECP process. The morphological results showed that ECP can improve surface finish. Surface roughness values are enhanced by 97.2 %, 96.9 % and 53.2%, in terms of Sa, Sq and Sz, respectively.

Keywords: Additive manufacturing, electrochemical polishing, electron-beam melting, surface texture.

1. INTRODUCTION

The potential of additive manufacturing (AM) technologies in the industry is an undeniable fact due to the impact on the production of complex, and porous parts. However, the direct use of AM parts is limited because of the high levels of roughness on the part surfaces. Electropolishing (ECP) could be an alternative method for surface enhancement of AMed parts. ECP has the possibility of modifying complex geometries and porous parts by using environmentally friendly electrolytic solutions (Acquesta & Monetta, 2021).

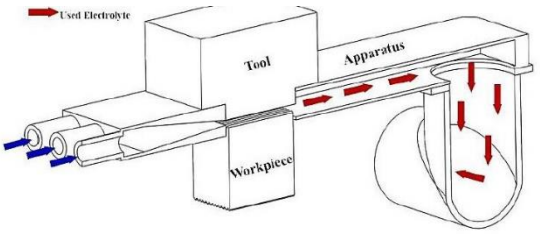

Figure 1. Schematic representation of the ECP process (Demirtas et al., 2021).

Figure 1 represents the schematic view of the ECP process. The ECP treatment refers to the electrochemical process, which creates a mirror-like surface on base metals by selectively removing specific particles from the surface. Teixeira reduced the surface roughness of Ti-6Al-4V parts by 50–70% using NaCl-ethylene glycol-based electrolyte and applying electric pulses (Teixeira, 2011). Besides, Lassell concluded the ECP process was not suitable for the Ti-6Al-4V surface finish in terms of Ra values, but successful in removing surface imperfections, such as laser scanning lines. The objective of the present work is to examine the effect of electrochemical polishing on the surface properties such as topography and roughness, of additive manufactured γ-TiAl part (Lassell, 2016).

2. MATERIALS AND METHODS

A cubic γ-TiAl part with the dimensions of 25×25×25 mm has been successfully produced by an ARCAM EBM machine (Figure 2).

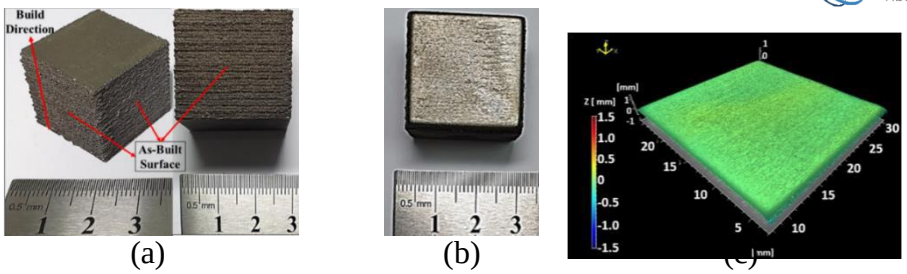

(a) (b) (c)

Figure 2. a) As-Built γ-TiAl part produced with EBM method, b) Electrochemical polished surface and c) morphological analysis of the AM part.

Electropolishing process has been applied onto the EBM - γ-TiAl part surface with an electrochemical Machining (ECM) set-up presented in (Demirtas et al., 2021). The specification of the set-up is presented in Table 1. Surface morphological assessments before and after ECP was examined via a white-light interferometer Polytec TopMap Metro.Lab TMS 150 to observe the changes.

Table 1. Specifications of ECM machine tool (Demirtas et al., 2021).

ECM Specification	**Value**
Travel distance in mm (X-Y-Z)	350*350*100
X-Y-Z movements	Recirculating Rolling guides
Max. movement speed (mm/min)	400
Motor type	Stepper
Motion transmission	16/5 ball screw

3. RESULTS AND DISCUSSION

ECP process and morphological analysis can be seen in Figure 2. As can be seen, the surface roughness has decreased significantly. Table 3 indicates the Sa, Sq and Sz values of both the as-built and ECP surfaces. The Sa, Sq and Sz values of the as-built surface are measured as 66.39 µm, 84.55 µm, and 706.88 µm respectively. Roughness values of the electrochemical polished surface Sa, Sq and Sz are 1.85 µm, 2.62 µm and 330.68 µm, respectively.

Table 2. Surface roughness values of As-Built and ECP surfaces.

	Sa (µm)	**Sq (µm)**	**Sz (µm)**
As-Built Surface	66.39	84.55	706.88
ECP Surface	1.85	2.62	330.68

4. CONCLUSIONS

ECP can be used to reduce surface roughness, especially complex parts. In this work, the ECP process was applied to the surface of the γ-TiAl part produced by the EBM method. As a result, the surface roughness of the AM part could be reduced by 97.2 %, 96.9 % and 53.2%, in terms of Sa, Sq and Sz, respectively.

REFERENCES

Acquesta, A., & Monetta, T. (2021). The Electropolishing of Additively Manufactured Parts in Titanium: State of the Art. *Advanced Engineering Materials, 23*(12).

Demirtas, H., Yilmaz, O., L., S., A., G., Bilgin, G. M., Orhangul, A., Nesli, S. (2021). Surface quality improvement using electro chemical machining process for γ-TiAl parts produced by electron beam melting. *Procedia CIRP, 102*, 240-245.

Lassell, A. (2016). *The electropolishing of electron beam melting, additively manufactured TI6AL4V titanium : relevance, process parameters and surface finish.*

Teixeira, A. F. (2011). *Development of an Electropolishing Method for Titanium Materials*.

INVESTIGATION OF FLUID FLOW CHANNEL GEOMETRIES FOR FUEL MANIFOLD BASED ON ADDITIVE MANUFACTURING PROCESS LIMITS

Ataberk Konukseven[1], Gokhan Dursun[2], Tarık Taha DEMİRTAŞ[1], Deniz Yurdakul[1], Bora Gençer, YETIŞER1, Murat Kadri AKTAŞ[1]
[1]*TOBB University of Economics and Technology, akonukseven@etu.edu.tr*
[2]*Tusas Engine Industries*

ABSTRACT

Fuel manifold is gas turbine engine part that connects multiple inputs and outlets with liquid flow channels. The advantages of additive manufacturing (AM) technologies offer rapid production as well as customized designs with part consolidation for fuel manifolds. However, AM part surface roughness depends on the design and process parameters affecting the part performance with fluid flow. The poor surface quality and AM process limits decrease the part efficiency due to fluid pressure drop and reduced flow rate of fuel manifolds. This study focuses on the comparison of fluid pressure drop and flow rate of fuel manifold designed with varying additive fluid channel geometries based on AM process limits. Results show that quadrangle geometry provided the lowest pressure loss for the desired manifold geometry. In addition, the outlet velocity analysis showed that triangle cross section geometry has lowest deviation between outlets. Results will be evaluated based on surface roughness of samples.

Keywords: Additive Manufacturing, Microchannels, Design for Additive Manufacturing, Surface roughness

1. INTRODUCTION

Additive manufacturing is a term for layer-oriented and fast-growing manufacturing technology introduced as rapid prototyping in the late 1980s. The term rapid prototyping describes a process for creating a representative of a system or part before the final part and commercialization. In a product development process, physical prototypes are created directly from digital data offering various opportunities for new product design [1]. Additive manufacturing also provides significant advantages in terms of reducing the manufacturing process steps whilst other manufacturing processes require multiple and iterative steps to be performed [2].

The design and additive manufacturing of parts with fluid flow channels relate to a wide variety of applications. When designing such parts, manufacturing constraints need to be considered for additive manufacturing depending on the material, machine, and process parameters. There are certain limitations in the production of parts with flow channels using the laser powder bed fusion (LPBF) technique due to process capability. A fuel manifold is a geometry with multiple inlets and outlets where small channels are connected by larger ones. Within the scope of the study, the support structures is avoided for fuel manifolds and various AM channel geometries are adopted. The fuel manifold part is redesigned based on LPBF design suggestions and flow characteristics of different flow channels are analyzed.

2. MATERIALS AND METHODS

Fuel manifold parts are designed based on LPBF suggestions with seven different cross-section geometries using Computer Aided Design (CAD) modelling. CFD (Computational Fluid Dynamics) with Inconel 718 is conducted in order to see flow characteristics depending on the various geometries. Pressure drop and flow rate of fuel is revealed with respect to various geometries and compared with nominal part. Fuel manifold has 14 outlet, however, only 7 outlet from half of the part is considered for analysis to decrease computational time. Cross section of geometries are shown in Fig. 1. CFD analysis will be repeated with surface roughness consideration.

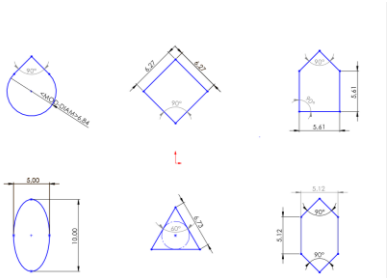

Figure 1. Cross section of manifold used for CFD analysis

3. RESULTS AND DISCUSSION

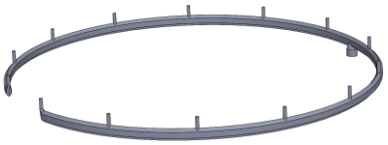

Figure 2 shows the pressure drop of seven outlets of the components.
Results show that quadrangle geometry provided the lowest pressure loss for the desired manifold geometry as the pressure of fluid decreased from 5000 kPa to 4997 kPa.

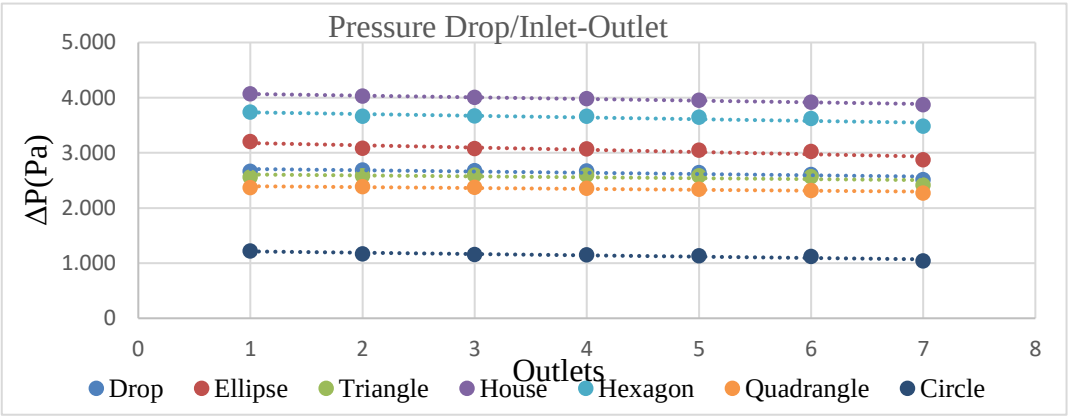

Figure 2. Pressure drop of various geometries

4. CONCLUSIONS

In the project, it was aimed to observe the effects on the flow by making changes in the flow cross-sectional areas, taking into account the constraints of additive manufacturing.
CFD analyzes were made and the most appropriate cross-sectional areas taken from the literature were selected according to the desired criteria and their effects on the flow were reported.
As a result, according to the data obtained, the section geometry with the lowest pressure loss was determined as quadrengular and the part was designed.

REFERENCES

References should be listed in alphabetical order and presented in a format according to APA6th Style.
[1] Ian Gibson, I. G. (2015). Additive manufacturing technologies 3D printing, rapid prototyping, and direct digital manufacturing.
[2] Biedermann, M., Beutler, P., & Meboldt, M. (2021). Automated design of additive manufactured flow components with consideration of overhang constraint. Additive Manufacturing, 46, 102119.

INVESTIGATION OF LASER POWDER BED FUSION DEFECT INSPECTION BY IN-SITU MONITORING AND COMPUTED TOMOGRAPHY

Çağdaş Şen[1], Oğuz Acar[1], Soner Ören[1], Emre Özeren[1], Akın Orhangül[1]
[1]*TUSAS Engine Industries, Inc., cagdas.sen@tei.com.tr*

ABSTRACT

Complex processing nature of LPBF technology requires close monitoring of the component quality both in-situ and ex-situ. Defects unique to LPBF cause degradation in final component quality and process productivity. Novel characterization methods are being implemented in the AM industry for detection and characterization of defects. In-situ process monitoring (PM) enables inspection of the build quality during the production process. X-ray computed tomography (XCT) is a post-process non-destructive inspection technology allowing internal feature characterization, dimensional and material inspection of both inner and outer geometry.

This study aims to investigate the possibility of utilizing in-situ process monitoring for different types of LPBF defects detection. For this purpose, samples were designed and produced with different simulated defects intentionally embedded. These samples were monitored and inspected using a photodiode and a high-speed camera based in-situ PM system, a micro XCT system and conventional methods via destructively cutting samples. Defect morphology, location and geometrical properties were investigated for each varying inspection method. Integration of in-situ PM into the characterization of LPBF process and components were discussed and a correlation between different inspection methods was presented in the study.

Keywords: Additive manufacturing (AM), Process monitoring (PM), X-ray computed tomography (XCT), Laser powder bed fusion (LPBF), Defect inspection

1. INTRODUCTION

One of the widely used additive manufacturing (AM) technologies, laser powder bed fusion (LPBF) offers design freedom, production ease of complex geometries and rapid prototyping for the metallic components via layer by layer build up. Besides its advantages, intricate laser and powder interaction in LPBF generates defects and anomalies that are new and not standardized yet. AM defects can be classified broadly in three categories; powder related (powder characteristics, trapped gas etc.), process related (lack of fusion, balling, keyhole, spattering, surface roughness, residual stress induced defects etc.) and post-processing related defects (thermally induced porosity, surface processing induced defects etc.) [1]. There are several ex-situ and in-situ methods to monitor and characterize these defects both destructively and non–destructively. Real-time defect detection and closed-loop control of parameters using in-situ PM offers great opportunities in the field of AM, despite its limitations of resolution, restricted field of view and data load [2]. In this study different inspection methods will be compared, defects analysis using emerging in-situ process monitoring technology will be presented.

2. MATERIALS AND METHODS

Samples design choices of the geometries made to provide simplicity to manufacturing and measurement tasks. Main limitation to sample designs was X-ray attenuation mechanics of the XCT process. In order to get sufficient and homogeneous X-ray penetration simple prismatic samples without any complex feature were designed. For each investigated defect different samples were built. By doing so easier control in manufacturing and traceability after manufacturing is achieved.

The sample geometries, designed to have specific defects, were produced in Concept Laser M2 S5 Dual-Laser system using Ti6Al4V ELI virgin powder. Particle sizes of the powder are in the range of 15-53 microns. Different process parameters with different volumetric energy densities utilized in the production for a certain set of defects, besides the standard process parameter set.

XCT operation conducted using RX Solutions EasyTom micro CT system with a 240 kV X-ray source. Each sample scanned separately with constant X-ray parameters; X-ray voltage, X-ray current and exposure time. Before each measurement calibration cycle conducted to remove residual effects of previous measurements on detector. All samples measured in the same magnification ratio resulting same voxel size for better comparison.

QM Meltpool 3D, licensed by Concept Laser GmbH, was used as the in-situ process monitoring system. The system consists of the infrared high-speed camera and the photodiode, which are located in the optical rail between the laser source and the scanning system of the machine. In this study, two types of

melt-pool data which are raw data and mapping were used for the interpretation of defects. The raw data was collected from the XY position of the scanner and the signals of the photodiode and camera sensors. The mapping was done with a combination of part geometry and the raw data for each layer.
After the manufacturing and characterization using both PM and XCT, samples were cut by aligning specifically the defects to be inspected. For this purpose, destructed samples were investigated using optical methods to capture the form and position of the defects.

3. RESULTS AND DISCUSSION

In-situ process monitoring were used to investigate different simulated defects real time during the production process. Samples were then inspected using XCT, which enables the internal part inspection. Defect size, diameter, location and morphology detectability limitations for different inspection methods were compared. It was seen that the in-situ PM is capable of capturing the defects to a certain size. Furthermore XCT is more capable of detecting defects considering their size and percentage, despite process' high cost and considerably slow speed. For the volumetric porosity inspection, correlation was conducted by taking into account the whole sample porosity distribution. Figure 1 presents a cylindrical sample with two different porosity percentage levels resulting from varying processing volumetric energy densities.

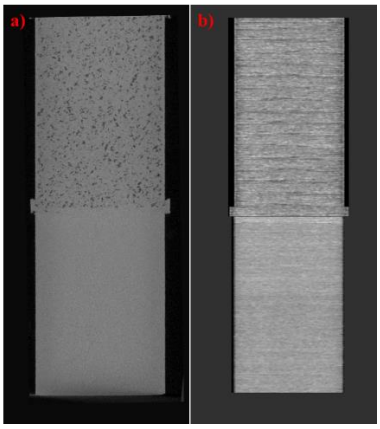

Figure 1. A LPBF cylindrical sample slice with varying porosity levels investigated a) using XCT b) using in-situ meltpool PM system.

4. CONCLUSIONS

Integrating the metrology into the process chamber offers advantages such as automation of the process, continuous monitoring of process chain and better process efficiency rates. It also offers AM process cost reduction by detecting the defects earlier in the process chain. Efficiency and limitations of in-situ PM system is analyzed in this study, also the PM and XCT defect inspection precision demonstrated by comparing the results with destructive methods. Future work will be to investigate the accuracy of PM system for different type of geometries and defects.

REFERENCES

1. Mostafaei, A., Zhao, C., He, Y., Reza Ghiaasiaan, S., Shi, B., & Shao, S. et al. (2022). Defects and anomalies in powder bed fusion metal additive manufacturing. Current Opinion In Solid State And Materials Science, 26(2), 100974.
2. Everton, S., Hirsch, M., Stravroulakis, P., Leach, R., & Clare, A. (2016). Review of in-situ process monitoring and in-situ metrology for metal additive manufacturing. Materials &Amp; Design, 95, 431-445.

INVESTIGATION OF SKINCORE STRATEGY TO INCREASE PRODUCTIVITY FOR LARGE PARTS IN LASER POWDER BED FUSION SYSTEM

Oguz Kaan OZTURK[1], Taner KARAGOZ[2]
[1]*okozturk@coskunoz.com.tr*
[2]*tkaragoz@coskunoz.com.tr*

ABSTRACT

Selective laser melting technology allows the production of complex parts that cannot be produced by conventional methods. With many different types of metal powder, parts in different sizes can be produced for different sector needs. Especially the production of large and high density parts can take long build times and risky. Residual stresses during production can be minimized by using different scanning strategies. However, this type of scanning strategy significantly reduces the production speed. At this point, the separation of the part into two bodies as shell and core with different scanning strategies gives the opportunity to minimize the residual stresses without compromising the production speed. In this study, it is aimed to determine the mechanical and microstructure properties of the parts produced by this method.

Keywords: hull&core, residual stress, chess strategy, stripe strategy

1. INTRODUCTION

In selective laser melting technology, metal powder can reach temperatures over 1000 C instantly, with the effect of high laser powers on the powder. This causes a high residual stress in the part. This rate can be much higher, especially in large dimension and full filled parts. High residual stress during production causes distortions and cracks on the part. Also during support removing process distortions may occur. Stress relieving heat treatments applied after production are not always sufficient to reduce defects.

There are some scanning strategies for different purposes in selective laser melting technologies. Especially in parts with high residual stress, the chess scanning strategy, which scans the surface by dividing it into small cells, is used. However, the scanning speed in this method is quite low. While minimizing the thermal deposition of large-sized parts, it extends the production time considerably. In this study, it is aimed to minimize the residual stress without sacrificing the production time by separating the part into two bodies and combining different scanning strategies.

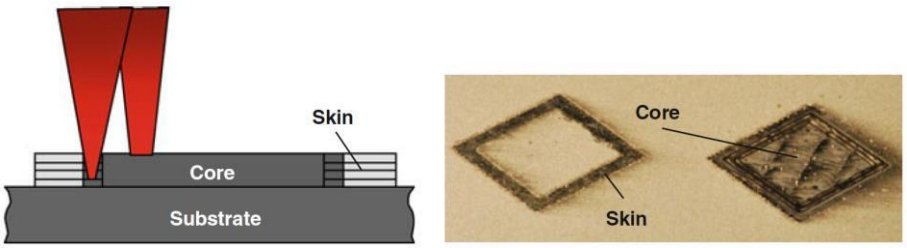

Figure 1. Scanning of Hull and Core [1]

2. MATERIALS AND METHODS

In this study, different scanning strategies will be combined to minimize the distortions and cracks caused by high residual stress in the parts produced with selective laser melting. The part volume will be divided into two bodies as the outer shell and the core. The bodies will be scanned with different scanning strategies. The large outer part is the area that stress concentrations are most frequently encountered.
In chess scanning strategy, the area is divided into small sections and scanned. In outer area, it will be preferred to minimize residual stresses. In the inner part, the stripe scanning strategy will be used to tolerate the decrease in production speed in the outer shell. In this way, the balance of stress deposition and production speed will be maintained. The parts produced in different shell/core combinations will be analyzed with various mechanical and microstructural tests. After the tests, the optimum part and parameter will be determined in terms of properties such as density and strength.

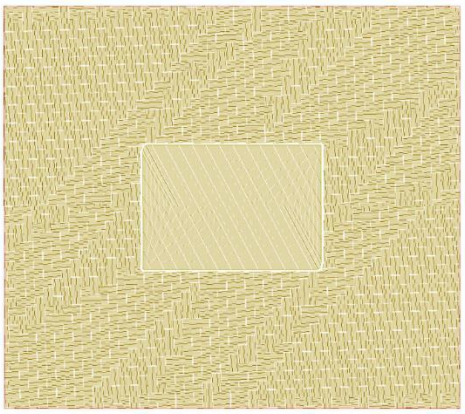

Figure 2. Hull and Core

3. RESULTS AND DISCUSSION

After the tests, it will be seen that the distortions and cracks especially in large cross-sectional and full fileed parts are minimized. This study will find a solution to the questions of maintaining the balance of the production time of the parts and density of the parts.

4. CONCLUSION

The optimum shell/core ratio, which will be determined according to the mechanical and microstructure test results, will be determined. With this ratio, errors cause of residual stress will be prevented, especially for that large cross section area parts.

REFERENCES

[1] Poprawe, R., Hinke, C., Meiners, W., Schrage, J., Bremen, S., & Merkt, S. (2015). *SLM Production Systems: Recent Developments in Process Development, Machine Concepts and Component Design* (pp. 49–65). https://doi.org/10.1007/978-3-319-12304-2_5

INVESTIGATION OF THE EFFECT OF LATTICE PARAMETERS ON MECHANICAL PROPERTIES AND RELATIVE DENSITY IN OPTIMIZATION OF LATTICE STRUCTURES IN ADDITIVE MANUFACTURING

Mutlu, F.[1], Kayacan, M.C.[2]
[1]*Department of Mechanical Engineering, Suleyman Demirel University, Isparta, Turkey fehmimutlu@sdu.edu.tr*
[2]*Department of Mechanical Engineering, Suleyman Demirel University, Isparta, Turkey cengizkayacan@sdu.edu.tr*

ABSTRACT

Due to energy and material savings importance of the design of light mechanical parts is increasing rapidly. Lattice structures are good method for designing parts with lightweight and multifunctional properties. With development of Additive Manufacturing (AM) technology, idea of obtaining lightweight and high-strength parts with lattice structures, which are difficult to manufacture with traditional manufacturing methods, is of interest. To obtain high specific strength parts with lattice structures, it is necessary to determine effective parameters by optimizing lattice parameters.

In this study, parameter optimization was performed on effective parameters of lattice structures, cell type, unit strut length and diameter. Analyzes were carried out under static conditions on three-point bending test pieces obtained at variable densities. In the parameter optimization studies, three types of lattice cells were used Simple Cubic (SC), Body Centred Cubic (BCC), and Face Centred Cubic (FCC). In the analysis studies, by comparing relative densities according to yield strength for different lattice structures, were determined optimum lattice parameters for minimum weight and highest strength. The obtained results were compared with literature.

Keywords: Lattice Structures, Additive Manufacturing, Lattice Parameters, Topology Optimization

1. INTRODUCTION

Lattice structures are structures obtained by repeating lattice unit cells in design space. The fact that these structures have various properties such as their special mechanical behavior, energy absorption ability, heat transfer and acoustic damping has been frequently topic of optimization studies (Chuang,2021). Lattice structures are preferred in studies and industry because of their high stiffness/weight ratio and to reduce cost and manufacturing time of parts. Lattice structures appear as areas of use in theaerospace, aviation and automotive industries (Dong, 2020).In this study, was investigated effect of lattice parameters on mechanical properties and density in optimization of lattice structures in additive manufacturing (AM). In the optimization of lattice structures, a test piece was obtained with different lattice parameters and simulation studies were carried out with the three-point bending analysis. In the parameter study of lattice optimization study, were investigated cell type, lattice unit cell size and struth element diameter. With help of these parameters, variable density lattice structures were obtained and determined effects of parameters on mechanical properties.

2. MATERIALS AND METHODS

In the optimization study of the lattice structures, method of creating lattice structures, lattice parameters and methods used in validation analyzes is given below in accordance with methodology.
Material: Ti6Al4V, which is frequently preferred in AM methods, was used as material of finite element analysis (FEA) lattice structures. Finite Element Analysis (FEA): Stress and deformation behaviors of lattice structures, which are mechanical properties, were analyzed using ANSYS Workbench software with the three-point bending test. In the analysis study, a single 130N load was applied from middle of lattice structures obtained in parameter study. Figure 1 shows lattice structure design area, dimensions and boundary conditions.

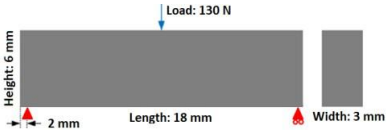

Figure 1. Three-point bending test loading and boundary conditions

Creation of lattice structures: ANSYS Spaceclaim® commercial software was used to create lattice structures in the study.

3. RESULTS AND DISCUSSION

In the study, geometric dimensions and relative densities of SC, BCC and FCC structures with different unit cell sizes according to analysis results at yield strength point are shown in Table 1.

Table 1. Geometric dimensions and relative densities of lattice structures with literature comparison

Unit cell type	Struth element diameter -d (mm)	Struth element length-a (mm)	Relative density decrease (%ρ)	Literature comparison		
				d	%ρ decrease	Ref.
SC	0,4	1,3	82,21	0,7	55	Dhiman, 2021
	0,5	**1,85**	**85,96**			
	0,6	2,15	85,04			
BCC	0,4	2,45	82,18	0,5	85	Jin, 2021
	0,5	2,8	79,83			
	0,6	2,85	70,66			
FCC	0,4	2,3	83,15	0,2	80	Tanlak, 2017
	0,5	2,8	83,05			
	0,6	3	78,20			

4. CONCLUSIONS

Highest relative density reduction (hence weight reduction) at yield strength point was determined inSC lattice structure at rate of 85.96%. As the optimum lattice parameters in SC lattice structure; struthelement length and diameter are 1,85 mm and 0,5 mm, respectively.

REFERENCES

Chuang, W. A. N. G., Jihong, Z. H. U., Manqiao, W. U., Jie, H. O. U., Han, Z. H. O. U., Lu, M. E. N. G.,.. & Zhang, W. (2021). Multi-scale design and optimization for solid-lattice hybrid structures and their application to aerospace vehicle components. Chinese Journal of Aeronautics, 34(5), 386-398.

Dhiman, S., Singh, M., Sidhu, S. S., Bahraminasab, M., Pimenov, D. Y., & Mikolajczyk, T. (2021). CubicLattice Structures of Ti6Al4V under Compressive Loading: Towards Assessing the Performance for Hard Tissue Implants Alternative. Materials, 14 (14), 3866.

Dong, G., Tang, Y., Li, D., & Zhao, Y. F. (2020). Design and optimization of solid lattice hybrid structuresfabricated by additive manufacturing. Additive Manufacturing, 33, 101116.

Jin, Q. Y., Yu, J. H., Ha, K. S., Lee, W. J., & Park, S. H. (2021). Multi-dimensional lattices design for ultrahigh specific strength metallic structure in additive manufacturing. Materials & Design, 201, 109479.

Tanlak, N., De Lange, D. F., & Van Paepegem, W. (2017). Numerical prediction of the printable density range of lattice structures for additive manufacturing. Materials & Design, 133, 549-558.

LASER WELDABILITY OF LASER POWDER BED FUSED ALSI7MG0.6

Kenan Kaan Yetil[1], Simone D'Arcangelo, Barbara Previtali, Ali Gökhan Demir
[1]*Politecnico di Milano, kenankaan.yetil@polimi.it*

ABSTRACT

Laser Powder Bed Fusion (LPBF) allows to manufacture components with lightweight and near net shape suited to aerospace and aviation applications employing Al-alloys. The process is highly suited to one-of-a-kind or small batch production of small to medium sized parts. As the maturity of the process and its end-users increase, the demand for larger components becomes more relevant. The increase of part size by increasing the size of the LPBF machine inevitably increases the cost and the complexity of the employed system. Moreover, the parts produced by multiple lasers in a large powder bed may have issues related to residual stresses and part deformation. On top of that, the cost of process failure during producing of large parts is much higher in comparison. In the light of these, the use of joining operations, in particular welding, appears as a suitable option for the production of large components via LPBF. Indeed, the process lends itself well to also producing dedicated joint edge preparations, thickness and section variation within the location of the welded joint. Amongst different processes, laser welding stands out as a viable option as it can provide narrower weld seam and heat affected zone, produce less deformation on the parts and be automated with cartesian or robotic manipulators.

In the literature, laser weldability of some LPBF produced alloys such as Stainless Steel, Titanium and Inconel have been studied, and relatively successful welds with low relative densities were obtained (Jokisch et al., 2019; Matilainen, Pekkarinen, & Salminen, 2016; Wits & Jauregui Becker, 2015). However, as being one of the most commonly used materials in aerospace, automotive and aviation industries, laser welding of LPBF produced aluminum alloys still requires a further understanding. Various researchers made efforts on the laser weldability of the LPBF produced aluminum alloys, and the biggest challenge emerged as significantly high percentage of porosity, hence poor mechanical properties (Mäkikangas, Rautio, Mustakangas, & Mäntyjärvi, 2019; Möller, Schnabel, Scurria, Jöckel, & Baumgartner, 2021; Zhang et al., 2019). While the previous results show the overall problem, a greater understanding of the pore formation causes is required. From this perspective, the use of oscillating beams and wire feeding as more recent solutions appear to be neglected as well.

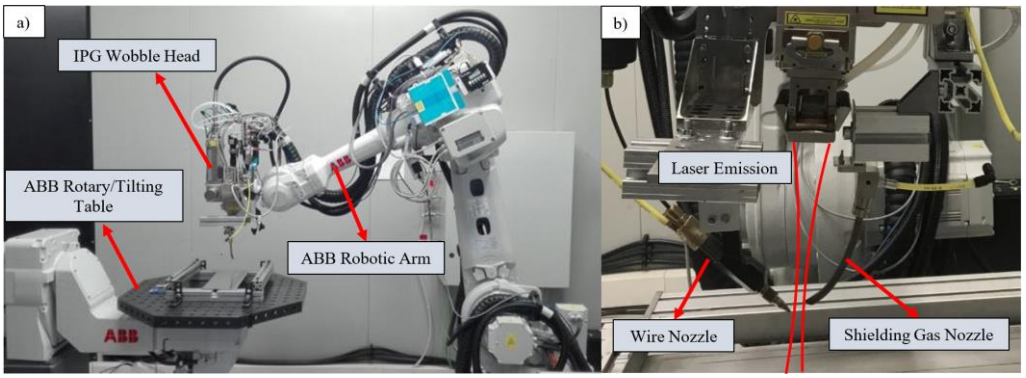

Figure 1. Welding system consists of a) robotic and beam oscillation units and b) wire feeding and shielding.

Accordingly, in this work laser weldability of LPBF produced AlSi7Mg0.6 is assessed with novel beam oscillation and wire feeding solutions. Flat plate specimens with 50 mm x 75 mm x 3 mm dimensions were produced with AlSi7Mg0.7 using an industrial LPBF system (Renishaw AM250) with sufficient part density (>99%). The welds were realized using an IPG YLS-6000 continuous wave infrared laser with a maximum power output of 6000 W. As seen in Figure 1.a), the laser system was equipped with a 6 degree of freedom ABB IRB 4600 robotic arm with ABB IRPB A-250 rotary-tilting table. In order to expand the research, IPG D50 Wobbling Head was used to virtually increase the beam size by oscillating it in a circling manner with certain frequency and amplitude values utilizing a galvanometric mirror system. On the other hand, As seen in Figure 1.b), the effect of the filler wire was investigated using an Al 5356 filler wire with a diameter of 1.2 mm. The filler wire was fed using Abicor Binzel MFS-V3 and all welds were shielded using an Argon flow.

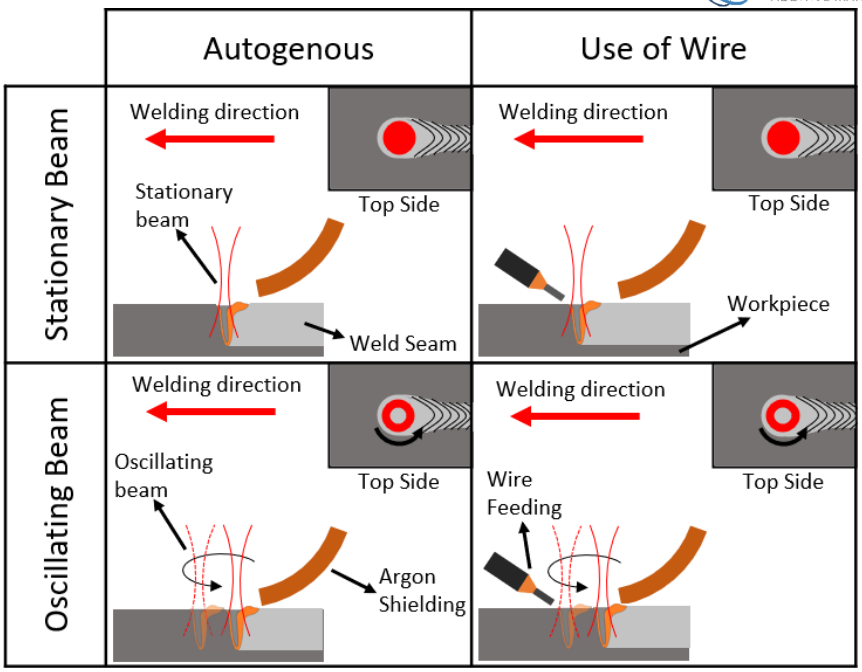

Figure 2. Representative bead on plate weld conditions.

Full pass weld conditions were sought in different weld configurations comparing beam oscillation and wire feeding solutions opposed to autogenous laser beam welding without oscillation. Figure 2. shows representative welds obtained through oscillating and stationary beams with and without the filler wire. The welding conditions were analysed further for the understanding the cause of the excessive porosity. Initial mechanical characterization was also carried out to assess the influence of the welding strategy.

REFERENCES

Jokisch, T., Marko, A., Gook, S., Üstündag, Ö., Gumenyuk, A., & Rethmeier, M. (2019). Laser welding of SLM-manufactured tubes made of IN625 and IN718. *Materials*, *12*(18). https://doi.org/10.3390/ma12182967

Mäkikangas, J., Rautio, T., Mustakangas, A., & Mäntyjärvi, K. (2019). Laser welding of AlSi10Mg aluminium-based alloy produced by Selective Laser Melting (SLM). *Procedia Manufacturing*, *36*, 88–94. Elsevier B.V. https://doi.org/10.1016/j.promfg.2019.08.013

Matilainen, V. P., Pekkarinen, J., & Salminen, A. (2016). Weldability of additive manufactured stainless steel. *Physics Procedia*, *83*, 808–817. Elsevier B.V. https://doi.org/10.1016/j.phpro.2016.08.083

Möller, B., Schnabel, K., Scurria, M., Jöckel, A., & Baumgartner, J. (2021). Fatigue assessment of laser beam welds between AlSi10Mg AM-structures and conventionally manufactured aluminum by local approaches. *Procedia Structural Integrity*, *34*, 160–165. https://doi.org/10.1016/j.prostr.2021.12.023

Wits, W. W., & Jauregui Becker, J. M. (2015). Laser beam welding of titanium additive manufactured parts. *Procedia CIRP*, *28*, 70–75. Elsevier B.V. https://doi.org/10.1016/j.procir.2015.04.013

Zhang, C., Bao, Y., Zhu, H., Nie, X., Zhang, W., Zhang, S., & Zeng, X. (2019). A comparison between laser and TIG welding of selective laser melted AlSi10Mg. *Optics and Laser Technology*, *120*. https://doi.org/10.1016/j.optlastec.2019.105696

MECHANICAL PROPERTIES OF CONTINUOUS CARBON FIBER-REINFORCED THERMOPLASTIC PARTS PRODUCED BY FUSED FILAMENT FABRICATION

Güneş Güngör[1], Fatih Bulun[1], Sertaç Altınok[1], İbrahim Erden Tekin[1], Mehmet Kepenekci[2], Ümit Aytar[1], Hakan Yavaş[1], Mete Bakır[1], Sezer Özerinç[1,2]

[1]*Turkish Aerospace Industries Corporation, Ankara, Turkey*
gunes.gungor@tai.com.tr, fatih.bulun1@tai.com.tr, sertac.altinok@tai.com.tr, ibrahim.tekin@tai.com.tr, uaytar@tai.com.tr, hakan.yavas@tai.com.tr, mete.bakir@tai.com.tr

[2]*Department of Mechanical Engineering, Middle East Technical University, Ankara, Turkey*
mehmet.kepenekci@metu.edu.tr, ozerinc@metu.edu.tr

ABSTRACT

The use of continuous fiber (CF) upgrades conventional fused filament fabrication (FFF) and enables the production of carbon fiber-reinforced composites in a versatile fashion. The key feature of continuous fiber-reinforced FFF (CFR-FFF) is its capability to spatially control the fiber orientation – an additional design parameter that is not available in the conventional production of fiber-reinforced composites. Anisotropic mechanical properties of fiber-reinforced composites combined with this new capability provide new opportunities for the design of parts with spatially and directionally varying strength for demanding structural applications. In this work, we assessed the potential of CFR-FFF by exploring the fiber layout – mechanical property relationships in carbon fiber reinforced nylon specimens. The results show that both the modulus and tensile strength strongly depend on the fiber orientation. The findings demonstrate the great potential of CFR-FFF for the design and implementation of structural parts with enhanced load-bearing capacity. Future studies should combine these efforts with the advancements in topology optimization for achieving optimum performance.

Keywords: Additive Manufacturing, Fused Filament Fabrication, Carbon Fiber Reinforced Polymers, Mechanical Properties

1. INTRODUCTION

Fused filament fabrication (FFF) is a well-established additive manufacturing (AM) technique that allows the 3D printing of thermoplastic parts (Bakır, Atik, and Özerinç 2021). Recent advances in AM technology have enabled the implementation of continuous fibers in the printed parts, which we refer to as continuous fiber-reinforced fused filament fabrication (CFR-FFF) (Li et al. 2022). This additional capability offers considerable improvement in mechanical properties that makes the approach suitable for load-bearing applications, where conventional thermoplastics do not meet the strength and stiffness requirements.

Continuous fiber-reinforced polymers are well-characterized due to their wide use in the aerospace industry. The fibers in the commercially available CFRP prepregs are available in either unidirectional or woven forms. CFR-FFF, on the other hand, enables the printing of the continuous fiber in any trajectory and in any desired orientation in each layer. Effective facilitation of this capability requires a thorough understanding of the relationships between the process parameters, the fiber layout, and the mechanical performance of the printed parts.

This work aims to experimentally investigate the effect of CFR-FFF process parameters such as fiber orientation on the mechanical properties of printed parts, with a focus on carbon-fiber reinforced nylon parts.

2. MATERIALS AND METHODS

A Markforged X7 (MA, USA) CFR-FFF printed continuous carbon fiber-reinforced tensile testing parts by using an Onyx matrix, which is a chopped micro carbon fiber filled nylon-based composite filament. The rectangular prism-shaped specimens had dimensions of 250 mm × 25 mm × 2.5 mm. The printer deposited the thermoplastic and the fiber components in separate layers through two dedicated printing heads. The infill ratio was 100%, layer thickness was 0.125 mm and specimen orientation was flat for all specimens. The other printing parameters such as nozzle temperature, printing speed, and feed rate are automatically set by the instrument for optimum printing quality.

An Instron 5900 Universal Testing Machine (MA, USA) performed the tensile tests according to the ASTM D3039 – Tensile Testing of Polymer Matrix Composites. Mechanical testing provided the strength and elastic modulus of the printed parts.

3. RESULTS AND DISCUSSION

Figure 8(a) and (b) shows the stress-strain response of fiber-reinforced specimens with fiber orientations being parallel (0°) and perpendicular (90°) to the loading axis, respectively. The 0° specimens exhibited considerably higher strength and elastic modulus.

When the fibers are parallel to the loading direction, they dominate the mechanical response, which is reflected in the superior mechanical properties. When the fibers are perpendicular to the loading direction, both the modulus and strength are primarily determined by the stiffness and load carrying capacity of the polymer matrix, resulting in values that are comparable to specimens without any continuous fiber.

The matrix material is also a composite consisting of nylon and chopped carbon fibers, developed by Markforged. Considering the mechanical properties of 3D printed nylon parts without fibers (Hasçelik et al. 2021), the composite matrix provides an appreciable amount of improvement in the mechanical properties.

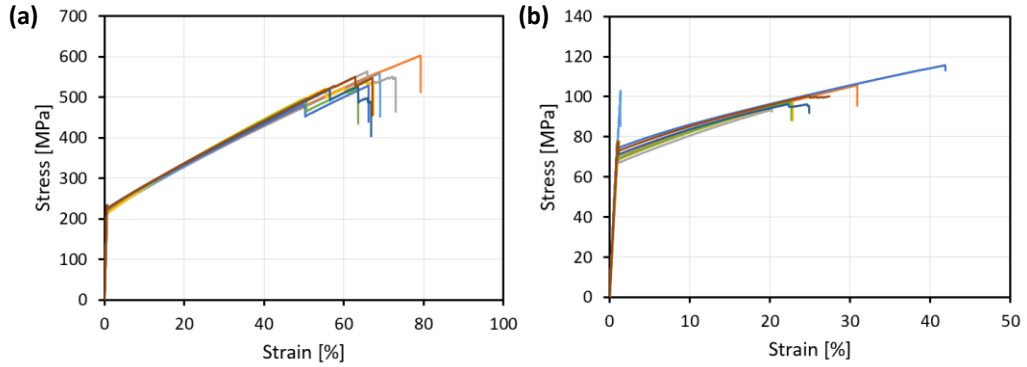

Figure 7. Stress-strain data of continuous carbon fiber-reinforced specimens with 100% infill. a) Fibers parallel to the loading direction. (b) Fibers perpendicular to the loading direction.

4. CONCLUSIONS

The experimental work demonstrated the major role that the fiber orientation plays on the mechanical behavior of continuous carbon-fiber reinforced polymer parts produced by fused filament fabrication (CCFR-FFF). The CCFR-FFF technology provides a new and versatile approach to the production of load-bearing structural parts. However, care should be taken in the design of the parts due to the strongly anisotropic behavior.

REFERENCES

Bakır, Ali Alperen, Resul Atik, and Sezer Özerinç. 2021. "Mechanical Properties of Thermoplastic Parts Produced by Fused Deposition Modeling:A Review." *Rapid Prototyping Journal* 27(3):537–61. doi: 10.1108/RPJ-03-2020-0061.

Hasçelik, Sabit, Ömer T. Öztürk, and Sezer Özerinç. 2021. "Mechanical Properties of Nylon Parts Produced by Fused Deposition Modeling." *International Journal of Modern Manufacturing Technologies* XIII(2): 2067–3604. doi.org/ 10.54684/ijmmt.2021.13.2.34

Li, Jiahui, Yvonne Durandet, Xiaodong Huang, Guangyong Sun, and Dong Ruan. 2022. "Additively Manufactured Fiber-Reinforced Composites: A Review of Mechanical Behavior and Opportunities." *Journal of Materials Science & Technology* 119:219–44. doi: 10.1016/j.jmst.2021.11.063.

MICROSTRUCTURE AND BONDING MECHANISM EVALUATION FOR BI-METALLIC SS 316-INCONEL718 PRODUCED BY DIRECTED ENERGY DEPOSTION PROCESS

Mustafa Kaş[1], Oguzhan Yilmaz[1], Büşra Aslan[1], Osman Kırlı[2], Bahadır Yücel[2] and Murathan Dak[2]
[1] *Advanced Manufacturing Technologies Research Group (AMTRG), Faculty of Engineering, Gazi University, 06570, Maltepe, Ankara, Turkiye*
[2] *UniqueTech Engineering Ltd. R&D Department, Şekerpınar Mahallesi, Marmara Geri Dönüşümcüler Sanayi Sitesi, Ayçiçek Sokak, No:25/B Çayırova-KOCAELİ*

ABSTRACT

Bimetallic applications on functional parts produced via additive manufacturing methods have been worked by my researchers in order to obtain multi-directional benefits. One of the most compatible bimetallic application is the combination of SS316 and Inconel 718 pair which has a potential application in aerospace, energy and chemical industries. In this study, SS 316 deposited on the Inconel 718 substrate and Inconel 718 deposited on the SS 316 substrate by directed energy deposition additive manufacturing method were investigated. The bonding characteristics and performance, microstructure, micro hardness behavior at bonding region were examined in detail. Since the melting points and thermal conductivity of the binary materials are not very different, bonding was generally considered successful in terms of delamination. On the other hand, in the microstructure examinations, intermetallic structures that deteriorate the material characteristics were encountered and it was determined that these structures caused regional cracking and changes in the micro hardness values.

Keywords: Additive manufacturing, directed energy deposition, bimetals

1. INTRODUCTION

Inconel 718 has been for high temperatures and harsh environment conditions (Hosseini and Popovich 2019). SS 316 alloy have superior strength, ductility, corrosion resistance and creep resistance at high and low temperatures. Due to good chemical compatibility and similar thermo-physical properties, Fe and Ni-based material combinations are relatively easy to manufacture and show good properties. However, undesirable metallurgical effects may still occur. Many metallurgical failures may become possible when Inconel718 and SS316L alloys melted together. (Jeng et al. 2007). Common problems encountered in joining different materials are inter-metallic formation, solubility limit problem, incompatibility of thermal properties and dilution problems. Most of materials have limited solid solubility and form intermetallic phases in their intermediate composition. By considering the binary phase diagrams of the alloys, a first-order decision can be made about the probability of intermetallic formations. In order to bond two different metals, thermal properties such as melting temperature, coefficient of thermal expansion, thermal conductivity must be similar. In melting processes, the temperature difference not only causes inhomogeneous heat flow and dilution, but also causes cracking in the alloy with low melting point during solidification (Kah and Jukka Martikainen 2013). Similar problems arise when bonding different materials with significantly different thermal conductivity (Anon n.d.). As the heat is dissipated from the material with higher thermal conductivity, unbalanced heat flow occurs at the transition interface. Dilution is a condition that must be considered. If it is not well controlled, dilution can fundamentally alter the material properties and metallurgy and it cause problems ranging from undesirable precipitation to hot cracking (DuPont, J. N. 2011).

2. MATERIALS AND METHODS

In this research work, single-bead depositions were produced via robotic additive manufacturing system in order to investigate the effects of directed energy deposition (DED) process parameters of each material combination on the microstructure and bonding. From the literature studies and the results obtained from preliminary studies, laser power (1000-1400 W), scanning speed (600-750 mm/min) and powder feed rate (3-4 rev/min) were used in the workshop tests. Microstructure analysis and hardness tests were carried out for the test parts. Metallographic investigations were done by etching and examining samples under optical microscope and scanning electron microscopy. Micro hardness measurements were made in the build direction. In addition, the samples were subjected to compositional analysis by EDS analysis.

3. RESULTS AND DISCUSSION

It was observed that a large number of MC and NbC carbides and precipitates were formed when SS 316 and Inconel 718 were directly deposited as seen in Figure 1.a. This formation has affected the corrosion resistance and brittleness at the interfaces of the two materials negatively. In order to overcome these failures, the problems mentioned above should be clearly identified and their formation mechanisms should be kept under control. When analyzing the bonding zone, the effect of alloying elements and impurities has to be taken into account. For example, nickel super alloys often contain small amounts of niobium, which forms precipitates of strengthening. However, in the region where nickel transitions with stainless steel, these niobiums form brittle compounds as shown in Figure 1.b that are rich in Nb with stainless steel and these compounds form interdendritic zones where mechanical properties deteriorate. The microstructure morphology was examined, grains in the structures produced by DED formed cellular or columnar. Grain orientations were not in a clear direction like powder bed systems and dendritic grains was observed at irregular orientation. Melt pools that were shorter in length and high in depth because of the high energy input per unit area significantly affected the direction of the heat flow locally. EDS line scan profile of Inconel 718 deposited on SS 316 showed that with the transition from Inconel 718 to SS316 elements such as Cr and Fe stayed almost the same, and the amount of Ni and Mo decreased.

a) b)

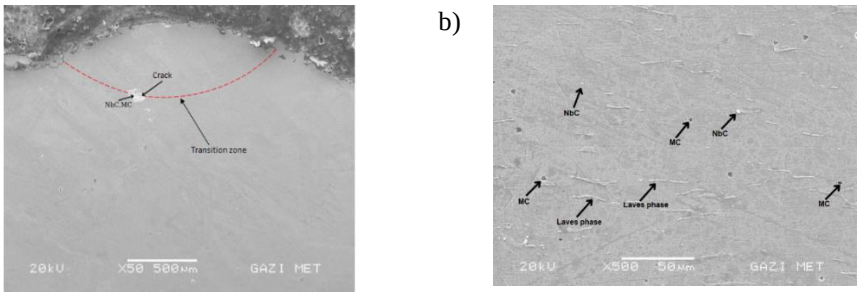

Figure 1. Microstructure of Inconel 718 bead deposited on SS 316 substrate

4. CONCLUSIONS

This study claimed that bi-metallic bonding of SS316 and Inconel 718 by DED process bonding characteristics was successful in terms of deposition and delamination. There are no observed deposition defects. Conversely microstructure evaluations showed that undesirable phases formed at the bonding region. Since these phases deteriorate the microstructure and mechanical properties by forming intermetallic formations. Because of the formation of such harmful phases is not only dependent on the thermodynamics, but also on the kinetics that will change according to the production process and the thermal history of the transition zone. EDS analysis results showed that material transition between adjacent layers from SS316 to Inconel 718 occurs in gradient, not at a sharp interface as designed.

REFERENCES

Anon. n.d. “AWS Bookstore. WHC4.06 CLAD AND DISSIMILAR METALS.” Retrieved July 21, 2022 (https://pubs.aws.org/p/1002/whc406-clad-and-dissimilar-metals).

Hosseini, E., and V. A. Popovich. 2019. “A Review of Mechanical Properties of Additively Manufactured Inconel 718.” *Additive Manufacturing* 30:100877. doi: 10.1016/J.ADDMA.2019.100877.

Jeng, S. L., H. T. Lee, T. E. Weirich, and W. P. Rebach. 2007. “Microstructual Study of the Dissimilar Joints of Alloy 690 and SUS 304L Stainless Steel.” *MATERIALS TRANSACTIONS* 48(3):481–89. doi: 10.2320/MATERTRANS.48.481.

Kah, Paul, and Madan Shrestha Jukka Martikainen. 2013. “Trends in Joining Dissimilar Metals by Welding.” Pp. 269–76 in *Applied Mechanics and Materials*. Vol. 440. Trans Tech Publications Ltd.

MICROSTRUCTURE AND STRENGTH OF 3D PRINTED PART USING MICROPLASMA WIRE ARC ADDITIVE MANUFACTURING

Mohd Rizal Alkahari[1,2], Nor Ana Rosli[2], Shajahan Maidin[1,3], Faiz Redza Ramli[2]
[1]*Advanced Manufacturing Center, Universiti Teknikal Malaysia Melaka, Hang Tuah Jaya, Durian Tunggal, Melaka, Malaysia, rizalalkahari@utem.edu.my*
[2]*Faculty of Mechanical Engineering, Universiti Teknikal Malaysia Melaka, Hang Tuah Jaya, Durian Tunggal, Melaka, Malaysia,*
[3]*Faculty of Manufacturing Engineering, Universiti Teknikal Malaysia Melaka, Hang Tuah Jaya, Durian Tunggal, Melaka, Malaysia,*

ABSTRACT

Additive Manufacturing (AM) is one of the significant thrusts in Industrial Revolution (IR 4.0). Nevertheless, one of the barriers for its wider adoption is lack of understanding on factors that affect the characteristics of the 3D printed/AM structure and high price of metal AM system. The research study tries to address this issue by studying the strength and microstructure from in house developed low-cost wire arc additive manufacturing (µPWAAM). Furthermore, application of micro plasma in WAAM is limited compared to other heat source. Hence, in this study, µPWAAM component with 50 mm height was additively manufactured and investigated. The microstructure shows there is existence of cellular structure near the substrate, columnar dendrites in the middle region and equiaxed dendrite at the top layer. The highest tensile strength of the part was recorded at 640.4 MPa. The study demonstrates that acceptable microstructure and strength of part can be produced by using low cost µPWAAM.

Keywords: Wire arc additive manufacturing, additive manufacturing, 3D printing,

1. INTRODUCTION

Additive manufacturing (AM) or also known as 3D printing is an emerging process and increasingly becoming an important commercial manufacturing technology. AM is regarded as one of the important pillars for Industry 4.0 (IR4.0). Through AM, several metallic materials including the important engineering materials steel, aluminum and titanium may be processed and become a viable alternative for an increasing number of applications. Despite of its potential, high cost of metal AM limits its wide adoption in industry, research, and academic institutions. WAAM is one of cost effective and attractive option to metal AM. WAAM has gained worldwide attention recently especially its vast application of customized design in large part fabrication. Nevertheless, WAAM still facing technical obstacles to meet industry requirement. WAAM part is known for issues related to low strength, high residual stress, poor surface roughness, distortion, dimensional accuracy, and others (Lee, 2020). One of the reasons is excessive heat with large size of melt pool size during additive manufacturing of the components (Rosli et al, 2021). Realizing this, low cost WAAM system has been developed and integrated with micro plasma welding is used in this study. Later, microstructure and strength of the additively manufactured parts were investigated.

2. MATERIALS AND METHODS

The machine used in the study was designed and developed in house using PC based controller and connected to 4 axis 3D printer. A micro plasma arc welding from EWM 25 was used as a welding power source during the printing process. The position of the MPAW torch and outer filler wire was perpendicular to the substrate, and the external wire feeding was set at fixed angle. The plasma gas was 99.99% purity argon, and the inert shielding gas of MPAW is mixed gasses (96% argon + 4% hydrogen). SS 316L material wall was additively manufactured using solid filler wire with a 1.2 mm on SS 304 plate which was set as the substrate.

The torch is attached to the z axis and moves accordingly based on the computer aided design (CAD) data which is transferred to the machine. Travel speed of the torch was set at 36.625 mm/min and deposited continuously. 3D printed component with the height of 50mm and length of 150mm was produced. After the printing, the components were cut using wire electrical discharge machining (WEDM) based on ASTM E8-04 (ASTM, 2013) standard for strength test and the microstructure of the additively manufactured parts were also observed.

3. RESULTS AND DISCUSSION

The part produced relatively smooth and clear from any visually observable defect, pore and crack. From the microstructural point of view, there is variation in the microstructure consisting of cellular, columnar and equiaxed dendrite structures at various regions away from the substrate. This is indicated in Figure 1. It is observed that the first few initial layer has a narrow shape. This is due to the high temperature gradient between the substrate and the melt pool (Rosli et al, 2021). The substrate is relatively cold and removes significant amount of heat from the molten pool. As a result, undulated surface was obtained and formation of narrow and tall shape due to rapid cooling trough significant heat loss trough a substrate (Lee, 2020). There is also existence of cellular structure near the substrate, columnar dendrites in the middle and equiaxed dendrite at the top layer.

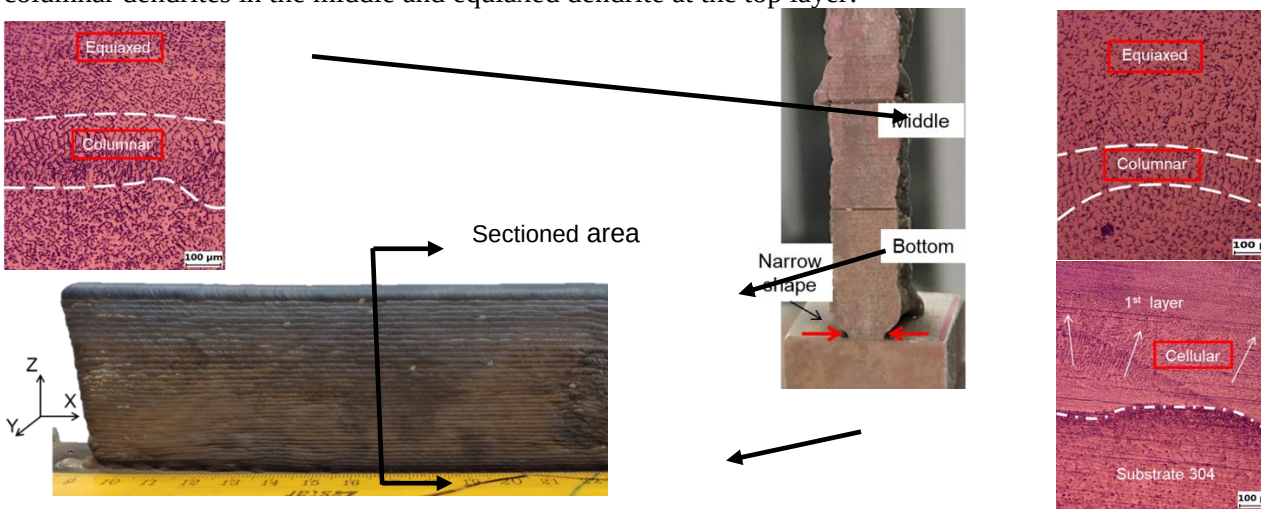

Figure 1. µPWAAM Part With Its Cross-Section And Microstructure At Various Position

4. CONCLUSIONS

The study has successfully manufactured sound and acceptable metal component in terms of the microstructure and strength from in house developed low cost µPWAAM system. The average tensile strength of the additively manufactured sample was recorded at 640.4 MPa. The study opens up new potential where further study on other properties such as fatigue, permeability, surface integrity and others that can be produced from µPWAAM may be performed in the future.

5. REFERENCES

ASTM Standard (2013). Test Methods for Tension Testing of Metallic Materials. ASTM International. https://doi.org/10.1520/e0008_e0008m-13

Rosli, N. A., Alkahari, M. R., Abdollah, M. F., Maidin, S., Ramli, F. R., & Herawan, S. G. (2021). Review on effect of heat input for wire arc additive manufacturing process. Journal of Materials Research and Technology, 11, 2127–2145. https://doi.org/10.1016/j.jmrt.2021.02.002

Lee, S. H. (2020). CMT-based wire arc additive manufacturing using 316L stainless steel: Effect of heat accumulation on the multi-layer deposits. Metals, 10(2), 278. https://doi.org/10.3390/met10020278

MICROSTRUCTURES AND MECHANICAL PROPERTIES OF OXIDE DISPERSION STRENGHTENED INCONEL 718 ALLOYS PRODUCED BY SELECTIVE LASER MELTING

M. Yesim Yalcin[1], A. Alkim Gokbayrak[2], C. Bora Derin[3], Eda Aydogan[4], Bahattin Koc[5]
[1] *Middle East Technical University, Ankara, 06800, Turkey, yesim.yalcin@metu.edu.tr*
[2] *Middle East Technical University, Ankara, 06800, Turkey, alkim.gokbayrak@metu.edu.tr*
[3] *Istanbul Technical University, Istanbul, 34467, Turkey, bderin@itu.edu.tr*
[4] *Middle East Technical University, Ankara, 06800, Turkey, aydogane@metu.edu.tr*
[5] *Sabanci University, Istanbul, 34906, Turkey, bahattin.koc@sabanciuniv.edu*

ABSTRACT

In this study, three novel alloys of ODS-IN718 have been designed and produced. The alloy compositions have been determined by using CALPHAD based FactSage Software. Designed ODS-IN718 alloys of "In718 – Y_2O_3 (ODS1); In718 – Y_2O_3 – FeO (ODS2); In718 – Y_2O_3 – FeO – Hf (ODS3)" are produced by Selective Laser Melting (SLM) technique with various power and velocity parameters to optimize production parameters. In order to dissolve the non-equilibrium phases, which are detrimental to the mechanical properties, to anneal existing nano-oxides, to maximize the number densities of nano-oxides, and other strengthening phases of γ'/γ″, novel heat treatment process is applied based on the thermochemical calculations. The samples are solutionized/annealed at 1050 °C for 1 hour followed by aging at 650 °C for 5 h. It is observed that experimental results are consistent with the thermochemical modelling calculations in terms of existence of phases and their amounts. Moreover, after FeO and Hf additions, an increase in number density of nano-oxides and a decrease in nano-oxide sizes were observed. Increase in nano-oxide number density and decrease in size contributed strengthening of ODS-IN718 alloy.

Keywords: Additive manufacturing, ODS – Inconel 718, nano-oxide, Selective Laser Melting, FactSage

1. INTRODUCTION

Inconel 718 (IN718) is a nickel-based superalloy with high-temperature stability (Davis, 2000) . Lately, additive manufacturing techniques such as selective laser melting (SLM) are used as promising alternative production methods to conventional methods. Oxide dispersion strengthening mechanism (ODS) is an effective way to improve the stability of the alloy at higher temperatures. By preventing the dislocation motion, ODS increases the mechanical properties of the alloy and keeps the grain growth limited by Zener pining effect (K. Huang & Logé, 2016). Higher coherency between oxides and the matrix increases the mechanical properties. Therefore, obtaining the oxides in nanoscale and homogeneously distributed gives better results in terms of mechanical properties (Miller, Russell, & Hoelzer, 2006). In this study, Inconel 718 alloy is strengthened by oxide dispersion strengthening using three different composition grades. Effects of Y_2O_3, FeO and Hf additions on microstructural and mechanical properties are investigated. The thermochemical calculations have been carried out by using FactSage 8.0 software to decide FeO, Hf and Y_2O_3 amounts to be added into IN718.

2. MATERIALS AND METHODS

In order to determine the alloy composition, thermochemical calculations have been done based on FactSage 8.0. Therefore, the amount of the Y_2O_3, FeO and Hf amounts for obtaining the maximum number of nano-oxide particle densities were determined. IN718 powders have a particle size distribution between 20-55 μm. FeO, Hf and Y_2O_3 powders have particle size distribution below 100 nm, below 80 μm, and between 18-38 nm, respectively. Chemical composition of In718 alloy was analyzed by Inductively Coupled Plasma (ICP) method. In addition, the elemental analysis was conducted in order to determine the oxygen amount in the IN718 alloy powders.

First, ODS alloys were mechanically alloyed for 10 mins without using grinding balls. Then, mechanically alloyed powders were used for SLM productions which were carried out by using a parameter set of 40 μm layer thickness, 110 μm hatch spacing, ,67º rotation strategy and various power and velocity values on a C45 steel base plate in Argon environment. A novel heat treatment was applied (1050ºC for 1 hour +650ºC for 5 hours). All processes were carried out under Argon atmosphere.

ODS-IN718 alloys' microstructures were examined by using optical microscopy (OM) and scanning electron microscopy (SEM). Moreover, EBSD and TEM analyzes are conducted. Microhardness tests were conducted with 1kg diamond tip and 10 sec holding time. Room temperature and high temperature

in-situ tensile tests are conducted according to ISO 6892-1 and ISO 6892-2 standards.

3. RESULTS AND DISCUSSION

For all the three grades, densifications greater than 99.7% are achieved in as-built state. Moreover, 318±7, 327±9, and 348±8 HV hardness values are obtained for ODS1, ODS2, and ODS3, respectively. According to SEM analysis, some irregular shaped coarse-sized oxides existed in ODS1 microstructure. On the contrary, oxides existing in ODS2 and ODS3 microstructure had mostly spherical shapes. Moreover, a decrease in oxide sizes and increase in oxide amounts were obtained for ODS2 and ODS3 grades compared to ODS1 as shown in Fig1.

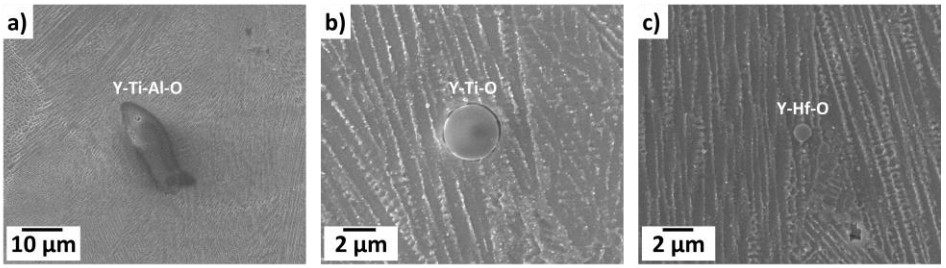

Figure1: SEM micrographs of a) ODS1; b) ODS2; c) ODS3 alloys showing oxides existing in the microstructure in as-built condition

4. CONCLUSION

It is observed that additions of FeO and Hf have an effect on oxide types formed in the matrix. Moreover, reduction in oxide dispersions' sizes are observed related with FeO and Hf additions. According to tensile tests performed on ODS1 alloy at 700°C, increase in hardness is observed. As future work, a novel heat treatment will be applied to as-built samples of ODS2 and ODS3 alloys. OM, SEM, EBSD analyzes, hardness measurements, TEM characterizations and in-situ tensile tests will be completed for as-built and heat-treated samples of ODS2 and ODS3.

REFERENCES

Davis, J. R. (2000). *ASM specialty handbook: Nickel, cobalt, and their alloys*. ASM International.

Huang, K., & Logé, R. E. (2016). Zener Pinning. In *Reference Module in Materials Science and Materials Engineering*. https://doi.org/10.1016/b978-0-12-803581-8.03211-2

Miller, M. K., Russell, K. F., & Hoelzer, D. T. (2006). Characterization of precipitates in MA/ODS ferritic alloys. *Journal of Nuclear Materials*, *351*(1–3), 261–268. https://doi.org/10.1016/j.jnucmat.2006.02.004

MULTI-TRACK, MULTI-LAYER FINITE ELEMENT ANALYSIS OF THE TEMPERATURE FIELD DURING SELECTIVE LAYER MELTING OF 316L STAINLESS STEEL

Saad Waqar[1], Hamaid Mehmood Khan[2], Saad Akram[1], Ebubekir Koc[2]
[1]*Department of Mechanical Engineering. Institute of Space Technology. Islamabad Pakistan, saad.waqar@IST.edu.pk*
[2] *Fatih Sultan Mehmet Vakif University, Aluminum Test Training, and Research Center (ALUTEAM), 34445, Beyoglu, Istanbul, Turkey, hamaid.khan@gmail.com*

ABSTRACT

Selective laser melting (SLM) is a layer-by-layer additive manufacturing technique which involves the application of high-power laser beam for powder melting. The rapid melting and solidification during SLM control the material and physical properties of fabricated components. An accurate estimation of these phenomena is critical to predict the behavior of fabricated components. Given the multi-track multilayer structure of the real SLM process, thermal and physical elements display variations that play a crucial role in shaping the overall mechanical and microstructural behavior of SLM components. To address these concerns, the SLM process of a four-layer component with numerous tracks was modelled, as well as the element birth and death approach to handle layer construction during simulation. Using an existing FEM model, this paper discusses the evolution behavior of the melt-pool shape and thermal variables such as cooling rate, thermal gradient, and solidification rates of SLM 316L SS across many tracks and layers. In addition, the effect of different processing parameters in a multi-track multi-layer SLM was explored.

Keywords: selective laser melting, 316L, cooling rate, thermal gradient, residual stress, additive manufacturing, solidification rate.

NEW APPROACH FOR USAGE OF VIRGIN AND REUSED POWDERS TOGETHER IN LASER POWDER BED FUSION

Taner KARAGOZ[1], Oguz Kaan OZTURK[2]
[1]*tkaragoz@coskunoz.com.tr*
[2]*okozturk@coskunoz.com.tr*

ABSTRACT

Laser powder bed fusion systems allow the use of many different metal alloy powders. The powders used as virgin at the beginning are sieved after production and continue to be used in a reused form. Virgin powder gives the desired results in production with its low humidity and correct particle size. During production, the laser beam does not only affect the meltpool area. With the effect of high temperatures, it causes consolidation in the surrounding particles and reduces the particle size quality. Although the powders are resized in sieving, virgin quality powder cannot be obtained. The same density and strength value should not be expected in the productions made by using these powders alone or together in several percentages.

Keywords: virgin powder, reused powder, sieving, microstructure

1. INTRODUCTION

After the virgin powders are produced with atomization, they are separated into sizes with sieves of various mesh sizes. In laser powder bed fusion systems, mostly 10-30µm and 15-45µm powders are used. When these powders are used as virgin, parts of desired density and quality can be produced due to optimum particle size and low humidity. Cause of the high temperature during production, sintered small solid particles may form due to merge of the particles and arcs during scanning. The sieving process after production is applied to separate such particles.

Although the sieving process is carried out, various defects occur in the shape of the powder particles. This situation directly affects the internal structure of the manufactured part. When the productions made with virgin powder and reused powder are compared, there will be microstructural and mechanical differences in the parts.

In this study, various productions will be made by mixing virgin and reused powders alone or in certain percentages. After the production, powder samples will be taken from the production area and the particle structure will be examined. In addition, density tests and microstructure analyzes will be made with the parts built in the productions.

2. MATERIALS AND METHODS

Production will start with the brand new powder that will be opened at the beginning of the work. In subsequent productions, the powders will be used alone or mixed in certain percentages. Powder samples to be taken from the production area after production will be examined by SEM and EDS. In each production made in different combinations, parts will be produced for density measurement and mechanical tests.
With the results, the optimum percentage in the use of virgin and reused powders will be obtained. With this ratio, the reused powders in future productions will be used effectively.

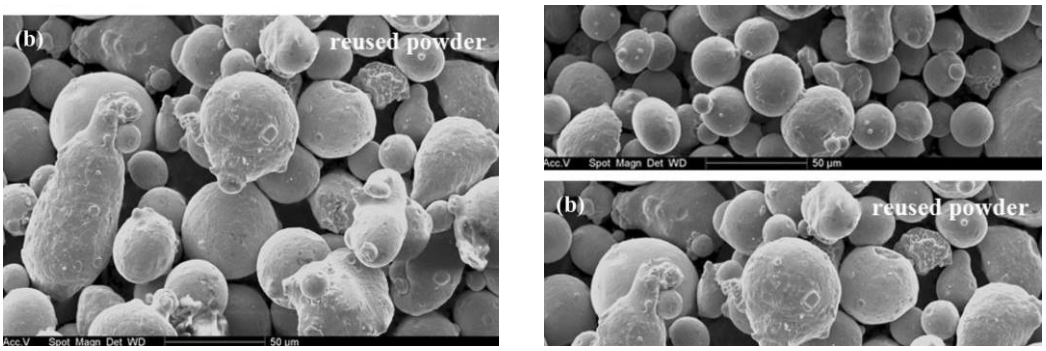

Figure 1. Virgin and Reused Powder Particles[1]

3. RESULTS AND DISCUSSION

As a result of the tests, the particle shape change experienced by a metal powder during its use will be seen. The effect of these changes on density will be examined. With the results obtained, the optimum combination of reused and virgin powders to be used during production will be obtained.

4. CONCLUSIONS

Efficient use of reused powders is very important for the sustainability of processes in laser powder bed fusion systems. Optimum virgin and reused ratio should be used in order not to compromise on part quality while ensuring sustainability.

REFERENCES

[1] Zhang, J., Hu, B., Zhang, Y., Guo, X., Wu, L., Park, H. Y., Lee, J. H., & Jung, Y. G. (2018). Comparison of virgin and reused 15-5 PH stainless steel powders for laser powder bed fusion process. *Progress in Additive Manufacturing*, *3*(1–2), 11–14. https://doi.org/10.1007/s40964-018-0038-2

NOVAL DESIGN OF ANTI-BACKLASH MOTOR BRACKET MECHANISM AND BENCHMARK TEST

Umut GÖVEZ[1] Mümin ÖZSİPAHİ[1] Emre ERCAN[1] Cengiz KÖSEOĞLU[1] Onat AŞIK[1] Berk İzgi DANIŞ[1] Evren TAN[1]
[1]*ASELSAN Inc., Yenimahalle, 06370, Turkey, ugovez@aselsan.com.tr*

ABSTRACT

Anti-backlash mechanisms are used to eliminate the backlash in the standard gear meshing, because of that, a revolute joint should be designed to obtain minimum clearance as possible. The main objective of the study is to re-design anti-backlash motor bracket mechanism by using design for additive manufacturing. The anti-backlash motor bracket mechanism has the "fixed bracket" which is connected to the "moving bracket" with a revolute joint and is composed of six mechanical components. The steel brackets are designed to conform traditional manufacturing, which leads to a weight of 4.15 kg. Re-design of the brackets, static analyses, topology - post topology optimizations and performance benchmarks were carried out respectively. Finally, the total weight of the consolidated bracket was reduced from 4.15 kg to 0.70 kg. Manufacturing was performed in ARCAM A2X system which is available at ASELSAN. Ti6Al4V powder was used as raw material, where the design and analysis parameters were tuned accordingly. The initial number of six mechanical components were consolidated to one component, reducing the logistical workload drastically.

Keywords: Design for Additive Manufacturing, Electron Beam Melting, Revolute Joint, Topology Optimization.

1. INTRODUCTION

Additive Manufacturing (AM) recently presents an increasing growth regarding the production of mechanical parts, due to its outstanding characteristics in comparison to conventional processes. AM methods facilitate the production of parts with unique and complex geometries without requiring subsequent operations or processes [1]. AM has become important in the industry with the development of technology as the variety of powder materials have increased, including metals. In order to fully benefit from these advantages of AM over traditional production methods, it is necessary to make specific and innovative designs for the AM [2]. One of the biggest advantages of additive manufacturing technology is that it enables the consolidated production of structures produced in multiple parts by traditional production methods [3,4]. In consolidated part design for AM, it is difficult to manufacture joints as one piece and to achieve fits that can meet industrial needs. It's not possible with AM to achieve the tight tolerances used in traditional methods. Therefore, innovative design approaches are required. The motivation of the team is to re-design the fixed and moving brackets with the revolute joint of anti-backlash mechanism using additive manufacturing. The aim is to reduce the weight of the brackets and to eliminate the mechanical parts used in the revolute joint while keeping the functionality of the mechanism. Geometrical tolerances are very critical for a functional component and the manufacturing process plays an important role to determine the tolerances [5]. At the same time, consolidated revolute joint was designed and clearance between shaft and housing minimized. The rules of this design are taken from the previous studies [5,6].

2. MATERIALS AND METHODS

For anti-backlash mechanism, fixed bracket is connected to the moving bracket with a revolute joint composed of six mechanical parts. The brackets made of AISI 4140 designed to conform traditional manufacturing, which leads to a weight of 4.15 kg. Topology optimization method was applied in order to reduce the weight of the brackets by using the Altair Inspire software. Contacts and different load cases were applied to construct the model in the software. Several topology optimization studies were performed, aiming at different objectives such as maximizing stiffness, frequency, etc. Unique revolute joint was re-designed to obtain a consolidated product for additive manufacturing using Siemens NX software. Hence additional assembly steps are not needed after the additive manufacturing process. The geometry of this joint was designed to obtain required axial and radial clearances, and also to ensure the clearance value between the shaft and the hole in order to prevent the parts from sticking during production. Using the outcomes of the topology optimization studies, fixed and moving brackets were re-designed using Inspire's "Polynurbs" feature resulting a unique organic texture. Production has been done by Arcam A2X E-PBF with Ti6Al4V material. Final product is shown in Figure 1. Afterwards, different functional and structural tests will be conducted such as, mechanical shock and vibration

respectively in order to validate the anti-backlash mechanism based on MIL-STD 810.

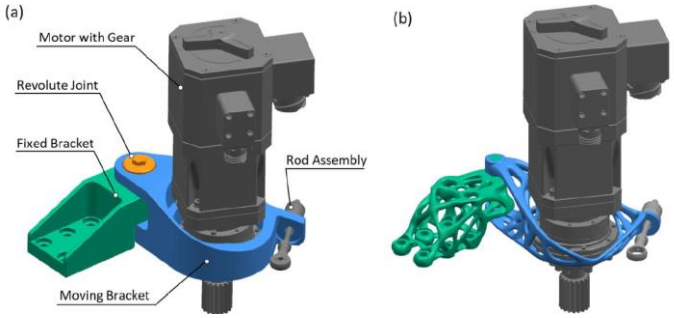

Figure 1. Anti-backlash mechanism (a) six-part traditional design, (b) consolidated design.

3. RESULTS AND DISCUSSION

For the final form of the product the weight decreases to 700 g, i.e. above 80% weight reduction is achieved while preserving the durability and functionality of the mechanism. After the topology and post topology optimizations structural analysis is done again, as a result, strength requirements are still maintained while the minimum safety factor is kept as 2. The initial six mechanical components were consolidated to one component. Additive manufacturing was performed in ARCAM A2X E-PBF machine. Functional performance benchmarks were carried out in the laboratory. After the production it is observed that axial and radial clearances exceeding the limits of E-PBF were obtained without problems; the consolidated joint meet the required functionality.

4. CONCLUSIONS

For re-designed anti-backlash motor bracket mechanism, weight and part reduction was achieved; anti-backlash clearance was compared to the traditional design, and it was found sufficient. Thanks to topology optimization and design for additive manufacturing production, logistical workload was reduced, assembly time was improved.

REFERENCES

Umaras, Eduardo, and Marcos SG Tsuzuki(2017). "*Additive manufacturing-considerations on geometric accuracy and factors of influence*." IFAC-PapersOnLine 50.1: 14940-14945

Adam, G. A. and Zimmer, D. (2014). Design for Additive Manufacturing—Element transitions and aggregated structures. *Journal of Manufacturing Science and Technology*, 7(1), 20-28.

Chen, Y. and Lu, J. (2011). Minimise joint clearance in rapid fabrication of non-assembly mechanisms. *International Journal of Computer Integrated Manufacturing*, 24(8), 726-734.

Calì, J., Calian, D. A., Amati, C., Kleinberger, R., Steed, A., Kautz, J. and Weyrich, T. (2012). 3D-printing of non-assembly, articulated models. *Association for Computing Machinery Transactions on Graphics*, 31(6), 1-8.

Gövez, U., Yılmaz, O., Tan, E. and Gümüş, B. (2020). On The Improvement of Geometrical Outcomes of E-PBF Parts with a Novel Design Approach. *The 3rd International Conference for Electron Beam Additive Manufacturing, Erlangen.*

Gövez, U., Yılmaz, O., Tan, E. (2020). Design for additive manufacturing of consolidated revolute joints or electron beam melting. *Gazi University Mechanical Engineering, Ankara.*

ON THE MECHANICAL BEHAVIOR AND MICROSTRUCTURAL CHARACTERIZATION OF WIRE + ARC ADDITIVE MANUFACTURING OF MN-SI BASED STEEL ALLOY (ER70S-6)

Masoud Abbaszadeh[1], Nevzat Bol[1], O. Ece Kara[1], A. Ali Sen[1], Oğuzhan Yılmaz[2]
[1]*INTECRO Robotics company, Ankara, Turkey, Masoud.abbaszadeh@intecro.com.tr*
[2]*Advanced Manufacturing Technology Research Group (AMTRG), Gazi University, Ankara, Turkey, oguzhanyilmaz@gazi.edu.tr*

ABSTRACT

Wire + Arc Additive Manufacturing (WAAM) is relatively a novel manufacturing technology which uses metallic wire as the feedstock material and normal arc as the heat source to build up large scale near-net-shape parts. This process has attracted the attention of many industries such as aerospace, defense and automotive due to its ability to produce very near-net-shape components without complex tooling and molds offers potential for significant cost and lead time reductions. In this paper, the mechanical and metallurgical properties of the WAAM ER70S-6 are studied during tension loading as well as microhardness testing and its behavior is correlated with microstructural observations. The microstructure of WAAM ER70S-6 is assessed by optical microscopy (OM). The results show that the selected parameters for deposition of ER70S-6, leads to an isotropic mechanical behavior during tension loading. The microhardness level is not changing in different regions of WAAM-fabricated ER70S-6, confirming presence of relatively homogenous microstructure.

Acknowledgments: This work has received funding from the Scientific and Technological Research Council of Turkey (TÜBITAK) under the Grant Agreement No: 3200280 which is gratefully acknowledged.

Keywords: WAAM, Tension loading, optical microscopy, microhardness.

1. INTRODUCTION

Wire + Arc Additive Manufacturing (WAAM) is a cost-effective additive manufacturing (AM) technology that produces 3D metallic components by depositing thin layers of metals in a layer by layer fashion. Compared to other AM technologies, WAAM process is using metal wire instead of powder and arc as the heat source instead of laser or electron beam. In addition, this process has the highest deposition rate (up to 8 kg/h) compared to other AM technologies such as electron beam and laser deposition (Mariacira Liberini, 2017) that enables it to fabricate components with no dimensional limits (Derekar, 2018) in shorter time; the manufacturing time is reduced up to 60% by WAAM process (Yun Zhao, 2020).
In this study, the mechanical properties as well as microstructure of WAAM-fabricated ER70S-6 low carbon steel alloy were investigated by means of mechanical tests such as tensile and microhardness testing and microstructural evaluations such as optical microscopy (OM).

2. MATERIALS AND METHODS

In the current study, ER70S-6 filler wire with diameter of 1.2 mm was used to build a thin wall-shape structure with dimension of 230×9×195 mm^3 using wire + arc additive manufacturing process. To build such a structure, 110 layers of ER70S-6 with average layer height of 1.8 mm were deposited in a zigzag direction. ASTM A52 mild steel with dimension of 300×200×30 mm^3 was used as the substrate. A KUKA (KR6 R 1820 ARC HW) 6-axis industrial robot equipped with Fronius TPSi 500 welding power supply and a Fronius CMT torch was employed as the heat source for WAAM of the part. In order to avoid excessive heat accumulation during the deposition process, 90 s waiting time was implemented prior to the deposition of new layer. Argon with 93 % purity was used as shielding gas with gas flow of 18 L/min. The arc current and voltage were also considered to be 166 A and 15.3 V, respectively.
In order to assess the anisotropic behavior as well as mechanical properties of the WAAM-fabricated ER70S-6 during tension loading, the tensile specimens were cut from both longitudinal and normal directions according to TS EN ISO 68-92-1 standard.

3. RESULTS AND DISCUSSION

The stress-strain response of the WAAM-fabricated ER70S-6 low carbon steel alloy during the tensile loading in both longitudinal (deposition) and normal (building) directions are plotted in Figure 1. Moreover, the corresponding mechanical properties such as yield strength, ultimate tensile strength, and

elongation are summarized in Table 1. It is shown that the WAAM-fabricated ER70S-6 steel alloy shows nearly isotropic mechanical properties during tensile in longitudinal and normal directions; the mean value of the yield strength, ultimate tensile strength and elongation are 357 MPa, 482 MPa and 31 %, respectively. It should be mentioned that similar results in terms of isotropic behavior as well as tensile strength of WAAM-fabricated ER70S-6 steel alloy during tensile testing have been reported in the literature (Alireza Vahedi Nemani, 2020), (Tomer Ron, 2020).

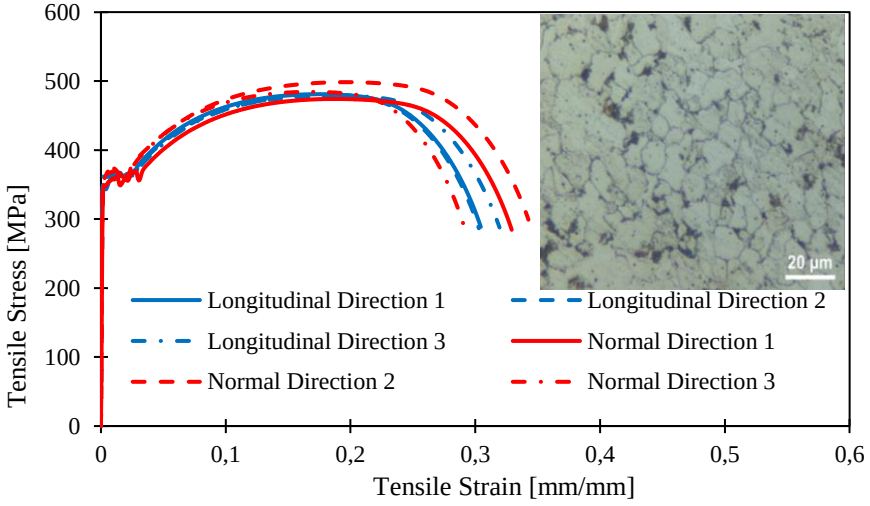

Figure 1. Stress-strain response of WAAM-fabricated ER70S-6 during tensile testing.

Table 1. A summary mechanical properties of WAAM-fabricated ER70S-6 during tension loading.

Test Direction	Yield Strength [MPa]	Ultimate Strength [Mpa]	Elongation [%]
Longitudinal	356.5±7.5	479.5±1.3	30±0.8
Normal	357.3±6.5	485±10	32±2

4. CONCLUSIONS

The mechanical properties and microstructure of wire + arc additive manufacturing of ER70S-6 steel alloy were investigated in this paper. Results indicated that the selected parameters, lead to anisotropic mechanical behavior of WAAM-fabricated ER70S-6 during tensile testing. It also shown that the grains are uniformly distributed in the different regions, i.e., inter-layer and inner-layer regions of the structure and the microstructure is homogeneous.

REFERENCES

Alireza Vahedi Nemani, M. G. (2020). On the Post-Printing Heat Treatment of a Wire Arc Additively Manufactured ER70S Part. *Materials, 13*(12), 2795. doi:https://doi.org/10.3390/ma13122795

Derekar, K. S. (2018). A review of wire arc additive manufacturing and advances in wire arc additive manufacturing of aluminium. *Materials Science and Technology, 34*(8), 895-916. doi:https://doi.org/10.1080/02670836.2018.1455012

Mariacira Liberini, A. A. (2017). Selection of Optimal Process Parameters for Wire Arc Additive Manufacturing. *Procedia CIRP, 62*, 470-474. doi:https://doi.org/10.1016/j.procir.2016.06.124

Tomer Ron, G. K. (2020). The Effect of Microstructural Imperfections on Corrosion Fatigue of Additively Manufactured ER70S-6 Alloy Produced by Wire Arc Deposition. *Metals, 10*(1), 98. doi:https://doi.org/10.3390/met10010098

Yun Zhao, Y. J. (2020). Process planning strategy for wire-arc additive manufacturing: Thermal behavior considerations. *Additive Manufacturing, 32*, 100935. doi:https://doi.org/10.1016/j.addma.2019.100935

OPTIMIZATION OF STRAIN ENERGY IN CRACK INDUCED STRUCTURE VIA MICRODEFECTS USING PERIDYNAMIC INFORMED TOPOLOGY OPTIMIZATION

Peyman Lahe Motlagh[1]
[1]*Department of Mechanical Engineering, Gebze Technical University, Kocaeli, Turkey,peyma.lahe@gtu.edu.tr*

ABSTRACT

Topology optimizations is vastly used to design light-weighted structures that used in industrial applications. Even tough classical continuum mechanics is implemented commonly to solve topology optimization problems, but it brings some restrictions to the modeling, analysis, and solution of complex structures with structural discontinuities. On the other hand, peridynamics (PD) theory can overcome these restrictions because of its nonlocal integration nature. PD eliminate the need for partial derivatives in equation of motion thus it is very suitable to include discontinuities. During additive manufacturing process occurrence of microcrack is inevitable so including microcracks during design stage helps to prevent unwanted future failure. This paper presents an application of peridynamics based topology optimization (PD-TO) to establish a framework to optimize of microcrack characteristics using genetic algorithm. To this end, the PD-TO model is derived using an in-house MATLAB code. By utilizing the genetic algorithm, best microcracks orientations and length are optimized. For each structure, strain energy density distributions are compared between different topologies. As a result, importance of predicting unwanted microcracks during design stage of a macrostructures is presented.

Keywords: Peridynamics, topology optimizations, genetic algorithm, microcracks.

1. INTRODUCTION

The occurrence of microcracks is inevitable during the manufacturing process, therefore including predefined microcracks within design domain and investigating their orientation and size effect can help for a better design criterion using PD-TO. During TO, a proper numerical method is needed to perform accurate structural analysis such as classical continuum mechanics (CCM) formulations in which particles interactions are considered between a particle and its nearest neighbor (Luo and Bao 2019). Some of CCM assumptions pose a modeling/analysis limitation for structures including damage, discontinuity, internal feature, or defect. Another approach to perform structural analysis during TO is non-local continuum theories referred to as Peridynamics (Anon 2000). In this approach, the material does not necessarily require remaining continuous during the simulations. Thus, it ideally becomes a robust approach for dealing with discontinuities such as cracks, damages, and defects. Few studies have applied PD directly to TO for designing cracked structures. For instance, Kefal et al. (Kefal et al. 2019) combined PD with BESO optimization schemes for structures with/without cracks. Moreover, a comparative study is performed by Motlagh and Kefal (Lahe Motlagh and Kefal 2021; Motlagh et al. 2021) to justify why TO algorithms should substitute peridynamics for the conventional FEM approach in the topology optimization of cracked structures. To the best of the authors' knowledge, there exist a need to justify whether many cracks can interfere with the final topology obtained from PD-TO algorithms. To this end, the main novelty of this study is to perform PD-TO simulations on a benchmark case including randomly oriented microcracks for minimizing compliance and by using genetic algorithm (GA) to figure out the best sets of length and orientations to achieve this goal. Furthermore, the strain energy of the benchmark problem is compared for each microcracks inclusion sequence.

2. MATERIALS AND METHODS

In PD, each particle i interact with all particles within its region, Horizon with the size of δ, $\{H = \mathbf{x} \in \beta: |\mathbf{x}' - \mathbf{x}| \leq \delta, for\ \delta > 0\}$. Figure 1. shows a region β and horizon of particle i with the size of δ.

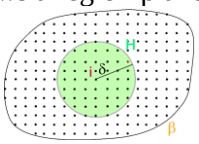

Figure 1. Horizon-Family of the material point $\boldsymbol{i}$

Equation of motion for sets of particles is defined as below as we all as micro-potential energy of each bond can be calculated as :

$$\rho(\mathbf{x})\ddot{\mathbf{u}}(\mathbf{x},t) = \int_H \mathbf{f}(\mathbf{u}' - \mathbf{u}, \mathbf{x}' - \mathbf{x}, t' - t)\mathrm{d}H + \mathbf{b}(\mathbf{x},t) \quad (1)$$

$$w = w(\boldsymbol{\xi},\boldsymbol{\eta},t) = \frac{1}{2} f s|\boldsymbol{\xi}| \text{ where } f = cs\frac{\mathbf{y}'-\mathbf{y}}{|\mathbf{y}'-\mathbf{y}|} \text{ and } c = \frac{9E}{\pi h \delta^3}$$

where $\rho(\mathbf{x})$, $\mathbf{b}(\mathbf{x},t)$ and $\ddot{\mathbf{u}}(\mathbf{x},t)$ are density, body force, and acceleration of particle $\mathbf{x}$ and $\boldsymbol{\xi}$, $\boldsymbol{\eta}$ and s represent relative position vector ($\boldsymbol{\xi} = \mathbf{x}' - \mathbf{x}$), displacement vector ($\boldsymbol{\eta} = \mathbf{u}' - \mathbf{u}$) and stretch between two particles ($s = \frac{|\mathbf{y}'-\mathbf{y}|-|\mathbf{x}'-\mathbf{x}|}{|\mathbf{x}'-\mathbf{x}|}$). f force density vector, E is the young modulus of isotropic material, h is the thickness of the domain and c is the bond constant. Compliance is an objective function generally used in TO with a target volume fraction, for the general optimization scheme, the constraints are as follows:

$$\min_{k_i} U(k_i) = \sum_{i=1}^{N} W(\mathbf{x}_i)V_i \;\; s.t. \begin{cases} \mathbf{KD} = \mathbf{B} \\ \frac{\sum_{i=1}^{N} k_i V_i}{\sum_{i=1}^{N} V_i} = \bar{V} \\ k_{min} \le k_i \le 1 \end{cases} \tag{2}$$

where minimization method is subjected to the global displacement solution, updated strain field, and maximum allowable volume constraint $\bar{V}$, the ratio of target volume to the total volume of design space.

3. RESULTS AND DISCUSSION

The main aspect of PD-TO studied in this paper is using GA for optimizing the strain energy of a structures. For this matter, a set of structure is studies with randomly oriented cracks with angle between -60° to 90° with sub-steps of 15° and length between of 25 to 100 mm with sub-steps of 25 mm. Each iteration of GA produced a set of randomly cracks with arbitrary length and size and this set is investigated in PD-TO. Figure 2. Shows a simply supported structure with and without cracks to emphasize the effect of optimizing the crack characteristics on the strain energy. Lowest strain energy is achieved when the microcracks are optimized with GA and its value is 245, compared to the original strain energy of structure (when there is no crack) about 30 percent reduction of strain energy is observed which help to produce a structure not only satisfy the lightweight design criteria but also have lower strain energy when it is loaded on the desired force.

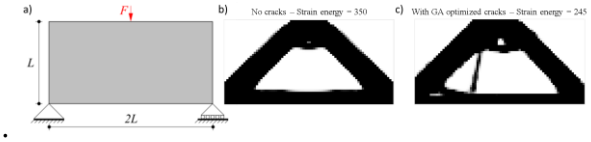

Figure 2. a) schematic of a simply supported beam, b) optimized topology of structure without cracks, c) optimized topology of structure with GA and inclusion of microcracks.

4. CONCLUSIONS

In this study, to design a light weighted structures TO is implemented using PD method. A set of randomly oriented crack with different length are distributed inside the domain and by using GA best orientation and length is selected. The results show about 30 percent reduction in strain energy. Future works will be implementing further benchmark problem and adding GA input with more crack characteristics.

REFERENCES

Anon. 2000. “Reformulation of Elasticity Theory for Discontinuities and Long-Range Forces.” *Journal of the Mechanics and Physics of Solids* 48(1):175–209. doi: 10.1016/S0022-5096(99)00029-0.

Kefal, Adnan, Abdolrasoul Sohouli, Erkan Oterkus, Mehmet Yildiz, and Afzal Suleman. 2019. “Topology Optimization of Cracked Structures Using Peridynamics.” *Continuum Mechanics and Thermodynamics* 31(6):1645–72. doi: 10.1007/s00161-019-00830-x.

PERIDYNAMIC INVESTIGATION OF SURFACE CRACKS IN OPTIMALITY CRITERION-BASED TOPOLOGY OPTIMIZATION FOR ADDITIVE MANUFACTURING

Abdullah Kendibilir[1,2,3], Mahmut Hudayi Bilgin[1,2,3], Adnan Kefal[1,2,3*]
[1] *Faculty of Engineering and Natural Sciences, Sabanci University, Tuzla, Istanbul 34956, Turkey*
[2] *Composite Technologies Center of Excellence, Sabanci University-Kordsa, Istanbul Technology Development Zone, Sanayi Mah. Teknopark Blvd. No: 1/1B, Pendik, 34906 Istanbul, Turkey*
[3] *Integrated Manufacturing Technologies Research and Application Center, Sabanci University, Tuzla, 34956, Istanbul, Turkey*
[*] *Corresponding author: adnankefal@sabanciuniv.edu (A. Kefal)*

ABSTRACT

Topology optimization (TO) is extensively used for reducing the weight of engineering parts that require higher performance in aerospace, automotive, and defense industries. Additive manufacturing (AM), a practical layer-by- layer material deposition process, is commonly employed to fabricate geometrically complex designs obtained from TO. However, AM processes may result in manufacturing-induced structural discontinuities (surface cracks or voids) that must be considered in the design stage. Nevertheless, most TO algorithms cannot realistically handle these structural cracks/defects since they mainly employ classical continuum-mechanics formulations combined with the finite element method (FEM). On the other hand, peridynamics (PD), a non-local meshless approach, can effectively model any structural discontinuity without the need for an additional effort by breaking non-local interactions. In this study, we combine PD and optimality criterion-based TO methods to investigate the effect of surface cracks on the three-dimensional structural design. For a comparative study, these cracks are also modeled using FEM-TO by eliminating the elements in the cracked region. Optimal geometries and total strain energies obtained from PD are compared with those from FEM for each benchmark case with/without surface cracks. Finally, the advantage of PD is revealed for modeling structural discontinuities in TO.

Keywords: Topology optimization, peridynamics, crack modelling, additive manufacturing, finite element method

1. INTRODUCTION

Topology optimization methods have been dedicated to decreasing the total weight of the critical engineering structures while satisfying the given constraints such as stress, volume fraction, etc. However, most of them do not consider structural discontinuities during the optimization. Therefore, we mainly focus on the investigation of the effective modeling of cracks and compare the performance of various TO methods (PD-TO and FEM-TO).

2. MATERIALS AND METHODS

In this study, we utilize PD and FEM-based TO methods to compare their performance in the TO of structures with surface cracks. Minimization of compliance in TO can be described in a general form as follows (Kefal et al., 2019):
For the solution of structural analysis (KD=B), we utilize two different approaches: PD and FEM. For discretization, FEM mesh includes eight-noded hexahedral elements whereas PD creates equally spaced uniform material particles. The optimality criteria method is selected for the design variable updating scheme during the optimization process (Hassani & Hinton, 1998).

3. RESULTS AND DISCUSSION

We modeled a cantilever beam which is a well-known benchmark problem in the literature (Figure 1.) The final material distributions for a benchmark case obtained from PD-TO are presented in Figure 2. Artificial density values continuously change in the structure where yellow and red colors represent 0 and 1 values, respectively. The cracked region was practically modeled for the PD-TO method by

tlagh et

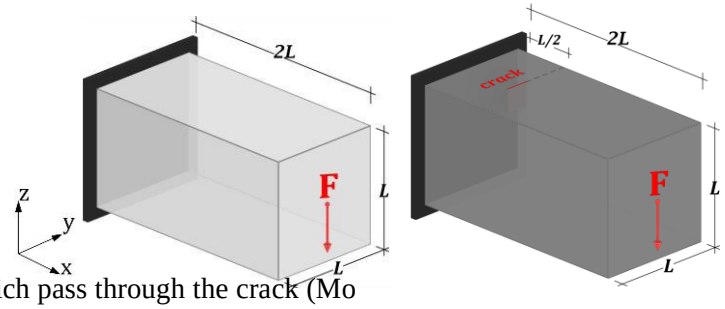

only breaking the PD bonds which pass through the crack (Mo

Figure 1. Design domain and boundary conditions for a cantilever beam; (a) without crack (b) with a crack in the back region.

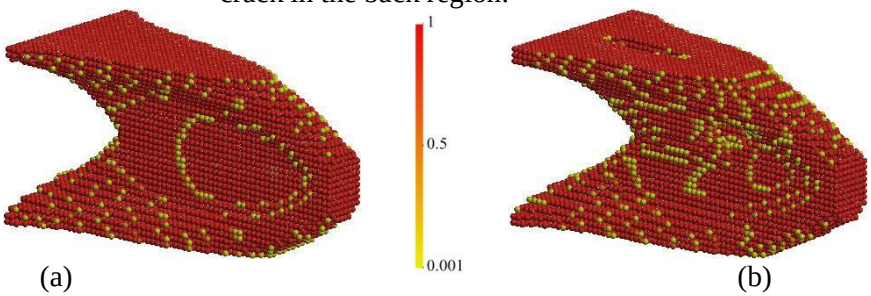

(a) (b)

Figure 2. Optimal topologies obtained from PD-TO for (a) without crack (b) with a crack in the back region.

4. CONCLUSIONS

It is revealed from Figure 2. that the crack involvement in the given domain significantly affects the final topologies. Crack tips are tightened by material stacking in these regions. However, in the normal direction of the crack, a certain amount of material is removed. The results of cracked cases obtained by PD-TO and FEM-TO are compared with each other to determine which method provides better solutions in the existence of any structural discontinuities. Accordingly, the extensive comparisons will be provided in the full submission file.

REFERENCES

Hassani, B., & Hinton, E. (1998). A review of homogenization and topology optimization III—topology optimization using optimality criteria. *Computers & structures*, *69*(6), 739-756.

Kefal, A., Sohouli, A., Oterkus, E., Yildiz, M., & Suleman, A. (2019). Topology optimization of cracked structures using peridynamics. *Continuum Mechanics and Thermodynamics*, *31*(6), 1645-1672.

Motlagh, P. L., Kendibilir, A., Koc, B., & Kefal, A. (2021). Peridynamics-informed effect of micro-cracks on topology optimization of lightweight structures. *Journal of Additive Manufacturing Technologies*, *1*(3), 610-610.

POLYACRYLIC ACID-BASED SHAPE-MEMORY, SELF-HEALING HYDROGELS FABRICATED BY STEREOLITHOGRAPHY

Tuerdimaimaiti Abudula, Oguz Okay
Department of Chemistry, Istanbul Technical University, 34469 Maslak, Istanbul, Turkey
abudulat@itu.edu.tr, okayo@itu.edu.tr

ABSTRACT

Additive manufacturing of smart materials holds great promises for numerous applications, such as soft robotics, aerospace, sensors, and healthcare industries. Polyacrylic acid-based hydrogels are attractive smart materials widely used in the medical field owing to their supreme biocompatibility, good moisture absorptivity, and suitability for physiochemical modification.[1,2] Herein, we present a stereolithography (SLA)-based additive manufacturing strategy of shape-memory and self-healing hydrogels copolymerized of hydrophilic acrylic acid within hydrophobic hexadecyl acrylate (C16A) chains. SLA printing of the hydrogels can be performed in a commercial resin printer, and the crosslinking of the copolymer can be achieved via hydrophobic interaction without chemical crosslinks.[3] The melting temperature of the hydrophobic, crystalline domain in the hydrogels can be tuned between 37~41 ºC by changing C16A content, which allows them to possess a shape-memory effect near their melting point. This unique property of the hydrogels provides us with a magic possibility to switch their shapes near human body temperature (36-45 ºC). Additionally, the printed hydrogels exhibited 4-6 MPa of tensile strength and 2.5-250% of stretchability together with a brittle-to-ductile transition by increasing the C16A content. Finally, the temperature-induced self-healing ability of the printed hydrogels after physical and structural damages makes them remarkably interesting for various biomedical applications.

References:

1 Yin, M. J. *et al.* Rapid 3D patterning of poly (acrylic acid) ionic hydrogel for miniature pH sensors. *Advanced Materials* **28**, 1394-1399 (2016).

2 Xin, C. *et al.* Environmentally Adaptive Shape-Morphing Microrobots for Localized Cancer Cell Treatment. *ACS nano* **15**, 18048-18059 (2021).

3 Tuncaboylu, D. C., Sari, M., Oppermann, W. & Okay, O. Tough and self-healing hydrogels formed via hydrophobic interactions. *Macromolecules* **44**, 4997-5005 (2011).

POLYMER-METAL HONEYCOMB COMPOSITES PRODUCED BY ADDITIVE MANUFACTURING AND ELECTROPLATING

Roozbeh Neshani[1], Olgun Yılmaz[2], Davis J. McGregor[3], Sameh Tawfick[3], William P. King[3], İshak Karakaya[2], Sezer Özerinç[4]
[1]*Department of Micro and Nanotechnology, Middle East Technical University, Ankara, Turkey*
roozbeh.neshani@metu.edu.tr
[2]*Department of Metallurgical and Materials Engineering, Middle East Technical University, Ankara, Turkey*
olguny@metu.edu.tr, kkaya@metu.edu.tr
[3]*Department of Mechanical Science and Engineering, University of Illinois at Urbana-Champaign, Urbana, United States, davisjm2@illinois.edu,* wpk@illinois.edu, *tawfick@illinois.edu*
[4]*Department of Mechanical Engineering, Middle East Technical University, Ankara, Turkey*
ozerinc@metu.edu.tr

ABSTRACT

Polymer-metal honeycomb composites (PMHC) that combine polymer additive manufacturing and electroplating have been reported in this study. Digital Light Synthesis, a recently developed rapid vat photopolymerization process, printed rigid polyurethane honeycomb structures. Electroless Cu coating followed by NiCo electroplating up to a thickness of 100 μm provided the composite structure. The coating process improves the elastic modulus and strength of the honeycomb parts and enables their use in lightweight structural applications. The developed PMHC structures provide a route for the cost-effective manufacturing of structural parts by eliminating the need for a metal 3D printer. Tuning the lattice geometry and coating parameters offers a versatile design space for implementing a wide range of structural parts with the desired mechanical response.

Keywords: Additive Manufacturing, Digital Light Synthesis, Composite Materials, Honeycomb Structures, Electroplating

1. INTRODUCTION

Lattice Structures, open-cell geometries of repeating topologically ordered unit cells, offer high specific mechanical properties, especially suitable for lightweight structures and impact-absorbing applications (Gibson and Ashby 1997). While additive manufacturing has enabled the effective production of complex lattice structures (Nazir et al. 2019), the high cost of metal 3D printers and slow production rates have so far limited the applicability of the approach. Recent advances in polymer additive manufacturing offer cost-effective rapid production of high-resolution polymeric parts, including lattice structures. Combining the polymer AM of lattice parts with the well-established and low-cost electroplating process is a promising way to develop new composite structural materials for lightweight applications. This work reports on the development of polymer-metal honeycomb composites (PMHC) that combine polymer additive manufacturing and electroplating. Digital Light Synthesis (DLS) has been the choice for the AM of the polymeric parts due to the high manufacturing speed and accuracy (Tumbleston et al. 2015). Steps of surface activation, electroless plating, and electroplating ensured uniform and defect-free coatings on the non-conducting substrate, followed by mechanical testing to demonstrate the strength enhancement.

2. MATERIALS AND METHODS

The RPU 70 (Carbon Inc., USA) resin selected for this work offers mechanical properties comparable to ABS, with an elastic modulus of 1.7 GPa and ultimate tensile strength of 40 MPa (Carbon 3D Inc. 2020). An M2 DLS printer (Carbon Inc. USA), printed the honeycomb lattice specimens with overall dimensions of 48.5 mm × 48 mm × 30 mm. The specimens had 9 × 8 cell arrangement and a wall thickness of 0.5 mm, resulting in 23% solid volume fraction. A standard activation procedure (etching, cleaning, catalyzation) prepared the surface for electroless plating inside a bath of Cu salt. A 3D printed custom setup ensured the precise placement of the Ni 201 anodes through the specimen, submerged in a Ni-Co electrolyte bath. The parts were electroplated for 180 minutes, yielding a coating thickness of around 100 μm. The mechanical response of the uncoated and coated parts was tested according to ASTM D1621 Standard Test Method for Compressive Properties of Rigid Cellular Plastics (ASTM Committee 2016). A Z250 universal testing machine (Zwick/Roell, Germany) compressed the samples at strain rate of 0.00167 s^{-1} (10% of the sample height per minute). A Fujifilm X-S10 mirrorless camera recorded the mechanical response of the samples at 240 frames per second.

3. RESULTS AND DISCUSSION

Figure 8(a) shows the photographs of uncoated, electroless Cu coated, and Ni-Co electroplated specimens. Figure 1(b) shows the stress-strain response of the respective specimens. The uncoated specimen exhibited an apparent elastic modulus of 26.2 MPa and maximum compressive strength of 1.32 MPa. The coated specimen's corresponding elastic modulus and maximum compressive strength were 156 MPa, and 3.32 MPa, respectively. Therefore, the 100 µm thick coatings improved modulus and strength by 500% and 150%, respectively.

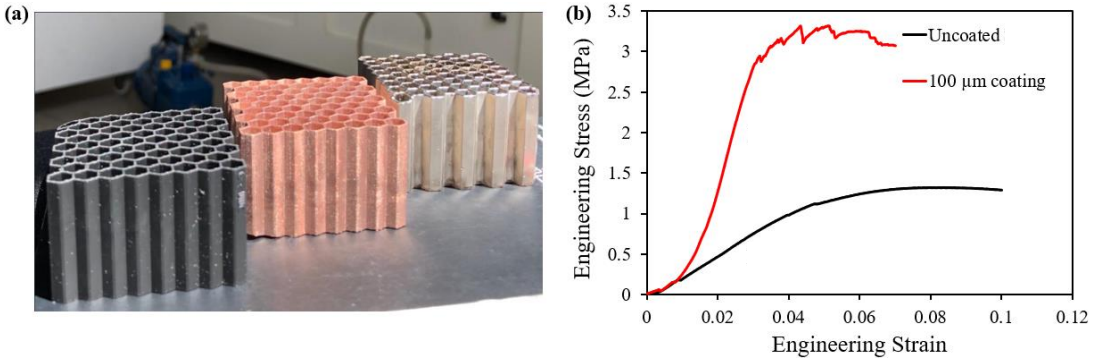

Figure 8. (a) From left to right, uncoated, copper-coated, and NiCo coated specimens. (b) Mechanical response of 100 µm coated sample compared to an uncoated sample.

4. CONCLUSIONS

Polymer-metal honeycomb composites have been successfully demonstrated by polymer 3D printing and NiCo electroplating, providing superior mechanical properties. The developed material architecture offers new routes for developing high specific strength structures and impact absorbers.

REFERENCES

ASTM Committee. 2016. "Standard Test Method for Compressive Properties of Rigid Cellular Plastics." Retrieved April 7, 2022 (https://www.astm.org/d1621-16.html).

Carbon 3D Inc. 2020. "Carbon-RPU-70-Datasheet-TDS.Pdf." Retrieved January 3, 2022 (https://3dprinting.com/wp-content/uploads/carbon-RPU-70-datasheet-TDS.pdf).

Gibson, Lorna J., and Michael F. Ashby. 1997. *Cellular Solids: Structure and Properties*. 2nd ed. Cambridge: Cambridge University Press.

Nazir, Aamer, Kalayu Mekonen Abate, Ajeet Kumar, and Jeng-Ywan Jeng. 2019. "A State-of-the-Art Review on Types, Design, Optimization, and Additive Manufacturing of Cellular Structures." *The International Journal of Advanced Manufacturing Technology* 104(9):3489–3510. doi: 10.1007/s00170-019-04085-3.

Tumbleston, John R., David Shirvanyants, Nikita Ermoshkin, Rima Janusziewicz, Ashley R. Johnson, David Kelly, Kai Chen, Robert Pinschmidt, Jason P. Rolland, Alexander Ermoshkin, Edward T. Samulski, and Joseph M. DeSimone. 2015. "Continuous Liquid Interface Production of 3D Objects." *Science* 347(6228):1349–52. doi: 10.1126/science.aaa2397.

POST-PROCESSING OF SURFACE TOPOGRAPHY DATA FOR AS-BUILT METAL ADDITIVE SURFACE TEXTURE CHARACTERIZATION

Theresa Buchenau[1*], Hauke Brüning[1], Marc Amkreutz[1]
[1]*Fraunhofer Institute for Manufacturing Technology and Advanced Materials IFAM, Bremen, Germany*
** Corresponding author, email: theresa.buchenau@ifam.fraunhofer.*

ABSTRACT

Surfaces of additively manufactured metal parts from powder-based processes typically show powder particle agglomerations and other features, resulting in high surface roughness. Proper characterization of those surfaces is necessary in order to assess part quality with respect to coatability, mechanical performance or corrosion resistance for use in aerospace, automotive, medical and more industrial applications.

Optical surface texture measurement allows for collection of areal surface data, while the established contact stylus method only captures line profile data.

When applying optical methods for surface topography measurements, proper data acquisition and post-processing in order to assess surface texture may be complex. A number of variables can be adjusted, such as different measurement settings, approaches to outlier removal, evaluated area size or form removal.

This work shows the influence of selected measurement and post-processing variables on data obtained from confocal microscopy for as-built Ti6Al4V and AlSi7Mg0.6 from laser powder bed fusion.

The aim is to show the influence of variation in measurement and post-processing on calculated surface texture parameters and stress the importance of proper documentation in order to achieve meaningful, reproducible data for quality assurance.

Keywords: Laser Powder Bed Fusion, Surface Texture Characterization, Optical Metrology, Confocal Microscopy

1. MATERIALS AND METHODS

2.1 Laser Scanning Confocal Microscopy

In laser scanning confocal microscopy (LSCM), the surface is scanned by a laser in different focal planes, only exposing the area portion in focus. The 3D surface representation is created by layering data across the focal planes (Leach, 2011). The used instrument in this study is the Keyence VK 9700. The method is listed as suitable method for areal surface texture characterization in ISO 25178. Data acquisition and post-processing are not yet included in the standard.

2.2 Samples

Considered surfaces are as-built condition from laser powder bed fusion (LPBF), AlSi7Mg0.6 (Fig.1, left) and Ti6Al-4V (Fig. 1, right). Typical powder particle agglomerations of different sizes are visible in both scanning electron microscopy (SEM) images.

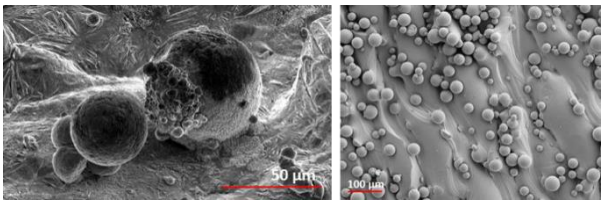

Figure 1. Powder Particle Agglomerations on As-built AlSi7Mg0.6 *(left)* and Ti6Al4V *(right)* Surfaces from Laser Powder Bed Fusion

2. RESULTS AND DISCUSSION

Typical confocal microscopy raw data shows large spikes (see Fig. 2, also refer to Thompson 2017), that occur around the edges of powder particles. Comparing the raw data to the microscopic images (i.e. Fig. 1[1]) clearly shows these spikes are not physically present on the measured surfaces, leading to the assumption that they are measurement artefacts. Taking a closer look at the data shows that the spikes have the size of the measured z-range, as illustrated in Fig. 2. The figure shows identical location with variation of the pre-set z-range, which means that the size of the artefact does not seem to depend on a

surface feature, but on a measurement setting.
However, the origin of the spikes is indeed related to specific features, namely particle agglomerations. Confocal microscopy is a line-of-sight method and as-built LPBF show undercuts, which can hence not be captured. On the boundaries of attached particles, the instrument detects two signals, one from the boundary and one from the surface below[1], leading to the display of a spike artefact.

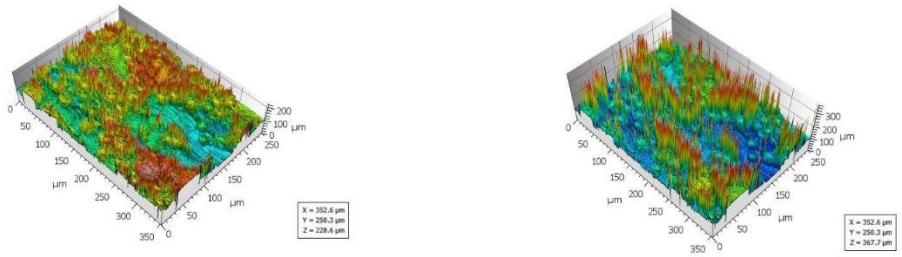

Figure 2. Spikes in Confocal Raw Data of As-built Ti6Al4V. Left and Right Images Show Identical Locations on the Surface with Different Z-Range Setting

3. CONCLUSIONS

These artefacts are only one example showing why optical methods, when applied to as-built metal additive surfaces, require special attention when it comes to post-processing. As data acquisition and post-processing is not yet included in the ISO 25178 standard, there are various option all resulting in different values for surface texture parameters.
The complete data evaluation showing and discussing a range of options with a final recommendation for processing of LSCM data for as-built metal additive surfaces will be given in the full paper.

REFERENCES

Bagehorn, S.; Mertens, T.; Greitemeier, D.; Carton, L.; Schoberth, A. (2015): Surface finishing of additive manufactured Ti-6Al-4V - A comparison of electrochemical and mechanical treatments. In *6th European Conference for Aerospace Sciences*.
ISO 25178: Geometric Product Specifications (GPS) - Surface texture: areal - Part 2: Terms, definitions and surface texture parameters, 2012.
Leach, R. K. (2011). Optical Measurement of Surface Topography. 10.1007/978-3-642-12012-1.
Grimm, T.; Wiora, G.; Witt, G. (2015): Characterization of typical surface effects in additive manufacturing with confocal microscopy. *Surface Topography: Metrology and Properties*, 3(1):014001.
Thompson, A.; Senin, N.; Giusca, C.; Leach, R. (2017). Topography of selectively laser melted surfaces: a comparison of different measurement methods. *CIRP Annals*, *66*(1), 543-546.
Townsend, A.; Senin, N.; Blunt, L.; Leach, R. K.; Taylor, J. S. (2016): Surface texture metrology for metal additive manufacturing: a review. In: *Precision Engineering 46*, S. 34–47. DOI: 10.1016/j.precisioneng.2016.06.001.
Triantaphyllou, A.; Giusca, C. L.; Macaulay, G. D.; Roerig, F.; Hoebel, M.; Leach, R. K. (2015): Surface texture measurement for additive manufacturing. In: *Surf. Topogr.: Metrol. Prop. 3 (2)*, S. 24002. DOI: 10.1088/2051-672X/3/2/024002.

PRELIMINARY INVESTIGATION OF TRIBOLOGICAL CHARACTERIZATION OF 3D PRINTED AN AMORPHOUS THERMOPLASTIC WITH DIFFERENT INFILL DENSITIES

Gülşah Akıncıoğlu[1], Enes ASLAN[1]
[1]*Department of Machine and Metal Technologies, Duzce University, Duzce, Turkey,*
gulsahakincioglu@duzce.edu.tr; enesaslan@duzce.edu.tr

ABSTRACT

Amorphous thermoplastic has been widely used in the automotive industry and outdoor applications such as sliding doors, due to its strong weather resistance, mechanical properties, and lightweight. This study aims to increase the lightness and also retain the wear resistance by producing samples with different infill densities. The samples were produced with a fusion filament production system with different filling densities. Friction tests were performed on pin-on disc device according to ASTM G99 standards. The hardness of the samples was measured with a Shore D test device. Worn surface examinations were made using digital microscope images. Wear rates based on the weight losses were evaluated after the wear test. The expected result of this study is to obtain a light and wear resistance product with less cost and material.

Keywords: Amorphous thermoplastic, Friction, worn surface, Fused filament fabrication

QUALIFICATION METHOD FOR THE PROCESS DEPENDENT FACTORS AND AFFECTING THE FATIGUE BEHAVIOR OF LASER POWDER BED FUSION METHODS FOR TI6AL4V

Ümit Aytar[1], Erdem Mermer[2]
[1]*Turkish Aerospace, uaytar@tai.com.tr*
[2]*Turkish Aerospace, erdem.mermer@tai.com.tr*

ABSTRACT

A main limiting factor for the adoption of additively manufactured (AM) parts into structural applications is the challenge of qualification. The other challenging factor is fatigue chracterization of part. The fatigue chracterization of LPBF metals is a fundemental step toward technology acceptance for structural applications. To speed qualification of LPBF, a rapid method that quantifies impacts of process variables on part structure, properties, and performance is required. Using a list of design requirements developed from literature, build experience, and needs from several major roadmapping efforts, a test artifact was designed to evaluate geometry-specific microstructure, dimensional accuracy, residual stress, chemistry, surface integrity, powder removal, and distortion. The LPBF artifact includes: four sides for geometric feature accuracy and surface integrity analysis, indication marks for accurate sectioning for metallography, and additional features specifically designed to evaluate residual stress, powder removal, mechanical properties and distortion. Microstructure is quantifiable on features including overhangs, islands, thin features, channels, lattice structures and bulk areas representing different thermal histories. This single geometry can be used for many purposes, including optimization of LPBF input variables, qualification and more. Ongoing work is continuing to improve the artifact design, testing its implementation across LPBF platforms, and using the artifact to concretely define process sensitivity currently limiting standardization and adoption of LPBF due to costs associated with defining process windows in terms of qualification and certification.

Keywords: Qualification, Laser Powder Bed Fusion, Ti6Al4V, Fatigue

1. INTRODUCTION

Selective laser melting (SLM) is an established powder-bed-fusion- based additive manufacturing (AM) process today [1] A wide variety of metallic materials have been processed to date by this process. In particular, AM of Ti-6Al-4V (wt.%) has received extensive attention due to both its broad applications in various industry sectors and its high cost of manufacture and long lead time by the conventional manufacturing processes.
In this study, Ti-6Al-4V alloy will be used with laser powder ped fusion method.

2. RESULTS AND DISCUSSION

This work is developing a qualification process that allows relationships across instruments, platforms, suppliers, and even alloy systems to be inferred using qualification test article. This allows predictions to be made across AM systems which can reduce the amount of data needed to qualify a new machine and certify a new part, greatly speeding the adoption of AM parts into aerospace parts without sacrificing the quality and reliability that drive the need for qualification. The goal is to enable qualification of AM parts with significantly reduced testing across various tools, vendors, and feedstocks by directly incorporating awareness of manufacturing issues such as melt pool scaling, powder reuse, and local thermal environment during a build.

3. CONCLUSIONS

The pre-selected geometry designed and managed by the authors for the benefit of research to advance LPBF qualification efforts and help lead to more widespread adoption of LPBF for Ti-6Al-4V alloys. Also this study will investigate the influence of microstructure, residual stress and orientation of LPBF produced Ti-6Al-4V on establishing parameters from a foundational perspective.

REFERENCES

[1] Edwards P, Ramulu M. Fatigue performance evaluation of SLM Ti- 6Al-4V. Mater. Sci. Eng. A

SURFACE CHARACTERIZATION OF ELECTRON BEAM MELTING PROCESSED γ-TIAL

Güney Mert Bilgin[1], Çağdaş Şen[1], Akın Orhangül[1]
[1]*TUSAS Engine Industries, Inc., guneymert.bilgin@tei.com.tr*

ABSTRACT

In recent years, γ-TiAl alloys find various application areas in aviation industry as they provide high temperature strength and oxidation resistance. Moreover, a significant weight gain is achieved when γ-TiAl alloys are preferred in comparison to their nickel based superalloy counterparts utilized in aero-engines. However γ-TiAl is extremely brittle at room temperature and thus severe material loss can not be avoided when a conventional subtractive production method is applied. Therefore a near-net shaping technology such as electron beam melting (EBM) is required to produce γ-TiAl parts in a certain geometry. On the other hand, due to the nature of EBM, the surface roughness of the produced parts is higher compared to its counterparts and requires secondary operations. In this study, EBM technology was applied to produce Ti-48Al-2Cr-2Nb representative turbine blade geometry with various process parameters in order to obtain better as-built surface quality. The EBM process variables, used to manufacture the highest quality Ti-48Al-2Cr-2Nb turbine blade surfaces, were determined according to the roughness and subsurface micro porosity measurements.

Keywords: Electron Beam Melting (EBM), Ti-48Al-2Cr-2Nb, Surface Roughness, X-ray computed tomography (XCT)

1. INTRODUCTION

Electron beam melting (EBM) is an additive manufacturing method where a focused electron beam is used to melt powders in each layers. Subsequently melted layers are fused to each other to create complex shaped parts. This layer by layer approach presents possibility of producing complex geometries and internal features. Besides there are noteworthy benefits of additive manufacturing namely design freedom, lower buy-to-fly ratio and ability to produce highly complex shapes with rapid fabrication. Recently, in conjunction with EBM, γ-TiAl alloys are being used in aerospace applications. Comparably lower density and good high-temperature strength properties make γ-TiAl alloys perfect candidate for innovative aero-engine applications, where good creep, oxidation resistance and lower weights are desired at high operating temperatures. Yet poor surface finish and as a result distorted geometrical form prevent EBM γ-TiAl parts to be used in as built form. Post-process operations, such as machining or surface improvement secondary processes, are generally needed to utilize γ-TiAl parts. Obtaining better surface finish can significantly reduce the post-process operation times and need. This study aims to investigate the possibility of enhancing as built EBM Ti-48Al-2Cr-2Nb surface quality by applying different scan contour process parameters. For EBM process, speed function and line offset parameters have the largest effect on the density and resultant surface roughness 1). Electron beam energy input, which is a cofactor of beam voltage, beam scan speed, beam current and track offset distance, has also a significant effect on the final part quality. Low energy input results in higher average porosity percentage that can be monitored using micro XCT 2). Ti-48Al-2Cr-2Nb representative turbine blade, which is a critical aero –engine component used in high temperature environments, samples were produced with different processing parameters and afterwards surface characteristics, porosity and sub-surface porosity were compared and analyzed.

2. MATERIALS AND METHODS

Gas atomized Ti-48Al-2Cr-2Nb prealloyed powder having 45 -150 µm average particle size was used in this study. The chemical composition of the powder is shown in Table 3.

Table 3. Ti-48Al-2Cr-2Nb Powder Chemical Composition (in wt. %)

Al	Cr	Nb	Fe	C	O	N	H	Ti
34.4	2.5	4.8	0.03	0.01	0.08	<0.01	0.0002	Balance

Arcam A2X EBM system having accelerating potential of 60 kV was applied to manufacture Ti-48Al-2Cr-2Nb samples. The preheating temperature of 1060°C and layer thickness of 90 µm process variables were kept constant throughout the EBM production which was done within a vacuum environment having an average 2.0 e^{-3} mBar. Infill of the all samples were scanned with 12 mA current, 0.200 mm line offset, and 1600 mm/s scan speed hatch variables in manual mode 3)4). Contour scans in

the form of multi-spots with different parameters were carried out to reduce the surface roughness and to ensure geometric accuracy of the produced parts. Accordingly, an experiment set consisting of beam currents varying between 5 to 10 mA, focus offsets from 0 to 12 mA and speed functions in between 4 and 8 was studied. The turbine blade surface obtained as a result of the EBM production without applying contour parameters was also compared with the experimental contour studies. The measurements were conducted from the as-built surfaces of the turbine blades and no additional secondary process was carried out. XCT measurements were conducted using RX Solutions EasyTom micro CT system with a 240 kV X-ray source. Pores within the samples were analyzed regarding their size and distribution. Surface characterization were made both using optical coherence scanning interferometry method and conventional tactile method. Due to highly irregular surface characteristics of EBM method, optical surface characterization method is employed to obtain areal surface parameters.

3. RESULTS AND DISCUSSION

9 different turbine blade samples were produced using EBM with different contour scan parameters. Resultant convex and concave surfaces were measured using both contact and optical methods. As built surface arithmetic mean height of the scale-limited surface (Sa) parameter is enhanced from 64 µm without contour scanning to 42 µm via adding three steps contour scanning and adjusting with contour scan parameters; beam speed, current and focus offset. Porosity analysis for different samples were conducted using micro XCT and sub-surface porosity analysis were also conducted using optical microscopy. Results will be elaborated within the full manuscript.

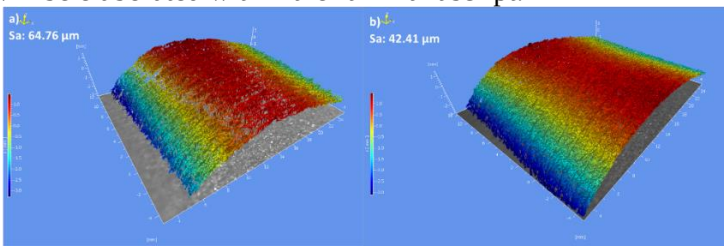

Figure 1. Ti-48Al-2Cr-2Nb samples produced via EBM a) without using contour scan b) with using improved contour scan parameters

4. CONCLUSIONS

Detailed results and conclusions will be elaborated within the full manuscript.

REFERENCES

1) Mohammad, A., Al-Ahmari, A., AlFaify, A., & Mohammed, M. (2017). Effect of melt parameters on density and surface roughness in electron beam melting of gamma titanium aluminide alloy. Rapid Prototyping Journal, 23(3), 474-485. doi: 10.1108/rpj-12-2014-0187
2) Mohammad, A., Alahmari, A., Mohammed, M., Renganayagalu, R., & Moiduddin, K. (2017). Effect of Energy Input on Microstructure and Mechanical Properties of Titanium Aluminide Alloy Fabricated by the Additive Manufacturing Process of Electron Beam Melting. Materials, 10(2), 211. doi: 10.3390/ma10020211
3) Seifi, M., Salem, A. A., Satko, D. P., Ackelid, U., Semiatin, S. L., & Lewandowski, J. J. (2017). Effects of HIP on microstructural heterogeneity, defect distribution and mechanical properties of additively manufactured EBM Ti-48Al-2Cr-2Nb. *Journal of Alloys and Compounds*, *729*, 1118-1135.
4) Lin, B., Chen, W., Yang, Y., Wu, F., & Li, Z. (2020). Anisotropy of microstructure and tensile properties of Ti–48Al–2Cr–2Nb fabricated by electron beam melting. *Journal of Alloys and Compounds*, *830*, 154684.

SURFACE ROUGHNESS ASSESSMENT OF POST-PROCESS EFFECTS ON LPBF ALLOY 718

Muhammed Baybars Gökcan[1a], Alican Taş[1b], Beyzanur Ertekin[1c], Zehranur Cavcar[1d], Emre Özeren[1e], Güney Mert Bilgin[1f], Göktuğ Kara[1g], Akın Orhangül[1h]
[1a]*TUSAS Engine Industries, Inc., MuhammedBaybars.Gokcan@tei.com.tr*
[1b]*TUSAS Engine Industries, Inc., Alican.Tas@tei.com.tr*
[1c]*TUSAS Engine Industries, Inc., Beyzanur.Ertekin@tei.com.tr*
[1d]*TUSAS Engine Industries, Inc., Zehranur.Cavcar@tei.com.tr*
[1e]*TUSAS Engine Industries, Inc., Emre.Ozeren@tei.com.tr*
[1f]*TUSAS Engine Industries, Inc., GuneyMert.Bilgin@tei.com.tr*
[1g]*TUSAS Engine Industries, Inc., Goktug.Kara@tei.com.tr*
[1h]*TUSAS Engine Industries, Inc., Akin.Orhangul@tei.com.tr*

ABSTRACT

Laser Powder Bed Fusion (L-PBF) is one of the promising Additive Manufacturing (AM) technologies to build relatively smooth surfaces belong to complex geometries with its overall technology readiness level. However, this may depend on the other parameters such as built orientation, support structures etc. Despite many advantages of AM, surface roughness of L-PBF'ed parts may still not be met in as-built condition the tight requirements of aviation industry.

In this study, the surface roughness assessment of L-PBF'ed as-built Alloy 718 parts using virgin powder is evaluated by utilizing several post processes beyond the industrial preferences, in aviation standards. The surface roughness is consequently optimized based on orientation in order to define robust manufacturing tolerances in AM of aviation parts. Closed clearances or smooth surface profiles are perfectly needed in those parts to improve several aspects such as fatigue life span. In the scope of this study, Grit Blast, Glass Bead Peen, Chemmill, Ultrapolish, Streamfinish and some of their combinations on five different sloping angles were studied, surface quality were evaluated with profilometer in addition to weight loss effects based on the stock loss method. The outcomes of the study will be used as reference in the future works of TEI.

Keywords: L-PBF, Alloy 718, Surface Roughness, Stock Loss.

1. INTRODUCTION

Laser Powder Bed Fusion (L-PBF) represents an efficient manufacturing alternative compared to conventional methods in terms of reduced lead-time per parts, ability to bring complex geometries and consolidated assemblies out at one shot. From these aspects, L-PBF becomes a popular method for aviation parts but it still needs to be improved in order to have robust outcomes in line with aviation standards. Surface roughness is one of these features and in the literature, there are some kind of studies that they have paid particular attention by dealing with hybrid to conventional (Brown, Li, Liu, Fang, & Guo, 2017) or several methods (Kaynak & Tascioglu, 2020). In this study, the effects to surface roughness of some sort of methodologies used in aviation were studied on as-built Alloy 718 specimens that are built in different sloping angles.

2. MATERIALS AND METHODS

Square prism samples with dimensions of 30 x 30 x 2 mm are manufactured from virgin Alloy 718 powders with same build parameters. The total number of specimens are counted per 5 different methods, namely Grit Blast (in two different parameters), Glass Bead Peen, Chemmill, Ultrapolish, Stream Finishing; and two of the combinations, namely Grid Blast + Chemmill and Grit Blast + the method will be selected based on the better outcomes from the comparison of Ultrapolish or Stream Finishing. The specimens are planned to fabricate in 5 different sloping angles per each method. The distribution of samples is shown in Fig. 1. The follow-up for each process has been provided by process cards.

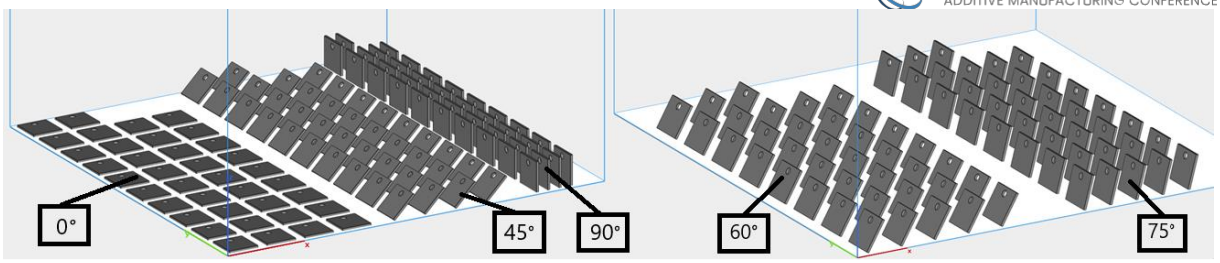

a **b**

Figure 9. Specimen sloping angles on built chamber **a.** 0°, 45° and 90°; **b.** 60° and 75°

For each post processes at each angle, 3 of trial specimens are provided to adjust robust process parameters except Grit Blast in which the number of trial specimens was 6. Resultantly, 2 specimens per each combination are planned to be applied the post processes. Each sample has 3 different direction of roughness measurement on upskin via profilometer, see Fig. 2. The initial and post processed weight measurements are recorded to define average offset to be added to the surface of fatigue specimens. Thus, the offset is expected to be removed by post processes in order to obtain smooth specimens.

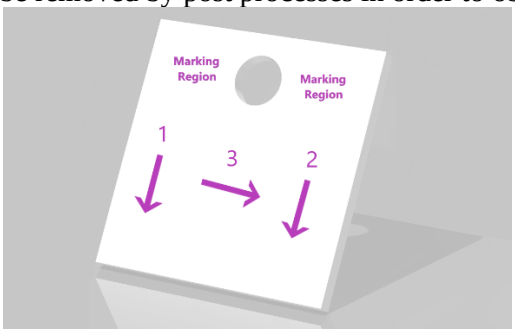

Figure 10. The direction of roughness measurements on specimen

3. RESULTS AND DISCUSSION

As an on-going period, the results of some of the studies are still being obtained. Thus, evaluation of studies is not concluded yet.

4. CONCLUSIONS

When the all results handled, the conclusion will be provided. The future work will be the assessment of effects of surface roughness on fatigue of aviation engine parts.

REFERENCES

Brown, D., Li, C., Liu, Z., Fang, X., & Guo, Y. (2017). Surface integrity of Inconel 718 by hybrid selective laser melting and milling. *Virtual and Physical Prototyping*, 26-31.

Kaynak, Y., & Tascioglu, Y. (2020). Post-processing efects on the surface characteristics of Inconel 718 alloy fabricated by selective laser melting additive manufacturing. *Progress in Additive Manufacturing*, 221-234.

SURFACE TREATMENT EFFECTS ON CHEMICAL MILLING PERFORMANCE OF L-PBF PRODUCED TI6AL4V ELI

Buket Parlak[1*], Oğuz Acar[1], Aslınur Ataklı[1], Emre Özeren[1]
*[1]TUSAS Engine Industries, Inc., *Buket.Taspinar@tei.com.tr*

ABSTRACT

Titanium is one of the most desirable engine material in compressor sections of engines due to its low density and high strength. Titanium suffers from oxygen entrapment by the reason of heat treatment, high temperature exposure and produced oxygen rich layer referred as alpha case. Laser Powder Bed Fusion (L-PBF) supports to produce the desired geometries that have high complexity. As casting method, L-PBF also encountered with alpha case due to high temperature melting but not high amount like casting. Since L-PBF produced parts that have high surface roughness, melted powders on surfaces, it is hard to remove alpha case totally. In this study, Ti6Al4V ELI parts were produced by L-PBF and measured alpha case levels before and after chemical milling. Abrasive blasting was used to facilitate chemical attack on parts surface to make smooth surface before chemical milling and chemical concentrations were changed to get proper and alpha case free surfaces.

Keywords: Additive Manufacturing, L-PBF, Titanium, Alpha Case, Chemical Milling

1. INTRODUCTION

Additive manufacturing is a production method in which parts are obtained by adding layers on top of each other. Laser Powder Bed Fusion (L-PBF) is one of the methods of powder bed fusion technology. The main working principle is based on melting powder into the bed by using laser power [1]. Additive manufacturing is mostly preferred to produce the parts as near net shape forms instead of traditional methods such as casting, forging. Titanium and its alloys are common materials used in many applications as aerospace applications especially compressor sections because of its strength to weight ratio, high corrosion resistance, and low density. Among the titanium alloys, Ti6AL4V is commonly used for cold section aero engine applications and contains two phases defined as alpha (body centered cubic structure) and beta (closed packed hexagonal structure) [2]. Increasing alpha and beta phases in the structure give raise to strength and reduced ductility respectively [2]. Titanium is mostly manufactured by investment casting method which brings high cost and long manufacturing delivery time and alpha case problems. Alpha case is an oxygen rich layer that is caused by heat treatment, casting, hot working and exposed to air at high temperature on titanium surface [2,3]. Since alpha case reduces tensile, fatigue properties due to brittle phase and make easy to crack initiation, titanium is not used without removal of this layer for high load and amplitude applications [4,5]. Mechanical and chemical method are applicable to remove this layer for casting, wrought parts. Due to the porous and non homogenous structure of additive based manufactured Ti6Al4V alloys, it is hard to totally remove alpha case by chemical milling methods. Although, L-PBF has advantages to obtain near net shape part production, it is necessary to work on removing the alpha case generated from L-PBF method and annealing heat treatment.

In this study, the effects of post processes and different chemical concentrations to be successfully achieved chemical milling process by the aim of removing alpha case from L-PBF-produced Ti6Al4V ELI surface has been studied.

2. MATERIALS AND METHODS

The geometries planned for alpha case control, were manufactured in Concept Laser M2 Series 5 machine. The machine has a dual-laser system and it is also capable of building plate heating up to 200 degrees Celsius. The production has been completed via non-virgin, Concept Laser branded, Ti6Al4V ELI powder with particle size distributions from 15 to 53 microns. Samples were manufactured at XY and Z directions. After production, parts were heat treated at 700°C for 2 hours with the aim of stress relief. Before removal of the alpha case, sand blasting process parameters were studied. Alpha case examinations were examined by using an optical microscope, Nikon Exlipse Ma200 branded. Surface roughness of all samples were measured by using profilometer after performing each sand blasting set. Chemical milling was performed as per ASTM B600. After chemical milling, samples were prepared by using Struers cutting machine mounted, polished and etched with Kroll's reagent and then amoniumbifloride to examine alpha case with proper magnifications.

3. RESULTS AND DISCUSSION

It is observed that alpha case removal was successfully achieved by application of sand blasting, as seen figure 1. It is clearly seen that sandblasting makes the surface more active against to chemical solutions.

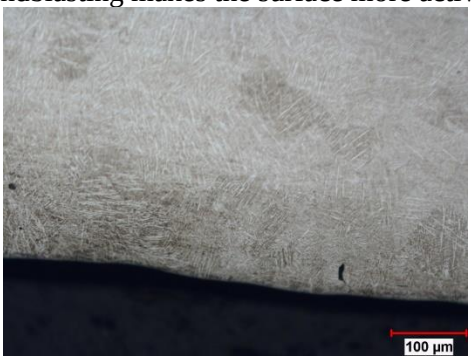

Figure 1. Alpha Case Examination (After Sand Blasting and Chemical Milling Processes).

4. CONCLUSIONS

Samples will be produced in XY and Z built directions (both as built and heat-treated conditions). Surface roughness of the parts will be measured and defined sand blasted parameters will be performed before chemical milling. Alpha case levels will be determined. Etch rate of chemical milling baths will be calculated, then parts will be processed to remove alpha case totally from additive part surfaces.

REFERENCES

[1] Dareh Baghi, A., Nafisi, S., Hashemi, R., Ebendorff-Heidepriem, H., & Ghomashchi, R. (2021). Effective Post processing of L-PBF fabricated ti-6al-4 v alloy: Machining vs thermal treatment. Journal of Manufacturing Processes, 68,m 1031–1046. https://doi.org/10.1016/j.jmapro.2021.06.035
[2] Donachie, M. J. (2010). Titanium: A technical guide. ASM International.
[3] Get the facts on... heat treatment. Get the Facts on... Heat Treatment | GE Additive. (n.d.). Retrieved April 30, 2022, from https://www.ge.com/additive/ja/node/1131
[4] Satko, D. P., Shaffer, J. B., Tiley, J. S., Semiatin, S. L., Pilchak, A. L., Kalidindi, S. R., Kosaka, Y., Glavicic, M. G., & Salem, A. A. (2016). Effect of microstructure on oxygen rich layer evolution and its impact on fatigue life during high-temperature application of α/β titanium. Acta Materialia, 107, 377–389. https://doi.org/10.1016/j.actamat.2016.01.058
[5] Zhai, Y., Galarraga, H., & Lados, D. A. (2015). Microstructure evolution, tensile properties, and fatigue damage mechanisms in ti-6al-4v alloys fabricated by two additive manufacturing techniques. Procedia Engineering, 114, 658–666. https://doi.org/10.1016/j.proeng.2015.08.007.

AMCTURKEY
ADDITIVE MANUFACTURING CONFERENCE

TEETH SUPPORT STRUCTURES EFFECT ON DIMENSIONAL DEVIATION OF LPBF PRINTED COMPONENTS WITH OVERHANG FEATURES

Kadir Günaydın[1], Orhan Gülcan[2], Alican Çelik[3] and Evren Yasa[4]
[1]*General Electric Aviation, Gebze, Kocaeli, Turkey, kadir.gunaydin@ge.com*
[2]*General Electric Aviation, Gebze, Kocaeli, Turkey, orhan.gulcan@ge.com*
[3]*General Electric Aviation, Gebze, Kocaeli, Turkey, alican.celik@ge.com*
[4]*Eskişehir Osman Gazi University, Mechanical Engineering Department, Eskişehir, Turkey, eyasa@ogu.edu.tr*

ABSTRACT

Support structures are the special structures that provides the integrity of overhang features in terms of dimensional accuracy and manufacturability without any collapse. Support structures need to be removed without forming any defect on main part after the build and minimizing the usage of these structures are in the scope of different studies. One of the prevalent support structure types is the teeth support structures which includes spaced repeated teeth for providing easy removal and better remnant. In this study, laser powder bed fusion technology is utilized to produce overhang features in the angle of 30° and different teeth parameters are used to find optimum teeth support dimension for achieving intended dimensional accuracy. The support thickness and spacing between two support pieces are the variables for forming different type of teeth support ranging. The manufactured parts are scanned with a 3D scanner blue light device. Results show that the optimum teeth support parameters.

Keywords**:** dimensional deviation, contactless support, LPBF

1. INTRODUCTION

Laser powder bed fusion (LPBF) or electron powder bed fusion (EPBF) technologies are two types of additive manufacturing (AM) technologies where metal powders and an energy source (laser in LPBF and electron in EPBF) are used to selectively scan and melt pre-laid powders on a build platform layer by layer to get near-net-shape products [1]. These novel technologies enable production of very complex and lightweight parts which are very difficult or sometimes impossible to produce with conventional manufacturing processes [2]. However, these technologies have some limitations, one of which is the necessity of support structures in especially overhang areas. Support structures are used to hold the part on the build platform and prevent it from distortions and dimensional deviations due to high thermal gradients during manufacturing [3]. This study focuses on the producibility of overhang features using teeth support structures and providing dimensional accuracy while creating feasibility for easy support removal option.

2. MATERIALS AND METHODS

Overhang specimens with 30^0 inclination angles with respect to build plate were modelled with Siemens NX software (Figure 1). Teeth supports with three different parameters (tooth support thickness - 0.76, 1.02, 1.27 and gap between supports - 0.51, 0.76, 1.02 mm) were used during production. Concept Laser M2 LPBF machine was used for the production of the specimens. In718 powder material and standard vendor process parameters were used. After production, supports and the final parts were removed from the build platform with GF Agiecharmilles wire electrical discharge machine. Specimens were scanned with ATOS ScanBox 4105 blue light device and GOM Inspect software was used to evaluate the dimensional deviations of the produced specimens from the original CAD geometry.

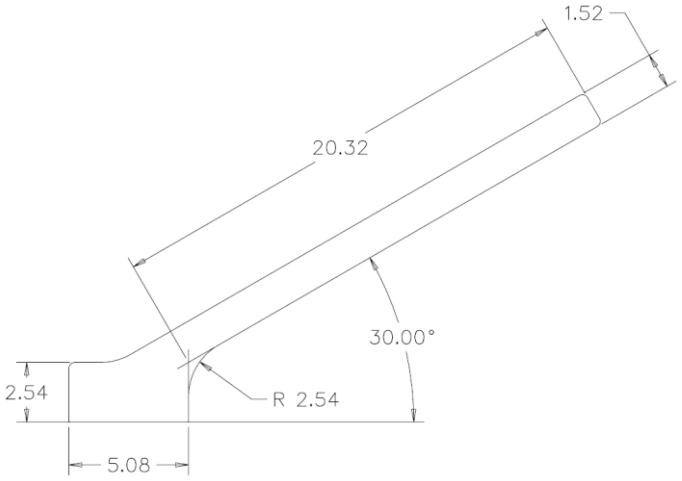

Figure 1. Overhang specimen

3. RESULTS AND DISCUSSION

For each teeth support value, three specimens and total 9 specimens were produced without any specific production problem (Figure 2).

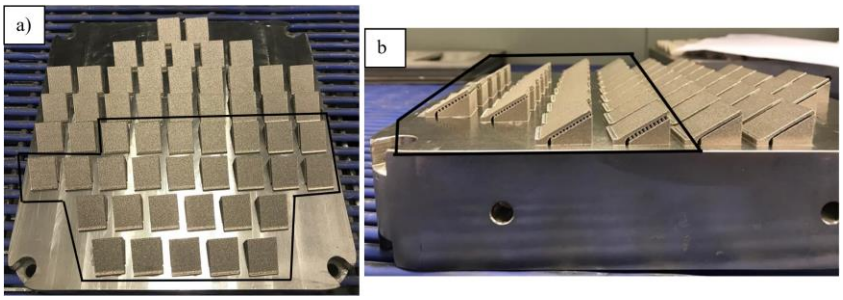

Figure 2. Produced specimens

4. CONCLUSIONS

The comparison between blue light scanned 3D data of the produced specimens and the original CAD data reveals that gap value between the support structures support thickness affects the dimensional variation of the overhang surface. As a future work, the effect of teeth support parameters on surface roughness, microhardness through thickness and microstructural changes will be investigated.

REFERENCES

Leary, M. 2020. “Powder bed fusion”, Editor(s): Martin Leary, In Additive Manufacturing Materials and Technologies, Design for Additive Manufacturing, Elsevier, 295-319. [https://doi.org/10.1016/B978-0-12-816721-2.00011-7].

Flores, I., Kretzschmar, N., Azman, A. H., Chekurov, S., Pedersen, D. B., Chaudhuri, A. 2020. “Implications of lattice structures on economics and productivity of metal powder bed fusion”, Additive Manufacturing, 31: 100947. [https://doi.org/10.1016/j.addma.2019.100947].

Jiang, J., Xu, X., Stringer, J. 2018. “Support structures for additive manufacturing: a review”, Journal of Manufacturing and Materials Processing, 2: 64.

THERMAL SIMULATION AND EXPERIMENTAL VERIFICATION STUDY FOR TI-6AL-4V ALLOY PROCESSED BY METAL LASER MELTING

Demiray M. A. , Sekerci B. Kayacan M. C.*, Gürgen M.
Department of Mechanical Engineering, Suleyman Demirel University, Isparta, Turkey
YETEM , Suleyman Demirel University, Isparta, Turkey
* *Corresponding author, email: cengizkayacan@sdu.edu.tr*

ABSTRACT

Prediction of the effect of process parameters is a challenging problem in selective laser melting (SLM) method. Although the simulation technics are the most widely used methods to predict temperature gradients / melt pool dimensions and their relations with parameters, they are also required some experimental verification manufacturings. In the present study, 3D thermal simulation of metal laser melting process and its experimental verification was conducted for different process parameters to provide a relation between pool dimensions, temperatures and process parameters. Both simulations and experimental manufacturing steps were conducted for 3 layers that each one includes 4 adjacent laser tracks for different scanning speed, laser power and hatching distance combination. Temperature gradients and melt pool dimensions were revealed as simulation results. Afterall, special substrate was designed to manufacture all Ti-6Al-4V multi tracks at once within all parameter combinations. Cross- sectional areas of multitrack specimens were investigated in optic microscope to observe melt pools and top surfaces of specimens were investigated by Scanning Electron Microscope (SEM). Both cross sectional investigations approved that our simulation results are accurately predict real manufacturing temperatures and pool dimensions within small errors.

Keywords: SLM, melt pool, simulation, Ti-6Al-4V

1. INTRODUCTION (11 FONT SIZE, BOLD, ALL CAPS)

Selective Laser Melting (SLM) method is the most common and promising Additive Manufacturing (AM) method all over the world. Due to SLM has many variables, the most challenging problem for SLM is the uncertainty of the effect of process parameters such as laser scanning speed, laser power, layer thickness and hatching distances which is a distance between adjacent laser lines.

In the last 10 years, simulation and modelling technics based on mathematical equations became the most applicable methods since the computer technology comes up with new skills[1-4]. Nonetheless, simulation predictions were required verifications at first by some experimental specimen investigations which can be done with some manufacturings with the same process parameters as in the simulations. Afterall, simulation become reliable for much more parameter combinations. This related study focused on the FE thermal modeling, simulation and experimental verification of the SLM process for Ti-6Al-4V to reveal a reliable simulation technic for different process parameters such as laser power, scanning speed and hatching distance.

2. MATERIALS AND METHODS

Simulation study conducted in ABAQUS finite element (FE) software by developing a fortran based subroutine to get laser power source onto substrate throughout bidirectional pattern. At the beginning, material properties were acquired from the literature for Ti-6Al-4V powder and solid material [5]. Then based on governing equations, (Goldak double ellipsoidal heat source for moving heat source, density, specific heat and conductivity equations, convection coefficient calculation) 3D model built in ABAQUS interface with the Neuman boundry conditions [6,7]. Simulation results were acquired as temperature history, maximum temperatures and melt pool dimensions at cross section of the laser tracks.

At the experimental side, process parameters that used in manufacturings were given in Table 1. An unique smaller substrate that divided into several laser track islands was designed to manufacture all combination from Table 1 at once and laser tracks were given in Figure 1 as manufactured on the small substrate. 4 adjacent laser tracks were manufactured on each island in EOS M280 Device during 3 layer with using EOS Ti-6AL-4V raw metal powder and argon as inert gas atmoshpere.

Table 1. Simulation Parameters

Laser Power (W)	130-150–170 - 190	Solidus and Liquidous (℃)	1600, 1650,
Scaning Speed (m/s)	0.75-1 - 1.25 - 1.5	Vaporization (℃)	2860
Hatching Distance (mm)	0.06-0.08 - 0.1 - 0.12	Latent Heat Of Fusion and Vapor (J/kg)	295000, 9860000
Beam Diam. (mm)	0.08	Porosity (%)	30
Layer Thick.(mm)	0.03	Absorptivity (%)	70
Powder Material	Ti6Al4V	Emissivity (%)	70

3. RESULTS AND DISCUSSION

This section shows the experimental melt pool investigations in comparison with simulation results. After that, melt pool dimension and process parameter relation was revealed as temperature related. Figure 2 shows the experimental cross sectional microscobic pictures of melt pool.

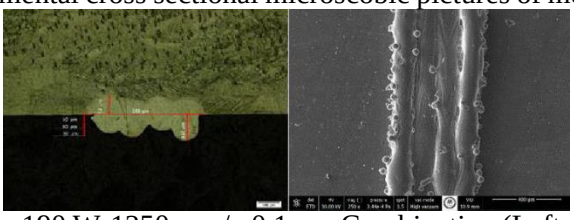

Figure 2. Melt Pools For 190 W-1250 mm/s-0.1mm Combination (Left: Optic Microscope Pictures at Cross Sectional Area. Right: Top Surfaces Under SEM)

4. CONCLUSIONS

In this study, 3D thermal simulation predictions were revealed as temperature and melt pool dimensions for 64 different process parameter combinations. Experimental verification were conducted by cross sectional specimen investigations for melt pool dimensions. It was revealed that simulation predictions are reliable in a range of % 15-25 error values and temperature-melt pool-process parameter relations were revealed.

REFERENCES

Zeng K., Pal D., Stucker B., 2012. “A review of thermal analysis methods in laser sintering and selective laser melting”, Proceedings of Solid Freeform Fabrication Symposium Austin, TX 60, 796-814.

Lavery N., P., Brown S.G.R., Sienz J., Cherry J., Belblidia F., 2014. “A review of computational modelling of additive layer, manufacturing - multi-scale and multi-physics”, International Conference on Sustainable Design and Manufacturing Cardiff, Wales, UK 28-30 April 2014.

Schoinochoritis B., Chantzis D., Salonitis K., 2017. “Simulation of metallic powder bed additive manufacturing processes with the finite element method: A critical review”, Proceedings of the Institution of Mechanical Engineers, Part B: Journal of Engineering Manufacture, 231(1):96-117. doi:10.1177/0954405414567522

Moraes D. A. and Czekanski A., 2018. “Parametric thermal FE analysis on the laser power input and powder effective thermal conductivity during selective laser melting of SS304L”, Journal of Manufacturing and Materials Processing 2(3): 47.

Mills KC., 2002. “Recommended values of thermophysical properties for selected commercial Alloys”, Wiltshire, England; Woodhead.

Bejan, A., & Kraus, A. D. 2003. “Heat transfer handbook”, New York: J. Wiley.

Goldak J., Chakravarti A. and Bibby M., 1984. “A new finite element model for welding heat sources”, Metallurgical Transactions B volume 15, pages 299–305..

THERMO-MICRO-MECHANICAL SIMULATION OF A TI-6AL-4V SINGLE WALL STRUCTURE MANUFACTURED BY DIRECTED ENERGY DEPOSITION

Merve Tunay[1], Cengiz Baykasoğlu[1], Oncu Akyildiz[2]
[1] *Hitit University, Faculty of Engineering, Department of Mechanical Engineering, Cevre Yolu Avenue, 19030, Corum, Turkey,* mervetunay@hitit.edu.tr, *cengizbaykasoglu@hitit.edu.tr*
[2] *Hitit University, Faculty of Engineering, Department of Metallurgical and Materials Engineering, Cevre Yolu Avenue, 19030, Corum, Turkey, oncuakyildiz@hitit.edu.tr*

ABSTRACT

In this study, thermo-micro-mechanical (TMM) finite element (FE) process model for a single wall deposition is developed to investigate the residual stresses and deformations occur during laser-based directed energy deposition (DED) process of Ti-6AL-4V. The effects of some process parameters (i.e., laser power and scanning speed) on the residual stress and deformation fields are also examined. The special focus is to evaluate the influence of solid-state phase transformations on the flow behavior of Ti-6AL-4V. At this point, the Johnson-Cook (JC) constitutive material model combined with a rule of mixtures is used to account for the effect of phase transformations on the flow behavior by considering strain, strain rate, temperature. The proposed TMM model provides useful information for a better understanding of process-microstructure-property relations in a DED-processed part.

Keywords: Additive manufacturing, directed energy deposition, thermo-micro-mechanical model, residual stress and deformation, finite element method

1. INTRODUCTION

During metal additive manufacturing (AM), process parameters and their effect on the thermal, microstructural and mechanical properties of a manufactured part need to be studied in detail. Recent studies demonstrate that the use of FE-based macroscale modeling is a good alternative to determine the effects of process parameters that are difficult to test experimentally (Shamsaei et al., 2015). In this study, a coupled thermo-micro-mechanical model based on the most recent observations and formulations in the literature has been proposed and applied to the DED process. The proposed model allows the prediction of thermal field, phase distribution, residual stresses and deformations during DED processes for different process parameters.

2. MATERIALS AND METHODS

A coupled TMM model is developed and used to simulate the DED process of ten layers single wall Ti-6Al-4V deposition having 8.75 mm height, 41.61 mm long and 2.45 mm width, using commercial software ABAQUS as shown in Figure 1.

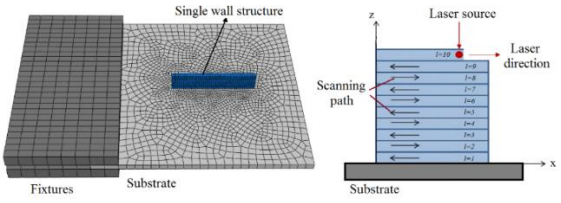

Figure 1. FE model and laser scanning direction of the single-wall structure.

Five different user subroutines are written in order to define the geometry, FE mesh, interactions, boundary conditions, heat source input, temperature dependent material properties and element activation definitions, etc. Goldak' s double ellipsoidal heat source model is implemented into the model to describe laser source (Goldak et al.,1984). The single wall deposition is modelled using the inactive/active element technique. The process parameters are selected as two different laser power (300 W and 400 W) and scanning speed (2 mm/s and 4 mm/s). The microstructure of the Ti-6Al-4V alloy is a mixture of α and β phases whose volumetric fractions can change significantly depending on thermal cycles during deposition processes. During the TMM simulations, the volume fractions of α and β phases are calculated according to the microstructural model presented in our previous study (Baykasoğlu et al., 2020). The individual contributions of the α and β phases to the yield stress of the

material are considered with the JC material plasticity model, in which the yield stress of each phase is evaluated in terms of strain, strain rate and temperature (Johnson & Cook, 1983). After determining the yield stress of each phase, the yield stress depending on the microstructure is calculated using the rule of mixtures (Pan et al., 2016).

3. RESULTS AND DISCUSSION

The residual stress (S11) and deflection values taken from the red lines shown in figures are given in Figure 2. As seen from the figure, the magnitude of deflection increases with the increasing laser power and decreasing scanning speed. With the increase of laser power from 300 W to 400 W, the maximum deformation values for laser scanning speeds of 2 mm/s and 4 mm/s increase by 85% and 36%, respectively. Similar to deflection values, residual stress values also increase with the increasing laser power and decreasing scanning speed. Particularly, the residual stress for 400 W laser power and 2 mm/s scanning speed reaches to 411 MPa in deposition area. Residual stress and deflection contours for 400 W and 2 mm/s are shown in Figure 2.

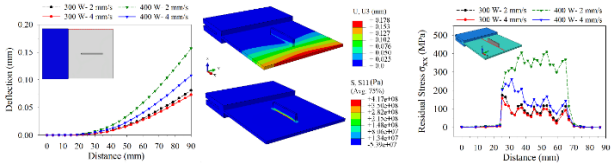

Figure 2. The deflections and residual stresses (S11) for different laser power and scanning speed.

4. CONCLUSIONS

This study introduces a TMM model to describe effect of process parameters on residual stresses and deflections for DED manufactured single-wall part. The simulation results demonstrated that the residual stresses and deflections decreased with the increase of laser scanning speed and decreasing of laser power. The proposed TMM process model with physics-based material constitutive model provides useful information for a better understanding the effects of process parameters on the residual stresses and deflections in a DED-processed part.

ACKNOWLEDGMENT

This research is partially supported by the Scientific and Technological Research Council of Turkey (TUBİTAK) under grant number 217M638.

REFERENCES

Baykasoğlu, C., Akyildiz, O., Tunay, M., & To, A. C. (2020). A Process-Microstructure Finite Element Simulation Framework for Predicting Phase Transformations and Microhardness for Directed Energy Deposition of Ti6Al4V. Additive Manufacturing, 35(March), 101252.

Goldak, J., Chakravarti, A., & Bibby, M. (1984). A New Finite Element Model for Welding Heat Sources. Metallurgical Transactions B, 15(2), 299–305.

Johnson, G. R., & Cook, W. H. (1983). A Constitutive Model and Data for Metals Subjected to Large Strains, High Strain Rates and High Temperatures. Proceedings of the 7th International Symposium on Ballistics, 21(1), 541–547.

Pan, Z., Liang, S. Y., Garmestani, H., & Shih, D. S. (2016). Prediction of Machining-Induced Phase Transformation and Grain Growth of Ti-6Al-4 V Alloy. International Journal of Advanced Manufacturing Technology, 87(1–4), 859–866.

Shamsaei, N., Yadollahi, A., Bian, L., & Thompson, S. M. (2015). An Overview of Direct Laser Deposition for Additive Manufacturing ; Part II : Mechanical Behavior ,Optimization and Control.

TOPOLOGY OPTIMIZATION OF THE CONSOLIDATED STRUCTURAL BRACKET AND VALIDATION BASED ON MIL-STD

Berk İzgi DANIŞ[1], Cengiz KÖSEOĞLU[1], Onat AŞIK[1], Umut GÖVEZ[1], Emre ERCAN[1], Evren TAN[1]
[1]*ASELSAN Inc., Yenimahalle, 06370, Turkey, bidanis@aselsan.com.tr*

ABSTRACT

The rapid advancement in topology optimization (TO) and additive manufacturing (AM) have altered the design workflow predominantly such as lightweighting and part consolidation. Due to strict design requirement, defense industry emerges the potential of these tools and have turned their attention through these approaches. This study presents the design workflow of a MIL-STD810 shock and vibration resistant structural bracket by means of TO in order to achieve mass reduction and part consolidation. The output of TO is redesigned where high level of combined loading conditions and design for AM (DfAM) rules were taken into account. Bracket was directly fabricated by Stereolithography (SLA) in order to check manufacturability. Afterwards, finite element analysis (FEA) is carried out to ensure the mechanical strength of the optimized structural bracket. Electron Beam Powder Bed Fusion (E-PBF) is utilized to manufacture it made of Ti6Al4V for further validation stage. With successful implementation of this study step by step, it is stated out that the mass of structural bracket is decreased by %52 while the first natural frequency is 2.2 times higher than the original one.

Keywords: Design for Additive Manufacturing, Electron Beam Melting, MIL-STD, Topology Optimizatio

1. INTRODUCTION

Nowadays, the defense industry is seeking for exploiting the full potential of additive manufacturing in order to achieve the fully integrated end-use products with validation according to military standard MIL-STD 810. In this regard, the usage of TO and the rapid development within additive manufacturing brings a design freedom and have shaped structural design positively. From mechanical point of view, the collaboration of these tools provides technical opportunities such as both lightweighting and part consolidation. There are numerous advanced industrial applications [1-4] available that redesigned for additive manufacturing by means of TO. With accomplished validation procedure, the components are ready to serve with full functionality. Fundamentally, TO is a type of structural optimization method derived from applied mathematics that suggests the optimum material layout within the design space under prescribed boundary conditions with manufacturing constraints in FEA while complying with mechanical design requirements [5]. However, the result of TO leads to a geometric complexity as a drawback and cannot be fabricated via the conventional manufacturing method. In order to eliminate these difficulties, AM is an eligible candidate for fabrication of lighter, organic, and complex shaped parts [6]. In this study, TO is carried out for structural bracket and then the result of TO is redesigned by considering DfAM rules. The optimized structural bracket made of Ti6Al4V powder is fabricated with use of E-PBF after the manufacturability check in SLA (Figure 1).

2. MATERIALS AND METHODS

The structural bracket is responsible of carrying both impact load and mass of the structural panel in a military system. The part originally consists of AL5083-H32 mechanical parts with AISI304 stainless fasteners. The consolidation and mass reduction have been performed by using TO. The analyses were conducted in ANSYS Discovery and ALTAIR Inspire. The boundary conditions and load cases were given as input by considering working environment of the part. The hole regions where the structural bracket connected to the main frame and skin panel have been excluded from the optimization.
The TO results have been compared and the one with minimum mass and maximum stiffness has been selected for production. The initial production has been performed by SLA to observe the producibility

and geometry of the part. After the design is validated the production has been performed by using E- PBF technology. CT inspection is coupled for observation of the defects and imperfections in the part before and after the mechanical tests which are shock and vibration according to MIL-STD-810 standard.

3. RESULTS AND DISCUSSION

Using the defined design space and given load cases inferred from design requirements of the part, the TO output is obtained. It can be seen from the topology output geometry that, as a result of 3-axis load case application, the supporting geometries are built in order to provide rigidity in all 3 axes. A structural analysis is conducted on the TO output and the regions with low safety factor are reinforced using PolyNURB module of ALTAIR Inspire. Initial design with 2.55 kg mass is reduced to 1.22 kg with the TO and post-topology processes. In addition, the other main aim of the work is successfully obtained where part is consolidated into a single part, from 5 main body parts and 24 fasteners. On the other hand, alongside aforementioned improvements, it is shown that the strength requirements are still fulfilled after performed structural analysis in ANSYS Workbench. The first natural frequency of the optimized part is also increased to 2.2 times of the initial value, to 933 Hz.

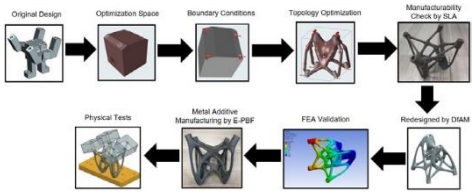

Figure 1 The Structural Bracket Design Workflow

4. CONCLUSIONS

In this study, improvements on production, assembly, production cost, natural frequency and mass the structural bracket that is actively used in a military system is achieved via TO. Following the design stage, the production of the optimized structure is also performed by an E-PBF Machine to pave the way for the related structural tests (impact, mechanical shock and vibration) on the part.

REFERENCES

1. Tomlin, M., & Meyer, J. (2011, May). Topology optimization of an additive layer manufactured
(ALM) aerospace part. In Proceeding of the 7th Altair CAE technology conference (pp. 1-9).
2. Eos.info. 2022. *3D Printing for Aerospace with EOS Technology*. [online] Available at:
<https://www.eos.info/en/all-3d-printing-applications/ruag-aerospace-3d-printed-satellite-components> [Accessed 9 May 2022].
3. 3D Printing Media Network - The Pulse of the AM Industry. 2022. *GE Aviation already 3D printed
30,000 fuel nozzles for its LEAP engine*. [online] Available at: <https://www.3dprintingmedia.network/ge-aviation-already-3d-printed-30000-fuel-nozzles-for-its-leap-engine/> [Accessed 9 May 2022].
4. Badır, M., Dagkolu, A., Sogutkıran, E. and Yılmaz, O., 2019. A New Design Approach for Additive
Manufacturing of Satellite Components. In: *AMC TURKEY*. İstanbul: AMC TURKEY, pp.86-88.
5. Gibson, I., Rosen, D., Stucker, B. and Khorasani, M., 2021. *Additive Manufacturing Technologies*.
Cham: Springer International Publishing.
6. Meng, L., Zhang, W., Quan, D., Shi, G., Tang, L., Hou, Y., Breitkopf, P., Zhu, J. and Gao, T., 2019.
From Topology Optimization Design to Additive Manufacturing: Today's Success and Tomorrow's Roadmap. *Archives of Computational Methods in Engineering*, 27(3), pp.805-830.

USING COBOTS FOR ADDITIVE MANUFACTURING OF BUILDING ELEMENTS

Efe Özkara[1,5], Çağla Meral Akgül[2,5], Mustafa Mert Ankaralı[3,5], Ulaş Yaman[4,5]
[1]*Department of Robotics, METU, Ankara, ozkara.efe@metu.edu.tr*
[2] *Department of Civil Engineering, METU, Ankara, Turkey, cmeral@metu.edu.tr*
[3] *Department of Electrical & Electronics Engineering METU, Ankara, Turkey, mertan@metu.edu.tr*
[4] *Department of Mechanical Engineering METU, Ankara, Turkey, uyaman@metu.edu.tr*
[5] *Center for Robotics & AI, METU, Ankara, Turkey*

ABSTRACT

Additive manufacturing aided construction has various benefits over traditional practices. The entire construction process can be shortened with improved quality control through digital fabrication. Production of high-quality complex geometries becomes possible without special formworks, easing the incorporation of functionality to the

3D printed components. The labor cost, especially critical for high-income regions, can be minimized. However, the structures which are mainly used in additive manufacturing makes the process harder in the scale of civil engineering due to product size, the amount of material used and the type of material. Therefore, adjusting the structure might help the process with another commonly used technique. Using collaborative robots (cobots) and platforms instead of the basic 3-D printing structure helps the mechanism reach further areas with work and cost- efficient construction using their ability and safety features and allow an active collaborative construction environment with humans.

Keywords: Collaborative robot (cobot), Additive Manufacturing, Building elements, end-effector, nozzle.

1. INTRODUCTION

Additive manufacturing is being more commonly used in rapid production of low quantity products. With scaling the size, this method can be used in much larger applications such as construction of various structures such as walls, columns, also relatively small structures such as gazebos and benches. The entire construction process can be shortened with improved quality control through digital fabrication. Production of high-quality complex geometries becomes possible without the need for special formworks. A collaborative robot (cobot) is a robot designed for processes which need collaboration with the operator and/or worker (El Zaatari, Marei, Li, & Usman, 2019; International & Robotics, 2019). Therefore, using a cobot with a platform attached underneath eliminates the problem of building a complete structure. Cobots has also various safety features and precautions, therefore maintaining a safe working environment for the operator. Considering the use of cobots for manufacturing in construction, the cobot must be optimized and programmed for simpler uses of additive manufacturing in relatively small scales.

2. MATERIALS AND METHODS

Cobots can be programmed for a variety of applications such as material handling, material removal, welding, dispensing, assembly etc. (El Zaatari et al., 2019; Universal Robots, 2020). This variety of applications proves that the cobots can be used for additive manufacturing with proper CNC and robotic programming and a suitable end-effector. The cobot used in the experiments can be seen on Figure 2, UR10e cobot from Universal Robots. A program can be written via the cobots interface or on a host computer and transferred to the cobot. Container is filled with clay and vibrated via a cement vibrator or a hammer to release all the air stucked in the container. After filling the container, it is connected to a hose and to the cobot. Then, the hose is filled with clay through to the nozzle. Lastly, the cobot is brought to the initial position and construction is started.

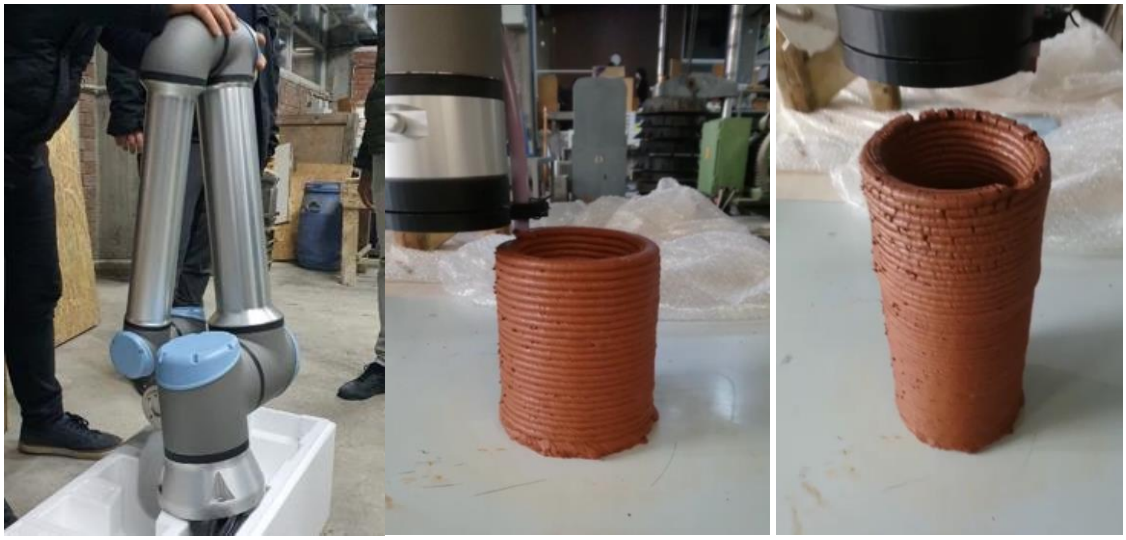

(a) (b)

(c)

Figure 2. (a) Cobot; (b) printing action; (c) printed hollow cylinder

3. RESULTS AND DISCUSSION

The cobot in action and the fabricated hollow cylinder can be seen in Figure 2 b-c. The cobot can easily 3D print desired patterns and shapes. However, the pattern must not have any sharp turns or overlapping patterns since the extruded beads overlap and it affects the layers and structural integrity. As seen from the figure, some errors occurred during 3D printing due to non-laminar flow of the material caused by the walls of the container and pressure flaws. Therefore, the method of material extrusion may be improved to obtain high quality structures.

4. CONCLUSIONS

A cobot can be used for additively manufacturing of a construction element. Optimizing the material injection may help manufacturing elements with better structural integrity. Using a wider nozzle may increase the durability of structures after construction.

REFERENCES

El Zaatari, S., Marei, M., Li, W., & Usman, Z. (2019, June 1). Cobot programming for collaborative industrial tasks: An overview. *Robotics and Autonomous Systems*, Vol. 116, pp. 162–180. Elsevier B.V. https://doi.org/10.1016/j.robot.2019.03.003

International, & Robotics, F. of. (2019). Demystifying Collaborative Industrial Robots. *Positioning Paper*, (October), 2–3. Retrieved from https://ifr.org/

Universal Robots. (2020). Cobot Applications. Retrieved May 5, 2022, from https://www.universal-robots.com/blog/cobot-applications/

VERIFICATION TESTS OF TI6AL4V ALLOY BY TIG BASED WAAM METHOD

Gani Melik Önder[1*], Mehmet Emre Çetinkaya[1], Ümit Aytar[2], Abdülcelil Bayar[2]
[1]*AlloyAdditive, Istanbul, Turkey*
[2]*Turkish Aerospace Industries, Inc., Ankara, Turkey*
**Corresponding author, email: ganimelikonder@alloyadditive.com*

ABSTRACT

The research and development for metal additive manufacturing of large-scale parts has been expanded in the recent years. Wire arc additive manufacturing (WAAM) has great potential by high deposition rate, reduced lead time and cost-effective solutions. With the ability to achieve lower buy-to-fly ratios, WAAM is substantial alternative for high-cost metals manufactured for aerospace industry. One of the essential alloys in this industry is Ti6Al4V with its high specific strength value. In this study, multilayer Ti6Al4V wall is deposited by TIG based WAAM method. Vertical and horizontal tensile test specimens are extracted from this wall according to ASTM E8 standards by wire-electrical discharge machining (Wire-EDM) and turning operations. Several verification tests such as X-ray inspection, alpha case measurement, microstructure analysis, and tensile tests are conducted. Very low amount of porosity is detected while suitable tensile test results compared to literature are achieved. It is appeared that developing the WAAM capabilities for full scale Ti6Al4V parts provide many advantages. **Keywords:** WAAM, TIG, Titanium, Ti6Al4V, Additive Manufacturing

1. INTRODUCTION

For production of large-scale parts, wire arc additive manufacturing (WAAM), a directed energy deposition method, has several advantages over conventional manufacturing and also other metal additive manufacturing methods in terms of cost and process time. High deposition rate, low initial machinery cost and low process consumable cost are main reasons of attention on WAAM in recent years. For example, instead of very long and difficult forging and machining operations of titanium parts in aerospace structures, WAAM is a prospective solution with the ability to manufacturing near net shapes and production with low buy-to-fly (BTF) ratios [1]. Unlike most of the academic and commercial WAAM by metal inert gas/gas metal arc welding (MIG/GMAW) method, tungsten inert gas/gas tungsten arc welding (TIG/GTAW) method is selected for WAAM of Ti6Al4V alloy in this work due to more controllable arc condition, independent wire feeding and lower surface roughness.

2. MATERIALS AND METHODS

Like in all metal additive manufacturing methods, there is a need for substrate which has to be similar material to feed material. Titanium plate (AMS4911) with 200x60x12mm dimensions was used as substrate for WAAM wall. Grinding and cleaning with ethanol were applied to the substrate. 1.2mm in diameter titanium welding wire (AWS5.16: ERTi-5) was used. A Lincoln Electric Aspect 300 AC/DC TIG welding machine was worked as heat source. An inert chamber with Ar gas was built due to titanium and its alloy's high oxygen affinity. Six axis industrial welding robot was used as motion system which was mounted with welding torch, local shielding device and wire feeding mechanism. Location of tensile specimens (ASTM E8) was decided in CAD model of wall. Horizontal(x-y) and vertical(z) specimens were extracted with Wire-EDM method to see the effect of anisotropy that stems from nature of additive manufacturing.

3. RESULTS AND DISCUSSION

A wall seen in Figure 1, 175x17x115mm dimensions in x-y-z directions, is built with WAAM for the mechanical characterization tests. 4 vertical and 7 horizontal tensile specimens are extracted from the wall via Wire-EDM machine. Specimens that are numbered as 1,4,5,7,8,11 are tested as built status without heat treatment. Before the tensile test, radiography test is applied to check porosity occurrence. Hardness values are measured on the 5 different zone on the specimens. Also, alpha case thickness is measured which is important brittle structure for titanium alloys. Finally, tensile test is applied to specimens. Result is seen in Table 1 is compared with literature and global manufacturing standards. Similar strength and elongation values are coming up with the literature.

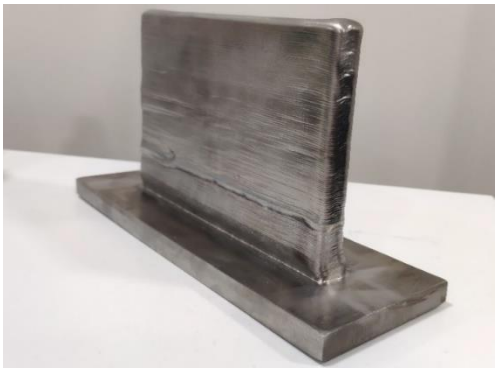

Figure 1. Ti6Al4V WAAM all for tensile specimens

Table 1. Tensile Test Results

Specimen	Direction	Yield Strength (MPa)	Tensile Strength (MPa)	Elongation(%)
1	z	~747	~904	18
4	z	754	863	25
5	x-y	869	970	16
7	x-y	817	915	15
8	x-y	801	902	18
11	x-y	788	930	17
Reference [2]	x-y	~830	~970	~8
Reference [2]	z	803	918	14
ASTM B265-20a	x-y	827	893	10
AMS4999	x-y	800	896	6
AMS4999	z	758	855	6

4. CONCLUSIONS

Ti6Al4V wall structure was produced by TIG based WAAM in this work. For verification efforts, non- destructive and destructive tests are conducted to specimens which were extracted from the wall. Tensile test shows that strength and elongation values are conforming to literature and standarts. As future work, fatigue tests will be conducted for fatigue life evaluation of specimen produced by WAAM.

REFERENCES

1. Williams, S. W., Martina, F., Addison, A. C., Ding, J., Pardal, G., Colegrove, P. (2016). Wire + arc additive manufacturing. Materials Science and Technology, 32(7), 641-647. doi:10.1179/1743284715y.0000000073
2. Wang, F., Williams, S., Colegrove, P., & Antonysamy, A. A. (2012). Microstructure and mechanical properties of wire and arc additive manufactured ti-6al-4v. Metallurgical and Materials Transactions A, 44(2), 968-977. doi:10.1007/s11661-012-1444-6

WIRE + ARC ADDITIVE MANUFACTURE OF 17-4 PH STAINLESS STEEL: EFFECT OF PROCESSING CONDITIONS ON THE GEOMETRICAL AND MECHANICAL PROPERTIES

Omer Faruk Yazici[1], Talha Muslim[2], Orkun Tekelioglu[3], Alperen Bayram[4]
[1] *Coşkunöz Holding R&D Center, ofyazici@coskunoz.com.tr*
[2] *Coşkunöz Holding R&D Center, tmuslim@coskunoz.com.tr*
[3] *Coşkunöz Holding R&D Center, otekelioglu@coskunoz.com.tr*
[4] *Coşkunöz Holding R&D Center, abayram@coskunoz.com.tr*

ABSTRACT

Wire + Arc Additive Manufacture (WAAM) is a well-known Additive Manufacturing method used to manufacture meter-sized parts at a comparatively lower cost, with less material wastage. A wide variety of metallic alloys can be processed using WAAM. 17-4 PH is a precipitate hardening stainless steel with high corrosion resistance and strength. It is important to understand how this alloy behaves when processed via WAAM. This study investigates how fracture critical parts can be successfully manufactured via WAAM. Single bead tracks were investigated for geometrical accuracy. Walled geometries were deposited to extract tensile coupons for mechanical characterization. A cylindrical part was successfully manufactured which underwent solutionizing and ageing heat treatment. The part was scanned in as-built and heat-treated conditions to account for deformation. The part underwent nondestructive testing to analyze internal defects such as porosity. This study shows that WAAM is a very suitable process for manufacturing medium to large-sized parts with relatively simple geometry.

Keywords: Additive manufacture, WAAM, Stainless steel, 17-4 PH

1. INTRODUCTION

Additive Manufacturing (AM) refers to a group of technologies that can be used to manufacture complex 3D parts directly from Computer-aided design (CAD) data. Wire + Arc Additive Manufacture (WAAM) uses an electric arc as a heat source, a metallic wire as the feedstock material, and a robot or a gantry system is used as a manipulator to deposit near net-shaped parts layer by layer. The continuous heating and cooling cycles experienced during WAAM result in a complex, inhomogeneous and anisotropic microstructure which intern affects the mechanical properties of the part. 17-4 PH stainless steel is a precipitate hardening material that is difficult to process conventionally and is very suitable to be processed via WAAM. Limited studies investigate how 17-4 PH can be effectively processed via WAAM hence presenting a gap. This study investigates how fracture critical parts can be successfully manufactured via WAAM. Single bead geometries were investigated. Walls were deposited to extract tensile coupons for mechanical characterization. Finally, the part was deposited and heat treated.

2. MATERIALS AND METHODS

Kuka KR 70 r 2100 robotic arm (KRC 4) and Fronius tps 500 I welding machine were used in the experiment. 17-4 PH wire of 1.2 mm diameter provided by Böhler Welding was used as the feedstock material. Unidirectional 60 mm long single bead tracks were deposited as shown in Figure 1.



Figure 1. 17-4 PH single bead tracks

Wire feed speed (m/min) and Travel speed (m/min) were varied whereas all other process parameters remained unchanged. Table 2 shows the range of process parameters used.

Table 2. Process Parameter ranges used in experimental trials

Parameter	Range
Wire feed speed (WFS)	3, 4.5, 6, 7.5, 9, 10.5
Travel speed (TS)	0.3, 0.45, 0.6, 0.75, 0.9, 1.05

Edges of the tracks were removed. Each track is sawed into 5 pieces at equidistant points. The heights, widths and depths are measured at the cross-section and averaged out. Figure 2 shows one of the cross-sectional measurements for sample 1.

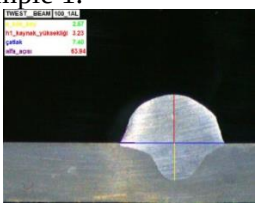

Figure 2. One of the cross-sectional measurements of the17-4 PH single bead tracks

An acceptability criterion was defined for the single bead geometry. A cylindrical part was deposited as shown in Figure 3.



Figure 3. Cylindrical parts deposited via WAAM

The process parameters used were: 4m/min wire feed rate, 1m/min torch speed, and 1.45mm layer thickness. All other parameters remain unchanged. The cylindrical part will be subjected to the following heat treatment condition: 1040 °C – 1 h, air-cooled to RT, 620 °C – 4 h, air-cooled. The part will be scanned before and after heat treatment and compared with the CAD data to account for the heat treatment. The cylindrical part will undergo X-RAY to account for any internal defects. The same process parameter combination will be used to deposit walls to extract tensile coupons for mechanical characterization. Figure 4 shows the schematic of the wall.

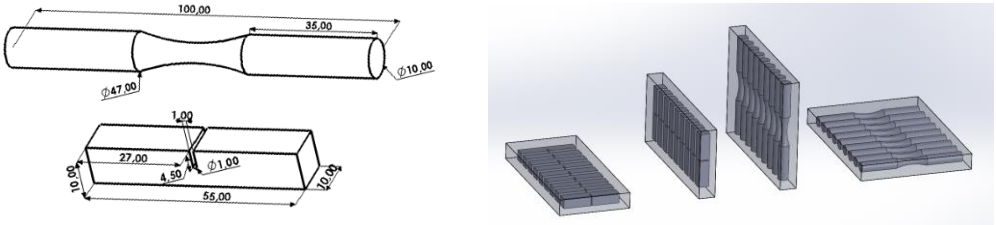

Figure 4. Schematic of the wall with tensile coupon location, size and orientation

3. RESULTS AND DISCUSSION

The authors want to bring to the attention of the reviewers that we have deposited the single bead tracks and the cylindrical part. Work is still going on heat treatment of the part and manufacturing of the wall to extract coupons for mechanical characterization. All results collected will be reported in detail during the presentation at AMC.

4. CONCLUSIONS

The study is still in progress. The part will be heat treated and the wall will be deposited to extract test coupons for mechanical characterization. All results will be reported in detail in the presentation.

WIRE ARC ADDITIVE MANUFACTURING OF THIN-WALLED LOW ALLOY STEEL COMPONENTS USING SOLID AND METAL CORED WIRES

Batuhan Turgut[1], Uğur Gürol[2] , Recep Önler[3]
[1]*Gedik Welding Inc, Gebze Technical University, bturgut@gedik.com.tr,*
[2]*Istanbul Gedik University, Gedik Welding Inc, ugurol@gedik.com.tr*
[3]*Gebze Technical University, ronler@gtu.edu.tr*

ABSTRACT

Wire Arc Additive Manufacturing method is an innovative technique that can easily produce large complex shaped metal parts with significantly reduced cost and build time compared to powder bed additive manufacturing methods. The approach allows additively manufacturing metal parts that can be welded. Metal cored wires which include a basic outer shell and filled with the desired alloying elements can be an important wire choice to reduce wire cost and provide additional flexibility. Due to their geometry, the generated arc profile and resultant thermal profile can be significantly different from the solid wires. This study presents a hardness test comparison of parts manufactured with the WAAM method at the same parameters using commercial AWS A5.18 ER 70 S-6 solid welding wire and AWS A5.18 E 70 C-6 M metal cored wire. It was observed that the metal cored wire results in higher hardness values compared to solid wire processed under identical conditions.

Keywords: WAAM, Additive Manufacturing, Gas Metal Arc Welding (GMAW), Hardness, Metal Cored Wire

1. INTRODUCTION

Wire Arc Additive Manufacturing method (WAAM), one of the DED processes, is a method that uses electric arc as heat source and welding wire as feeding material. Since it does not require special powder or a well-controlled environment, the WAAM method has less production costs than other metal additive manufacturing methods (Frazier, 2014; Williams et al., 2016). It was shown that the WAAM method is suitable to produce large-sized parts (Williams et al., 2016). The WAAM is a promising method due to its advantages such as higher deposition rate, higher energy efficiency and lower cost. (Ding et al., 2015; Yildiz et al., 2020) Although the knowledge and experience in the welding provides a decent base for WAAM, part geometries and thermal history differentiates the process from the welding.

The solid wires used in WAAM are usually produced by wire drawing and are generally mass-produced. For small quantity needs, metal-cored wires in which, the outer shell contains the base material, and the inner core includes the desired alloying elements can be more economical. However, the geometry of metal-cored wires changes the arc profile and in turn, the heat source is altered. Metal cored wires transmit the current through the wire strip during welding causing a higher current density, lower heat input and lower penetration (Lin et al., 2019). Thus, during WAAM operation, it is important to understand the consequences of the wire choice.

This study experimentally investigates the hardness of parts produced by metal cored wire in comparison with a solid wire with a similar composition. For this purpose, two parts were created with identical process parameters using solid and metal cored wires. The hardness variation from the base plate to the top layer was measured using a Vickers indenter.

2. MATERIALS AND METHODS

The WAAM operation was done on a robot cell which includes a 6-axis industrial welding robot (OTC Daihen FD-V8L) integrated with a GMAW welding machine (GeKaMac Power MIG GPS WB P500L) For comparison, an AWS A5.18 ER 70 S-6 as solid welding wire and AWS A5.18 E 70 C-6 M was used to create rectangular samples on a 12 mm thick low alloy steel substrate. Both the wires were used with 80 Amper current, 40 cm/min travelling speed under ArCO18 shielding gas with 15lt/min flow rate. A total of 60 layers were printed using both wires with 2 minutes dwell time after each layers. Both samples were manufactured on a 350x75x12 mm S355 base plate.

3. RESULTS AND DISCUSSION

It was observed that the metal cored wire produces lower layer height and larger wall thickness compared to solid wire. After the WAAM process was performed, the height of the component produced by using solid wire was measured 73 mm in 60 passes, and the height of the component produced by using metal cored wire was 65 mm in 60 passes. When the width of the produced parts is compared, it was measured that the metal cored wire was 0.3 mm thicker than the solid welding wire.

Figure 1 shows the Vickers hardness values obtained from the cross-section of the investigated workpieces. It was seen that due to repeated thermal cycle, the lower layer showed similar hardness values whereas with increasing height, the metal cored wire resulted in higher hardness values due to faster cooling as a result of larger wall.

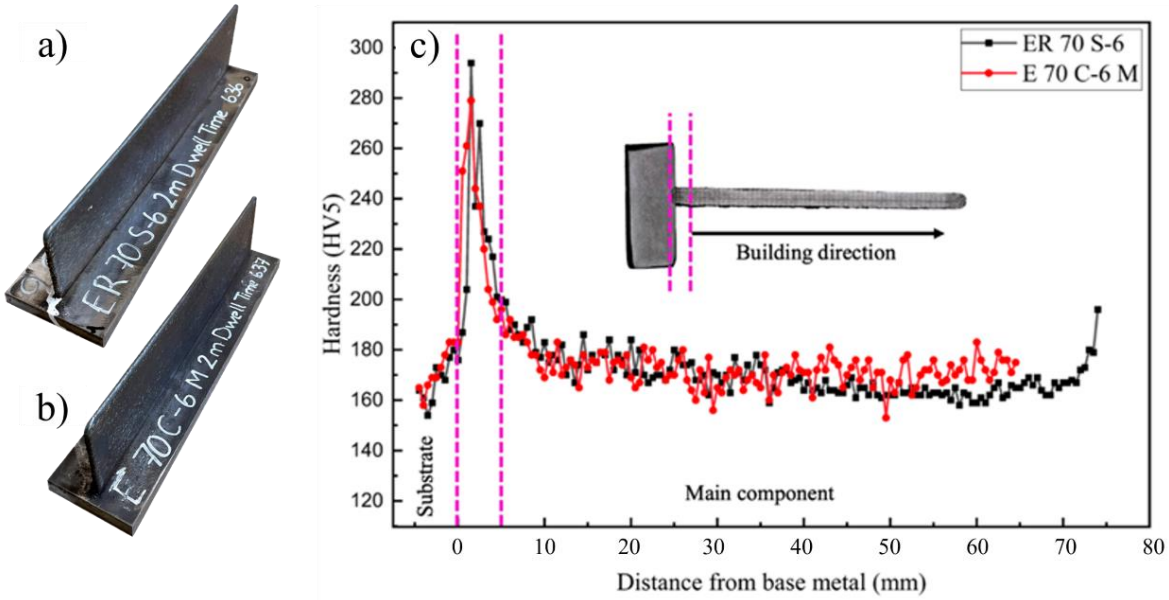

Figure 1. Manufactured parts using (a) solid wire ad (b) metal cored wire and (c) variation of Vickers Hardness on the cross-sections of the parts.

4. CONCLUSIONS

It was seen that the metal cored wire produces lower layer height and wider wall thicknesses compared to solid wire under the investigated process conditions. The hardness of the sample manufactured using solid wire was slightly higher on top layers possibly due to thermal history. Microstructure, and other mechanical properties need to be analysed for a complete comparison.

REFERENCES

Ding, D., Pan, Z., Cuiuri, D., & Li, H. (2015). A multi-bead overlapping model for robotic wire and arc additive manufacturing (WAAM). *Robotics and Computer-Integrated Manufacturing*, 31, 101–110. Retrieved from https://doi.org/10.1016/j.rcim.2014.08.008

Frazier, W. E. (2014). Metal additive manufacturing: A review. *Journal of Materials Engineering and Performance*. Springer New York LLC. Retrieved from https://doi.org/10.1007/s11665-014-0958-z

Suat Yildiz, A., Davut, K., Koc, B., & Yilmaz, O. (n.d.). Wire arc additive manufacturing of high-strength low alloy steels: study of process parameters and their influence on the bead geometry and mechanical characteristics. Retrieved from https://doi.org/10.1007/s00170-020-05482-9/Published